The University Of Sheffield.

The impact of soil microaggregates on bacterial competition

By

Mina Mohaghegh

A thesis submitted for the degree of Doctor of Philosophy

The University of Sheffield
Faculty of Science
Department of Physics and Astronomy

August 2022

To Mehdi, Aiden and my parents

Acknowledgements

I would like to express my gratitude to the people who supported me through my PhD journey. This PhD project was funded by the Imagine: Imaging Life studentship from University of Sheffield which I am very thankful for.

I would like to thank Prof. Simon Foster, Prof. Duncan Cameron, Prof. Michael Brockhurst, Pro. Ole Nybroe, Prof. Kevin Foster, Dr. Clair Turner, Dr. Andrew Fenton, Dr. Eleanor Harrison, Dr. Darren Robinson, Dr. Christa Walther and Dr. Wook Kim for their valuable discussion and feed-backs. For the opportunity to pursue my PhD and for his great support throughout my journey, I am extremely thankful to my supervisor, Dr. Mack Durham. Also, I would like to thank the F18 group (old and new crew) who represented the best combination of brilliant scientists and wonderful people. Drs. Kasia Wacnik, Bartek Salamaga, Milena von und zur Muhlen, Victoria Lund, Rebecca Hodges, Nicola Galley, Laia Pasquina Lemonche, Lucia Lafage, Mariana Tinajero-Trejo, and Jamie Wheeler. You guys are like my family and I am grateful for our friendship.

I am forever thankful to my parents for giving me the opportunities and experiences that have made me who I am today. Your unconditional love and support allowed me to live my life to the fullest. Maman and Baba, you are my everything and I love you more than I can put in words.

To my late sweet aunt, Khale Nadi, who was like a second mother to me. When I was studying in France, she used to call me every Saturday to ensure that I felt loved and supported. Her kindness touched the lives of many people and I feel grateful to have had her in my life.

My special thanks go to Aiden, who kept me company during the last few months I was in Sheffield and had an active presence in my belly while I was doing microscopic imaging. My precious Aiden, you have brought so much love and joy into our lives, and I feel extremely fortunate to be your mum. Love you so much.

Last but not least, I want to thank my one and only Mehdi who has always been there for me, supported me and loved me. Together, we have come a long way, and I could not ask for a better partner. Love you so much Mehdidou!

Abstract

Soil contains one of the planet's most diverse microbial communities, which live in intense competition with each other for nutrients and space. Microaggregates are small clusters that form within soil, composed of both clay and diverse organic materials and have a size between 20-250 μm. These small-scale structures allow bacteria to withstand environmental stresses and provide ecological niches that promote diversity. In addition, microaggregates are known to play a major role in the global carbon cycle because they can protect organic carbon from degradation by bacteria. Yet, little is known about how microaggregate structure impacts the competition between different bacterial genotypes.

To metabolise the organic material in soil, many bacteria secrete extracellular compounds that digest recalcitrant nutrients to a labile form which bacteria can readily metabolise. These enzymes typically have a significant production cost, however, in well-mixed systems these secretions can be used by bacterial genotypes that did not pay the cost of producing them. The aim of this thesis is to investigate how microaggregates affect the competition between bacterial strains that produce enzymes and those that lack enzyme production. This is accomplished through the development a laboratory-based model of microaggregates in which two strains of *Pseudomonas fluorescens* compete for nutrients. While wild-type cells produce an extracellular enzyme called AprX, that can allow them to digest casein into labile form, we engineered a clean deletion mutant ON2-Δ*aprX* that is unable to produce AprX thus cannot grow in casein-based media.

We compared the dynamics of bacterial competition in both media containing casein, which requires AprX for bacteria to utilise, and a control media contains casein that has already been pre-digested with proteinase K and is already labile. Both media were then tested in the both the presence and absence of clay, which is the main constituent of microaggregates. We optimised our experimental protocols to break the microaggregates efficiently with minimum damage to the bacteria, allowing us to quantify each bacterial strain accurately after completing the competition.

This laboratory-based model of microaggregates indicates that clay microaggregates can allow enzyme producing cells to grow faster than non-producing "cheaters" by transforming public goods into private goods. However, microscopic imaging suggests that the degree of genotypic patchiness within the microaggregate structure can exert a strong influence on the outcome of bacterial competition in microaggregates. In particular, when the genotypes are well-mixed together within microaggregates we find that wild-type cells and AprX mutants

tend to grow at a comparable rate.

The results of this study will allow us to gain a deeper understanding of how bacteria compete for resources in highly heterogeneous environments such as soil. While the research on bacterial competition in soil microaggregates is still in its infancy, this study represents a significant step forward in understanding how soil microaggregates shape the evolution of bacterial communities.

Declaration

This thesis is submitted to The University of Sheffield in support of my application for the degree of Doctor of Philosophy. I, the author, confirm that the thesis is my own work.

Contents

1 Introduction **1**

1.1 Introduction 1

1.1.1 Research question and challenges 4

1.2 Soil structure 6

1.2.1 Size and structure of aggregates 10

1.3 Stability of public good production 14

1.4 Bacterial competition 15

2 Development and characterisation of a strain of *P. fluorescens* that lacks the ability to produce the protease AprX **22**

2.1 Introduction 22

2.2 Aims of the chapter 24

2.3 Results 24

2.3.1 Construction of a protease deficient strain in *P. fluorescens* ON2 24

2.3.2 Developing media for bacterial competition 39

2.3.3 Characterisation of the *P.f ON2-ΔaprX* 41

2.4 Discussion and conclusion 54

3 Microaggregate Development **57**

3.1 Introduction 57

3.2 Clay preparation 60

3.2.1 General Protocol 60

3.2.2 Revised Protocol 65

3.2.3 Clay In Growth Media 67

3.2.4 Adjusting Clay Concentration 68

3.3 Microaggregate lab model development 69

3.3.1 Bacterial inoculation in the clay media 69

3.3.2 The impact of bacterial growth on microaggregate formation 71

3.3.3 Optimisation: Temperature and aeration rate . . . 73
3.3.4 Microaggregate formation over time . . . 75
3.4 Discussion and conclusion . . . 76

4 Bacterial competition in soil microaggregates 78
4.1 Introduction . . . 78
4.1.1 Aims of this chapter . . . 82
4.2 Experimental design of bacterial competition in clay environments . 82
4.2.1 Candidate bacterial strains and growth media . . . 83
4.2.2 Length of the experiment . . . 84
4.2.3 Optimising the bacterial competition experiment . . . 86
4.2.4 Post-competition treatments . . . 88
4.3 Breaking treatment techniques . . . 91
4.3.1 Breaking microaggregates with vortex . . . 92
4.3.2 Breaking microaggregates using a Homogeniser . . . 93
4.3.3 Breaking using ultrasonic energy to destabilise microaggregates . . . 95
4.3.4 Breaking aggregates chemically, using sodium pyrophosphate 97
4.3.5 Breaking aggregates using filters . . . 99
4.3.6 Applying pressure using fine syringes . . . 101
4.4 Data analysis . . . 103
4.4.1 Colony forming unit (CFU) counting . . . 103
4.4.2 Single Plate-Serial Dilution Spotting (SP-SDS) counting technique . . . 106
4.4.3 Counting using fluorescence microscopy . . . 107
4.5 Microscopic study on bacterial competition in microaggregates . . . 110
4.5.1 Epifluorescence microscopy . . . 114
4.5.2 Confocal microscopy . . . 124
4.6 Discussion and Conclusion . . . 126
4.6.1 Discussion . . . 126
4.6.2 Conclusion . . . 131

5 General Discussion 133
5.1 Discussion . . . 133
5.2 Future Research Directions . . . 138

List of Figures

1.1 Terrestrial carbon cycle with major processes that are mediated by soil microorganisms. Organic carbon in soil results from the interactions of several ecosystem processes, photosynthesis, respiration, and decomposition and the role of soil microorganisms is crucial in the carbon cycling process [14]. This process is composed of soil microbes including bacteria and fungi, decaying material from once-living organisms such as plants (fixation of atmospheric CO_2 into the plant biomass as the result of photosynthesis) and animal tissues, fecal material, and products formed from their decomposition [1]. 3

1.2 The hierarchical model of soil aggregate classification. Larger macroaggregates are composed of hyphae, plant roots, microaggregates, and small microaggregates. This image is adapted from Costa et al., 2018 [47] 7

1.3 Conceptual drawing of isolated soil aggregates during dry condition (left), and wet condition (right). Wet conditions allow for the transfer of nutrients, bacteria, virus and metabolites between soil aggregates. Images are adapted from Wilpiszeski et al., 2019 [51]. . . 8

1.4 Illustration of inter-aggregate and intra-aggregate pores. Image is reproduced from [61]. 9

1.5 Comparison of clay aggregates in sterilised soil and unsterilised soil using scanning electron microscopy. Due to lack of the bacteria in sterilised soil, only a few clay aggregates are present (a). However in unsterilised soil, high quantities of clay aggregates are observed (b), the white arrows pointing dense layers of microaggregates. Image (c) shows a detailed view of a microaggregate and its surfaces of minerals. The # signs in the image (c) show the mineral leaflets of the microaggregate. Images are adapted from Lunsdorf et al., 2000 [76]. 10

1.6 Clay is categorised in different types based on its physicochemical properties. Shown here are three main groups of clay called illite, smectite and kaolinite, which each have a different chemical properties and microstructure [81, 82, 83, 84]. The SEM microscopic images of illite, kaolinite and smectite clay particles are adapted from [85], [81] and [86] respectively. The schematic structural diagrams of different types of clay are adapted from [87]. 12

1.7 The face and edge of the clay particles contain negative and positive electric charges respectively that facilitate their attachment to particles, chemicals, and each other. The positively charged particles thus often attach on the face and negatively charged particles often attach to the edge of the clay particles. This property of the clay has a direct relation with the pH of the environment. 13

1.8 An illustration of possible outcomes of the bacterial competition. a) competition exclusion when the less competitive strains go extinct while others dominate the community, b) coexistence of the strains by consuming different resource types, c) coexistence of competitors through spatial separation. The image was adapted from Ghoul et al. 2016 [37]. 16

1.9 An illustration of cells in homogeneous and heterogeneous environments: a) in the homogeneous environment (such as shaken liquid culture), the secreted enzyme diffuses away from the producer and the product of the enzyme (digested casein in this case) can be consumed by neighbouring cells without paying the cost of enzyme production ("non-producer" cells). Therefore, the non-producer cells will grow faster than the producer cells, resulting in the non-producers outcompeting the producers. b) on the other hand, in heterogeneous environment (such as soil microaggregates in this case) the secreted enzyme will stay close to its producer cell due to the physical barrier conformed by the microaggregates such that the product is preferentially accessible to the producer cells. . . 19

1.10 An example of a clay aggregate inhabited by a bacterium (marked by a green circle and shown with orange B). The image was taken by TEM microscopy [147]. 21

2.1 A schematic illustration to show a cross section of a casein micelle with its subunits of k-casein peptide chains, submicelle and calcium phosphate, adapted from Walstra et al. 1999 [156]. 23

2.2 PCR revealed that the *aprX* gene in protease deficient strain, ON2-pd5, is still present, but the *inh* gene is affected by the Tn*5* transposon. PCR product in lane 1 to 3 belong to ON2-WT strain and while lanes 4 to 6 are PCR products from ON2-pd5. 1) amplified *aprX* with expected size of 1.5 kb, 2) amplified *inh* with expected size of 0.7 kb and 3) amplified *aprX* plus *inh* from the genomic DNA of ON2-WT with expected size of 2.2 kb. 4) amplified *aprX*, 5) amplified *inh* and 6) amplified *aprX* plus *inh* from the genomic DNA of ON2-pd5. PCR products representing *aprX*, *inh* and *aprX* plus *inh* were amplified using primers (aprXF, aprXR), (inhF, inhR) and (aprXF, inhR) respectively. The details of the primers are listed in Table 2.2. Sizes of a DNA ladder are shown in kb. 28

2.3 Construction of pGEM®-T::Δ*aprX* plasmid. The deleted version of *aprX* consists of ∼1kb upstream and downstream regions of the *aprX* gene which carries 15 bp of the upstream and 15 bp of the downstream of the *aprX* gene. The linearised pGEM®-T plasmid has a T-overhang at each end in order to facilitate the ligation of an insert into the plasmid. Therefore, an A-overhang was added to each end of the Δ*aprX* fragment. 32

2.4 Construction of pEX18::Δ*aprX*. a) The pEX18Gm was linearised by EcoRI and the purified Δ*aprX* fragment was cloned into it, resulting in pEX18::Δ*aprX*. b) Restriction enzyme digestion of pEX18::Δ*aprX* with EcoRI. The expected DNA band sizes of 2 and 5.8 kb are indicated with black arrows. Sizes of a DNA ladder are shown in kb. 34

2.5 Construction of ON2-Δ*aprX* with a clean deletion of the *aprX* gene. In ON2-Δ*aprX* the entire *aprX* gene except for its first 15 bp and last 15 bp is deleted (a). The deletion of the gene was confirmed by PCR (b), and sequencing and the new strain called ON2-Δ*aprX*. The expected DNA band size of 3.5 kb (ON2-WT) and 2.1 kb (ON2-Δ*aprX*) are indicated with black arrows. 36

2.6 Characterisation of the ON2-Δ*aprX* and ON2-WT strain. Comparing the growth of the new mutant strain, ON2-Δ*aprX*, with parental wildtype strain, ON2-WT in casein and digested casein media using a) CFU counting (Data presented as mean and standard deviation and data are compared using *t* test **** $p<0.0001$ and ns (not statistically significant) $p>0.05$), b) casein and digested casein agar and c) fluorescent microscopy imaging. All the samples were incubated at room temperature for 48 hours and the results confirmed the reduction of ON2-Δ*aprX* growth compared to ON2-WT as mono-culture in casein medium. The scale bars in microscopic images are 50 μm. 42

2.7 Measuring growth curve of ON2-WT and ON2-Δ*aprX* strains with and without labels in a) M63 and b) casein over a period of 50 hours. a) is the OD_{600} measurement of of ON2-WT (unlabelled, labelled with CFP-Km^r and YFP-SM^r) and ON2-Δ*aprX* (unlabelled, labelled with CFP-Km^r and YFP-SM^r) in M63 and b) is their growth curve in casein. The aim of this measurement was to detect the impact of fluorescent proteins or antibiotic resistant labels on ON2-WT and ON2-Δ*aprX* by comparing their growth with unlabelled strains. . . . 44

2.8 A schematic of surficial and subsurface colonies. In the sub-surface colony, the cells are sandwiched between agar and glass, which helps keep them two-dimensional. In contrast, cells in the surficial colony grew on top of the agar and quickly formed a multi-layer thick colony. It appeared that the high density of cells and their secretions interfered with the imaging of CFP- and YFP-labeled cells in the surficial colonies. Therefore, this study employed the subsurface method as it keeps colonies flatter, so that single cells can be more easily imaged with a fluorescence microscope for further investigation. 47

2.9 Growth of ON2-WT and ON2-Δ*aprX* strains using the subsurface method on casein agar after 16 hours. In all samples, the start point of inoculation was OD_{600} of 0.05, colonies were incubated at 25°C for 16 hours. Image (A) shows a mono-culture of ON2-WT-CFP and ON2-WT-YFP, (B) a mono-culture of the ON2-Δ*aprX*-CFP and ON2-Δ*aprX*-YFP, (C) a co-culture of the ON2-WT-CFP mixed with ON2-Δ*aprX*-YFP and (D) a co-culture of ON2-WT-YFP mixed with ON2-Δ*aprX*-CFP. The scale bars are 50 μm long. 49

2.10 Subsurface colonies on casein-agar surface. Both strains were equally represented at the time of inoculation (OD_{600} of 0.05), and the time of incubation is 5 days at 25°C. (A) wild type strain labelled with CFP and YFP. (B) ON2-Δ*aprX* strain labelled with CFP and YFP label. (C) Co-culture of the ON2-WT-CFP mixed with the ON2-Δ*aprX*-YFP strain. (D) Co-culture of ON2-WT-YFP and ON2-Δ*aprX*-CFP strains. The scale bars are 50 μm long. 51

2.11 Quantification of the ON2-WT-CFP and ON2-Δ*aprX*-YFP cells as mono-cultures in casein and M63 media using flow-cytometry. a) ON2-WT-CFP in M63 b) ON2-Δ*aprX*-YFP in M63, c) ON2-WT-CFP in casein and d) ON2-Δ*aprX*-YFP in casein. Initially, casein and digested casein media were used in the analyses, however, a high level of noise was observed in a cell-free blank of the casein media digested with proteinase K, and it was replaced with M63. A large reduction in the number of ON2-Δ*aprX* cells was observed in casein compared to ON2-WT cells using this method. However, due to the auto-fluorescence of the hectorite clay particles, this device ultimately was not used in this project as it could not distinguish cells from clay particles. 52

3.1 The composition and structure of soil, including microaggregates, macroaggregates, organic and inorganic matters. Image reproduced from [51]. 58

3.2 Detailed process of eliminating organic contaminants from clay particles using (a) sodium hypochlorite and (b) ethanol. The clay of case (a) absorbed the sodium hypochlorite, and even after multiple washings, the sodium hypochlorite was not washed away, which prevented bacteria from growing. In (b), the ethanol was used instead of sodium hypochlorite but it is likely because of the clay dehydration caused by ethanol [203], resulting in rapid sedimentation that prevented clay particles from being separated by size. 61

3.3 A comparison of clay treated with and without sodium hypochlorite. After 24 hours of incubation with clay samples, test tubes showed a significant change in colour (a). Ⓘ is the control sample of bacteria clay samples without sodium hypochlorite treatment and Ⓘⓘ is bacteria in a clay medium treated with sodium hypochlorite. Comparing (a)-Ⓘ and (a)-Ⓘⓘ, the significant difference suggests that the sodium hypochlorite attached to the clay particles caused a bactericidal effect. Sub-figure (b) is the result of CFU counting of both samples on LB agar plates without antibiotics (sample (b)-Ⓘ has been diluted five fold, whilst (b)-Ⓘⓘ has not). Sub-figure (c) is the result of fluorescent microscopic imaging of bacteria clay samples (sample (c)-Ⓘ has been diluted 2 times, whilst (c)-Ⓘⓘ has not). In the fluorescent microscopic result of sample (c)-Ⓘⓘ, the exposure time was enough to observe any GFP-labelled cell. These measurements confirmed the sodium hypochlorite treatment process renders the clay media unable to support bacterial growth. . . . 63

3.4 A comparison of sodium hypochlorite and ethanol-treated clay samples for bacterial growth. (a) and (b) are microscopic results of clay treated with sodium hypochlorite that confirm sodium hypochlorite has a bactericidal effect, preventing the growth of bacteria. Images (c) and (d) show that when clay was treated with ethanol, bacteria could grow in the clay sample, confirming that ethanol was washed away from the clay but the concentration of clay particles in the clay medium was inadequate. Because the clay particles sediment so rapidly in the bottom of the tube, the clay particles in the supernatant fraction of the clay sample were very fine in size with low concentration. 64

3.5 Revised clay preparation protocol to design a microaggregate structure. In this protocol, clay is prepared in M63 10X without glucose so it will sediment slowly enough to separate finer clay particles from clay aggregates. In this method, the supernatant was collected containing fine clay particles and diluted to M63 1X. 65

3.6 The finer clay particles are separated from larger clay aggregates in concentrated M63 via sedimentation. The sedimentation occurred over a period of 30 minutes and the finer clay particles (C) remained in the supernatant (SN) fraction. The photos were taken every two minutes from time zero to 30 minutes. 66

3.7 Clay M63 medium preparation. During the preparation of clay M63, the clay was autoclaved, but the rest of the medium was filtered before mixing with the clay. 67

3.8 Clay casein medium preparation. Since casein is sensitive to pH, all materials need to be thoroughly mixed together before adding casein to the clay medium. The pH of the clay casein medium was then adjusted with filtered sterilise HCL 0.1M. 68

3.9 Different concentrations of clay mixed with M63 10X medium: (a) 1 g as control, (b) 4 g and (c) 10 g of clay mixed with 50 ml of M63 10X. Incubation time for all three samples was 30 minutes at room temperature. 69

3.10 Schematic illustration of clay medium preparation with four times larger clay fraction. The clay samples were prepared according to the protocol and then the supernatants were removed after 30 minutes, mixed with sterilised distilled water and autoclaved. The autoclaved clay rested on the bench for an hour before removing the liquid fraction, then the clay fractions were mixed together to make a four-fold more concentrated clay sample. 70

3.11 A third of the blue tip was cut off to minimize structural damage to the microaggregate. 71

3.12 The stability of the microaggregate structure relies on bacterial activity and their extracellular products. The images in the top row were taken using a brightfield filter, while those in the bottom row were taken using a GFP filter. (a) and (b) are the mixture of clay and GFP labelled bacterial culture in M63 medium without glucose, (c) and (d) the same clay and bacterial culture but in a M63 with glucose. Samples were incubated at 30°C, with shaking at a speed of 220 rpm. 72

3.13 High-speed shaking provides more aeration for bacteria to grow but prevents the development of large microaggregates. The left images are bacterial culture in clay M63 medium incubated for 24 hours at 30°C with a shaking speed of 220 rpm. The right images are after adjusting temperature and aeration rate to 21°C and 110 rpm respectively. The samples were imaged using brightfield and GFP imaging. 74

3.14 Microaggregate formation and development over the period of 48 hours time. The mixture of clay and bacteria was imaged from time zero to 48 hours after incubation on a slow shaker at room temperature, 21°C. Results demonstrate microaggregate formation from clay particles to an early stage of microaggregate to a mature microaggregate with size around 250 μm. The images are taken by fluorescent microscope with brightfield and GFP filters. Bars are 50 μm. 76

4.1 The costs and benefits of producing public goods. Shown are the growth rates of populations consisting of producers and non-producers (e.g., of a digestive enzyme) and producers in a population started with a 50:50 mixture of both. The graphs show that non-producers spread and out-compete producers in a well-mixed environment. Image reproduced from [215] with permission. 79

4.2 The tragedy of the commons with public goods. Cheats (gray cells) who do not pay the cost of producing public goods (red circles) can still exploit the benefits of public goods produced by other cells (green cells). This allows for cheats to increase their reproductive rate. Image reproduced from [215] with permission. 80

4.3 An illustration of the process of optimisation before and after the bacterial competition experiment in order to accurately analyse the results. 83

4.4 The optimal duration of the bacterial competition was determined to be 48 hours. The ON2-WT and ON2-Δ*aprX* were prepared as mono-culture and co-culture in casein and casein with proteinase K (digested casein) media without clay and incubated on a slow shaker* at the room temperature with three different incubation times, (a) 24 hours, and (b) 48 hours. Based on the CFU counting results, after 24 hours of incubation, there was still nutrient available in the cultures, suggesting that the incubation time needs to be extended in order to maximise the time for bacterial competition. Also, by comparing CFU counting results at 48 hours time point with (c) 96 hours, the reduction in number of cells after 96 hours incubation suggests that the length of incubation was too prolonged for the cells. Based on these results, 48 hours of incubation will give the cell enough time to grow and compete in casein. 84

*Laboratory shaker: IKA KS 260 basic S002

4.5 The ON2-Δ*aprX* cells in a genotypically mixed bacterial populations within a microaggregate can benefit from the ON2-WT secreted AprX; (a) result of the CFU counting of ON2-WT-CFP-Km^r and ON2-Δ*aprX*-YFP-Sm^r, mono-cultures and co-culture from microaggregates fraction in casein with clay medium after 48 hours of incubation; (b) fluorescence microscopic image of ON2-WT-CFP-Km^r and ON2-Δ*aprX*-YFP-Sm^r co-culture in casein clay medium after 48 hours of incubation. Error bars indicate mean and standard deviation *** p<0.005, ns (not statistically significant) p>0.05. 87

4.6 Experiment optimised to increase genotypic patchiness in microaggregates. In the previous experiment, both strains were added to the clay medium at the same time (a), which caused well-mixed bacterial strains in the microaggregates. However, by growing each bacterial strain in clay media separately (b), microaggregate will be formed with individual bacterial genotypes, and then two monocultures were mixed to prepare a co-culture sample. During this process, bacteria with the same genotype grow in microaggregates and form a high level of genotypic patchiness. Such genotypically patchy bacterial populations are expected in soil microaggregates due to the structure of the soil which limits mixing of bacterial populations and the fact that bacteria are more likely to be attached to soil surfaces rather than being in a planktonic state. 89

4.7 ON2-WT and ON2-Δ*aprX* strains had approximately the same cell density in the start point samples prior to the initiation of bacterial competition. The CFU counting was utilised to determine the number of bacterial cells. The ON2-WT and ON2-Δ*aprX* cells in M63 media with and without clay as the start point samples were placed on the slow shaker alongside other samples at room temperature for 24 hours. The start point samples were treated to be counted, while the rest of the samples were prepared for the bacterial competition. The difference between ON2-WT and ON2-Δ*aprX* in M63 medium without clay was statistically not significant as well as their difference in M63 with clay. Error bars indicate mean and standard deviation. ns: not statistically significant. p>0.05. 90

4.8 Separating the liquid fraction from the microaggregates is necessary to accurately measure the bacterial populations within microaggregates. (a) Upon completing the incubation time on the slow shaker, the microaggregates are suspended in the liquid culture. (b) Microaggregates are allowed sediment to the bottom of the tube after sitting on the bench for 30 minutes. Therefore, (c) the liquid and microaggregate fractions were separated. From one another bacterial populations in the liquid fraction are in the planktonic state and should not be mixed with bacterial populations within microaggregates during the breaking phase. 90

4.9 Breaking soil microaggregates in order to release bacterial cells attached to the clay particles. 92

4.10 Microscopic images of different breaking techniques to break microaggregates. The samples are co-culture of ON2-WT and ON2-Δ*aprX* incubated in clay M63 for 48 hours at room temperature on the slow shaker. Then the supernatant fraction was removed and replaced with sterile PBS before breaking. After each breaking treatment, the samples were allowed to settle for 30 minutes on the bench at room temperature and the supernatant was collected for imaging using fluorescent microscopy with CFP and YFP filters. (a) samples treated by vortexer, (b) by vortexer and water bath sonication and (c) by vortexer, water-bath sonication and 30^G needle. For the purpose of microscopic imaging, ON2-WT was labelled with CFP and ON2-Δ*aprX* was labelled with YFP. Bars are 50 μm. 94

4.11 The effect of a homogeniser on cell viability. Homogeniser method was used to break aggregates and release cells inside microaggregates. The results shown in black are the ON2-WT in M63 clay that is agitated with speed 4 and results in white are agitated with speed 6. The control samples were only vortexed without being agitated by the homogeniser device. 95

4.12 Water-bath sonication was a more effective way to break microaggregates without damaging cells compared to the tip-sonication. The incubation time was 48 hours at room temperature with a shaking speed of 110 rpm. The sample used in this step was ON2-WT with and without presence of clay in M63 medium. In each treatment, a control sample was vortexed for one minute following a 48-hour incubation period. (a) is representing a schematic image of a tip-sonicator that directly sonicate the sample, (b) is the result of CFU counting of samples treated by the tip-sonication, (c) a schematic image of the water-bath sonication that sonicate samples indirectly through water, and (d) represent the CFU counting result of samples after treating by water-bath sonication. After 48 hours of incubation, samples without clay (shown in white) and with clay (shown in grey) were treated by sonication devices. 98

4.13 The SPT buffer did not sufficiently break microaggregates. The co-culture sample was incubated in clay casein medium for 48 hours, the supernatant was removed, and the clay fraction of the sample was mixed with 9 ml of the SPT buffer. The mixture was vortexed and transferred to water-bath sonication (a, b) and one sample (c, d) was treated only with SPT without vortex and sonication treatments and both samples were incubated on the slow shaker at room temperature for 24 hours. After 24 hours of incubation time, samples rested on the bench for 30 minutes until the solid and liquid phase were separated. The supernatants were collected to check the status of microaggregates after SPT treatment under microscope. Image (a) and (c) were taken with a bright-field filter and image (b, d) with YFP and CFP filters. No difference was observed between samples treated only with SPT and samples with vortex, water-bath sonication in SPT. Presence of small microaggregates with a significant number of cells attached to it shows SPT treatment was not an effective method to break and detach bacterial cells from microaggregates. 100

4.14 Using filters to separate cells from aggregates . Filters with smaller pores (5, 11, and 30 μm) were completely blocked by microaggregates. A few cells could find their way however the filtered sample was very transparent suggesting that the majority of the cells stayed with microaggregates. The 40 μm filter was the only filter that the supernatant could pass through but the microscopic images from filtered samples showed they also contained very few cells (data not shown). 102

4.15 In the casein clay medium, different bacterial populations are found within microaggregates. The CFU counting results show the number of bacteria in mono-culture and co-culture in (a) digested casein medium without clay, (b) digested casein medium with clay, (c) casein medium without clay, and (d, e) casein medium with clay. Casein was digested with 5 mg/L of proteinase K and the digested casein was used as the control medium for the two bacterial strains, since both strains were able to grow on the digested casein without the need for AprX. The outcome of the bacterial competition in casein medium sometimes showed that (d) the ON2-WT could grow faster than ON2-Δ*aprX* in casein medium with clay and their difference is significant (p<0.05). However, in biological repeats, the CFU counting result showed that both AprX-producer and non-producer cells grew similarly (e), which suggested that the microaggregate could not be the barrier to protect AprX from diffusing away. Data presented as mean and standard deviation and data are compared using t test *** p<0.005, * p<0.05, ns (not statistically significant) p>0.05.105

4.16 Additional colonies grew after the initial incubation period, resulting in incorrect SP-SDS counting. The samples were prepared for the breaking process (vortex (2 minutes), water-bath sonication (20 minutes) and needle breaking methods (five times)) after the competition was finished. Then bacterial cells were spotted on LB agar with respected antibiotics and incubated at room temperature for 48 hours before counting. (a) the SP-SDS CFU counting result of ON2-WT and ON2-Δ*aprX* in mono-cultures and co-culture in digested casein with clay and (b) in casein medium with clay. The start point samples for this experiment were counted and the result confirmed the similar number of ON2-WT and ON2-Δ*aprX* cells at the beginning of the bacterial competition experiment. If the number of cells in start point samples was unequal, the bacterial experiment was terminated and started with new sample preparation. Data presented as mean and standard deviation and data are compared using *t* test *** $p<0.005$, ns (not statistically significant) $p>0.05$. 108

4.17 Quantification of the number of ON2-WT and ON2-Δ*aprX* cells in co-culture samples in casein medium with clay confirms that ON2-WT cells are doing better in microaggregates. (a) counting repeats of ON2-WT mono-culture sample and ON2-Δ*aprX* cells, (b) counting repeats of co-culture samples that ON2-WT from co-culture was shown in dark grey and ON2-Δ*aprX* cell number in light grey and (c) the average of the CFU counting of the mono-culture and co-culture samples. The CFU counting results belong to mono-cultures and co-culture samples from the same experiment. In the majority of the co-culture repeats, the ON2-WT cells are growing faster than ON2-Δ*aprX* in casein medium with clay which indicates the being inside microaggregate have helped producer cells to have access to the digested casein. Data presented as mean and standard deviation and data are compared using *t* test, ns (not statistically significant) $p>0.05$, **** $p<0.0001$, * $p<0.05$. 111

4.18 Hectorite clay's autofluorescence poses a great challenge to fluorescent microscopy imaging of CFP-labelled bacteria within microaggregates. The fluorescent microscopic image (a) represents a microaggregate with ON2-WT-CFP and ON2-Δ*aprX*-YFP cells after 48 hours of incubation in digested casein. An area containing both bacterial populations in microaggregate is magnified in the region shown by the orange square. The cyan and yellow filters of the merged image were separated in order to observe CFP and YFP-labelled populations separately. In image (a) both clay aggregates and CFP-labelled cells appeared in cyan fluorescent channel but in (b) cells labelled with YFP label are very bright and distinguishable from the background noise. It was later demonstrated that the total number of the CFP-labelled cells is very similar to that of the YFP-labelled cells using CFU counting method. 112

4.19 Significant growth reduction of ON2-Δ*aprX*-YFP in casein clay environment. Mono-cultures of ON2-WT-CFP and ON2-Δ*aprX*-YFP after incubation in clay with digested casein (a,b) and clay with casein (c,d) for 48 hours. The overnight cultures of ON2-WT-CFP and ON2-Δ*aprX*-YFP were inoculated into clay media with OD_{600nm} of 0.01. Digested casein clay is an environment that both ON2-WT-CFP and ON2-Δ*aprX*-YFP can grow in this medium and form microaggregates. However, in the casein clay environment, the ON2-Δ*aprX*-YFP strain unlike ON2-WT-CFP (c) is unable to digest the casein to consume it and grow (d). Size of microaggregates in (d) are smaller compared to (c) and its structure seems to be more fragile as well. . 113

4.20 Well-mixed population of ON2-WT and ON2-Δ*aprX* when they grew in the pre-digested casein with clay medium. Two sets of co-culture were prepared, (a) and (b) ON2-WT-CFP mixed with ON2-Δ*aprX*-YFP and (c) and (d) ON2-WT-YFP was mixed with ON2-Δ*aprX*-CFP. The switching fluorescent labels were done to have a better observation of both bacterial populations in co-culture within microaggregates. Samples are prepared as it explained in Section 4.2.3.1. Bars are 50 μm. 117

4.21 Co-culture of ON2-WT and ON2-Δ*aprX* strains in the casein clay environment after 48 hours of incubation. (a) and (b)are the co-culture samples in which ON2-WT was labeled with CFP and ON2-Δ*aprX* with YFP, and (c) and (d) are images of the co-culture sample that ON2-WT was labelled with YFP and ON2-Δ*aprX* labelled with CFP. In the co-culture sample that ON2-WT was labelled with CFP (a), the microscopic image showed that the CFP-labeled cells were dominant compared to YFP-labeled cells. However, due to the autofluorescence feature of hectorite clay, distinguishing the CFP-labeled bacterial population from clay aggregates is difficult. By switching the fluorescent labels of the bacterial strains in co-culture, the microscopic images (c) revealed that the ON2-WT-YFP is the dominant population compared to ON2-Δ*aprX*-CFP in the casein clay environment. However, from the same samples in which images (a) and (b) were taken, there are microaggregates with well-mixed bacterial strains, ON2-WT and ON2-Δ*aprX*, as shown in image (b) and (d). These results indicated that there are different degrees of bacterial genotypic patchiness within microaggregates. Scale bars show 50 μm. 119

4.22 Microfluidic devices on fluorescent microscopy. Image (a) is showing the setup of an experiment using a microfluidic device, (b) a microfluidic device with linear channels and (c) a microfluidic device with porous channels. 121

4.23 Growth comparison of ON2-WT-CFP and ON2-Δ*aprX*-YFP as co-culture in casein and predigested casein (using proteinase K) media on the surface of the linear chamber of the microfluidic device. (a) result of co-culture growth in casein in different time points (from time 0 hour to 8 hours). (b) co-culture sample in predigested casein after 8 hours of incubation. Results show that the ON2-WT-CFP could grow faster than ON2-Δ*aprX*-YFP in the casein medium flows as the only source of nutrient (a). However, in the predigested casein (b), the ON2-Δ*aprX*-YFP cells grew faster than and formed bigger patches than ON2-WT-CFP. 123

4.24 Microfluidic device with porous chamber used to create a similar environment to soil microaggregates. The growth of ON2-WT-CFP and ON2-Δ*aprX*-YFP in the casein co-culture on the surface of a porous chamber was investigated. Image (a) is the look of the porous chamber before transferring the cells. In image (b) the co-culture samples were transferred in the porous chamber, (c) after 5 hours of incubation in casein and d) is when the co-culture sample in microaggregates was transferred in the porous chamber. ON2-WT was labelled with CFP and ON2-Δ*aprX* labelled with YFP. . . . 125

4.25 The structure of microaggregates depends on its base units, clay particles. Using confocal microscopy, the structure of the microaggregate was investigated. The sample was a mono-culture of ON2-WT-YFP in casein clay medium that was incubated for 48 hours at the slow shaker. Images from (a) to (i) show z-stacks of the microaggregate structure in cyan and the ON2-WT-YFP cells in yellow. The images taken with different z-stacks demonstrated bacterial movement in the microaggregate structure. The microaggregates built with larger clay particles contain larger pores. As a result of the presence of liquid in the clay media, bacterial cells are observed passing into the microaggregates through these pores. So, not all microaggregate structures are similar, and, depending on the pore size within the structure, the efficiency of the microaggregate as a physical barrier may differ. It is this phenomenon that explains the variation in the outcome of the bacterial competition. 127

5.1 The role of an adhesive agent, LapA protein, on microaggregate formation. LapA acts as an adhesive agent on the cell surface of *P. fluorescens*. During periods of stress, (a) high level of inorganic phosphate acts as a signal to activate LapD which suppresses activity of LapG (LapG degrades LapA). Therefore, LapA accumulates on the cell surface and facilitates attachment of cells to other cells or surfaces. When the stress is eliminated, (b) LapD becomes inactive so LapG degrades the LapA protein that leads cells to return to their planktonic state. (c) Brightfield microscopic images of *P. fluorescens* Pf0-1 WT, Pf0-1-Δ*lapG* and Pf0-1-Δ*lapA* after 24 hours of incubation at room temperature with slow shaking speed. 140

5.2 Confocal imaging of a co-culture sample, ON2-WT-CFP and ON2-Δ*aprX*-YFP in digested casein clay using Airy-scan microscopy. Using the spectral demixing feature of Airy-scan microscope, a unique signal from the wavelength of the hectorite clay was identified. This signal was marked with red colour which is easily distinguished from CFP and YFP labelled cells. Imaging the mixture of ON2-WT-CFP and ON2-Δ*aprX*-YFP in digested casein clay. 142

List of Tables

1.1 Impact of some bacterial activities on organic carbon reservoir in soil 4

2.1 Bacterial strains used in this project. 25
2.2 Primers used in this study (relevant restriction sites are underlined). 26
2.3 Ingredients of PCR reaction used to amplify the *aprX* and *inh* genes in ON2-WT and ON2-pd5 strains using Gotaq DNA polymerase. . . 27
2.4 PCR program to amplify the *aprX* and *inh* genes in ON2-WT and ON2-pd5 strains. 27
2.5 PCR reaction to amplify upstream and downstream of the *aprX* gene with EcoRI at each extremity. 30
2.6 PCR programme to amplify EcoRI-Δ*aprX* fragment. 31
2.7 Details of ligation mixture. 31
2.8 PCR mixture to confirm the Δ*aprX* insert in the pGEM®-T plasmid. . 31
2.9 Digestion mixture with EcoRI. 35
2.10 Material for ligation of pEX18Gm and Δ*aprX*. 35
2.11 Bacterial strains and plasmid used in this project. 38

Chapter 1

Introduction

1.1 Introduction

The increasing atmospheric concentration of greenhouse gases, particularly those containing carbon such as CO_2, is a consequence of human activities and is associated with climate change [1]. Land and ocean ecosystems are the major natural carbon sinks that limit the increase of CO_2 in the atmosphere by absorbing and sequestering nearly half of emitted CO_2. The soil carbon pool is approximately 3.1 times larger than the atmospheric pool of 800 GT [2] and only the ocean has a larger carbon pool, at about 38,400 GT of carbon. However, most of the sequestered carbon in the ocean is inorganic forms [3]. Given the magnitude of the exchange of carbon between soil and the atmosphere, and the serious concerns over human disruption of the global carbon cycle, it is essential to understand the stability and turnover of carbon held with soil [4].

The organic carbon stored in the soil, called soil organic carbon (SOC), and it is the largest terrestrial carbon pool (about two times larger than carbon storage in above ground biomass or the atmosphere [5]), which is an important component of the global carbon cycle. In terrestrial carbon cycle, shown in Fig. 1.1, plants and soil microorganisms fix carbon from the atmosphere (CO_2) to organic materials by photosynthesis and carbon fixation respectively [6, 7]. The fixed carbon then returns to the atmosphere by different pathways including bacterial decomposition and respiration of live organisms [8].

However, the increase in anthropogenic emission of greenhouse gases into the atmosphere has been disturbed the balance between CO_2 uptake by ecosystems and CO_2 loss to the atmosphere. accelerated CO_2 and global climate changing are associated with the increase observed in the average global surface temperature of 1°C since the late 19th century, an average increase of 0.08°C/decade [9].

The rising temperature is affecting and will continue to affect ecosystems and living organisms worldwide. When the temperature rises, evaporation is accelerated which results in soil humidity reduction. The combination of high temperature and low soil humidity causes plant productivity to be decreased, which ultimately leads to a decrease in soil organic matter (SOM) [10, 11]. On the other hand, soil microbial activity is enhanced with increasing temperature [12], which results in higher decomposition of SOMs. The high rate of bacterial decomposition leads to a higher respiration and a higher SOC output [13]. A few examples of bacterial activity on storage of SOC are given in Table 1.1.

Furthermore, the survival of all living organisms depends on the reservoir of necessary elements from the Earth [15]. Earth is a closed system with a finite supply of essential elements containing hydrogen (H), oxygen (O), carbon (C), nitrogen (N), etc, of which recycling of these elements is essential to avoid exhaustion [4, 14]. The role of microorganisms is fundamental in breaking down and transforming dead organic material into forms that can be used by other organisms [16, 17]. This is why the microbial enzyme systems involved are so essential as a key component of Earth's biogeochemical cycles [18, 4]. However, studying bacterial contributions to climate change through carbon cycle feedback are far from straightforward and little is known about bacterial interaction and traits in soil and its impact on the soil carbon cycling [19, 20, 21]

Achieving an understanding of bacterial processes has been difficult because (i) they take place at the micro-scale, (ii) the soil conditions in the soil fluctuate spatially and temporally, and (iii) there are a large number of interacting organisms and abiotic parameters. Thanks to advances in molecular tools, the diversity of soil microorganisms and their role in carbon cycling has been revealed to a greater extent.

Bacterial interaction networks are not separable from the soil carbon cycle and they often face competition for mainly limited resources and space in the soil environments [28]. Within the scope of this thesis, "interactions" will be defined as any process that has the potential to positively or negatively impact the survival or reproduction of microorganisms.

Several studies indicated that the outcome of bacterial competition, which determines the dominant bacterial population, changes the structure of the bacterial community in soil, which can have a profound effect on the process of carbon cycling in soil [29, 30]. For instance, changes in bacterial diversity frequently correlate with changes in their metabolisms and respiration rate [31]. Therefore, the bacterial population that survived and became dominant has an important impact on carbon turnover rate in soil [32]. Bacteria produce and secrete extracellular

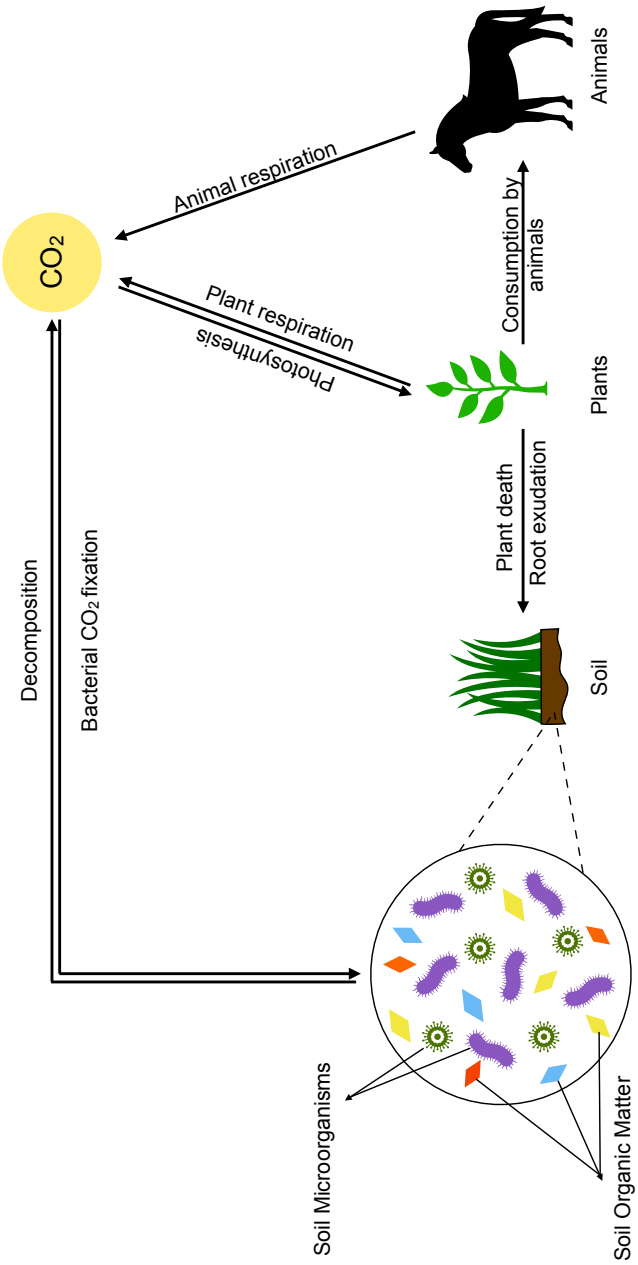

Figure 1.1: Terrestrial carbon cycle with major processes that are mediated by soil microorganisms. Organic carbon in soil results from the interactions of several ecosystem processes, photosynthesis, respiration, and decomposition and the role of soil microorganisms is crucial in the carbon cycling process [14]. This process is composed of soil microbes including bacteria and fungi, decaying material from once-living organisms such as plants (fixation of atmospheric CO_2 into the plant biomass as the result of photosynthesis) and animal tissues, fecal material, and products formed from their decomposition [1].

Table 1.1: Impact of some bacterial activities on organic carbon reservoir in soil

Type of behaviour	Effect on SOC storage	Potential mechanisms
Toxin production [22]	$\pm$	Bacterial growth inhibition might increase the level of SOC (from bacterial decomposition).
Cross-feeding [23] or syntrophy [24]	$-$	Facilitates SOM degradation in anoxic environments which increases the rate of SOC degradation.
Siderophore cheating [25]	$\pm$	May increase or decrease SOC degradation depending on the relative metabolic costs of siderophore production and growth rates of the cheater and producer.
Bacterial sporulation [26]	$+$	Reduction of degradation of soil organic matter including SOC by lowering total enzyme production.
Biofilm formation [27]	$\pm$	High carbon allocation to EPS and humic substances increase storage though associated production costs may cause greater CO_2 flux.

enzymes to have access to the nutrients they need to grow. Generally, the secreted enzymes are not exclusive to the cells secreting them. Local cell neighbours can also benefit from these enzymes and their products, resulting in developing a competition between the cells secreting the enzyme and their neighbours. Consequently, the availability of extracellular enzymes and their products plays an important role in the survival of bacteria in soil, and subsequently, the community of bacteria [33]. The nature of bacterial interaction in soil is influenced by soil structure and its surrounding environment. The aggregate-based structure of soil is defined as complex and spatially highly heterogeneous, which influences biotic, physical and chemical aspects of the soil [34]. Therefore, this thesis discusses how soil microaggregate spatial structure may influence interactions between bacteria.

1.1.1 Research question and challenges

The bacteria within a community can experience both interspecies and or intraspecies competition for limited resources and space in soil environments [35]. For instance, they can benefit from the production of enzymes, which can allow them to access nutrients derived from non-labile compounds by digesting it to a labile form. However, this strategy requires a considerable investment in enzyme

synthesis and excretion [36].

Extracellular products, secreted by bacteria that are not exclusive to only the producer cell, for example molecules to scavenge iron or digest proteins, belong to a class of chemical compounds called "*public goods*" [37]. The production of these soluble, nutrient-rich products is costly for the producing cell and the cost-to-benefit ratio must be sufficiently directed to the producing cells to remain evolutionary stable [38, 39, 40].

In an environment with a high diffusion rate, like in liquid, the risk of exploitation of public goods by non-producer neighbour cells is higher. As it will be discussed in Section 1.3, there have been extensive studies on the evolutionary stability of public good in homogeneous environments and spatially heterogeneous environments like biofilms. In short, as the rate of secreted public good dispersal is increased in liquid environments, the risk of its consumption by other cells "cheaters" will increase. In this case the competitive ability of the producing cells declined due to exploitation of its product by cheaters which causes high cost-to-benefit for the producing cells [41].

However, in case of the environments with spatial structure, such as aggregates and biofilms, the diffusion rate is lower (more disturbed) compared to liquid cultures and even the producing cells and non-producing cells can be physically separated which lead in transformation of the public good to *"private good"*. Consequently, the nature of bacterial interaction in an aggregate-based structure like soil with an extremely diverse microbial community, inter-connected in a complex web of trophic interactions [42, 43], can be completely different than in a liquid-based environment.

Previous modelling studies have suggested that limited enzyme diffusion and presence of a heterogeneous spatial structure in bacterial culture, promote coexistence strategies of producing bacteria and non-producing bacteria. However, studying bacterial interaction in soil is a difficult task and experimental study to investigate bacterial competition in soil at micro-scale is rare. Therefore, developing an experimental model is essential to study bacterial competition in soil where the soil content is simplified to only clay, which represent the smallest fraction of soil aggregates i.e., microaggregates (details regarding soil aggregates will be explained in Section 1.2), and the greatly diverse bacterial population is reduced to considered model microorganisms.

The aim of the present study is to contribute to a more comprehensive understanding of bacterial competition in soil microaggregates using molecular and microscopic approaches. Our objectives are as follows:

- Development and characterisation of a mutant strain for bacterial competi-

tion (Chapter 2).

- Development of a laboratory model of microaggregate (Chapter 3).
- Development of bacterial competition in soil microaggregates and characterisation and quantification of bacterial population after completing bacterial competition in microaggregates (Chapter 4).

The rest of this chapter is as follows. First, the structure of soil is introduced and discussed in Section 1.2. Then, an introduction to the evolutionary stability of public good will be given in Section 1.3. Furthermore, the bacterial competition in homogeneous and heterogeneous environments will be explained in Section 1.4.

1.2 Soil structure

Soil structure refers to the three-dimensional arrangement of organic and mineral complexes (aggregates) and pore spaces within and between aggregates [44]. This parameter is often indirectly quantified as the size distribution of aggregates or the stability of aggregates exposed to standardised disintegrating forces [34, 44]). Soil aggregates are classified into two main size fractions, microaggregate (< 250 μm) and macroaggregate (> 250 μm diameter). The different types of soil structure which occur on different size scales are placed in a hierarchical order.

Soil structure is also a key factor in its functioning, its ability to support plant and animal life, and soil carbon sequestration. The basic components of soil are minerals, organic matter, water and air. The typical soil consists of approximately 45% minerals, 5% organic matter, 20-30% water, and 20%-30% air. The minerals including sand (63 μm to 200 μm), silt (2 μm to 63 μm) and clay (0.1 μm to 2 μm), which consequently determine the three-dimensional geometric structure of the soil. The combination of these mineral particles and SOM, make primary soil aggregates, which is the base of the soil structure [45]. Between and within the aggregate structure, there are spaces called pores that can be found filled with air or liquid [46]. Aggregates and pores are distinct features of soil, which have an important role in carbon storage in soil.

Aggregates

Soil aggregates are the major physical properties of soil which can help protect organic matter from biodegradation [48]. They have a key role in regulating soil organic matter dynamics including carbon cycling [49]. The physical structure of aggregates protects soil microbial communities against its predators. Also, the physical properties of aggregates affect the soil water flow [50], which can cause

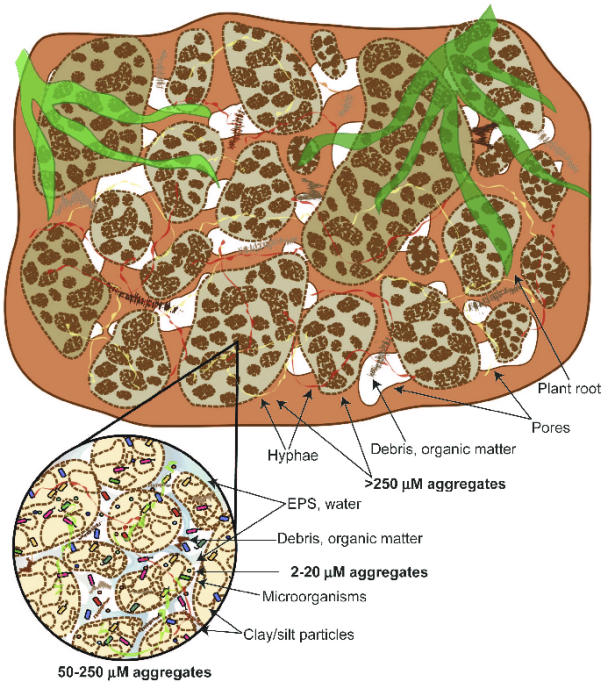

Figure 1.2: The hierarchical model of soil aggregate classification. Larger macroaggregates are composed of hyphae, plant roots, microaggregates, and small microaggregates. This image is adapted from Costa et al., 2018 [47]

changes in connectivity of aggregates which have a profound effect on the bacterial communities and their dispersal of the biochemical properties. In the wet condition, the intra-aggregate communities can be connected and transport their biochemical materials from one another and act like "bacterial villages" (shown in Fig. 1.3 right) [51]. On the other hand, in dry conditions, the bacterial community within aggregates are isolated from outside (shown in Fig. 1.3 left). The mineral particles that are the base unit of the aggregates, have the ability of nutrient sorption and desorption [52] and based on their chemical properties, the adsorption rate in soil fractions are different. The physical and chemical properties of aggregates also control microbial community structure [53] which directly determine quality and function of the soil. Hence, the stability of soil aggregates plays a crucial role in soil structural quality which affects many physical and biogeochemical processes in the terrestrial ecosystems [54].

Furthermore, the diffusion of gases and solutes in soils which determine the quality of soil, depends on pore size and pore connectivity in the soil. Consequently, effective diffusivity is directly related to porosity of the soil aggregates that will be explained in detail below.

Pores

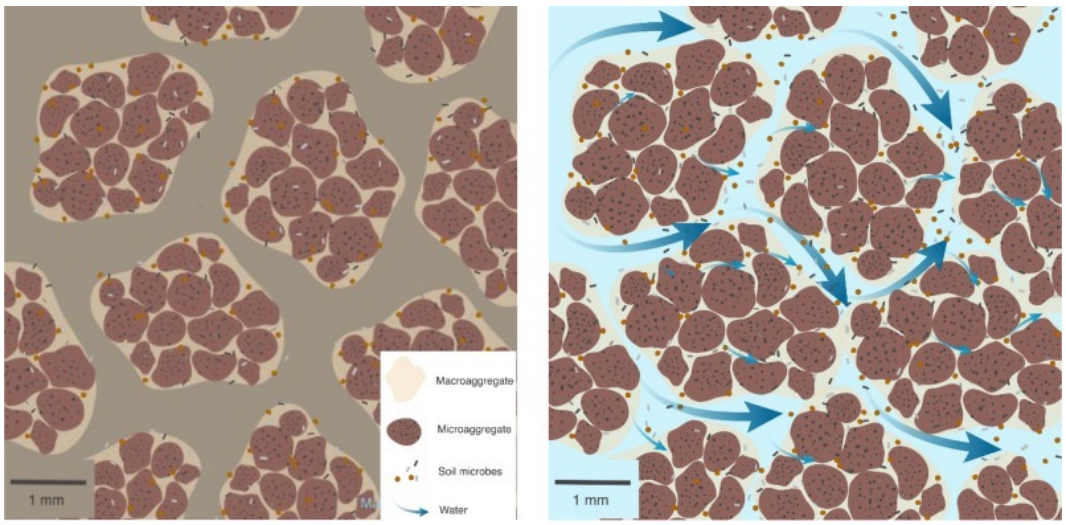

Figure 1.3: Conceptual drawing of isolated soil aggregates during dry condition (left), and wet condition (right). Wet conditions allow for the transfer of nutrients, bacteria, virus and metabolites between soil aggregates. Images are adapted from Wilpiszeski et al., 2019 [51].

Pore spaces range from 10 to 30μm in inter-aggregate pore spaces (i.e., between neighbouring aggregates) to 1 to 2 μm within intra-aggregate pores, illustrated in Fig. 1.4. Pores provide connectivity within microhabitat as they enable the flow of water, nutrients and the diffusion of gases to sustain microbial activity. The pore system also enables the connection of spatially separated bacterial microcolonies, allowing interactions to occur. However, the flow movement is restricted due to the variation in porosity within different types of soils and the not total soil volume is composed of pores [55].

The creation of pores in soil depends on many factors but earthworms are known to be responsible for modifying the porosity of soil [56]. Earthworms burrow through soil and by creating pathways for aeration and water flow, they play an important role in increasing the porosity of the soil and soil structure [57, 58]. Pore distribution in soil varies as some of them exist between soil aggregates and others are located within aggregates, and they are mainly filled with water and air [59]. These spaces serve as a biological habitat for a wide variety of microorganisms, which collectively play a major role in global biogeochemical cycling [60].

Based on the size of the pores, they are classified as macropores and micropores. The macropores are large soil pores, usually between aggregates, that are generally greater than 0.08 mm in diameter and drain freely by gravity which allow easy movement of water and air. They provide habitat for soil organisms and plant roots can grow into them. It is estimated each gram of soil, hosts between

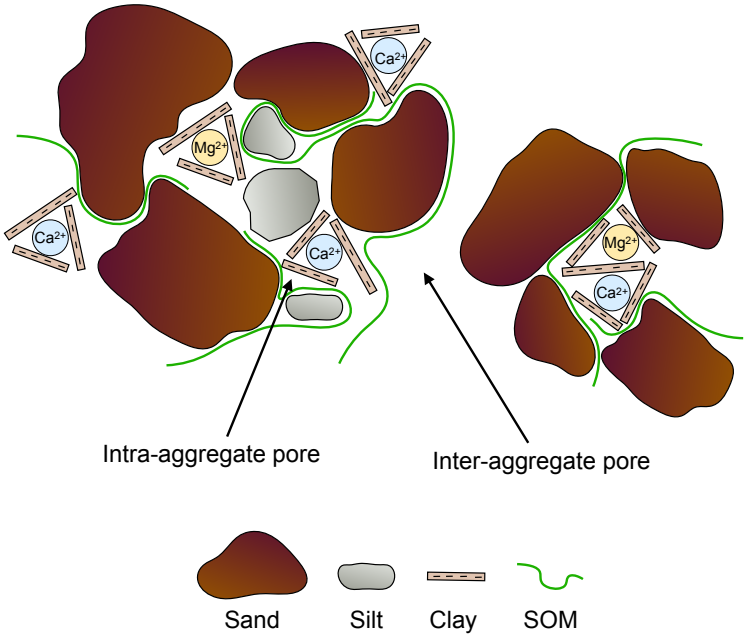

Figure 1.4: Illustration of inter-aggregate and intra-aggregate pores. Image is reproduced from [61].

$\times 10^2$ to $\times 10^6$ number of bacterial phylotypes with highest bacterial diversity compared to other ecosystems [62, 63, 64, 65, 66] that require soil organic matter (SOM) as a source of food. With diameters less than 0.08 mm, micropores are the small soil pores usually found within the structure of microaggregates. About 95%-99% of the SOM can be found in micropores with maximum access restriction for soil microorganisms [67] which makes this soil fraction remarkably important in carbon cycling. By storing carbons in nanopores, microaggregates can possibly protect SOC from decomposition by soil microorganisms and potentially reduce the rate of climate changing.

SOC highly influences the stability of aggregates [68] and it is a major regulator of the soil microbial diversity in the soil [69]. Bacteria synthesis enzymes that facilitate degradation of soil-binding organic materials. However, this process requires availability of SOC, as an energy source, for bacteria. The concentration of SOC and its stability varies in different size aggregates [70, 71, 72]. For instance, the smaller size of aggregates, microaggregate, are less susceptible to change than larger aggregates, macroaggregates [73]. Previous studies confirmed that microaggregates have great capacity to protect carbon sequestration in the soil [74, 75] which also can suggest that it might be a suitable environment for bacteria to grow. Following the size and structure of aggregates will be introduced in detail.

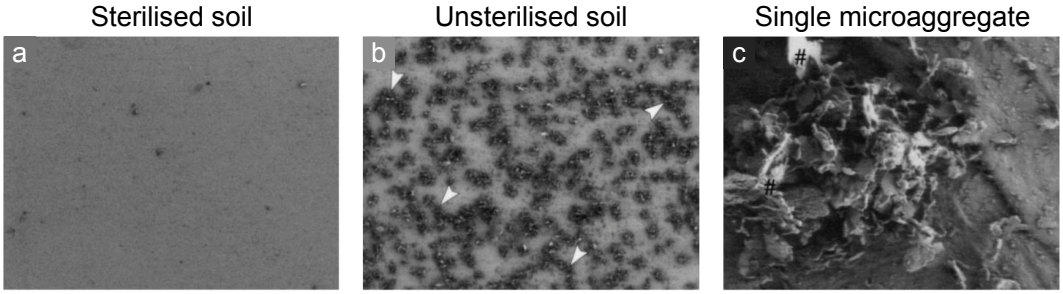

Figure 1.5: Comparison of clay aggregates in sterilised soil and unsterilised soil using scanning electron microscopy. Due to lack of the bacteria in sterilised soil, only a few clay aggregates are present (a). However in unsterilised soil, high quantities of clay aggregates are observed (b), the white arrows pointing dense layers of microaggregates. Image (c) shows a detailed view of a microaggregate and its surfaces of minerals. The # signs in the image (c) show the mineral leaflets of the microaggregate. Images are adapted from Lunsdorf et al., 2000 [76].

1.2.1 Size and structure of aggregates

Aggregate size classes were shown to have a significant impact on soil properties, affecting both carbon retention and the bacterial community composition of the soil. The size of aggregates is a key determinant of soil structure and have an important role in storage of SOM including SOC. Based on the stability of the soils against ultrasonic excitation, soil is built of macroaggregates and microaggregates, with macroaggregates being the consequence of weakly associated microaggregates [77]. Based on the size of microaggregate, the active biological population in this fraction of soil is mainly bacteria.

In general soil aggregates are broken down into two categories, macroaggregates and microaggregates and microaggregates ($< 250\mu$m) as illustrated in Fig. 1.2. Macroaggregates are more transient than microaggregates – because of their organic-binding agents, roots and hyphae – and are more rapidly degradable than the older humified material. These characteristics make the mineral-organic complexes bind the microaggregates.

- Macroaggregates

  Macroaggregates with size of (250μm to 2mm) are a collection of sand, silt and clay particles, microaggregates, and organic matter [78]. The content of

macroaggregates is very diverse, containing a broad range of minerals, organic matter, and biotic materials that are bound together by various physical, chemical and biological processes. The accumulation of SOM inside the microaggregate makes this fraction important in soil structure. However, organic matter in this fraction of soil is more transient than microaggregates meaning that the organic-binding agents are more rapidly degradable. Therefore, the structure of the macroaggregates is constantly transitioning and is less stable. Due to this characteristic of macroaggregate, SOM accumulation that is considerably high in this fraction, faces decomposition by microbial process or oxidisation due to exposure to oxygen. Macroaggregates are formed when fresh plant residue is decomposed by fungi and bacteria [79]. Fungal hyphae and bacterial extracellular polysaccharides serve as nucleation cores to accrete larger masses of slightly decomposed SOM that become macroaggregates. These macroaggregates are constantly weathering in the soil to produce more microaggregates within SOM that are inaccessible to microbial decomposition [80]. The organic matter in this fraction of soil is more transient than microaggregates meaning that the organic-binding agents are more rapidly degradable. The macroaggregates are composed of diverse mineral, organic and biotic materials.

- Microaggregates:

  The size of microaggregates is in the range of 20μm to 250μm and they are known to be the most robust and stable fraction in soil [88]. The primary structure of microaggregates are formed by a combination of clay particles and SOM and then gradually develop by attaching these primary structures together through biological processes [89, 90]. Microorganisms contribute actively to the stability of microaggregates [91, 92, 93] and without their secreted substrates, the structure of microaggregates is more fragile (as it is shown in Fig. 1.5).

  Based on the physio-chemical properties of the clay, it is classified in different groups. Clay is primarily composed of a combination of alumina and silica sheets whose microscale configuration defines the particle size, chemical composition, surface charge properties, cation exchange capacity and water retention properties of clay [94]. The principal clay minerals found in soils can be classified as illite, kaolinite and montmorillonite (smectite) (as shown in Fig. 1.6). There are different types of clay in nature and depending on clay, the formation of microaggregate can differ. The versatile nature of clay is attributed to the presence of clay minerals, which impart significant

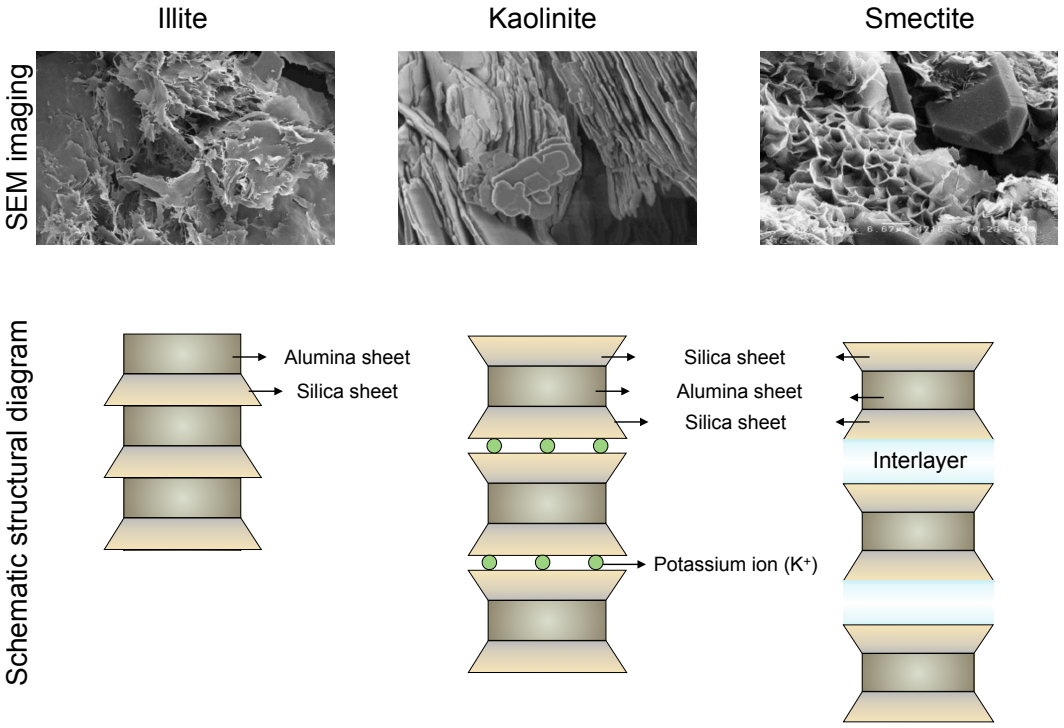

Figure 1.6: Clay is categorised in different types based on its physicochemical properties. Shown here are three main groups of clay called illite, smectite and kaolinite, which each have a different chemical properties and microstructure [81, 82, 83, 84]. The SEM microscopic images of illite, kaolinite and smectite clay particles are adapted from [85], [81] and [86] respectively. The schematic structural diagrams of different types of clay are adapted from [87].

physical properties to the raw materials, such as particle size and shape, ion exchange, hydration and swelling, plasticity, rheological properties, colour properties and reactions with organic and inorganic compounds.

In general, the surface of a clay particle is negatively charged and the edges are positively charged, which allows organic and mineral particles to adhere together to form micro-structured clay particles [95, 96]. This unique property allows clay to attach to various surfaces with different charges. As it is illustrated in Fig. 1.7, the positively charged particles attach on the surface of the clay particle and at the edge of the clay particle, the negatively charged particles can adhere. These compound particles then act as composite building units and include the so-called 'organo-mineral associations' [97, 98, 99], nano-sized, organo-mineral composites as part of the 'presumed building blocks' [100] or 'mineral-organic associations' [101]. Some types of clay are suitable for bacteria to grow and some have opposite features. In this project, the considered clay is from smectite clay that is well-known in studying soil microbial communities which allow to study bacterial interaction within microaggregates.

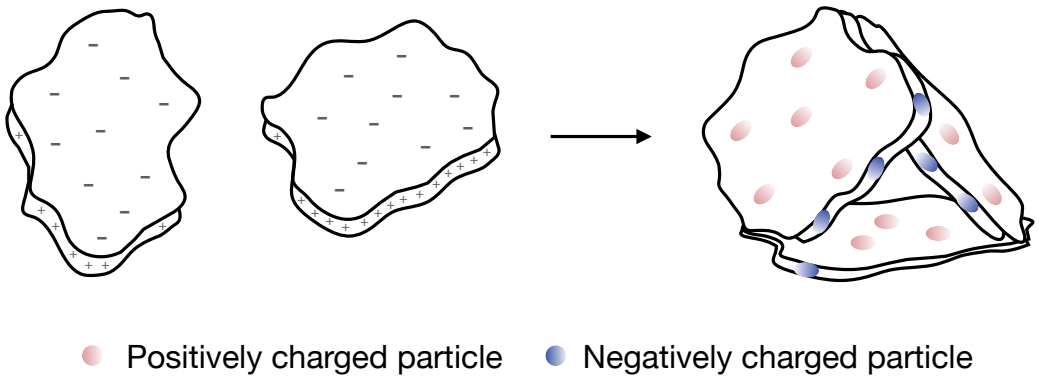

Figure 1.7: The face and edge of the clay particles contain negative and positive electric charges respectively that facilitate their attachment to particles, chemicals, and each other. The positively charged particles thus often attach on the face and negatively charged particles often attach to the edge of the clay particles. This property of the clay has a direct relation with the pH of the environment.

This fraction of soil is known to be the most stable fraction with robust structure. It has been generally recognised that micro-scale heterogeneity in soil environments can have a substantial effect on many soil physical, chemical, and biological processes driving physical protection of SOM [102]. However, the knowledge of micro-scale soil fraction is still in infancy.

Microaggregates consist primarily of mineral, organic, and biological soil com-

ponents that act as building units, adhesives, and cements; and described as a three-dimensional, microporous, and chemically heterogeneous structure [103].

Microorganisms contribute actively to the stability of microaggregates [104]. Living microorganisms can adhere to soil minerals by forming direct electrostatic bonds [105]. The microbial cell walls involved in these bonds are frequently stable against biotic decomposition and many of them persist after the death of the bacterium [106]. Microbial products and their interactions with soil particles, such as clay minerals, promote the crosslink between individual building units, particularly in microaggregates < 20 μm [107]. Of particular importance for the formation and stabilization of microaggregates are the gel-like, water-rich macro molecular organic mixtures, namely extracellular polymeric substances (EPS) [108].

Soil microorganisms use EPS for cell attachment to mineral surfaces and the adsorption of EPS to mineral surfaces fosters the aggregation of mineral particles [47]. Such mechanisms with the help of high microbial activity are shown to be of particular importance in the formation of microaggregates. The comparison between microaggregates in sterilised and unsterilised soil (shown in Fig. 1.5(a) and (b), respectively) indicates the importance of bacterial activities in forming microaggregates. The addition of OM to soils stimulates microaggregate formation by enhancing microbial activity and hence the production of EPS, which aids binding of soil particles [109, 110, 103].

1.3 Stability of public good production

The breakdown of organic matter is a fundamental biogeochemical process in soil that is mostly regulated by microbial activities. Bacteria secrete extracellular enzymes to speed up biochemical reactions which help them to adapt to their environment and grow [111]. The extracellular enzymes produced by bacteria break down soil organic matter compounds into smaller molecules that can be taken up and metabolised by bacteria [112, 113]. Therefore, a major part in the nutrient and carbon cycle process relies on bacterial extracellular enzymes.

It is true that bacteria can benefit from enzyme production by gaining access to energy and nutrients found in complex compounds, but the process of enzyme synthesis and excretion also requires a substantial resource investment [114]. It is estimated that enzyme production consumes between 1% - 5% of the energy in enzyme producing bacterial cell [115, 116], which requires a large amount of labile nutrients like carbon and nitrogen, in order to compensate for the energy loss [30].

The production of enzymes is regulated by its producer cell; however, once the enzyme is secreted, it becomes available to its local neighbour cells and the

producer has no control over how it will be consumed [117]. As long as the producing cell is able to metabolise its own product, the cost to benefit ratio of enzyme production will be sufficient to allow the cell to continue to grow and produce enzymes [118].

However, in natural habitats where bacteria live in communities, it is more likely that the neighbouring cells will also be able to take advantage of the secreted enzyme and its byproduct without bearing the cost of its production [119, 120, 121]. The product of extracellular enzymes provide essential nutrients for bacterial growth which include carbon, nitrogen, phosphorus, etc, [122, 123, 124, 125]. Since the concentration of these nutrients differs between environments, bacteria have to compete to have access to these limited resources.

Consequently, non-producing cells, also known as "cheaters", will grow faster as a result of having access to the free nutrients, and as they grow faster, they require more nutrients. This will result in cheaters exploiting the public good secreted from producers. Based on this scenario, the natural selection should favor the cheaters variants that by avoiding the cost of enzyme production, they increased their individual fitness compared to the producers by exploiting the public goods [126]. Therefore, the producers need a strategy to keep their secretions for their benefit in order to remain evolutionary stable.

In the following, the bacterial competition in different environments will be addressed and the outcome of bacterial competition in these environments will be discussed.

1.4 Bacterial competition

Most natural environments harbor a stunningly diverse collection of bacterial species which are in constant competition mainly over nutrients and spaces [28]. Previous studies reported that in an environment with high nutrient resources, microbial groups grow faster and continue to expand as a mixed group. On the other hand, low nutrient abundance leads to high selection for bacterial competition [127]. Bacterial competition can be classified in two main ways: a) direct way in which bacterial cells damage one another through their defence mechanisms, b) indirect way where bacteria compete through resource consumption (also known as exploitative competition) [37].

In exploitative competition, which is the subject of this project, one strain (producer) produces enzyme (also known as "public good") that can break down nonlabile nutrient to a digested form while the other non-producer strain ("cheater") consumes the limited resource produced by the producer strain, and restricts the

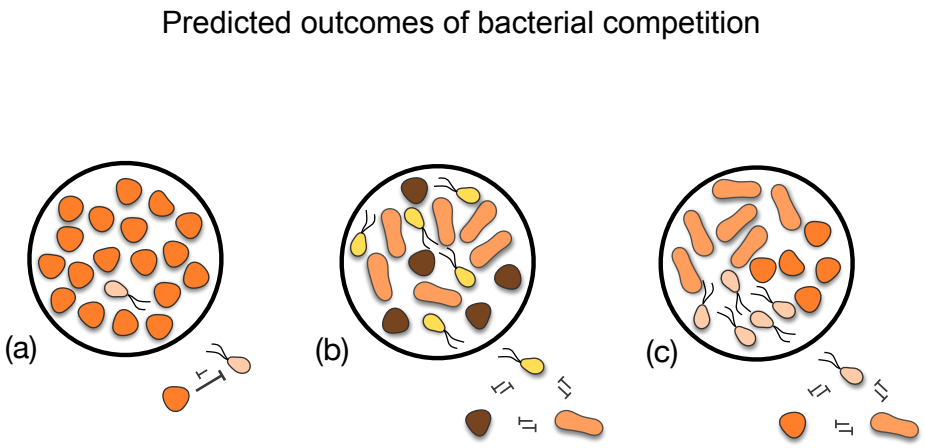

Figure 1.8: An illustration of possible outcomes of the bacterial competition. a) competition exclusion when the less competitive strains go extinct while others dominate the community, b) coexistence of the strains by consuming different resource types, c) coexistence of competitors through spatial separation. The image was adapted from Ghoul et al. 2016 [37].

supply to its competitor. Therefore, the cheater strain can outcompete the producer strain by consuming the public good secreted from the producer strain without paying the cost of its production. However, there are a number of mechanisms by which public goods can be transformed into private goods in microbial communities. This selective mechanism widely depends on the cooperative system [128] and the producers can only remain evolutionary stable against exploitation if the cost-to-benefit ratio of public good production is sufficient for them to grow [40, 39, 38]. Three ecologically stable outcomes regarding the bacterial competition are predicted and experimentally accepted as follows: i) less competitive strain will be distinct by the more competitive strain (shown in Fig. 1.8(a)), ii) both strains coexist by consuming different sources of nutrients than each other (shown in Fig. 1.8(b)) and iii) both strains coexist due to being separated in two different spatial structures (as shown in Fig. 1.8(c)).

A bacterial competition can be affected by many factors including nutrient availability [127], growth rate and motility of the bacterial species [28] and spatial structure of the environment [129]. Previous studies reported that in an environment with high nutrient resources, bacteria groups remain well mixed and continue to expand as a mixed group with high genetic diversity. In this case, natural selection is no longer expected for higher fitness of the bacterial groups as each genotype is benefiting from the nutrients and has its own evolutionary interests [127]. However, when nutrients are limited, the bacterial growth will be affected and most cell division will be prevented. This condition causes population bottlenecks as the natural selection is required to increase the group fitness and consequently reduce the genetic diversity [130, 131].

In a low nutrient environment, bacteria attached on a surface grow as clonal patches with genetically identical cells which allows them to exchange growth-promoting secretions and also segregates them from other genetically different strains [38, 132]. The creation of clonal patches is crucial for evolutionary adaptation of bacteria, especially when they are under stress. The bacterial genotypic patchiness can be determined by many factors but previous studies confirmed that one of important factors is when nutrients are limited in bacterial culture [127]. For instance, when two bacterial strains are in an environment where their access to digested nutrients is limited by an enzyme produced by one of the strains, the competitive behaviour can be generated between two strains. The non-producing cells can consume the digested nutrients without paying the cost of producing the enzyme, which leads to outcompeting the producer strain by exploiting their secreted enzyme. By genotypic patchiness, the producing cells will be spatially segregated from the non-producing cells which will limit cross-feeding, favoring

producer strains over non-producer strains. However, the impact of spatial segregation on bacterial competition can vary in different environments [128].

Previous studies showed that change in the frequency of bacterial strains can affect the outcome of bacterial competition [133]. Initial proportion of cells in a competitive environment is very important to determine the outcome of the competition. In a competitive environment, when the producer strain is in minority, it outcompetes the non-producer strain. Also, when the non-producer strain is initiated at low frequency, it will be surrounded by the plenty of digested nutrients provided by the producers that allow them to grow and become more abundant. When the non-producers become more abundant, the total enzyme production becomes low, which leads them to become the victim of their own success. Therefore, this regime of negative frequency-dependent selection gives cells with low initial start point a competitive advantage. Such frequency-dependent selection can maintain coexistence of cooperators and cheaters even in unstructured habitats [134]. Nevertheless, in aggregate-based habitats like soil, coexistence of different social strategies are predicted to be more stable since cheaters can only exploit local cooperators [135]. The interaction between enzyme production and the physical properties of soil is expected to crucially affect cheating strategies in soil and thereby ecosystem functioning [136].

Another factor affected by the spatial structured environment is fluid flow. The bacterial competition is often affected by the fluid flow in the environment as it can move bacteria, bacterial secretions and the soluble nutrients digested by the enzymes [137]. Therefore, secretion of the producer strains can be diffused away in a liquid culture with flow which leads to lower concentration of digested nutrients for the producer cells, as illustrated in Fig. 1.9(a). The dispersion in a homogeneous environment allows the non-producer strain to gain access to the digested nutrients without incurring the cost of enzyme production, which is unfavorable to the producer cells and can result in the exploitation of the producer strain by growing faster in the co-culture [138]. Nevertheless, a spatially heterogeneous environment tends to attenuate the fluid flow that supplies bacterial cells with nutrients and facilitates their dispersal [139].

In general, any environment that is not uniformly mixed is considered a heterogeneous environment. Previous studies uncovered that the presence of a spatial structure in the microbial environment can affect the outcome of the competition [119, 140, 37]. However, most of the studies on bacterial competition has been performed in liquid cultures, which eliminate the effect of spatial structure which is included in majority of microbial environments [141] and play a key role in bacterial interaction [142, 130]. Mathematical models and some laboratory experiments

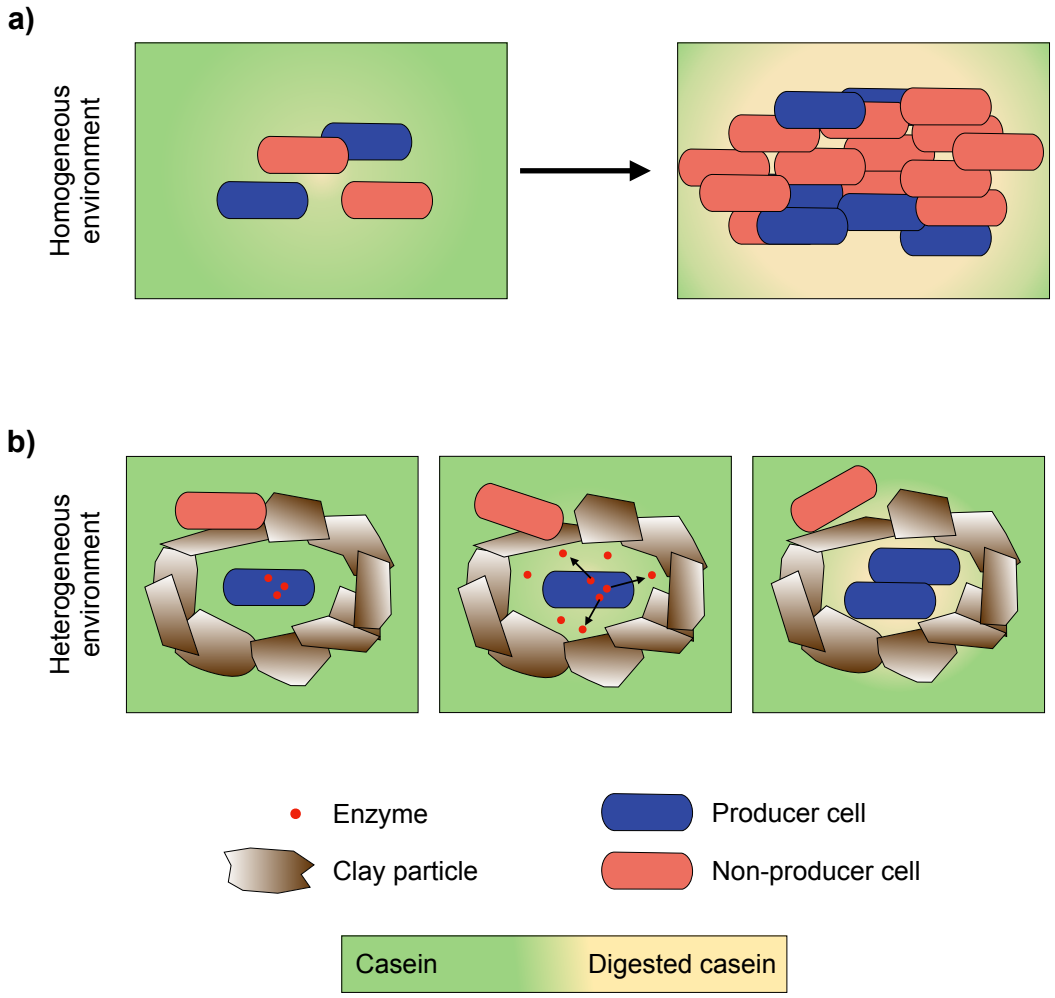

Figure 1.9: An illustration of cells in homogeneous and heterogeneous environments: a) in the homogeneous environment (such as shaken liquid culture), the secreted enzyme diffuses away from the producer and the product of the enzyme (digested casein in this case) can be consumed by neighbouring cells without paying the cost of enzyme production ("non-producer" cells). Therefore, the non-producer cells will grow faster than the producer cells, resulting in the non-producers outcompeting the producers. b) on the other hand, in heterogeneous environment (such as soil microaggregates in this case) the secreted enzyme will stay close to its producer cell due to the physical barrier conformed by the microaggregates such that the product is preferentially accessible to the producer cells.

suggested that spatial heterogeneity and capability of microbial populations to disperse over their habitat can lead to significant changes in sharing a common habitat whether secreted enzymes will be public or remain private [129, 132].

The spatial segregation will increase the distance between two strains, which leads to enzyme protection for the producer strain against non-producer [133]. In this study the spatial segregation was caused by thick biofilm formation but it can be extended to a broad range of heterogeneous environments. This phenomena was predicted in a mathematical model, developed in 1998, suggesting that microbial foraging by secreted enzymes would be beneficial for bacteria in an enclosed structure, while the production of extracellular enzymes in homogeneous environments may be a waste of resources [143]. The aggregate-based environment like soil is a good example of a heterogeneous environment where bacteria need to adopt a strategy to protect their enzyme from exploitation and growth [144]. Previous studies have proposed that the spatial structure of the soil encourages coexistence of the soil bacterial communities [145, 146]. Vetter et al. predicted that in an enclosed environment like soil aggregates, the concentration of bacterial secretions that might return to the producing bacterium is higher, while the production of extracellular enzymes in homogeneous environments may be a waste of resources [143].

Soil microaggregates with heterogeneous structure provide a unique spatial structure for bacteria to be surrounded by clay particles [147]. Figure 1.10, shows the early stage of a microaggregate, which consists of clay particles or stacks of leaflets that form an enclosed structure surrounding a bacterium cell (marked with a green circle). This structure can provide a physical barrier that the inside bacterial cell can be isolated from the outside environment. Moreover, previous research studies confirmed that clay particles enhance the biofilm formation of bacteria [148], which might be due to higher possibility of bacterial attachment to the clay surfaces when they are within microaggregates.

Therefore, we hypothesised that the biogeochemical feature of soil microaggregates can provide an environment where the producer cells within microaggregates can gain a competitive advantage over non-producer. A schematic image of this scenario is illustrated in Fig. 1.9(b), showing a producer cell (in blue) within a microaggregate structure in a growth medium (such as casein) for which bacteria require enzymes (red circles) to digest the nutrients. Due to the lower diffusion rate within the microaggregate structure and physical barrier of microaggregates, it is predicted that the secreted enzyme will be within a distance that is accessible to its producer, therefore resulting in a higher digested casein concentration accessible for the producer strain.

This thesis aims to investigate the impact of the spatial structure of the microaggregates on the bacterial competition and the structure of the bacterial community in the soil. The remainder of this thesis is structured as follows: Chapter 2 describes the development and characterisation of a mutant strain for bacterial competition. In Chapter 3, a laboratory model of microaggregates is developed and optimised. The design of the bacterial competition in microaggregates is addressed in chapter 4 as well as various methods employed to characterise and quantify the outcome of bacterial competition in microaggregates. Finally, in Chapter 5, a summary of the research findings of this thesis and several directions for further research in this topic are provided.

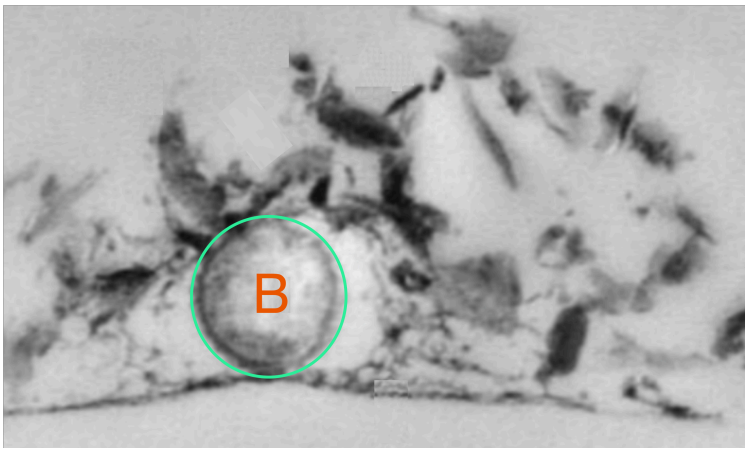

Figure 1.10: An example of a clay aggregate inhabited by a bacterium (marked by a green circle and shown with orange B). The image was taken by TEM microscopy [147].

Chapter 2

Development and characterisation of a strain of *P. fluorescens* that lacks the ability to produce the protease AprX

2.1 Introduction

Pseudomonas fluorescens is a soil bacterium that is known for its versatile metabolism [149]. Since 1950, *P. fluorescens* has attracted scientists' attention due to its significance in soil, agriculture, and the food industry [150]. While soil contains a wide variety of different nutrient sources, most of these are in non-labile form that cannot immediately be utilised by bacteria [112, 113]. Plants and animals are the major source of organic matter to the soil in which bacteria cannot decompose this form of complex organic material without secreting their extracellular enzymes [151]. In this process, the secreted extracellular enzymes break down the non-labile nutrients into more simple forms, such as amino acids and carbohydrates which allow them to grow on it [152]. *P. fluorescens* can produce and secrete a vast number of extracellular enzymes and proteins which allows this bacterium flexible to live in different environments such as soil, plants, fresh water and even in milk and dairy products [153, 154].

One of the proteases secreted by *P. fluorescens* is called AprX which is an alkaline metalloprotease and it is known to be for milk spoilage by digesting the main protein in milk, casein. Casein consists of four subunits, α_{S1}-, α_{S2}-, β- and κ-casein [155, 156]. The subunits are attached together by a strong electrostatic interaction and form molecular aggregates called micelles [157], as shown in Fig. 2.1. The first

biochemical and genetic characterisation of the AprX was published in 1998 [158] and found this caseinolytic metalloprotease was the key extracellular enzyme that allows *P. fluorescens* to grow in casein-based environments [41].

P. fluorescens ON2 is a well-characterised soil bacterium [159] and ON2-pd5 is a transposon-based mutant strain derived from this background. Due to the non-proteolytic phenotype of ON2-pd5, ON2-WT and ON2-pd5 strains have been extensively studied in projects focusing on bacterial competition and interaction [160, 41, 161]. In previous studies, casein has been used as a recalcitrant nutrient in the growth medium that *P. fluorescens* ON2 cells must secrete the AprX enzyme to digest casein in order to grow. For this project, the two *P. fluorescens* ON2 strains, AprX producer and AprX non-producer, were selected as bacterial candidates for bacterial competition and casein and predigested casein (using proteinase K) media were chosen as competitive and control environments, respectively. In order to study the effect of microaggregates on bacterial competition, these media will be mixed with clay in order to create an environment similar to microaggregates.

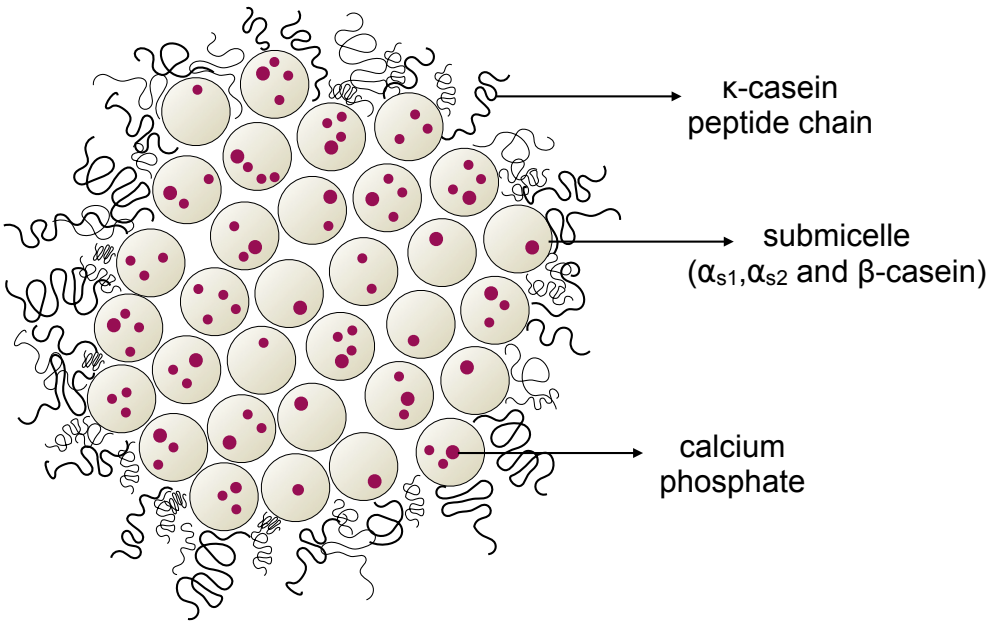

Figure 2.1: A schematic illustration to show a cross section of a casein micelle with its subunits of k-casein peptide chains, submicelle and calcium phosphate, adapted from Walstra et al. 1999 [156].

2.2 Aims of the chapter

The purpose of this chapter is to construct a clean deletion mutant in *P. fluorescens* ON2 background to compete with the ON2-WT strain over digested casein protein in casein medium. The gene responsible for the protease-deficient phenotype of the ON2-pd5 strain will also be identified. Afterwards, casein medium and predigested casein medium using proteinase K will be developed, and the formula of these media will be optimised.

This chapter is organised as follows: identifying the *aprX* gene in *P. fluorescens* ON2, construction of AprX deficient strain, labelling cells with fluorescent proteins and antibiotic resistant cassettes, developing media for bacterial competition and characterisation of the mutant strain with clean deletion of *aprX* gene in comparison to ON2-WT.

2.3 Results

2.3.1 Construction of a protease deficient strain in *P. fluorescens* ON2

P. fluorescens ON2 was first isolated from freshwater sediment by Christoffersen et al. in 1997 [159]. In previous studies, Worm et al., and Allison et al., [41, 126], found that the transposon-based mutant with AprX-deficient phenotype, ON2-pd5, was able to outcompete its protease-producing counterparts, ON2-WT, in casein liquid medium, where casein was digested by AprX, secreted from ON2-WT cells. Despite its disadvantage of being an AprX protease deficient, it was hypothesised that the ON2-pd5 strain was able to conserve energy by not producing AprX, which enabled it to grow more rapidly [126]. While previous studies have confirmed the protease deficiency of ON2-pd5, the gene responsible for this phenotype was not discussed. There are therefore no clear indication if this phenotype is caused by the disruption of the *aprX* gene or downstream genes such as an inhibitor gene, *inh*, or ABC transporter system genes, *aprD*, *aprE* and *aprF* by the mini-Tn*5* transposon insertion that was used to construct this mutant. To determine if disruption of *aprX* is responsible for protease deficiency, a clean deletion of the gene *aprX* was performed to determine the molecular basis of the protease deficient strain. The bacterial strains used in this study are listed in Table 2.1.

Table 2.1: Bacterial strains used in this project.

Strain	Description	Source
ON2-WT	*P. fluorescens* ON2 WT	Steven D. Allison
ON2-pd5	pJBA28-Tn5	Steven D. Allison
ON2-Δ*aprX*	clean deletion of *aprX* gene	This study

2.3.1.1 Identification of the gene responsible for the proteinase deficient strain in *P. fluorescens* ON2

The *aprX* and *inh* genes were first partially annotated by Liao et al., in 1997 using blastn program (AB015053; AF083061)*. Based on their research, milk gelation is primarily the result of an alkaline exo-enzyme of a molecular weight of 50 kDa secreted by *P. fluorescens*. The authors reported that in a 7.3-kb fragment of the genome of *P. fluorescens* there is a gene responsible for production of this enzyme as well as its downstream genes, namely a proteinase inhibitor (*inh*) and a type I ABC transporter (*aprD, aprE* and *aprF*). Following the synthesis of the AprX enzyme, its translocation across the cell membrane is carried out by the type I ABC transporter [162, 41]. Worm et al., created a protease deficient mutant strain of *P. fluorescens*, called ON2-pd5 [41] to study the interactions between proteolytic (ON2-WT) and non-proteolytic strains (ON2-pd5) in liquid media. This strain was constructed by inserting a mini-Tn*5* transposon into the 7.3 kb region of the genome where the *aprX* gene is located. This process led to a protease deficiency phenotype in proteolytic activity of the ON2-pd5 strain. While the ON2-pd5 strain exhibited a non-proteolytic phenotype, it was unclear whether this resulted from a disruption of the *aprX* gene or other genes downstream located within the 7.3 kb region.

Therefore, the first step was to identify the responsible gene for the ON2-pd5 phenotype. In order to accomplish this, the *aprX* and *inh* genes were PCR amplified from the genomic DNA of the ON2-WT and ON2-pd5 strains using aprXF and aprXR, and inhF and inhR primers. The details of the primers are provided in Table 2.2 plus the PCR reaction and program are listed in Table 2.3, and Table 2.4 respectively. In Fig. 2.2 the agarose gel results indicated that the mini-Tn*5* transposon did not disturb the *aprX* gene, as a ∼1.5 kb band representing the gene *aprX* is still evident in both the ON2-WT and ON2-pd5 genomes. However, no

*The blastn program is a general purpose nucleotide search and alignment program that can be used to align tRNA or rRNA sequences as well as mRNA or genomic DNA sequences containing a mix of coding and non-coding regions.

Table 2.2: Primers used in this study (relevant restriction sites are underlined).

Name	Primer sequence	Amplifying region	Source
aprXF	GAGTGATAGGACGATCTC	Amplification of *aprX*, forward primer	This study
aprXR	CATCTTTCGCTCCATCCTAGA	Amplification of *aprX*, reverse primer	This study
inhF	GACATCATCTACGGTGGT	Amplification of *inh*, forward primer	This study
inhR	TTGCAGTACAACTTCCGT	Amplification of *inh*, reverse primer	This study
UEcoXF	GAATTCTGCTCAACGACATCTGG	Amplification of upstream of *aprX* with EcoRI at the beginning, forward primer	This study
UEcoXR	TACATCACGCTACGATGTC-TTTTACTTTTGACATAAACGTAC	Amplification of upstream of *aprX* with EcoRI at the beginning, reverse primer	This study
DEcoXF	GTTTATGTCAAAAGTAAAA-GACATCGTAGCGTGATGTA	Amplification of downstream of *aprX* with EcoRI at the beginning, forward primer	This study
DEcoXR	CTTAAGAATCACGAACAGATAGATGGG	Amplification of downstream of *aprX* with EcoRI at the beginning, forward primer	This study

PCR products were observed for the *inh* gene in ON2-pd5 strain indicating that the mini-Tn*5* has affected the downstream gene(s) of the *aprX* as it is shown in Fig. 2.2. This result suggests that the protease deficiency phenotype of the ON2-pd5 strain is not due to the lack of AprX production but it is because of a disruption of its downstream gene, *inh*. Also, it was unclear whether or not the ABC transporter genes were affected as a result of a disruption of *inh*.

It has been identified that AprX in particular is responsible for hydrolysing casein in milk [163]. Unlike previous studies that utilised a transposon-based mutant as a non-proteolytic strain, in this study an AprX-deficient strain was created by unmarked deletion of the *aprX* gene, which is directly responsible for inability of the mutant strain to growth in casein. This approach was used to determine

Table 2.3: Ingredients of PCR reaction used to amplify the *aprX* and *inh* genes in ON2-WT and ON2-pd5 strains using Gotaq DNA polymerase.

PCR material	Quantity
Gotaq® buffer (5×)	5 μl
Betaine (final concentration 1M)	5 μl
dNTPs (0.2mM)	0.5 μl
Gotaq® DNA polymerase (5U/μl)	0.125 μl
Primer forward (10 μM)	1.25 μl
Primer reverse(10 μM)	1.25 μl
gDNA	50-100 ng
dH_2O	Up to 25 μl

Table 2.4: PCR program to amplify the *aprX* and *inh* genes in ON2-WT and ON2-pd5 strains.

Cycle number	Stage	Temperature	Time
1	Initial denaturation	95°C	2 minutes
30	Denaturation	95°C	40 seconds
	Annealing	51°C	40 seconds
	Extension	72°C	1 min/kb
1	Final extension	72°C	3-5 minutes

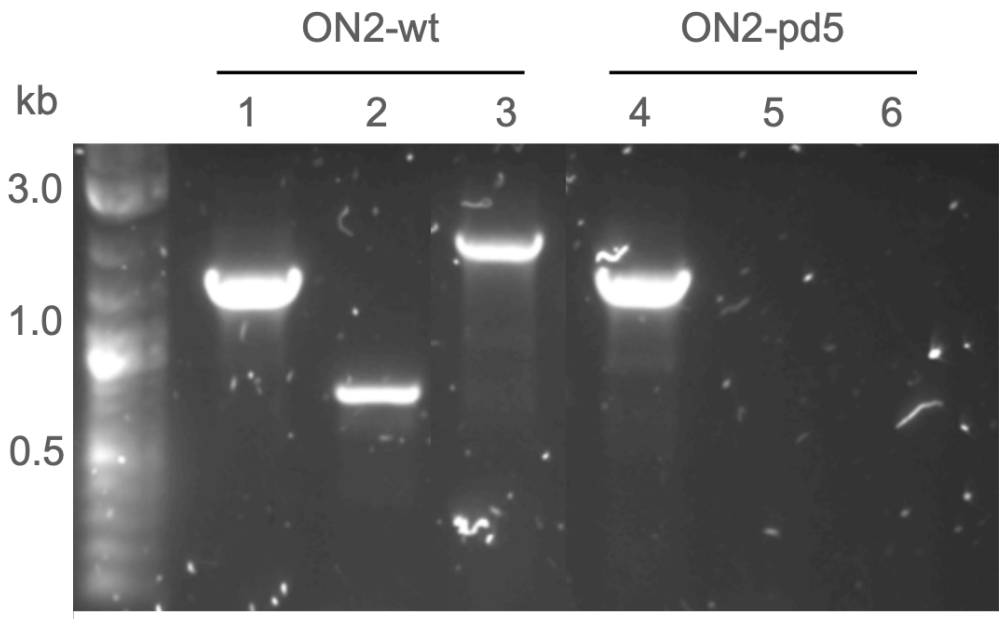

Figure 2.2: PCR revealed that the *aprX* gene in protease deficient strain, ON2-pd5, is still present, but the *inh* gene is affected by the Tn*5* transposon. PCR product in lane 1 to 3 belong to ON2-WT strain and while lanes 4 to 6 are PCR products from ON2-pd5. 1) amplified *aprX* with expected size of 1.5 kb, 2) amplified *inh* with expected size of 0.7 kb and 3) amplified *aprX* plus *inh* from the genomic DNA of ON2-WT with expected size of 2.2 kb. 4) amplified *aprX*, 5) amplified *inh* and 6) amplified *aprX* plus *inh* from the genomic DNA of ON2-pd5. PCR products representing *aprX*, *inh* and *aprX* plus *inh* were amplified using primers (aprXF, aprXR), (inhF, inhR) and (aprXF, inhR) respectively. The details of the primers are listed in Table 2.2. Sizes of a DNA ladder are shown in kb.

whether the inability of the mutant strain to grow in casein occurs as a result of the absence of the *aprX* gene and not by an upstream or downstream gene(s). The ON2-Δ*aprX* strain was constructed through a two-step allelic replacement procedure [164] and the details of the process are discussed in the following section.

2.3.1.2 Construction of unmarked *aprX* deletion in *P. fluorescens* ON2, ON2-Δ*aprX*

In 2015, Allison et al., sequenced a 94 kbp contig from extracted genomic DNA of the ON2-WT strain as reference sequence with GenBank accession KJ540107. They reported that this contig contained the extracellular protease operon as confirmed by BLASTn alignment to a 434 bp sequence upstream of the Tn*5* insertion point with GenBank accession KJ540106 [126]. The sequence with KJ540106 accession number contained the area corresponding to the Tn*5* transposon where the *aprX* gene was ended and the *inh* gene started. Liao et al., in [158], revealed the sequence corresponding to the beginning of the *aprX* gene, as an alkaline protease. In this project, the start codon of the *aprX* gene was searched in the 94 kb sequence of the genomic DNA of the *P. fluorescens* ON2 (GenBank accession KJ540107) and a homologous sequence to this fragment was found. This sequence was located to the upstream of the Tn*5* transposon in ON2-pd5. By counting the number of nucleotides between the start codon and stop codon of the *aprX*, the size of the gene was calculated to be ∼1.5 kb. This size of the nucleotide sequence is equivalent to the estimated molecular mass of the AprX which is 50 kDa and for the rest of this chapter, this sequence was considered to be the *aprX* gene.

In order to generate an isogenic non-AprX producer in *P. fluorescens* ON2, first a deleted version of *aprX* consisting of ∼1kb upstream and downstream regions of the *aprX* gene was constructed. The upstream fragment included a 1 kb upstream of the *aprX* start codon and first 15 bp of *aprX*, while the downstream fragment included the last 15 bp of *aprX* and 1kb downstream of the *aprX* stop codon. The total of 30 bp of the *aprX* gene is not expected to produce a functional AprX protease and it was just to secure the outcome of the amplified product. The primers used in this study are provided in Table 2.2. The primers were engineered to incorporate an EcoRI restriction site to the 5′ end of the upstream fragment and to the 3′ end of the downstream fragment. This was an important step that allowed for cloning the complete deletion cassette (Δ*aprX*) from one plasmid to another. In the next step the amplified upstream and downstream fragments were combined into one fragment by overlapping PCR using UEcoXF and DEcoXR primers. The details of the PCR reaction and program are presented in Table 2.5 and Table 2.6.

Next, the deletion cassette Δ*aprX* and pGEM®-T were ligated. The pGEM®-

Table 2.5: PCR reaction to amplify upstream and downstream of the *aprX* gene with EcoRI at each extremity.

PCR material	Quantity
Phusion HF buffer (5×)	5 μl
Betaine (final concentration 1M)	5 μl
dNTPs (0.2 mM)	0.5 μl
Phusion HF DNA polymerase (0.02U)	0.25 μl
Primer forward (10 μM)	1.25 μl
Primer reverse (10 μM)	1.25 μl
Upstream DNA fragment	10 ng
Downstream DNA fragment	10 ng

T (Promega) is a linearised plasmid with a single T-overhang at each end which harbours an ampicillin resistant gene for the purpose of antibiotic selection. The T-overhang makes the pGEM®-T sticky to facilitate ligation with a DNA insert containing an A-overhang. Therefore, an A-overhang was added to each end of the the Δ*aprX* fragment by adding 0.5 μl of GoTaq DNA polymerase (5U/μl) and 0.5 μl dNTPs (0.2 mM) to the PCR mixture containing the Δ*aprX* fragment and incubation at the 68°C for 20 minutes. A molar ratio of 3:1 Δ*aprX* insert to pGEM®-T plasmid was added to the ligation mixture in a total volume of 10 μl. The ligation reaction, listed in Table 2.7 was stored at 4°C overnight for a maximum transformation yield. An illustration of the cloning process of the Δ*aprX* into pGEM®-T is shown in Fig. 2.3. Then the ligation product was transformed into *E. coli* EC100 competent cells by heat shock. Transformants were selected on LB agar media containing ampicillin (100 μg ml^{-1}), 5-bromo-4-chloro-3-indolyl-β-D-galactoside (X-Gal) (80 μg ml^{-1}) and IPTG (0.5 mM) at 37°C, such that dark blue colonies indicated successful transformation.

The pGEM®-T::Δ*aprX* cloning was confirmed by colony PCR on one blue colony that grew on the LB agar containing ampicillin medium (the detail of the PCR reaction are presented in Table 2.8). In the following, the pGEM®-T::Δ*aprX* was extracted from the *E. coli* EC100 cells and purified from agarose gel. The extracted pGEM®-T::Δ*aprX* was digested with EcoRI enzyme to isolate the Δ*aprX* fragment, and was ligated into an EcoRI cut suicide vector called pEX18Gm. The details of the restriction enzyme digestion reaction can be found in Table 2.9. Briefly, 1 μl of EcoRI mixed with 2 μl CutSmart buffer (10X) and maximum 1 μg of the plasmid,

Table 2.6: PCR programme to amplify EcoRI-Δ*aprX* fragment.

Cycle number	PCR programme	Temperature	Time
1	Initial denaturation	98°C	30 seconds
30	Denaturation	98°C	10 seconds
	Annealing	50°C	10 seconds
	Extension	72°C	1 min/kb
1	Final extension	72°C	3-5 minutes

Table 2.7: Details of ligation mixture.

Ligation material	Quantity
Insert DNA (14.5 ng/μl)	3.5 μl
Linearised vector (50 ng/μl)	1 μl
T4 DNA Ligase (3 Weiss units/μl)	1 μl
2× Rapid Ligation Buffer, T4 DNA ligase	5 μl
dH_2O	To final volume of 10μl

Table 2.8: PCR mixture to confirm the Δ*aprX* insert in the pGEM®-T plasmid.

PCR material	Quantity
Phusion buffer (5×)	5 μl
Betain	5 μl
dNTPs	0.5 μl
Phusion polymerase	0.25 μl
Primer (10 μM)	1.25 μl
Primer (10 μM)	1.25 μl
DNA template	50-100 ng
dH_2O	11.75 μl

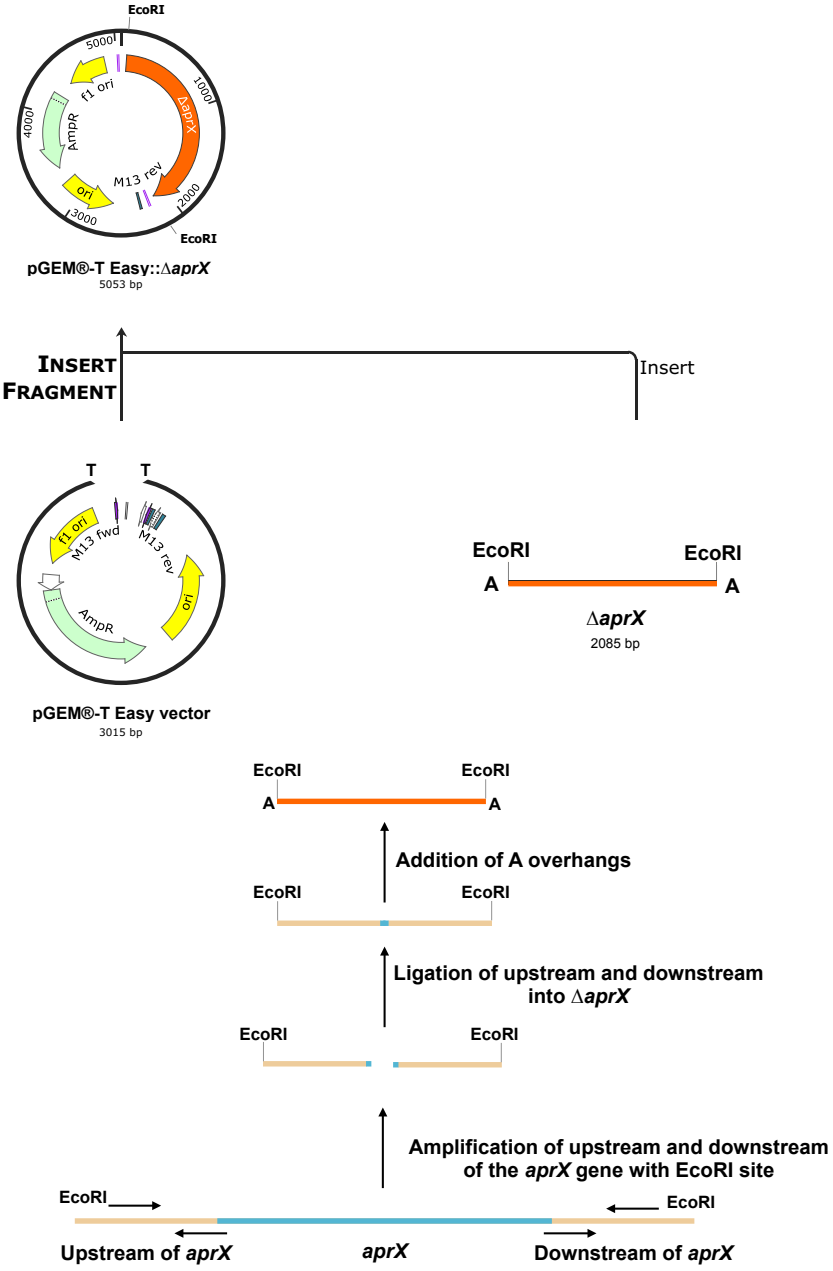

Figure 2.3: Construction of pGEM®-T::Δ*aprX* plasmid. The deleted version of *aprX* consists of ∼1kb upstream and downstream regions of the *aprX* gene which carries 15 bp of the upstream and 15 bp of the downstream of the *aprX* gene. The linearised pGEM®-T plasmid has a T-overhang at each end in order to facilitate the ligation of an insert into the plasmid. Therefore, an A-overhang was added to each end of the Δ*aprX* fragment.

and was then incubated at 37°C for 30 minutes. In order to prevent religation of the linearised pEX18Gm plasmid, Antarctic phosphatase mixture, listed in Table 2.10, was added to the pEX18Gm digestion mixture and incubated at 37°C for another 30 minutes. The Antarctic phosphatase removes the phosphorylated ends of linearised pEX18Gm to prevent open plasmid religation rate during cloning. The linearised pEX18Gm plasmid and Δ*aprX* fragments were purified and mixed with the ligation mixture explained above. The reaction was gently mixed by pipetting and resting at 4°C overnight for higher yield of transformant. The next step will be transformation of pEX18Gm::Δ*aprX* into a chemically competent cell, *E. coli* S17-1 λ pir.

The protocol of preparing S17-1 λ pir competent cell was inspired from Chan et al. 2013 paper [165]. Briefly, the *E. coli* S17 cell was grown overnight at 37°C in LB liquid. Next day, 100 μl of the overnight culture was diluted in a Falcon tube containing 40 ml liquid LB and incubated at 37°C for 3 hours until cells reached to the exponential phase (OD_{600} of 0.3-0.5). Cells were placed on ice for 15 minutes, before they were centrifuged at 3200*g at 4°C for 10 minutes. Then, cells were gently resuspended in 2 ml of prefreezed $CaCl_2$ 0.1M and incubated on ice for 1 hour. After this incubation time, the cells were centrifuged at speed of 3200*g at 4°C for 10 minutes and resuspended in $CaCl_2$ 0.1 M and 15% glycerol. The competent cells were aliquoted in pre-chilled eppendorf tubes and stored at -80°C until they were used in the transformation experiment.

The overnight ligate mixture at 4°C was transformed into the *E. coli* S17-1 λ pir competent cells by the heat-shock method and incubating the mixture at 42°C for 1 minute before immediately placing them on ice for 5 minutes. During the heat shock, the electrostatic repulsion between pEX18Gm::Δ*aprX* plasmid and *E. coli* S17-1 λ cell membrane was counteracted due to presence of $CaCl_2$. The high temperature creates pores in the membrane of the *E. coli* S17-1 λ cells that allowed pEX18Gm::Δ*aprX* to enter into the cells [166]. Then 900 ml of freshly made LB was added to the mixture and it was incubated at 37°C in a shaking incubator for two hours prior plating out. Transformants were selected on LB agar media supplemented with gentamicin (30 μg ml^{-1}), X-Gal (80 μg ml^{-1}) and IPTG (0.5 mM). The cloning strategy of the resulting pEX18-Gm::Δ*aprX* plasmid is illustrated in Fig. 2.4(a). Presence of pEX18-Gm::Δ*aprX* in *E. coli* S17-1 λ pir was confirmed first by colony PCR and then sequencing. Additionally, the plasmid was purified from the *E. coli* S17-1 λ pir cell and digested by EcoRI in order to confirm the cloning was successful. The result in Fig. 2.4(b) showed two bands corresponding to the 2 kb fragment of Δ*aprX* and 5.8 kb fragment of linearised pEX18Gm.

Next, the pEX18Gm::Δ*aprX* plasmid was transformed into the recipient cell, *P.*

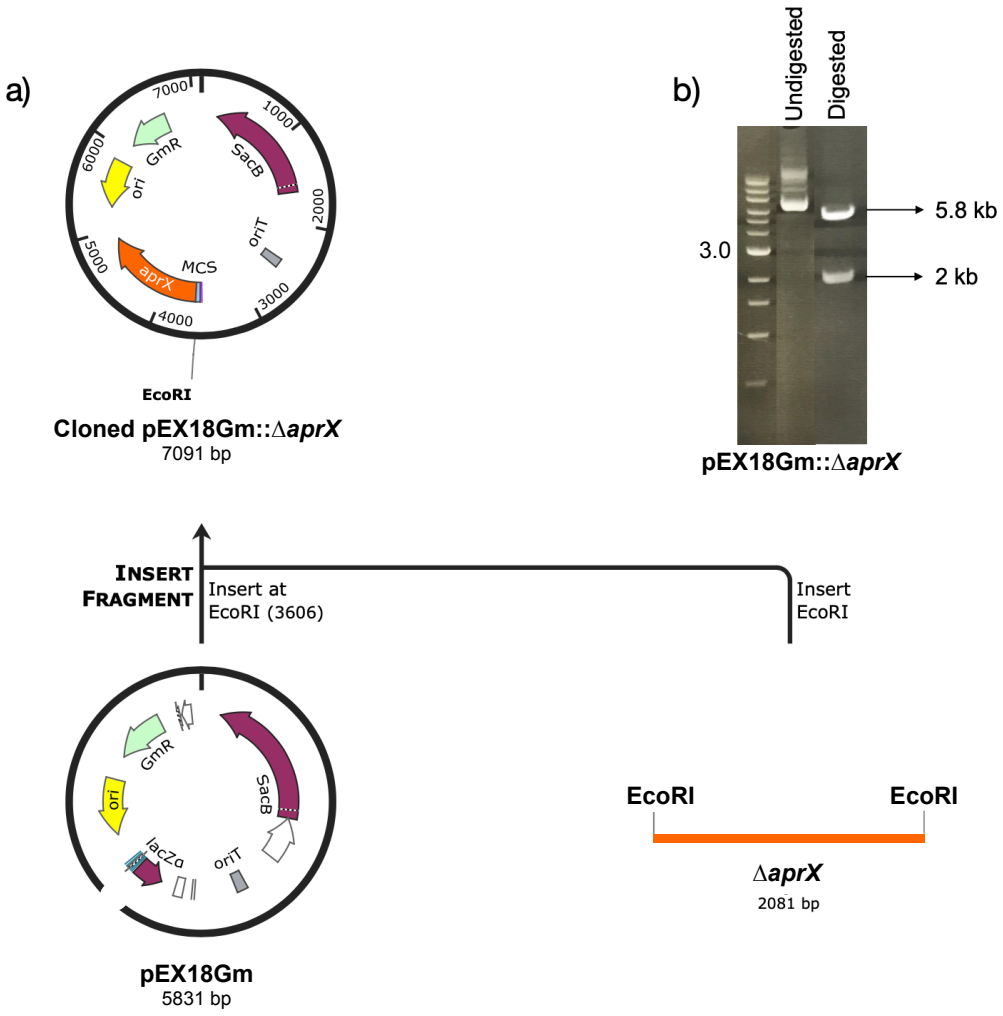

Figure 2.4: Construction of pEX18::Δ*aprX*. a) The pEX18Gm was linearised by EcoRI and the purified Δ*aprX* fragment was cloned into it, resulting in pEX18::Δ*aprX*. b) Restriction enzyme digestion of pEX18::Δ*aprX* with EcoRI. The expected DNA band sizes of 2 and 5.8 kb are indicated with black arrows. Sizes of a DNA ladder are shown in kb.

Table 2.9: Digestion mixture with EcoRI.

Digestion material	Quantity
CutSmart Buffer (10×)	2 μl
EcoRI	1μl
plasmid	Final concentration up to 1 μg
dH_2O	To final volume of 20 μl

Table 2.10: Material for ligation of pEX18Gm and Δ*aprX*.

pEX18Gm ligation material	Quantity
Antarctic Phosphatase Reaction Buffer (10X),	2 μl
Antarctic Phosphatase	(5 units)

fluorescens ON2-WT strain, using a three-strain mating protocol [167]. To achieve this, first the recipient cells, *P. fluorescens* ON2-WT, as well as the donor cells, *E. coli* pEX18Gm::Δ*aprX*, and a helper strain, *E. coli* SM10 λ pir, were grown individually on fresh LB agar plates (Lennox 35 g l^{-1}, Sigma-Aldrich). *P. fluorescens* ON2-WT was grown on LB agar without any antibiotics and incubated at 30°C, the donor strain was incubated on LB agar with 30 μg ml^{-1} gentamicin 37°C, while the helper strain was grown on LB agar with 100 μg ml^{-1} ampicillin at 37°C. In the next step, all three strains were mixed and incubated on fresh LB agar plate without any antibiotic overnight at 30°C. The resulting mixture was resuspended in a tube with 2 ml of fresh liquid LB (Lennox, 20 g l^{-1}, Fisher Scientific) and then spread on cetrimide agar plates (Sigma Aldrich) without antibiotics as a selective medium for *P. fluorescens* and were grown overnight at 30°C.

In the mixture of the three-strain cells, gentamicin could not select the *P. fluorescens* cells with pEX18Gm::Δ*aprX* against the *E. coli* pEX18Gm::Δ*aprX* (as donor strain). Therefore, cetrimide was used as a selective medium. Cetrimide is a toxic substance to many bacteria including *E. coli* since it induces the release of phosphorus and nitrogen, which inhibits their growth [168]. This medium has been used to select for *P. aeruginosa* for many years however, *P. fluorescens* and *P. putida* are also capable of growing on cetrimide at 30°C, so this medium was used to select for *P. fluorescens* in this study.

To isolate ON2-Δ*aprX* mutant with unmarked *aprX* deletion, it is necessary to select cells that have excised the plasmid but integrated the Δ*aprX* allele in place

of the *aprX* allele on their chromosome. The cells with integrated plasmid into their chromosome have a gene called *SacB* that makes cells sensitive to sucrose. Therefore, on LB agar containing 5% sucrose without any antibiotics, cells with double-crossover events in their genomes and the replacement of gene *aprX* with the Δ*aprX* fragment are selected. It is necessary to double check the excision of the plasmid from the selected cells. Therefore, replica plating was done on LB agar with gentamicin (30 μg ml^{-1}) and LB agar without antibiotic for the selected colonies. The colonies that grew on the LB agar without any antibiotics but not on the LB agar plate with antibiotic were isolated as the cells with unmarked *aprX* deletion (Fig. 2.5(a)). The clean deletion of the *aprX* gene was confirmed by PCR on the genomic DNA of the isolated cells using primers UEcoXF and DEcoXR, as shown in Fig. 2.5(b). The final construct was then verified by sequencing, and the resulting strain was named *P. fluorescens* ON2-Δ*aprX*.

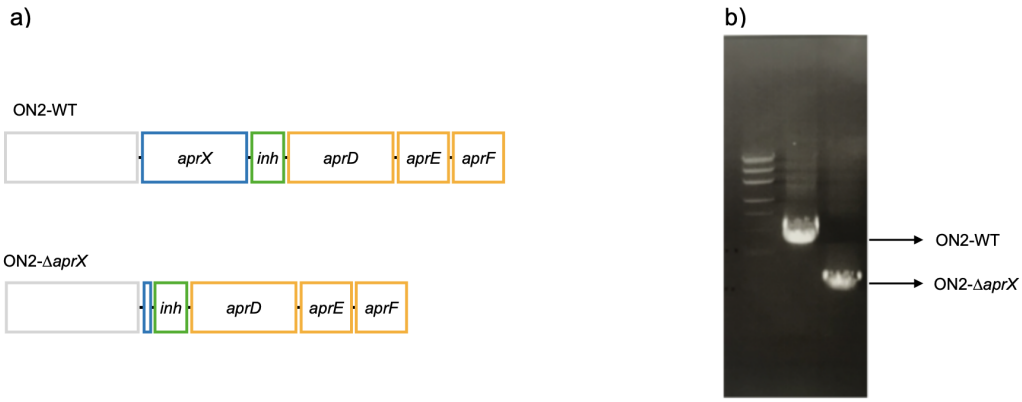

Figure 2.5: Construction of ON2-Δ*aprX* with a clean deletion of the *aprX* gene. In ON2-Δ*aprX* the entire *aprX* gene except for its first 15 bp and last 15 bp is deleted (a). The deletion of the gene was confirmed by PCR (b), and sequencing and the new strain called ON2-Δ*aprX*. The expected DNA band size of 3.5 kb (ON2-WT) and 2.1 kb (ON2-Δ*aprX*) are indicated with black arrows.

2.3.1.3 Construction of fluorescent strains

One of the objectives of this project was to examine bacterial competition in microaggregate structures using fluorescence microscopy. In the competition experiments, the competing bacterial strains were co-cultured in media with or without clay. The mixture of clay and bacterial cells create structures called microaggregates that will be discussed in detail in Chapter 3. The protease deficient strain, ON2-Δ*aprX*, along with ON2-WT were directly competed in both the presence and absence of clay to understand how their relative fitness is controlled by the spatial

structure introduced by the clay aggregates.

To distinguish each strain in the co-culture using fluorescence microscopy, it is essential to label them with different fluorophores. The spectral profiles of considered fluorophores should be well separated to minimise crosstalk between the two channels. For instance, YFP (Yellow Fluorescent Protein) with a peak emission of 530 nm is a yellow derivative of GFP (Green Fluorescent Protein) with peak emission value of 509 nm [169]. These two fluorescent proteins are known to be bright fluorescent labels and were utilised in many research studies. However, their spectral peaks are separated by only $\sim$20 nm [170]. Consequently, cells with YFP and GFP labels in a co-culture are not readily distinguishable from one another and could not be used in the microscopic study of this project. Besides fluorophores, synthetic dyes were also considered to label bacteria. However, this idea was dismissed due to the high risk of breaking microaggregates during extra pipetting and incubation.

CFP (Cyan Fluorescent Protein) with peak emission values of 475 nm, and RFP (Red Fluorescent Protein) with peak of emission of 583 nm potentially were good candidates for dual colour fluorescent imaging. Cells marked with RFP mixed with YFP labelled cells were tested, however, the intensity of the RFP labelled cells was not sufficiently bright in fluorescent microscopic imaging compared to YFP labelled cells in co-culture samples (data is not shown). Therefore, the RFP label was not a suitable option for this study.

Finally, a mixture of CFP labelled cells and YFP labelled cells that belonged to a different *P. fluorescence* background was tested by fluorescence microscopy. CFP and YFP labelled *P. fluorescens* were easily distinguished from one another using fluorescent microscopy. Therefore, fluorescent strains of ON2-WT and ON2-Δ*aprX* were constructed as described below. Both ON2-WT and ON2-Δ*aprX* strains were labelled with CFP and YFP using a Gm^r mini-Tn7 [171] vector via a three-strain mating protocol. The three strains used in this method were a receiver strain – *P. fluorescens* ON2-WT or ON2-Δ*aprX* – a donor strain – *E. coli* with the mini-Tn7 vector containing a gene encoding either CFP or YFP – and a helper strain – *E. coli* SM10 λ pir which provides genes necessary for conjugation. The list of strains is provided in Table 2.11. First, *P. fluorescens* ON2 was grown on LB agar without any antibiotics at 30°C, the donor strains were grown on LB agar with 30 μg ml^{-1} gentamicin at 37 °C and the helper strain on LB agar with 100 μg ml^{-1} ampicillin at 37 °C. All three strains were mixed together and incubated on fresh LB agar without any antibiotics at 30°C overnight. The resulting mixture was suspended in a tube with 2 ml fresh liquid LB (Lennox, 20 g l^{-1}, Fisher Scientific) and *P. fluorescens* cells were selected on cetrimide agar plates (Sigma Aldrich) without

Table 2.11: Bacterial strains and plasmid used in this project.

Strain	Plasmid	Antibiotic resistance	Source
E. coli JM105-CFP (constitutive-promoter)	pBK-miniTn7-ecfp-	chloramphenicol 25 μg ml^{-1} , gentamicin 10 μg ml^{-1}	Soren Molin[172]
E. coli JM105-YFP (constitutive-promoter)	pBK-miniTn7-eyfp	chloramphenicol 25 μg ml^{-1} , gentamicin 10 μg ml^{-1}	Soren Molin[172]
E. coli SM10-λ-pir-Helper	pUX-BF13	ampicillin 100 μg ml^{-1}	Soren Molin[172]
E. coli S17-1 λ-pir (conjugative strain)	pHRB2	kanamycin 50 μg ml^{-1}	Wook Kim
E. coli S17-1 λ-pir (conjugative strain)	pUC18miniTn7T-Sm	streptomycin 50 μg ml^{-1}	Wook Kim

antibiotics by overnight incubation at 30°C.

The reason why *P. fluorescens* ON2 was selected on cetrimide against *E. coli* donor and helper strains is that the *P. fluorescens* ON2 is naturally resistant to ampicillin, whereas the *E. coli* strains contained Gm^r and Amp^r cassettes therefore neither of these antibiotics could be used to select for fluorescently labelled *P. fluorescens* ON2 strains. The fluorescent labelling was therefore confirmed by visualising *P. fluorescens* ON2-WT-CFP, ON2-WT-YFP, ON2-Δ*aprX*-CFP and ON2-Δ*aprX*-YFP strains using fluorescence microscopy. Imaging showed that construction of the fluorescent strains was successful (as shown in Fig. 2.6(a) i,ii). The next step was to introduce an antibiotic resistance marker to the fluorescent strains so that colony forming units (CFU) could be measured in direct competition experiments.

2.3.1.4 Antibiotic cassette insertion

The insertion of an antibiotic resistance cassette into the genome of bacteria can be favorable (in media containing antibiotics), unfavorable or neutral to the fitness of a cell [173]. Therefore, choosing an antibiotic resistance cassette that is neutral to the cell is extremely important, especially in projects that study bacterial growth. According to previous studies, the kanamycin (Km^r) and Streptomycin (Sm^r) resistance cassettes have been found to have no affect the relative fitness of *P. fluorescens* [174]. Thus, *P. fluorescens* wildtype and ON2-Δ*aprX* strains were tagged with the Km^r and Sm^r resistance cassette in order to be able to select for each strain in co-cultures. The strains with a Sm resistance cassette did not grow on kanamycin-containing media, and vice versa.

The antibiotic resistance cassettes were inserted using the three-strain mating protocol, the donor, receiver and helper strains that were discussed earlier (Section 2.3.1.3). *E. coli* S17-1 λ pir is a conjugating strain that harbours plasmids for the Km^r (pHRB2) and the Sm^r (pUC18TminiTn7T) resistance cassettes. The list of plasmids can be found in Table 2.11. The donor, receiver, and helper strains were first grown independently with appropriate antibiotics and incubation temperature for each strain. Three were then mixed together on LB agar without antibiotics to allow the antibiotic resistance cassette to be transferred to the receiver strain by conjugation.

The ON2-WT-CFP and ON2-Δ*aprX*-YFP strains with Km^r and Sm^r resistance cassettes were selected on the cetrimide agar plates containing the appropriate antibiotics, Km (50 μg ml^{-1}) and Sm (50 μg ml^{-1}). In order to determine whether any changes have occurred due to the introduction of the antibiotic cassette, the growth rate of the resulting ON2-WT-CFP-Km^r, ON2-WT-YFP-Km^r, ON2-Δ*aprX*-CFP-Sm^r and ON2-Δ*aprX*-YFP-Sm^r strains was compared with that of the unlabelled strains, ON2-WT and ON2-Δ*aprX* in the following section.

2.3.2 Developing media for bacterial competition

Casein medium has been used in many studies (in different forms e.g. casein protein, casamino acid, etc.), from the characterisation of the exo-enzymes responsible for digesting casein [161] to the study of bacterial competition [41]. In this project, the casein medium was prepared according to a protocol proposed in [161]. The original protocol mandated that 25% ($^v/_v$) of the liquid casein medium is made of a minimal medium, M63, containing 2.0 g l^{-1} of $(NH4_2)_2$ SO_4, 13.6 g l^{-1} of KH_2PO_4, 0.5 mg l^{-1} of $FeSO_4$ $[H_2O]_7$, and 0.2% ($^w/_v$) of glucose. The carbon and nitrogen sources in the M63 allow all bacteria to grow at a similar rate at the begin-

ning of the competition experiment without the secretion of proteases like AprX. In the casein medium, therefore, there is always an additional nutrient provided by M63 with glucose medium, that helps bacteria grow in the early stages. Once M63 nutrients are used up, the bacteria start digesting casein using the AprX exoenzyme [175]. However, glucose present in M63 provides added nutrients to the liquid casein medium, allowing the protease deficient strain, ON2-pd5, to survive in casein for a longer period of time. This could affect the outcome of the bacterial competition by delaying the start point of the "competition".

To rectify this issue, the protocol was modified, and a new method of preparing liquid casein was developed for this project. In the revised protocol, casein medium still contains 25% (v/v) of M63, but glucose has been removed. It should be noted that the presence of M63 in liquid media in this project is not for its nutritional value, but rather because it is necessary for the preparation of media with clay (to be discussed in detail in chapter 3). Therefore, in order to provide an equal basis for the media with and without clay, the M63 medium was used throughout.

Casein is a heat- and pH-sensitive protein that is soluble in alkaline media. To solubilise casein, 2 M KOH as a strong alkaline solution was used. In a Duran bottle, 0.4% (w/v) of casein powder (Sigma-Aldrich) was dissolved in 1% (v/v) 2 M KOH, 4% (v/v) PBS and mixed with M63 medium (0.25 $\times$ in dH_2O) until the casein solution more transparent and appeared to be dissolved. Then 1 mM $MgSO_4$, 0.35 mM $CaCl_2$ and 25% (v/v) of M63 without glucose were added. The pH of the casein medium was adjusted using HCl. In order to avoid the HCl from precipitating the casein, it was important to dilute HCl to 0.1 M and then add it drop by drop to the casein medium.

Because of the heat sensitivity of casein, all media containing casein were filtered through a bottle-top vacuum filter with a 0.22 μm filter size. Once the protocol for preparation the casein media was established, growth of the ON2-WT and ON2-Δ*aprX* strains in media containing either casein (casein medium) or digested casein (described below) was tested and their growth rates were compared. The growth of ON2-Δ*aprX* in the casein medium was substantially attenuated compared to ON2-WT (shown in Fig. 2.6 mono-cultures in casein). These results indicated that except for the casein protein, there is very little additional nutrients in the casein medium which makes it impossible for the protease deficient strain to undergo appreciable growth in absence of a suitable protease.

As a control medium, digested liquid casein was used to test for bacterial growth. Sterile liquid casein was digested by using 5 μg ml^{-1} of filter sterilised proteinase K (Sigma-Aldrich). Due to the enzymatic activity of proteinase K en-

zyme, the colour of the mixture changed from transparent to milky when the enzyme was added to the casein medium. Consequently, it was not possible to filter sterilise the mixture as precipitated casein blocked the filter pores. Hence, the casein was filtered before adding the proteinase K and the filter sterilised enzyme was then added to the liquid casein near a flame to prevent contamination. To ensure the proteinase K had sufficient time to work, casein digestion was carried out on a shaker overnight at 37°C. Following incubation, the colour of the digested casein medium returned to transparent. The ON2-WT and ON2-Δ*aprX* strains grew similarly in digested casein as mono-cultures (shown in Fig. 2.6(a) in digested casein). Beside digested casein, bacterial growth in M63 with glucose was also measured because M63 is the base of casein media with clay and it is important to assess bacterial growth in it as well as the considered media for bacterial competition. The CFU result demonstrated in Fig. 2.6(a) in M63 and digested casein, showed that ON2-WT and ON2-Δ*aprX* strains have similar growth in M63 as it was observed in digested casein.

2.3.3 Characterisation of the *P.f ON2-ΔaprX*

In this study, the *aprX* gene was cleanly deleted for the first time in *P. fluoresces* ON2. Hence, the newly constructed ON2-Δ*aprX* strain had to be characterised in order to determine the effects of the AprX absence on the ON2-Δ*aprX* strain. To this end, the phenotype of the ON2-Δ*aprX* strain was investigated using casein agar and digested casein agar. To enumerate the number of cells of each strain, different counting methods including spectrophotometry (to measure bacterial optical density), colony forming unit (CFU) counting, flow-cytometry and fluorescence microscopy were used.

The fitness of ON2-Δ*aprX* was compared to its parental strain, ON2-WT. For all experiments the bacterial sample preparation for ON2-Δ*aprX* characterisation can be summarised as follows: all strains were streaked on LB agar without antibiotics and incubated at 30°C for 24 hours until single colonies were seen. One fully grown single colony for each strain was selected and transferred to freshly made liquid LB without antibiotics and incubated at 30°C in a Stuart IS600 incubator shaker at 220 rpm. Next day, the optical density at 600 nm (OD_{600}) of the samples was measured and fresh liquid LB was added to overnight culture to obtain an OD_{600} of 0.05. The bacteria were grown at 30°C and 220 rpm until they reached the exponential phase (OD_{600} of 0.2) at which cells were collected and subsequently used to initialise competition experiments.

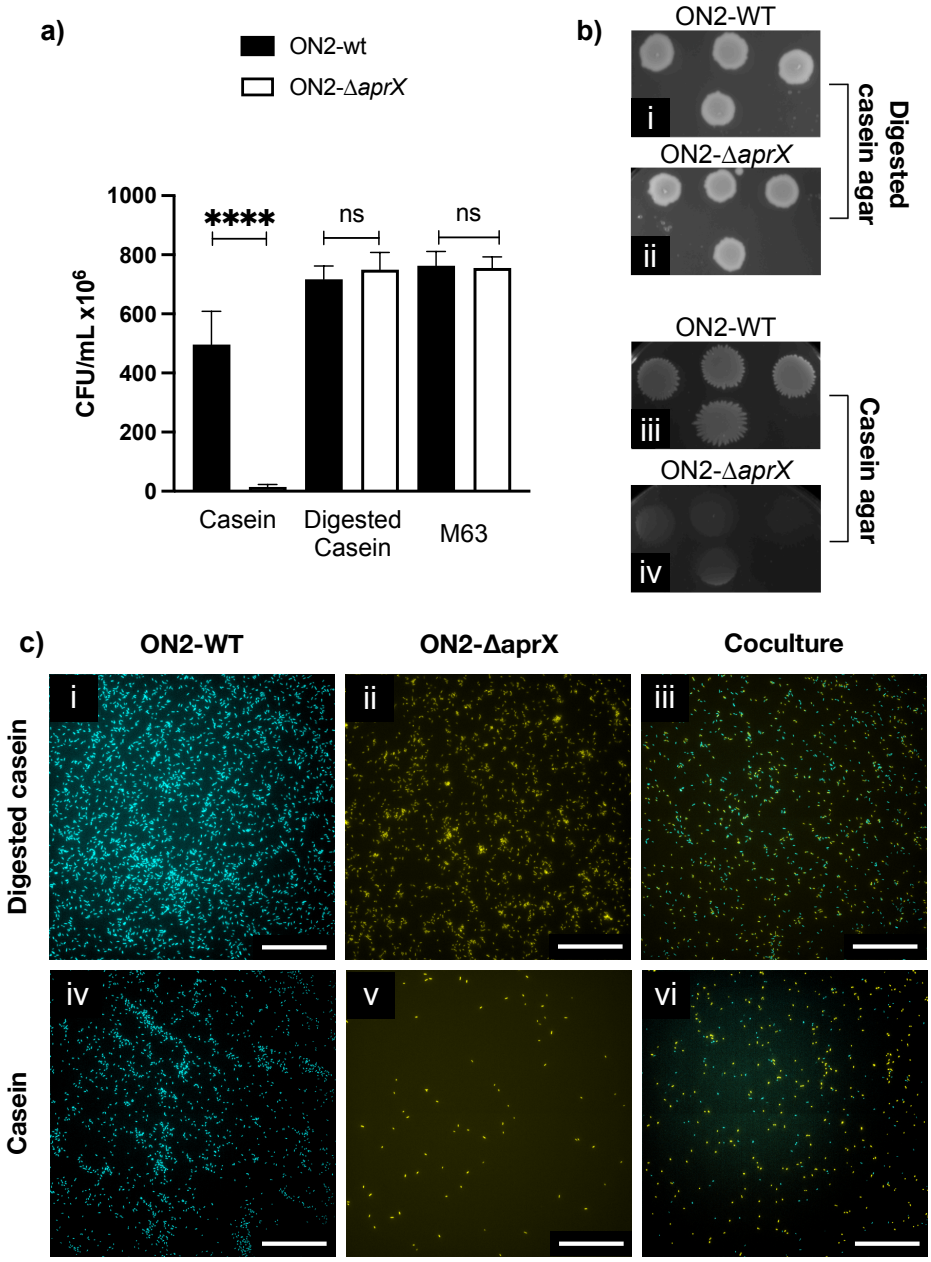

Figure 2.6: Characterisation of the ON2-Δ*aprX* and ON2-WT strain. Comparing the growth of the new mutant strain, ON2-Δ*aprX*, with parental wildtype strain, ON2-WT in casein and digested casein media using a) CFU counting (Data presented as mean and standard deviation and data are compared using *t* test **** p<0.0001 and ns (not statistically significant) p>0.05), b) casein and digested casein agar and c) fluorescent microscopy imaging. All the samples were incubated at room temperature for 48 hours and the results confirmed the reduction of ON2-Δ*aprX* growth compared to ON2-WT as mono-culture in casein medium. The scale bars in microscopic images are 50 μm.

2.3.3.1 Optical density measurement

Among the important characteristics of a bacterial strain are its growth rate and lag time. Bacterial growth can be affected by genetic manipulations in unexpected ways, and isolated mutants may have a different pattern of growth when compared with WT strains [176]. Furthermore, because of its proteolytic inactivity, ON-Δ*aprX* was expected to behave in a similar way to ON2-pd5, which both are not able to digest the casein protein. Optical density measurement OD_{600}) of these two strains were performed by using a VICTOR plate reader in order to compare their growth rates.

First, cells were grown overnight and used to prepare pre-cultures as described above. The optical density (OD_{600}) of the cultures was measured using the Biochrom WPA Biowave DNA spectrophotometer and Semi-micro PS cuvettes (Fisherbrand). To obtain an accurate reading, the samples were diluted in an appropriate medium in order to achieve readings between 0.1 and 0.9. Cells grown to the exponential phase (OD_{600} of 0.2) were inoculated in media containing casein or digested casein. Cell cultures were prepared in 96 well-plates and incubated in the plate reader at 30°C, with shaking. Readings were taken every 20 minutes for 50 hours. It should be noted that the casein blank can get precipitated resulting in noisy casein blank (data is not shown). To assess the impact of fluorescent and antibiotic resistance markers, growth of six strains was investigated: ON2-WT (unlabelled), ON2-WT-CFP-Km^r, ON2-WT-YFP-Sm^r, ON2-Δ*aprX* (unlabelled), ON2-Δ*aprX*-CFP-Km^r and ON2-Δ*aprX*-YFP-Sm^r. The results are shown in Fig. 2.7.

In the case of bacterial growth in digested casein 2.7(a), all the strains showed a similar pattern of growth. However, in the case of casein medium Fig. 2.7(b), the growth of ON2-Δ*aprX* strains was greatly compromised compared to ON2-WT. The low growth rate of the ON2-Δ*aprX* strain in liquid casein confirms that this strain is unable to digest casein due to the lack of AprX production and utilise it for growth. Observations of the double-hump observed in Fig. 2.7(b) for ON2-WT cells are due to the presence of two sources of carbon, one from the M63 medium that the cells grew in to reach the exponential phase, the other being casein, which the ON2-WT changed its metabolism to to digest it. Additionally, none of antibiotic resistance cassettes and fluorescent proteins had an appreciable impact on the strains as they all grew with a similar growth rate as the unlabelled isogenic strain.

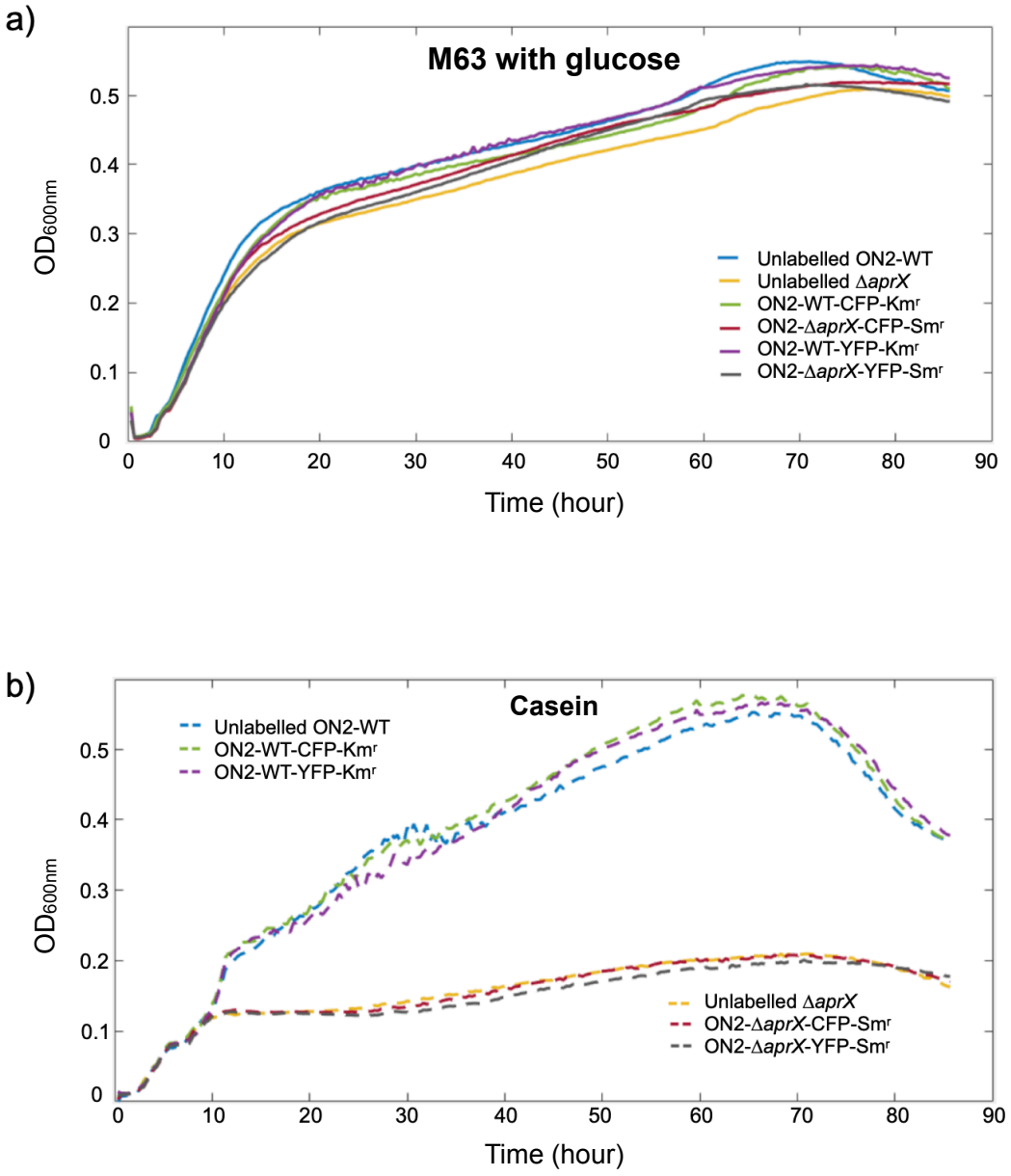

Figure 2.7: Measuring growth curve of ON2-WT and ON2-Δ*aprX* strains with and without labels in a) M63 and b) casein over a period of 50 hours. a) is the OD_{600} measurement of of ON2-WT (unlabelled, labelled with CFP-Km^r and YFP-SM^r) and ON2-Δ*aprX* (unlabelled, labelled with CFP-Km^r and YFP-SM^r) in M63 and b) is their growth curve in casein. The aim of this measurement was to detect the impact of fluorescent proteins or antibiotic resistant labels on ON2-WT and ON2-Δ*aprX* by comparing their growth with unlabelled strains.

2.3.3.2 Bacterial growth on agar pads

A preliminary experiment was conducted to evaluate the growth of ON2-WT and ON2-Δ*aprX* cells on casein and digested casein agar pads. In this experiment, the purpose was to (a) observe the colony formation of each genotype on casein and digested casein agar, and (b) observe their growth differences as mono-cultures versus co-cultures using Nikon Ti-E inverted fluorescence microscopy with CFI Plan Apochromat 20X Lambda air objective. This project uses casein as a medium for bacterial competition, and the agar pad assay has been conducted only on casein agar to compare the growth of AprX producers and non-producers. For this purpose, each of the bacterial strains, ON2-WT and ON2-Δ*aprX*, are labelled with both CFP and YFP. Therefore, four strains of ON2-WT-CFP, ON2-WT-YFP, ON2-Δ*aprX*-CFP and ON2-Δ*aprX*-YFP are used in this experiment.

Colony formation: In order to characterise the colony formation of ON2-Δ*aprX* on agar, ON2-WT and ON2-Δ*aprX* were inoculated on the surface of freshly prepared digested casein and casein agar without antibiotics to compare bacterial growth. First, both strains were grown in LB liquid medium without antibiotics overnight at 30°C, on a Stuart IS600 incubator shaker at 220 rpm for 24 hours. The samples from overnight culture were inoculated into fresh LB liquid and incubated at 30°C, 220 rpm until they reached exponential phase (OD_{600} of 0.2). A 20 μl drop of the cell culture was placed on digested casein agar and the covered dishes were incubated at 30°C for 48 hours. After incubation, colonies of both strains appeared on the digested casein agar. The results shown in Fig. 2.6 b (i, ii) confirm that the clean deletion of the *aprX* gene did not appear to negatively affect the growth of the ON2-Δ*aprX* cells as the mutant grew similarly to the ON2-WT strain on digested casein agar.

The next step was to compare the growth of the ON2-WT and ON2-Δ*aprX* cells on casein agar which requires the AprX protease to utilise. Since casein is a thermo-sensitive protein, rather than using the standard agar, a low melting temperature agarose (Sigma Aldrich) instead was used. Agarose was autoclaved, cooled down to 37°C, and its pH was adjusted as explained in Section 2.3.2. As a control, digested casein agar was prepared using digested casein with double concentration mixed with agarose. Next, 20 μl of exponentially grown cells was spotted on the surface of the casein agar and digested casein agar.

The small amount of growth of the ON-Δ*aprX* strain was observed on casein agar which was speculated to be due to the presence of liquid LB coming from the droplet of cells grown to exponential phase. The liquid LB provided additional labile nutrients for cells on the casein agar and facilitated the slight growth of ON-Δ*aprX* which is slightly visible as shown in Fig. 2.6(b, iv). As shown in Fig.

2.6(b, iii) and (b, iv), the difference in growth between ON2-WT and the mutant indicates that bacteria require the AprX protease to digest casein to be able to grow on media where casein is the only available nutrient. These experiments, in isolation, are not definitive. The appearance of colonies, however, is "consistent" with our previous CFU counting results in casein, shown in Fig. 2.6(a).

Bacterial growth in mono-culture vs co-culture: Samples are prepared as described above. Briefly, cells from exponential phase (OD_{600} 0.2) were collected and in the case of mono-cultures, a 1:1 ratio of ON2-WT-CFP and ON2-WT-YFP with OD_{600} 0.05 were mixed and based on the required microscopic technique, a droplet of the mixture was placed on the casein and digested casein agar plates. This process was repeated in the case of ON2-Δ*aprX* mono-culture. In case of co-cultures, a 1:1 ratio of ON2-WT-CFP, ON2-Δ*aprX*-YFP and a 1:1 ratio of ON2-WT-YFP, ON2-Δ*aprX*-CFP with OD_{600} of 0.05 were mixed and a droplet of the mixture was placed on the casein and digested casein agar plates. Glass bottom Petri dishes (MatTek) with glass thickness of 175 μm were used for samples that were imaged on the microscope.

There are two techniques used to capture bacterial growth on agar, namely the "surficial assay" and "subsurface assay" [177]. For both assays, a 3 mm thick layer of the casein agar was poured into a Petri dish, which was allowed to solidify under a laminar fume hood. Then a casein agar pad, which was 2 cm $\times$ 2 cm square, was cut and placed on the surface of a glass slide. Having prepared the agar, the following section discusses the details of the methods used to prepare the surficial and subsurface assays.

1. In surficial assay, a 10 μl droplet of bacterial sample with initial OD_{600} of 0.05 was spotted on the surface of the casein agar pad and was dried by keeping it close to the flame in order to prevent any contamination. Then the casein agar pad containing bacterial cells was transferred to the centre of the glass bottom Petri dish. One side of the casein agar pad was attached to the glass while the other side, which contained a droplet of bacterial sample, was exposed to the air as shown in Fig. 2.8(a). The lid of the Petri dish was put on and to prevent evaporation, it was sealed with parafilm (Bemis) and the sample was incubated at room temperature for 8 hours. Using this method, the cells quickly form a multi-layer thick colony that for imaging them, an air objective was required. However, it was difficult to see individual cells and fine scale structure as the air objective has a lower numerical aperture compared to an oil-immersion objective. Therefore, to investigate the bacterial interaction in greater depth, the subsurface assay was also used.

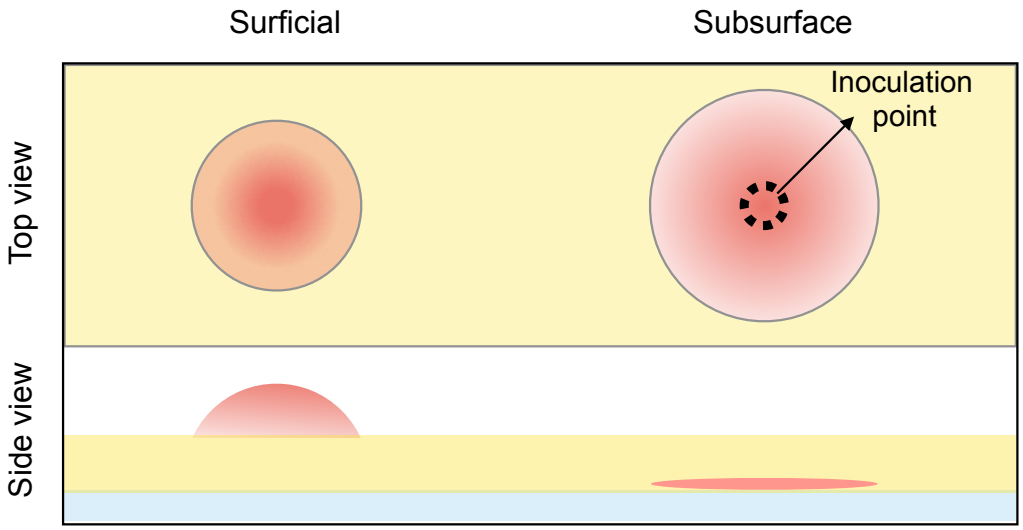

Figure 2.8: A schematic of surficial and subsurface colonies. In the sub-surface colony, the cells are sandwiched between agar and glass, which helps keep them two-dimensional. In contrast, cells in the surficial colony grew on top of the agar and quickly formed a multi-layer thick colony. It appeared that the high density of cells and their secretions interfered with the imaging of CFP- and YFP-labeled cells in the surficial colonies. Therefore, this study employed the subsurface method as it keeps colonies flatter, so that single cells can be more easily imaged with a fluorescence microscope for further investigation.

2. The subsurface assay provides high-resolution imaging necessary to gain a better understanding of bacterial interactions on casein agar surfaces. In subsurface assay, a 1 μl droplet of the bacterial culture with an OD_{600} of 0.05 was spotted on the top surface of the agar pad and left to dry near the flame until no visible liquid remained on the surface. Then the casein agar pad was carefully inverted and placed on a glass-bottomed Petri dish and cells were imaged . In this method, the cells were sandwiched between casein agar pad and the glass coverslip, as shown in Fig. 2.8(b), where they formed a monolayer. To prevent evaporation, contamination, or shrinkage of the agar during the experiment, the glass bottom Petri dishes were covered with their lids and sealed with the Parafilm. Also, it is imperative to use freshly prepared casein agar pads every time in this experiment to ensure the consistency between experiments. The samples were imaged at two points of time, after 16 hours and 5 days of incubation at room temperature. These two time points showed the state of wildtype and mutant in co-culture at the beginning and at the end of the competition on the casein agar pad. As the cells are sandwiched between agar and a glass slide, they grow in a more two-dimensional manner, making microscopic images more informative, because single cells can be easily observed.

   As shown in Fig. 2.9(A), the mono-culture of ON2-WT-CFP and ON2-WT-YFP exhibited substantial growth after 16 hours on the casein agar and none of the CFP or YFP labelled cells had any advantages over the other. However, as it can be seen in Fig. 2.9(B), the ON2-Δ*aprX*-CFP with ON2-Δ*aprX*-YFP does not show the same level of growth as in the ON2-WT mono-culture colony (Fig. 2.9(A)). No difference between CFP and YFP labels were observed. In the case of co-culture ON2-WT-CFP and ON2-Δ*aprX*-YFP shown in Fig. 2.9(C), the substantial growth of CFP labelled cells, which represent WT strain, is observed compared to YFP labelled cells that represent ON2-Δ*aprX* strain. In this case, the opposite colour represents substantial growth of YFP-labelled cells relative to CFP-labelled cells when the ON2-WT was labelled with YFP and the ON2-Δ*aprX* with CFP, shown in the Fig. 2.9(D).

   Figure 2.10 illustrates the results of the same samples that were imaged after five days of incubation period. The wildtype mono-culture, ON2-WT-CFP mixed with ON2-YFP, showed the same pattern of equal growing of CFP- and YFP-labelled cells that grew to a multi-layer bacterial cell shown in Fig. 2.10(A). The ON2-Δ*aprX* mono-culture with CFP and YFP cells in Fig. 2.10(B) also showed similar growth for CFP- and YFP-labelled cells. The ON2-Δ*aprX* cells however, did not exhibit substantial growth at five days compared with

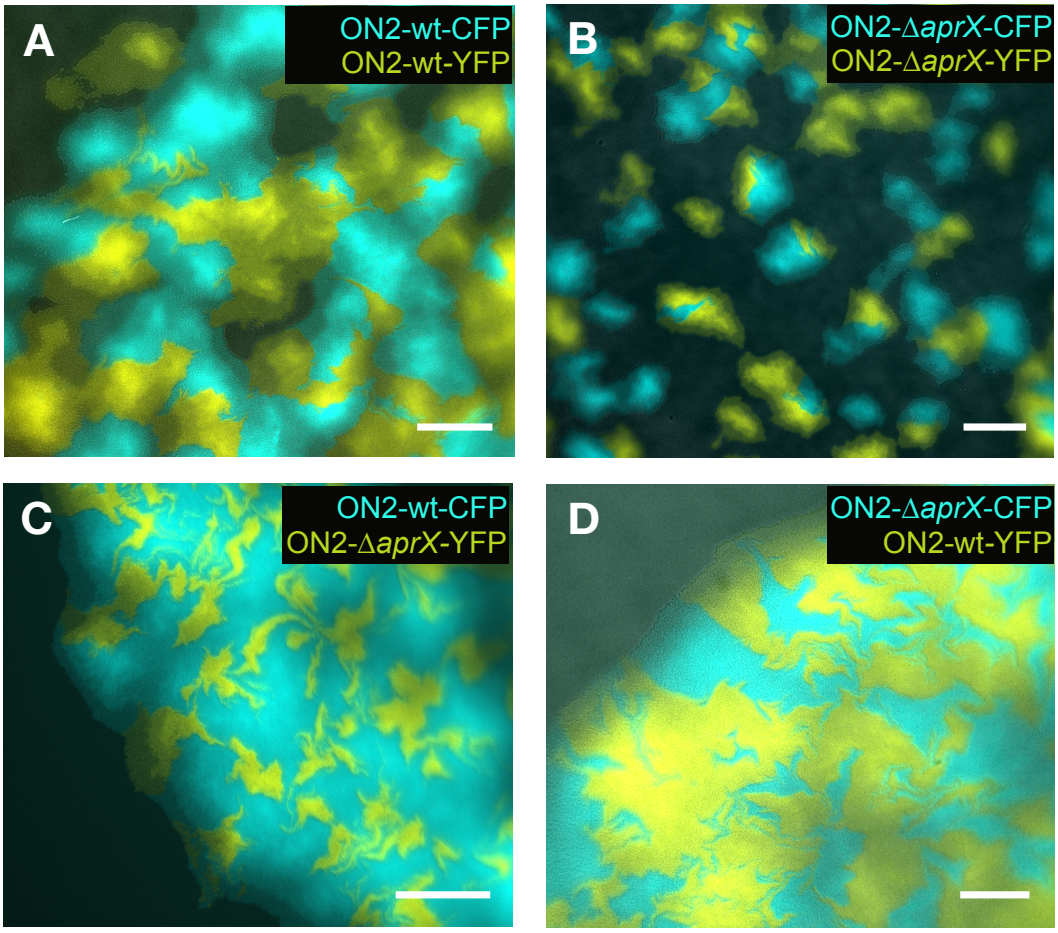

Figure 2.9: Growth of ON2-WT and ON2-Δ*aprX* strains using the subsurface method on casein agar after 16 hours. In all samples, the start point of inoculation was OD_{600} of 0.05, colonies were incubated at 25°C for 16 hours. Image (A) shows a mono-culture of ON2-WT-CFP and ON2-WT-YFP, (B) a mono-culture of the ON2-Δ*aprX*-CFP and ON2-Δ*aprX*-YFP, (C) a co-culture of the ON2-WT-CFP mixed with ON2-Δ*aprX*-YFP and (D) a co-culture of ON2-WT-YFP mixed with ON2-Δ*aprX*-CFP. The scale bars are 50 μm long.

16 hours, suggesting that they are dependent on AprX enzyme to digest the casein for them to grow.

In the case of the co-cultures, multi-layer structures formed after five days of incubation at room temperature. The microscopic images presented in Fig. 2.10(C and D) showed that after 5 days of incubation, both ON2-WT and ON2-Δ*aprX* strains had similar growth in co-culture samples. Based on these results, it is likely that the secreted AprX by ON2-WT cells had digested casein which was diffused to the ON2-Δ*aprX* cells after 5 days of incubation, allowing them to grow similarly as ON2-WT cells.

In summary, macroscopic images of colonies of the AprX-producer and AprX non-producer strains on casein and digested casein agar pads qualitatively recapitulated our previous findings. Also, by using fluorescence microscopy, the growth difference between two populations of ON2-WT and ON2-Δ*aprX* was visually observed and followed the changes over the period of five days. The microscopic imaging indicated that the two fluorescent labels did not differentially affect cell growth. After 16 hours of incubation, the wildtype cells showed more growth compared to the mutant cells. However, after 5 days of incubation, the ON2-WT and ON2-Δ*aprX* populations showed similar amount of growth on the casein agar pad when in co-culture. These results suggest that after five days of incubation, the casein broken down by the wildtype cells had diffused such that it was readily accessible to the non-producing mutant.

2.3.3.3 Flow-cytometry

Flow cytometry is an accurate technique used to count the number of cells or particles in liquid samples and determine their chemical and physical properties [178]. This method measures three parameters: forward scattering, side scattering, and fluorescence emission. The forward scattering provides the information about the size of the cell. On the other hand, side scattering provides information such as granularity and complexity of the particles. The fluorescence emission can be used to identify different bacterial strains in a sample when cells labelled with different fluorescent proteins.

A preliminary test using flow-cytometry was performed to determine whether this technique could be used to quantify the number of CFU and YFP labelled cells in a co-culture. First mono-cultures of ON2-WT and ON2-Δ*aprX* labelled with CFP and YFP respectively were tested. Cells were grown to exponential phase before being inoculated into casein and digested casein liquid media. Cells were

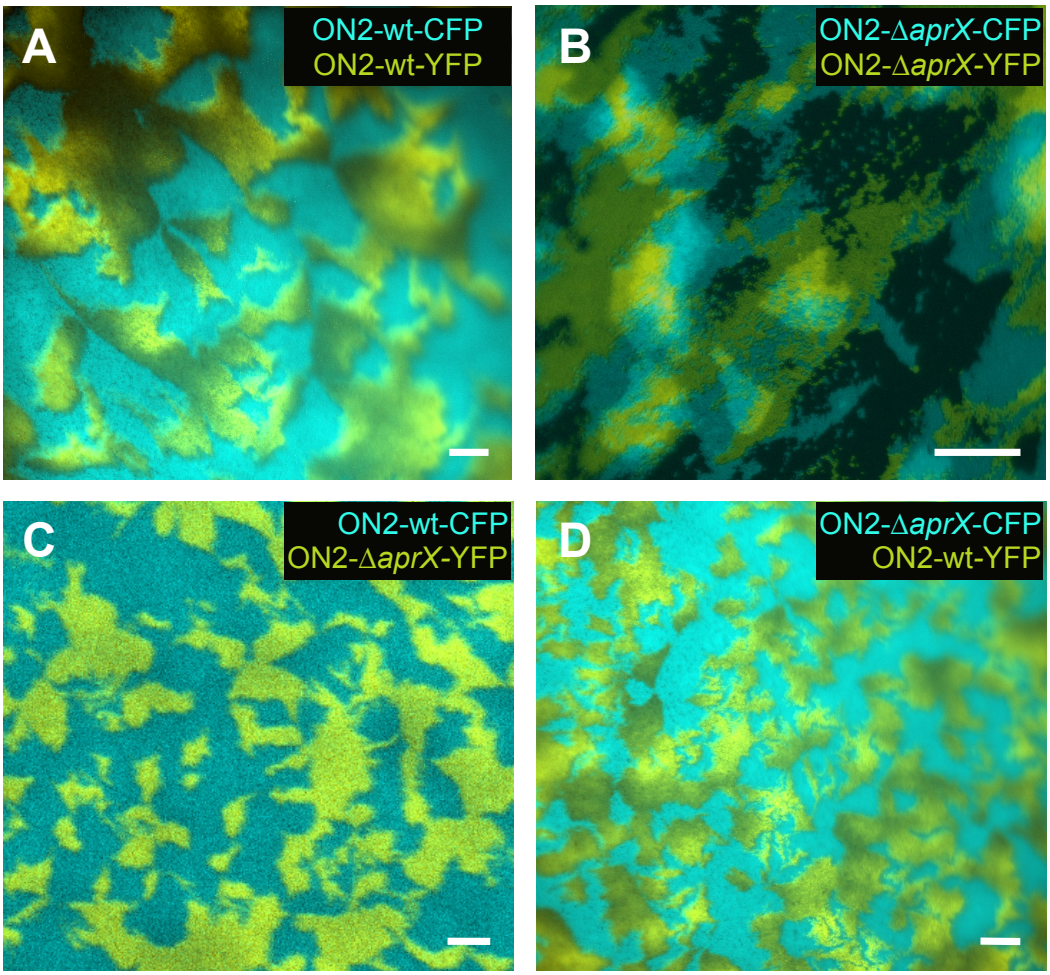

Figure 2.10: Subsurface colonies on casein-agar surface. Both strains were equally represented at the time of inoculation (OD_{600} of 0.05), and the time of incubation is 5 days at 25°C. (A) wild type strain labelled with CFP and YFP. (B) ON2-Δ*aprX* strain labelled with CFP and YFP label. (C) Co-culture of the ON2-WT-CFP mixed with the ON2-Δ*aprX*-YFP strain. (D) Co-culture of ON2-WT-YFP and ON2-Δ*aprX*-CFP strains. The scale bars are 50 μm long.

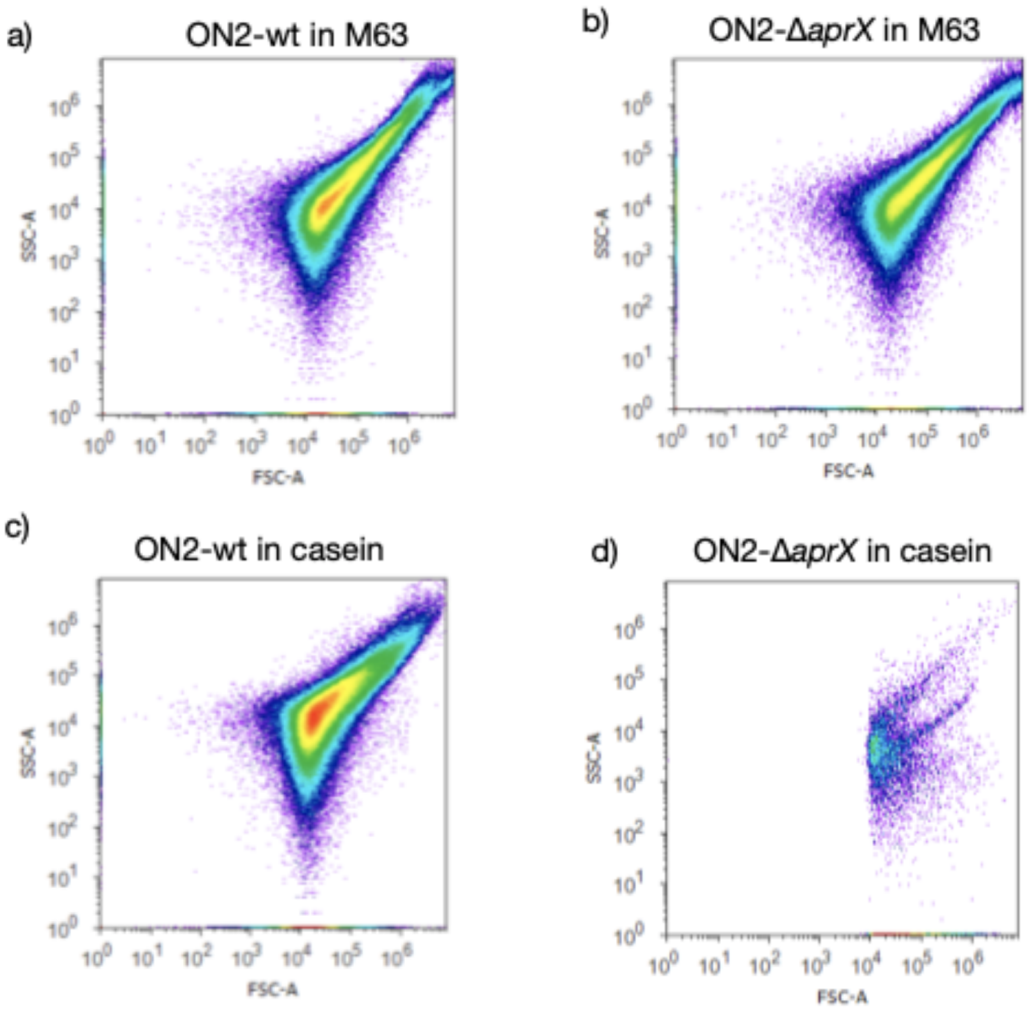

Figure 2.11: Quantification of the ON2-WT-CFP and ON2-Δ*aprX*-YFP cells as mono-cultures in casein and M63 media using flow-cytometry. a) ON2-WT-CFP in M63 b) ON2-Δ*aprX*-YFP in M63, c) ON2-WT-CFP in casein and d) ON2-Δ*aprX*-YFP in casein. Initially, casein and digested casein media were used in the analyses, however, a high level of noise was observed in a cell-free blank of the casein media digested with proteinase K, and it was replaced with M63. A large reduction in the number of ON2-Δ*aprX* cells was observed in casein compared to ON2-WT cells using this method. However, due to the auto-fluorescence of the hectorite clay particles, this device ultimately was not used in this project as it could not distinguish cells from clay particles.

incubated for 24 hours at 30°C with shaking at 220 rpm. The samples were then diluted fivefold in PBS for an accurate flow-cytometry reading. However, a blank sample of the digested casein without cells produced a noisy signal and thus this medium was replaced with M63 with a glucose medium in which bacteria grew very similarly.

The flow-cytometry results shown in Fig. 2.11 are for the mono-culture samples of ON2-WT and ON2-Δ*aprX* strains in M63 and casein media. Forward scatter (FSC) and Side scatter (SSC) are two parameters that are commonly used to identify cells of interest based on size and granularity. These plots showed a similar number of ON2-WT and ON2-Δ*aprX* cells grew in M63 with glucose medium (Fig. 2.11 a,b) which is in agreement with previous data Fig. 2.7(a). However, when the clay was added to the media, we encountered considerable obstacles using flow-cytometry for this study. Due to the auto-fluorescence of hectorite clay particles, the noise from cell-free blank media with clay produced signals similar to those observed when CFP-labelled cells were in the media (data not shown). Since the presence of clay in bacterial samples is an essential component of this research study, therefore, this technique was not used in any of our final analyses.

2.3.3.4 CFU counting

The Colony Forming Unit (CFU) allows one to measure the number of bacteria per milliliter present in a bacterial culture sample. This method will be discussed in detail in Chapter 4. In the current chapter, it was used to compare the number of bacteria on LB agar supplemented with appropriate antibiotics. The ON2-WT-CFP-Km^r and ON2-Δ*aprX*-YFP-Sm^r were grown in mono-cultures using the protocol explained before (Section 2.3.3.2). Cells in the exponential phase were inoculated in liquid casein and digested casein media without antibiotics for 24 hours on the incubator shaker at 30°C and 220 rpm. Following the incubation period, the samples were vortexed and diluted in PBS to reach the desired OD_{600}. Next, 100 μl of the sample were spread on LB agar containing an appropriate antibiotics (kanamycin or streptomycin) and incubated overnight at 30°C. It should be noted that for the optimal results the number of colonies should range from 25 to 250 on a single plate for an accurate count.

Results of the CFU counting are shown in Fig. 2.6(a) and demonstrate that both strains were capable of growing in the presence of their respective antibiotics, and the colonies have fully developed into single colonies (cells did not grow on LB agar plates containing antibiotics for which they did not possess the required cassette). Thus, the selection of each ON2-WT-CFP-Km^r and ON2-Δ*aprX*-YFP-Sm^r in form of co-cultures should be straightforward on LB agar plates with appropri-

ate antibiotics. As expected and similar to the reported growth of ON2-pd5 [41], the number of ON2-Δ*aprX* cells in the casein medium was substantially lower than ON2-WT. However, ON2-Δ*aprX* showed similar growth to ON2-WT in digested casein medium Fig. 2.6(a). The result of counting CFUs for both strains in different media is in agreement with the fact that counting CFUs can accurately represent bacterial populations in different media.

Nevertheless, it was observed that in presence of clay particles, *P. fluorescens* cells tend to assemble into cell aggregates which can cause larger standard deviations in the counting measurements in technical repeats that measured the cell density of the same culture of bacteria. Therefore, in addition to all methods explained above, counting cells using fluorescence microscopy was done to detect if any large aggregates were present in the sample. Figure 2.6 c, shows the microscopic images of ON2-WT-CFP in digested casein Fig. 2.6 c (i) and casein Fig. 2.6 c (iv), ON2-Δ*aprX*-YFP in digested casein Fig. 2.6 c (ii) and casein Fig. 2.6 c (v), co-culture sample in digested casein Fig. 2.6 c (iii) and casein Fig. 2.6 c (vi). The microscopy visualisation supported these results showing a substantial reduction in the number of ON2-Δ*aprX*-YFP cells in casein medium compared to ON2-WT in casein, Fig. 2.6 c (v) and (iv) respectively. Also, the CFP and YFP-labelled cells were clearly visible under fluorescent microscopy in mono-cultures and co-cultures, confirming that the ON2-WT and ON2-Δ*aprX* strains should be clearly distinguishable in our subsequent analyses which used fluorescent microscopy to enumerate cells.

2.4 Discussion and conclusion

In previous studies, it has been shown that the ON2-pd5 strain lacks the ability to grow in casein medium mono-culture due to a deficiency in protease enzyme production [175]. This phenotype was caused by insertion of a transposon, mini-Tn*5*, into the region where the *aprX* gene and its downstream genes are located. Yet, it was not reported exactly where the transposon was located in the genome.

In this study, the *aprX* gene was annotated and, by using two-step allelic replacement, a clean deletion of *aprX* gene was made in a wildtype background and the resulting strain was named ON2-Δ*aprX*. The ON2-Δ*aprX* strain was grown in the casein medium and results showed that the strain follows the same phenotype as ON2-pd5. In ON2-pd5, the transposon was found to be located downstream of *aprX* in the *inh* gene, while the protease deficiency phenotype of ON2-Δ*aprX* was due to the clean deletion of the *aprX* gene. The protease deficiency of ON2-Δ*aprX* made it an ideal bacterial candidate to compete with ON2-WT in a casein-based

media to study bacterial competition in clay microaggregates.

Further preparations were carried out in order to label strains with fluorescent proteins, CFP and YFP, as well as antibiotic resistance cassettes, Sm^r and Km^r. It was necessary to label bacterial strains with two different fluorescent proteins to ensure the labels did not differentially affect bacterial fitness. Moreover, we quantified the number of the wt and mutant cells in co-cultures using antibiotic resistance cassettes to allow us to select strains using the appropriate antibiotics. The markers were carefully selected so that they had a neutral effect on bacterial growth.

There were also challenges encountered during the preparation of the liquid casein. Casein is a pH and heat-sensitive protein that can precipitate in low pH or degrade at temperatures above 40°C. Thus, several attempts were made to develop a protocol for solubilising casein and preparing liquid casein that could only be used by bacteria capable of producing and secreting AprX and not by ON2-Δ*aprX*. A control medium was developed, which also included casein but it was digested with 5 μg ml^{-1} proteinase K at 37°C overnight. The growth of ON2-WT and ON2-Δ*aprX* in digested casein and M63 with glucose was similar. We used M63 with glucose as a control growth medium instead of digested casein in flow-cytometry experiments due to the background noise caused by digested casein.

In this chapter, it was demonstrated that *P. fluorescens* without the gene *aprX* gene is a viable strain although its growth is severely compromised in casein medium due to its inability to produce AprX and digest casein. The optimised casein and digested casein media provided a platform for performing the experiments for the ultimate goal of this project, which is the bacterial competition within clay microaggregates. The preliminary tests that quantify the growth rate of wildtype and mutant strains demonstrated that the growth defect of ON2-Δ*aprX* in casein is caused by the lack of the *aprX* gene and not the fluorescent proteins, or antibiotic resistance cassettes. The microscopic study on the two-dimensional bacterial colonies on casein agar and digested casein agar allowed us to characterise the AprX non-producer cells by comparing their growth with AprX producer cells in both mono-culture and co-culture samples. The results of the co-culture experiment on casein agar showed that at the beginning (first 16 hours of incubation) the ON2-WT was able to grow more than ON2-Δ*aprX* on casein agar. However, after five days of incubation the digested casein was diffused in agar and ON2-Δ*aprX* was able to have access to it and grow similar to ON2-WT. To quantify the number of bacteria, a number of counting techniques were tested and it was found that the CFU counting method produced more reliable results in media with and without clay compared to using the flow-cytometry technique. In conclusion, this chap-

ter established the bacterial strains and media to use in the bacterial competition experiments in this study.

Chapter 3

Microaggregate Development

3.1 Introduction

Increasing carbon dioxide concentration in the atmosphere has prompted numerous research studies to explore mitigation strategies to combat climate change [21], [179]. The sequestration of carbon in soil is a promising way to reverse this trend [180]. Soil's ability to serve as a carbon sink depends on the total soil organic carbon (SOC), its characteristics, management, and climatic conditions [181]. Researchers have debated the fundamental mechanisms that protect carbon from degradation for decades [182]. However, new studies suggest that the persistence of SOC is more than a molecular property of carbon, but is also highly dependent on the surrounding environment and the interplay between bacteria and soil minerals [14].

Soils are heterogeneous, porous, and biologically active media, and their function is closely linked to their three-dimensional structure [183]. Soil aggregation is one of the specific and distinct features of soils that serve as microhabitats and directly influence microorganisms that live within and are influenced by them in return [184]. As such, microaggregates are the smallest fraction in the soil and are mainly made from silt and clay particles [185], (details are shown in Fig. 3.1). Advantages of microaggregates include their ability to hold organic materials for a very long time [186]. For instance, among the soil fractions, the carbon turnover time in microaggregates is significantly higher (e.g., 100-300 years) than that in macroaggregates (15-20 years) [187]. This indicates the importance of microaggregate in SOC storage, which impacts the soil productivity and quality- by preventing soil SOC decomposition caused by microbial activity – and ultimately governing carbon cycling [14].

It is important to understand how microaggregates are formed since they typ-

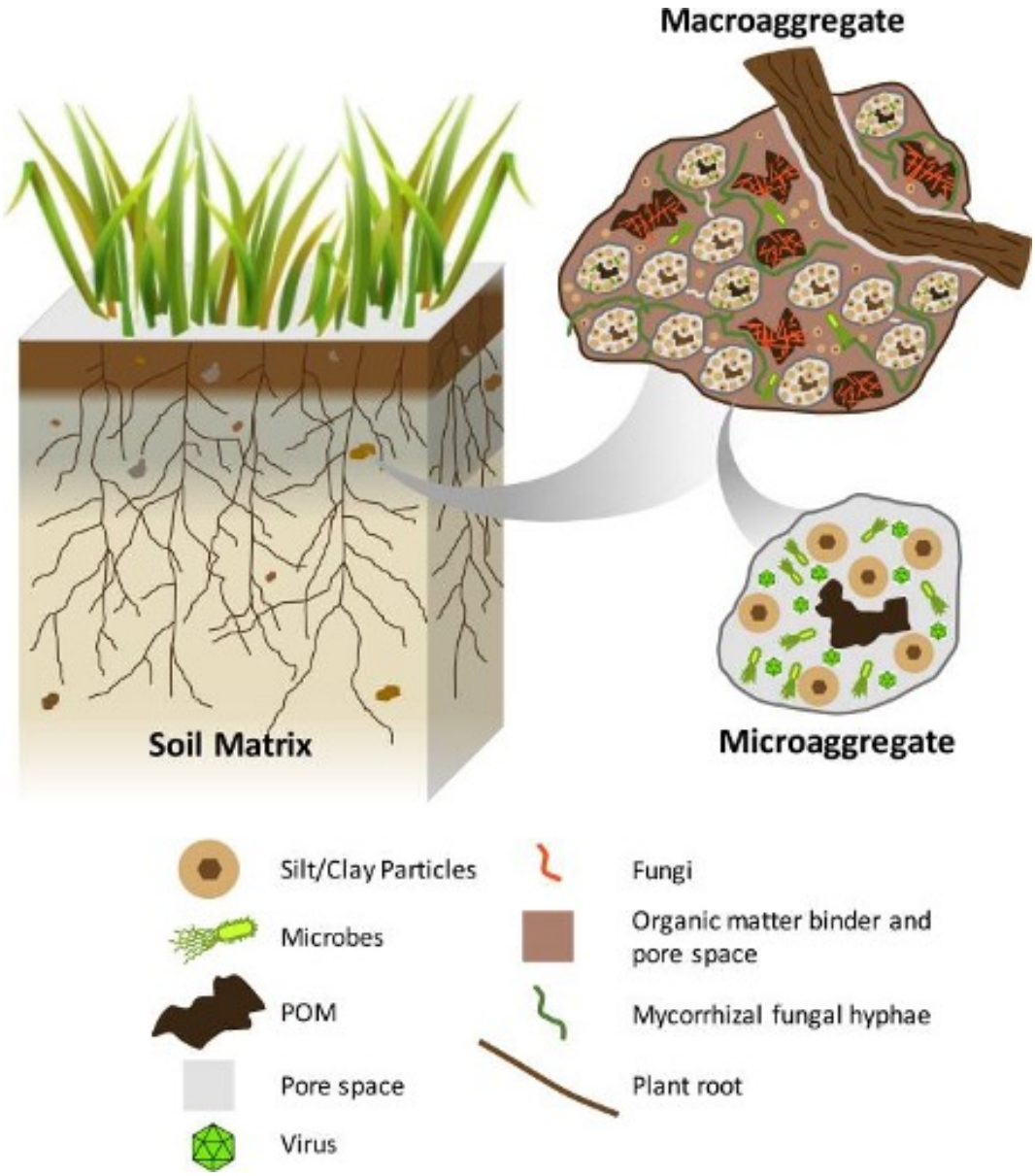

Figure 3.1: The composition and structure of soil, including microaggregates, macroaggregates, organic and inorganic matters. Image reproduced from [51].

ically consist of clay particles – with a diameter of less than 2μm – which cannot support structures as stable as microaggregates themselves. [147]. It was shown in [188, 189, 190], surface properties, such as different charges, allows organic materials to accumulate in the nano-sized pores of the clay surface and bond to the minerals to form microaggregate structures, however, this compound will not be mechanically sufficient to maintain the structure of the microaggregates. The microbial activities, like polysaccharide secretion, are essential to form a stable aggregation [47, 184]. While these studies concentrated on the macroaggregates fraction, further studies have confirmed that the role of microorganisms, particularly bacteria, is crucial in the formation and stabilization of microaggregates [191, 192]. Bacteria secrete their extracellular products to survive and when they are around clay, these secreted substances act as glue agents to cement the clay particles into clay aggregates and ultimately, form highly stable microaggregate structures [103]. The spatial structure of microaggregates is composed of a continuous system of interconnected voids and pores of varying size, shape and geometry, resulting in a morphologically complex biogeochemical network [193]. This network allows the transport of liquids and gases, dissolved compounds as well as colloidal particles within microaggregates [194]. Most soil microorganisms, like bacteria, live in interconnected communities that are closely associated with the aggregates of soil [195]. Temperature, pH, and moisture are the key factors in an environment that is favourable for bacterial growth [196]. Thus, the internal environment of the microaggregates can be a very favourable setting for bacteria [197].

Furthermore, microaggregates play a significant role in biogeochemical cycling, and soil biological activity and variability can reliably be predicted by studying this microscale fraction. For instance, it has been observed that microbial communities have irregular and uneven population distribution in soil [198, 199, 200]. On the other hand, the clay surrounding bacteria as a form of microaggregate can hinder the uptake of nutrients by impairing the flow [201]. Therefore, to fully understand the interactions between bacterial communities in microaggregates, it is necessary to understand the formation process of microaggregates within the presence of bacteria.

The aim of this chapter is to develop a lab model of microaggregates aiming to gain a better understanding on i) how microaggregates are formed, ii) the development of the microaggregate structure over time, and iii) the role of bacteria in stability of the microaggregates. In addition, the findings of this chapter will allow us to study interactions between bacterial genotypes studied in Chapter 4.

The organisation of the rest of this chapter is as follows. In section 3.2, the process of preparing clay particles based on a protocol from Alimova et al. [148]

to be used in the microaggregate lab model will be discussed. Next, in Section 3.3, an optimised protocol of developing a lab model microaggregate will be detailed. Finally, the main remarks of this chapter will be summed up in the conclusion section.

3.2 Clay preparation

As thoroughly discussed in Chapter 1, there are various types of clay – as the primary constituent of soil structure – with different physical and chemical properties. The majority of clay types are either innocuous or promote bacterial growth but some of them exhibit naturally bactericidal properties [201]. Hectorite* is a trioctahedral clay mineral with unique physical and chemical characteristics, such as swell/shrink ability, dispersibility, cation exchange capacity, surface reactivity and adsorption [202]. This type of clay has been extensively studied, and its ability to be mixed with a various range of liquid growth media makes it a suitable candidate for studying bacterial interactions with clay.

In order to develop a simplified laboratory model of a microaggregate, only hectorite clay and *P. fluorescens* ON2-WT bacterial strain (a detailed description of the bacterial strain was provided in Chapter 2) were used. In the following, a general protocol for preparing microaggregate will be outlined [148], and its limitations with respect to this project will be discussed. A revised protocol will then be introduced to correct the deficiencies of the previous protocol. Afterwards, it will be explained how the microaggregate lab model was developed, as well as how experiments were performed using the microaggregate lab model.

3.2.1 General Protocol

The initial protocol used to create a microaggregate followed the clay preparation method from Alimova et al. [148] who used sodium hypochlorite to decontaminate clay from potential nutrient sources (organic contamination). This protocol is outlined in Fig. 3.2 and explained as follows.

In an attempt to prepare the clay particles in the same way as [148], sodium hypochlorite (known as bleach) was used. Using sodium hypochlorite or hydrogen peroxide is a standard method to ensure the particles were free from any organic and inorganic contamination that might potentially interfere with bacterial growth [204]. To do this, a 200 mg of clay was incubated in 100 ml 5% sodium hypochlorite solution at 37°C for one hour. The decontaminated clay was then

*Chemical formula: $Na_{0.4}Mg_{2.7}Li_{0.3}Si_4O_{10}(OH)_2$

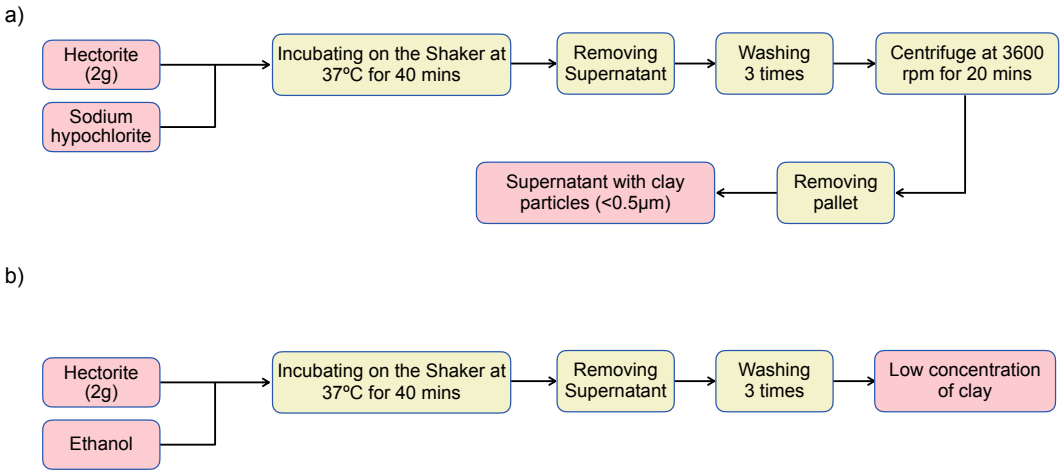

Figure 3.2: Detailed process of eliminating organic contaminants from clay particles using (a) sodium hypochlorite and (b) ethanol. The clay of case (a) absorbed the sodium hypochlorite, and even after multiple washings, the sodium hypochlorite was not washed away, which prevented bacteria from growing. In (b), the ethanol was used instead of sodium hypochlorite but it is likely because of the clay dehydration caused by ethanol [203], resulting in rapid sedimentation that prevented clay particles from being separated by size.

washed three times with sterilised distilled water (dH2O) in order to remove any remaining sodium hypochlorite solution from the clay particles. The clay was then mixed with 50 ml M63 with 0.2% (w/v) glucose. As it was explained in chapter two, the M63 with glucose is a minimal growth medium with glucose as a carbon source. The mixture of clay and the M63 then centrifuged at 3600 rpm for 20 minutes to make the larger clay particles (>500 nm in diameter) and non-clay minerals contamination sediment to the bottom of the tube. The supernatant, containing smaller particles (<500 nm in diameter), was then carefully collected and autoclaved at 121°C for 40 minutes to eliminate any potential bacterial contamination. Then the sterile-filtered $MgSO_4$ and $CaCl_2$ were added to the clay mixture and the pH was adjusted to 7 using sterile-filtered KOH. The sterility of the clay suspension was tested by placing 100 ml of the clay sample on a Luria Bertani (LB) agar plate without antibiotics and incubating at 25°C for 48 hours. There was no sign of contamination on the LB agar plates (results are not shown).

To ensure that the clay treated by sodium hypochlorite was not toxic to bacterial cells, the following experiment was conducted. A 1:1 ratio of clay and LB liquid medium was mixed to achieve a total volume of 10 ml. Then 100 μl of *P.f* ON2-WT overnight culture was inoculated in the clay medium and incubated at 30°C, 220 rpm for 24 hours. The same ratio of LB liquid and distilled water (without clay) was also prepared and 100 μl of *P.f* ON2-WT overnight culture was

added as a control sample for this experiment.

One way to determine whether bacteria were grown successfully in the medium is to observe the colour of the culture after the incubation time, in which the colour would have changed from being transparent to opaque. As illustrated in Fig. 3.3(a)-Ⓘ, the colour of the bacterial culture in the control sample was cloudy, suggesting that the bacteria were present at high concentrations. However, the colour of the medium with clay has not changed and has remained transparent (shown in Fig. 3.3(a)-Ⓘ), which indicated that bacteria was stifled by the sodium hypochlorite treated clay.

Aside from this qualitative assessment, there are a number of direct and indirect methods for quantifying the number of cells in a bacterial culture. Spectrophotometer is a standard method to measure the number of bacteria indirectly. The turbidity of the sample or its optical density indicates the bacterial content. However, the presence of clay particles in our bacterial cultures prevented us from using this method since it cannot distinguish clay from bacteria. To overcome this issue, a method of counting Colony Forming Unit (CFU) was used, in which a volume of 100 μl of the bacterial culture in clay medium was spread on a LB agar plate without antibiotics and bacteria in both the control and the clay sample were counted. The plates were incubated at 25°C for 24 hours. The control samples without bleach treated clay were countable as the control sample was diluted in PBS by a factor of five before spreading on the plate. On the other hand, the eight colonies growing on the LB agar plate corresponding to the clay sample were not diluted at all. As depicted in Fig. 3.3(c)-Ⓘ and (c)-Ⓘ as well as in Fig. 3.4(a) and (b), the microscopic study confirmed that the bacterial growth was strongly suppressed.

The above experiments have confirmed that sodium hypochlorite was not washed off of the clay and caused a toxic environment for bacteria which subsequently severely impacted their growth. The sodium hypochlorite is difficult to fully eliminate and after a triple wash, there may still be a residue of sodium hypochlorite in the clay, which may have acted as a toxic to bacterial growth. Therefore, the clay was subjected to a tenfold wash with sterilised distilled water, so as to completely remove any sodium hypochlorite solution. Despite repeating the washing process ten times, the sodium hypochlorite was not fully removed, as bacterial growth did not increase appreciably.

To test an alternative for decontaminating clay, ethanol was replaced with the sodium hypochlorite. Essentially, the idea behind this step was to use a solvent in which 1) clay could be mixed with and sedimented in and 2) can be easily removed from clay [205]. In this step, clay was mixed with ethanol 99% [Sigma-Aldrich]

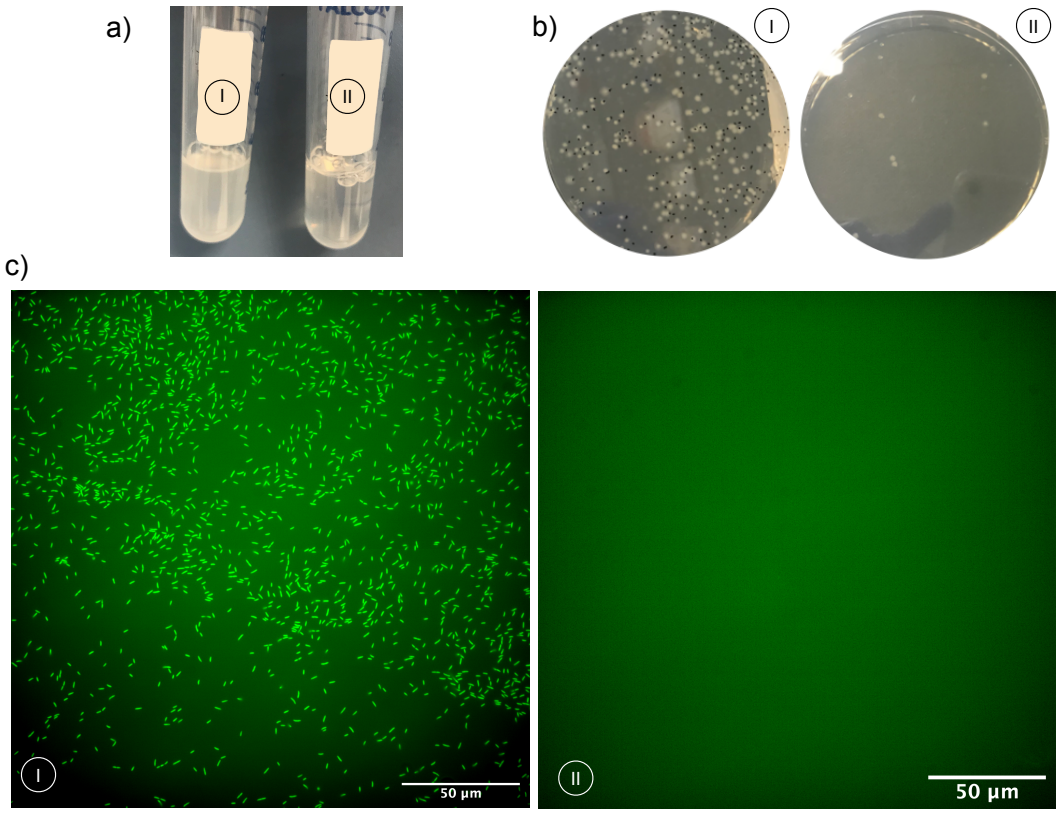

Figure 3.3: A comparison of clay treated with and without sodium hypochlorite. After 24 hours of incubation with clay samples, test tubes showed a significant change in colour (a). Ⓘ is the control sample of bacteria clay samples without sodium hypochlorite treatment and Ⓘ Ⓘ is bacteria in a clay medium treated with sodium hypochlorite. Comparing (a)-Ⓘ and (a)-Ⓘ Ⓘ, the significant difference suggests that the sodium hypochlorite attached to the clay particles caused a bactericidal effect. Sub-figure (b) is the result of CFU counting of both samples on LB agar plates without antibiotics (sample (b)-Ⓘ has been diluted five fold, whilst (b)-Ⓘ Ⓘ has not). Sub-figure (c) is the result of fluorescent microscopic imaging of bacteria clay samples (sample (c)-Ⓘ has been diluted 2 times, whilst (c)-Ⓘ Ⓘ has not). In the fluorescent microscopic result of sample (c)-Ⓘ Ⓘ, the exposure time was enough to observe any GFP-labelled cell. These measurements confirmed the sodium hypochlorite treatment process renders the clay media unable to support bacterial growth.

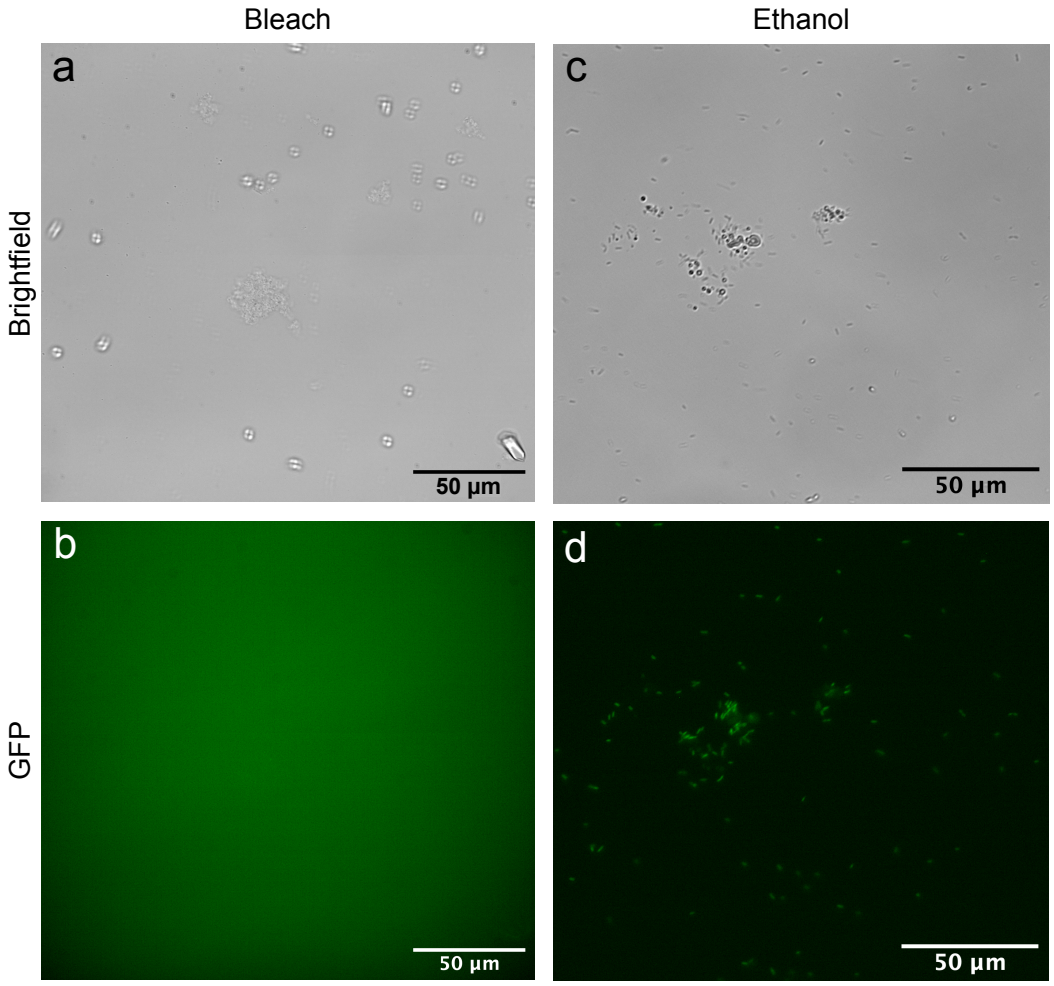

Figure 3.4: A comparison of sodium hypochlorite and ethanol-treated clay samples for bacterial growth. (a) and (b) are microscopic results of clay treated with sodium hypochlorite that confirm sodium hypochlorite has a bactericidal effect, preventing the growth of bacteria. Images (c) and (d) show that when clay was treated with ethanol, bacteria could grow in the clay sample, confirming that ethanol was washed away from the clay but the concentration of clay particles in the clay medium was inadequate. Because the clay particles sediment so rapidly in the bottom of the tube, the clay particles in the supernatant fraction of the clay sample were very fine in size with low concentration.

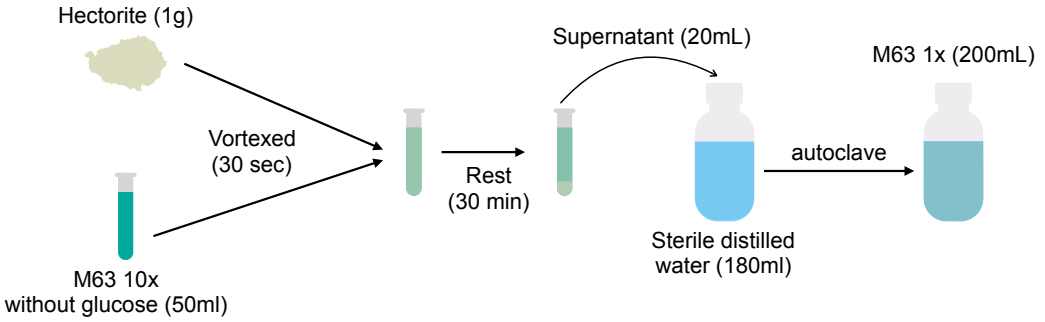

Figure 3.5: Revised clay preparation protocol to design a microaggregate structure. In this protocol, clay is prepared in M63 10X without glucose so it will sediment slowly enough to separate finer clay particles from clay aggregates. In this method, the supernatant was collected containing fine clay particles and diluted to M63 1X.

and the medium was incubated for 30 minutes at room temperature before it was washed. This method was not effective either, as the ethanol changed the dispersion of clay, which resulted in the clay sediment to the bottom of the Falcon tube. Therefore, only a very small amount of clay was observed in the supernatant, the microscopic results are shown in Fig. 3.4(c) and (d).

3.2.2 Revised Protocol

The following changes were made to address the shortcomings of the previously described protocols:

– The first challenge was the inability to remove sodium hypochlorite from the clay particles, thus creating a toxic environment for bacteria. Therefore, sodium hypochlorite has been fully eliminated in the revised protocol, and the autoclave step remained as the preferred method to ensure that particles were free from any organic contamination that might potentially interfere with bacterial growth. In this approach, the M63* was used as the medium. It should be noted that M63 is able to maintain its chemical properties at high temperatures, thus making it an excellent medium for autoclave processing.

– The second challenge: the low concentration of clay in the medium while using ethanol, ethanol needs to be replaced with a concentrated growth medium, i.e., M63, to allow the clay sediments to separate into phases that correspond to different clay particle sizes. In this approach, the concentration of M63 was tenfold

*The composition of M63 was thoroughly explained in Chapter 2.

increased. By increasing the concentration of the M63 larger clay aggregates sediment rapidly at the bottom of the tube, but small particles sediment more slowly and remain in the supernatant which can be easily collected.

As shown in Fig. 3.5, the clay sample preparation protocol was revised as follows:

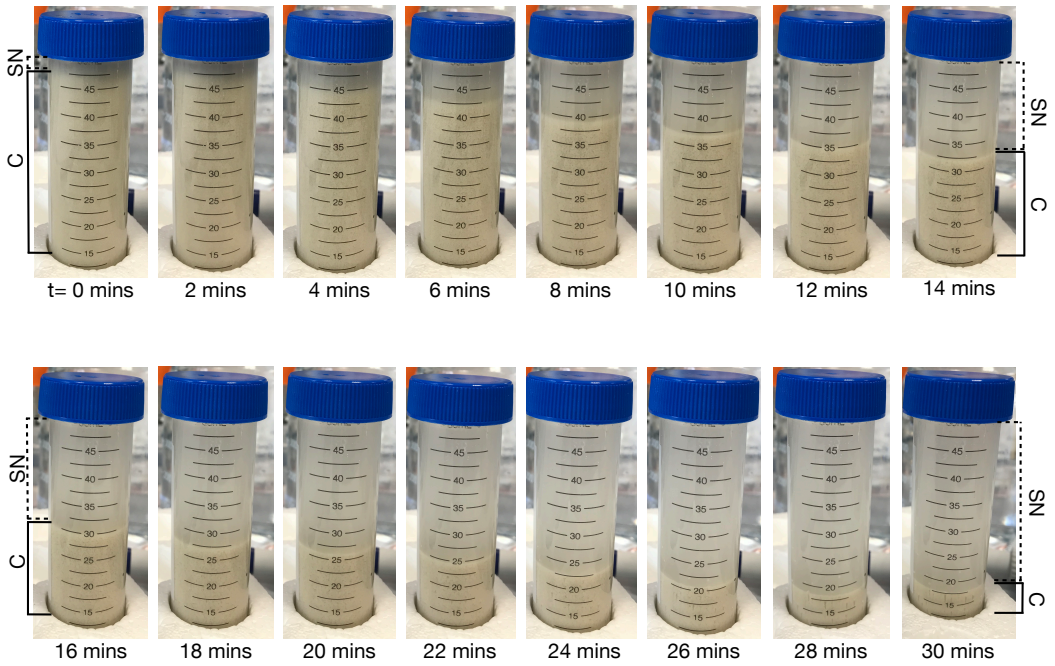

Figure 3.6: The finer clay particles are separated from larger clay aggregates in concentrated M63 via sedimentation. The sedimentation occurred over a period of 30 minutes and the finer clay particles (C) remained in the supernatant (SN) fraction. The photos were taken every two minutes from time zero to 30 minutes.

First, the M63 10X is prepared. It is important to note that M63 was prepared without glucose – as a source of carbon – and that the clay medium will not appreciably alter the carbon content of the media. Next, 1 g of hectorite clay was mixed with 50 ml of M63 10X, and the mixture was vortexed vigorously and then allowed to rest for 30 minutes as shown in 3.6. Then, 20 ml of supernatant, which contained the correct size/density of clay, was collected and diluted in 180 ml sterilised distilled water to get M63 1X. The mixture was then sterilised using autoclave for 20 minutes at 121°C.

Having the clay ready, the next step is to prepare the appropriate media required for bacterial competitions that will be used in Chapter 4. In the following, two different types of media will be developed: M63 and Casein.

3.2.3 Clay In Growth Media

– **M63 clay medium preparation:** To prepare the M63 clay medium, the sterile clay sample was mixed with sterile M63 1X with 0.2% (w/v) glucose. The autoclaved clay is 25% of the total volume of the M63 clay medium and the protocol for making M63 medium is explained as follows: The base M63 medium (pH 7.0) contained 2.0 g/l of $(NH4)_2SO_4$, 13.6 g/l of KH_2PO_4, 0.5 mg/l of $FeSO_4[H2O]_7$, and 0.2% (w/v) of glucose. Then the medium was supplemented with 1 mM of $MgSO_4$, 0.35 mM of $CaCl_2$. The protocol for making M63 with glucose medium was dissolved in sterilised distilled water and was filtered using a disposable vacuum filter (Corning). Then the filtered M63 1X with glucose was added to the sterilised clay and supplemented with the mixture of filtered $MgSO_4$ and $CaCl_2$. The pH was adjusted to 7.0, which is the optimum pH for bacterial growth, using filtered KOH 2M and the total volume will be filled up with sterilised distilled water to 200 ml. This procedure is shown in Fig. 3.7.

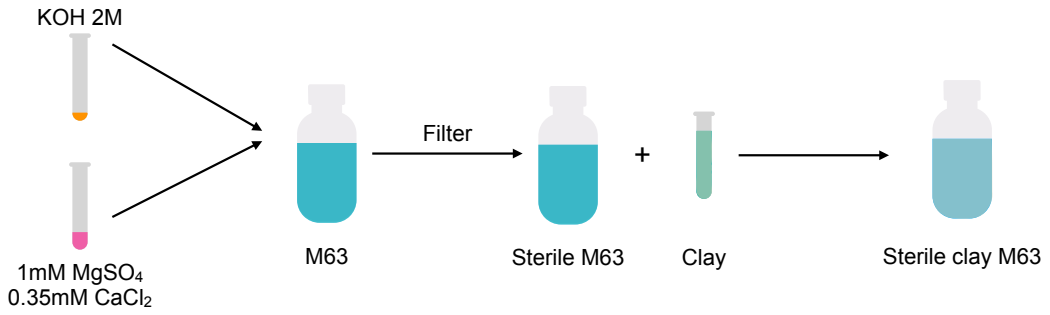

Figure 3.7: Clay M63 medium preparation. During the preparation of clay M63, the clay was autoclaved, but the rest of the medium was filtered before mixing with the clay.

– **Casein clay medium preparation:** Casein is an alkaline protein that is soluble in environments with pH above 7 *. The casein medium is pH sensitive and when the pH of the environment decreases, the casein precipitates. Therefore, the casein bottle should be on the stirrer throughout the entire preparation process to ensure that it is continuously well-mixed.

In both M63 with glucose clay medium and casein clay medium, the volume of autoclaved clay was 25% of the total volume of the media. The casein medium contains 0.4% (w/v) casein dissolved in 2M KOH and PBS. The dissolved casein was then diluted in sterilised distilled water and supplemented with 10μM of

*Further details are provided in Chapter 2.

$CaCl_2$, 20mM of $MgSO_4$. To sterilise the casein medium before adding it to the sterilise clay sample, the mixture was filtered. Then the sterilised clay sample was gradually added to the mixture of casein to prevent pH shock and casein precipitation. The pH of casein clay medium was adjusted to 7 using filtered HCl 0.1M. Adjusting pH in casein is very challenging as the HCl is a strong acid. Therefore, the HCl 0.1M needs to be added to the casein very slowly – on a drop-by-drop basis – with constant stirring. This procedure is shown in Fig. 3.8.

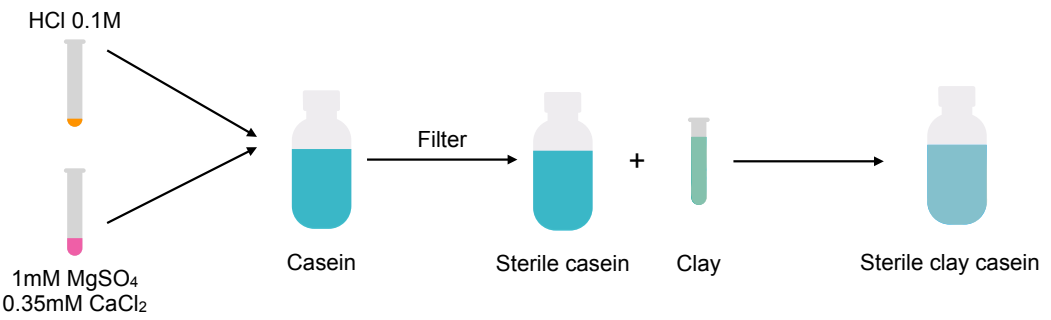

Figure 3.8: Clay casein medium preparation. Since casein is sensitive to pH, all materials need to be thoroughly mixed together before adding casein to the clay medium. The pH of the clay casein medium was then adjusted with filtered sterilise HCL 0.1M.

3.2.4 Adjusting Clay Concentration

As it will be explained in Chapter 4, the amount of clay to be used in the experiments needs to be optimised to provide a realistic representation of clay density found in soil microaggregates in the natural environment. Increasing the concentration of clay particles dispersed in the liquid medium increases the likelihood of bacterial attachment with clay particles, several samples containing different amounts of clay, e.g., 1 g, 4 g, 10 g, were prepared using the method described above. However, no noticeable changes to the concentration of clay in the fraction of the supernatant were observed (shown in Fig. 3.9), suggesting that the amount of clay in suspension saturates at 1 g per 50 ml of M63 10X.

To overcome this issue, the protocol was revised to find another way to increase the clay concentration in the media. In the revised protocol, the method of preparing the clay for 1 g concentration was repeated four times, resulting in four bottles of 200 ml clay in M63 1X. Then after autoclaving the bottles, 165 ml of the clear M63 1X (supernatant) was removed and 25 ml of clay from the bottom of the bottle was collected as a clay sample. This step was repeated for all the four

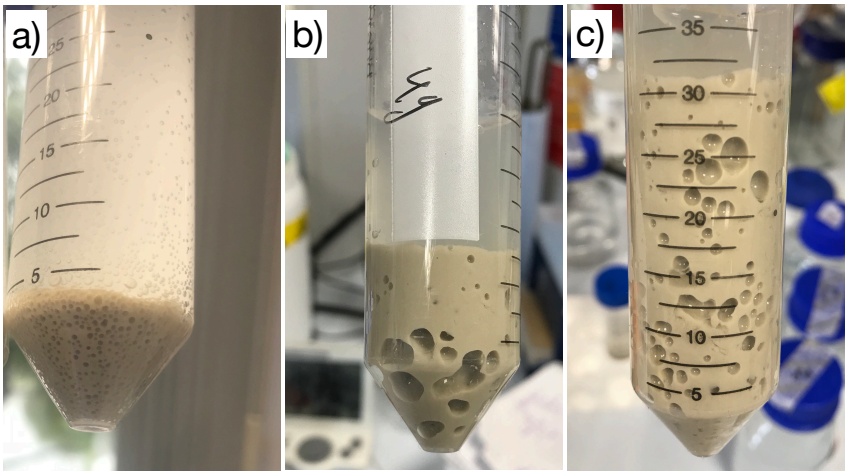

Figure 3.9: Different concentrations of clay mixed with M63 10X medium: (a) 1 g as control, (b) 4 g and (c) 10 g of clay mixed with 50 ml of M63 10X. Incubation time for all three samples was 30 minutes at room temperature.

bottles and the four 25 ml of the clay were combined to make a 100 ml clay sample with higher concentration as illustrated in Fig. 3.10.

3.3 Microaggregate lab model development

3.3.1 Bacterial inoculation in the clay media

Once the clay-medium was prepared, it is necessary to test the medium for bacterial growth and microaggregate formation. The process of introducing different genotypes of bacteria for each experiment will be thoroughly discussed in Chapter 4, however, in this section the procedure of mixing only one bacterial strain, ON2-WT, and its role in the microaggregate will be discussed.

First, a bacterial colony was resuspended in a rich medium, liquid LB, with the incubation temperature of 30°C and shaking speed of 200rpm for bacteria to grow overnight. When bacteria reached the stationary phase after 15 hours, the overnight cells were inoculated into a fresh liquid LB to reach the exponential phase. Then, bacteria was transferred to the clay medium to initiate the microaggregate formation process. In the following sections, three criteria that play an important role in the formation of microaggregates will be discussed.

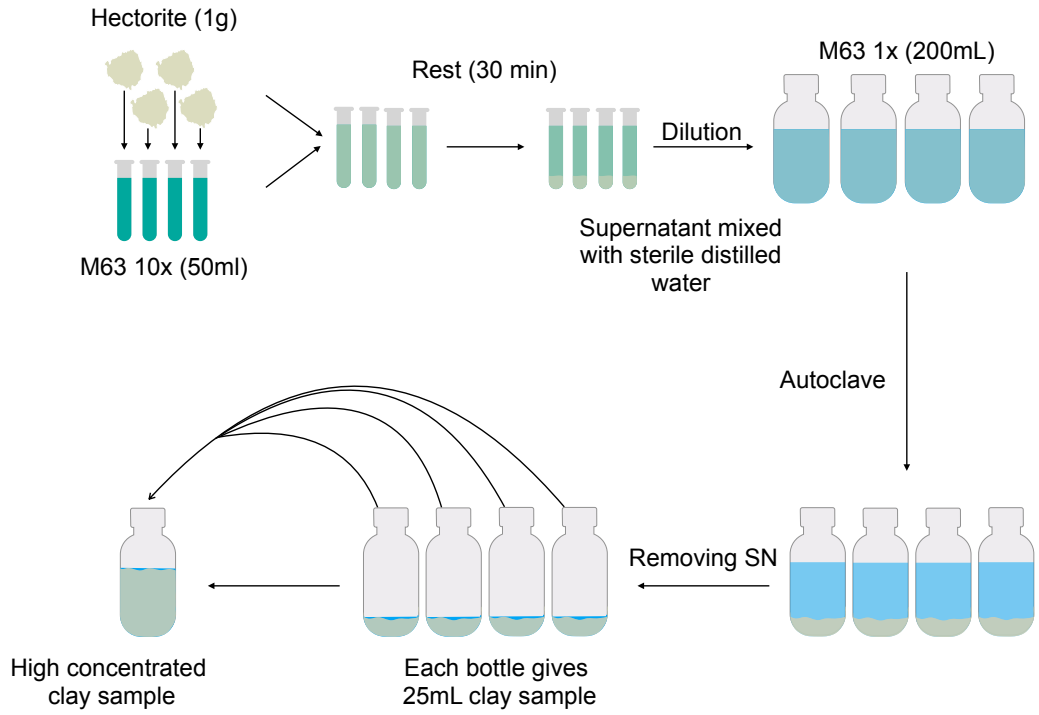

Figure 3.10: Schematic illustration of clay medium preparation with four times larger clay fraction. The clay samples were prepared according to the protocol and then the supernatants were removed after 30 minutes, mixed with sterilised distilled water and autoclaved. The autoclaved clay rested on the bench for an hour before removing the liquid fraction, then the clay fractions were mixed together to make a four-fold more concentrated clay sample.

3.3.2 The impact of bacterial growth on microaggregate formation

Carbon is an essential nutrient for bacteria [206], and lack of its availability will impact bacterial growth, which may influence microaggregate formation. To compare the structure of aggregates in media with and without glucose in the presence of bacteria the following experiment was conducted.

First, clay samples were prepared in M63 without glucose. A 0.2% (w/v) glucose-containing M63 with clay medium was also prepared as the control. Next, the ON2-WT bacteria was inoculated to both clay media, and the clay samples were then incubated for 24 hours in the incubator shaker *. The bacteria exhibit robust growth at a temperature of 30°C under well-mixed conditions. The incubator shaker was set on 30°C and the shaking rate of 220 rpm during the experiment. The samples were then transferred onto a microscope slide following the completion of the experiment. It needs to be noted that, for a microscopic study of the microaggregate fractions, microaggregates should be collected with care so that the structure of each microaggregate is preserved. In this regard, the largest pipette tip with capacity of 1000 μl, was used to extract the microaggregates from the sample. As shown in Fig. 3.11, a third of the tip was cut with sterilise scissors to reduce shear stress so the structure of the microaggregates stayed relatively intact.

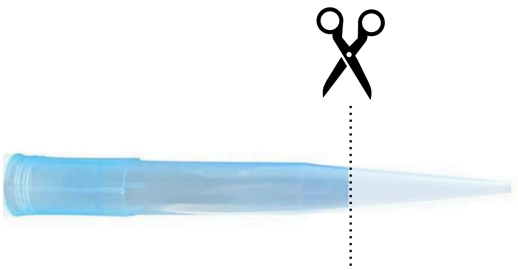

Figure 3.11: A third of the blue tip was cut off to minimize structural damage to the microaggregate.

As a result of the short incubation time, aggregates with a minimum size of 20 μm that may contain bacteria are considered microaggregates. Microaggregates are measured by their longest dimension. As can be seen in Fig. 3.12(a-b), the size of aggregates that were formed in clay medium without glucose, were considered to be at the smaller end of microaggregates. In contrast, Fig. 3.12(c-d) shows that the size of microaggregates in clay medium with glucose, is substantially larger.

Due to lack of source of carbon in the M63 sample without glucose, the bac-

*Stuart incubator orbital shaker SI600C

terial growth is remarkably lower than in M63 medium with glucose. The microscopic results of this experiment showed that higher bacterial growth in presence of glucose (shown in Fig. 3.12(d)) resulted in formation of larger aggregates compared to the sample in which bacterial growth was affected due to lack of glucose (shown in Fig. 3.12(b)). This finding can confirm the importance of bacterial activity and secretions in microaggregate formation by cementing clay particles together.

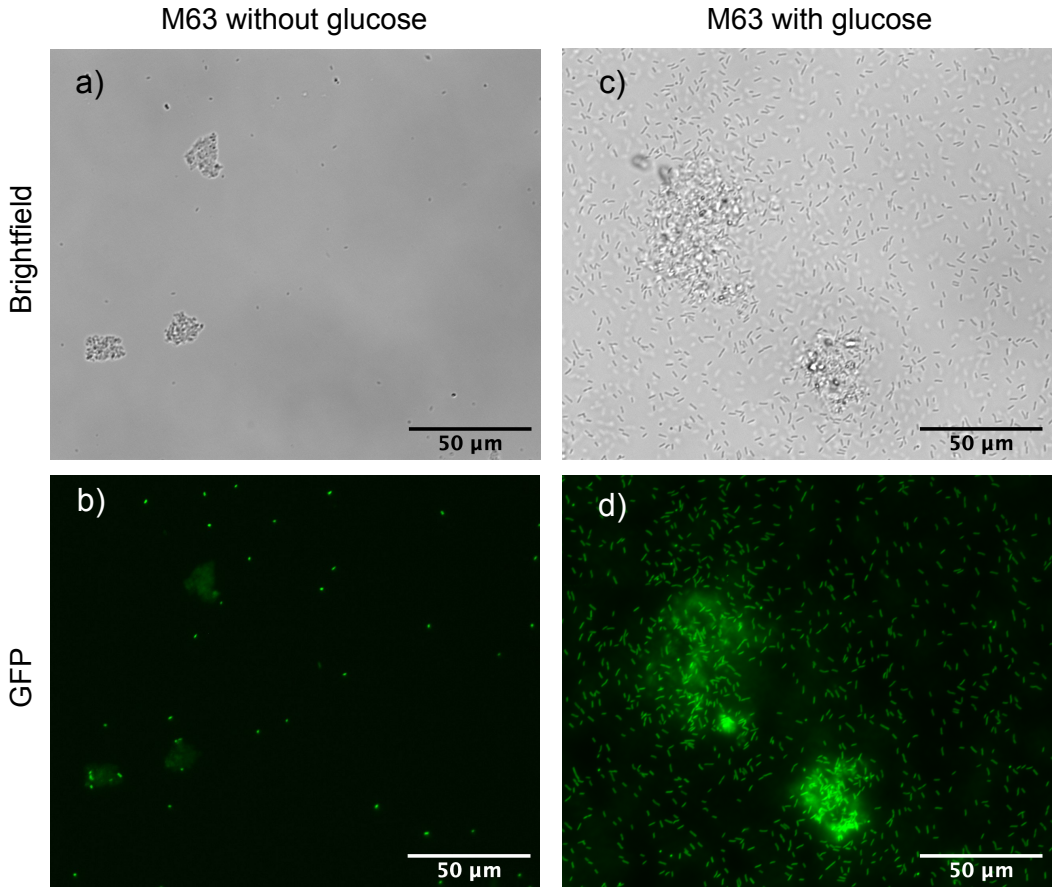

Figure 3.12: The stability of the microaggregate structure relies on bacterial activity and their extracellular products. The images in the top row were taken using a brightfield filter, while those in the bottom row were taken using a GFP filter. (a) and (b) are the mixture of clay and GFP labelled bacterial culture in M63 medium without glucose, (c) and (d) the same clay and bacterial culture but in a M63 with glucose. Samples were incubated at 30°C, with shaking at a speed of 220 rpm.

Microaggregates are typically between 20 μm to 250 μm in size. However, during microscope studies, it is observed that they are between 50-100 μm in size which is on the smaller end of the spectrum, indicating that the environment is not favourable for developing the microaggregates to the larger ones. Hence, a

revision of the incubation protocol for microaggregate formation is necessary to find an optimal condition for microaggregate formation. The following sections examine the influence of temperature, aeration rate, and time on microaggregate formation in order to determine optimal conditions.

3.3.3 Optimisation: Temperature and aeration rate

Initially, a protocol was created based on the optimal temperature and the aeration rate, which were set at 30°C and 220 rpm, respectively, using the incubator shaker for the growth of bacteria. Hence, these conditions were initially set as starting points. However, having incubator shaker speed of 220 rpm proved not to be an optimal situation for developing a microaggregate structure since the rapid agitation of the shaker can cause structural damage and result in the breakage of the microaggregate into smaller aggregates. This breakage will cause the bacteria to detach from the microaggregate and release into the liquid medium, where they will continue to grow.

In order to avoid this problem, the temperature and the shaking speed of the incubator should be optimised, and therefore, a variety of different temperatures and shaking speeds have been tested. In the optimised protocol, the incubation temperature was decreased to 21°C and an orbital shaker* was used to minimise the disruption caused by agitation. This shaker generated much less vigorous shaking compared to the one previously used. A speed of 110 rpm was chosen as the minimum speed at which the shaker could provide a constant orbital shaking. The revised protocol was applied to ON2-WT-GFP cells inoculated in 10 ml clay M63 medium with glucose and the tube samples were placed on the surface of the slow shaker in a horizontal position. The horizontal position of the tubes on the slow shaker causes the clay medium to slosh back and forth between the two ends of the tube, which results in a higher aeration rate which is an important factor for growth of the bacteria. The same preparation process was followed for the control sample, except that the incubator's temperature of 30°C and shaking speed of 220 rpm were applied. Prior to microscopic imaging, both samples were incubated for 24 hours.

The result of the revised protocol can be seen in Fig. 3.13(c-d), which displays a substantial change in the size of microaggregates. Under the slower agitation conditions, most of the microaggregates form larger aggregates that reach 150-200 μm in length. In the control sample, shown in Fig. 3.13(a-b), microaggregates with smaller size demonstrating that the combination of the incubation temperature and speed rate, which was 30°C and 220 rpm respectively, was not a suitable

*IKA KS 260 S002 laboratory shaker

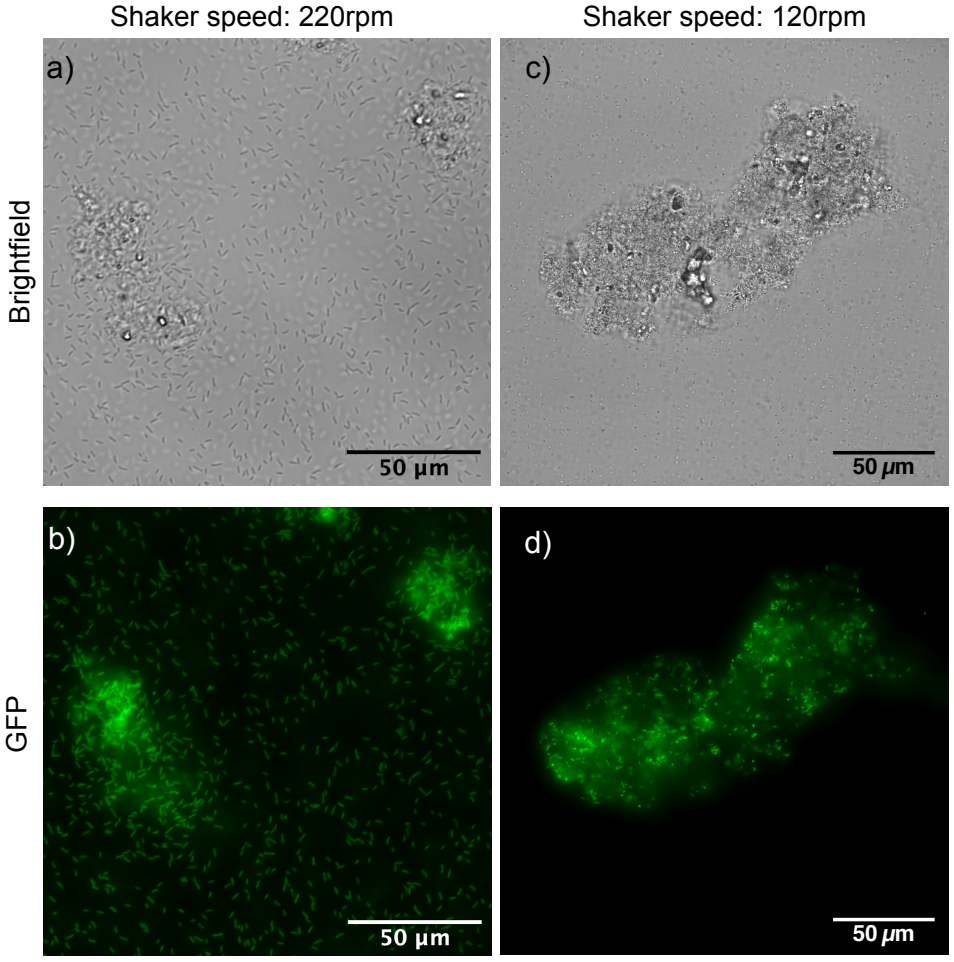

Figure 3.13: High-speed shaking provides more aeration for bacteria to grow but prevents the development of large microaggregates. The left images are bacterial culture in clay M63 medium incubated for 24 hours at 30°C with a shaking speed of 220 rpm. The right images are after adjusting temperature and aeration rate to 21°C and 110 rpm respectively. The samples were imaged using brightfield and GFP imaging.

condition for the mixture of bacteria and clay medium to develop larger aggregates. In contrast, by slightly slowing bacterial growth, the lower temperature, larger aggregates with higher cell density was observed in Fig. 3.13(c-d). The new protocol and settings can be used to study microaggregate structure, clay aggregate-bacteria interactions, and the process of microaggregate formation in greater detail.

3.3.4 Microaggregate formation over time

As shown in Fig. 3.14, the mixture of clay and bacteria could develop a microaggregate structure under optimum conditions. During the next 24 hours, the clay and bacteria gradually attached to each other and formed a stable structure. However, in general, there is very little information available about microaggregate formation in *in vitro*. We will examine different stages of microaggregate formation using fluorescent microscopy in this section.

For this experiment, four samples were prepared for imaging microaggregates at different times, i.e., 0, 6, 24, and 48 hours. On each sample, four 50 ml Falcon tubes of clay M63 medium were prepared and inoculated with bacteria with the same optical density of 0.05. The samples were vortexed and placed horizontally on the slow shaker at room temperature.

In Fig. 3.14, microaggregate formation is illustrated over time. At t = 0, there are individual clay particles and bacterial cells, in which no microaggregate structure can be seen. The interaction between clay and bacteria allows for the formation of aggregate structures, which are the earliest stages of microaggregates. At time-points of 24 hours and 48 hours, shown in Fig. 3.14(e-f) and (g-h), The aggregates were gradually developed into microaggregates with an expanded bacterial community and toward the larger end of defined microaggregate size range. Upon completion of the experiments, t = 48h, the aggregates have a size beyond 250 μm. This occurs when the microaggregates are joined together and form a larger aggregate.

This achievement was the result of developing a microaggregate laboratory model that created an environment in which bacteria could develop a complex and robust bacterial community within the aggregate. The microaggregate lab model appears to offer similar conditions to soil microaggregates with the ability to adapt to a range of media and bacteria. Thus, it allows us to study the interaction of bacteria within microaggregates and examine the impact of the microaggregates on bacterial life as will be thoroughly discussed in Chapter 4.

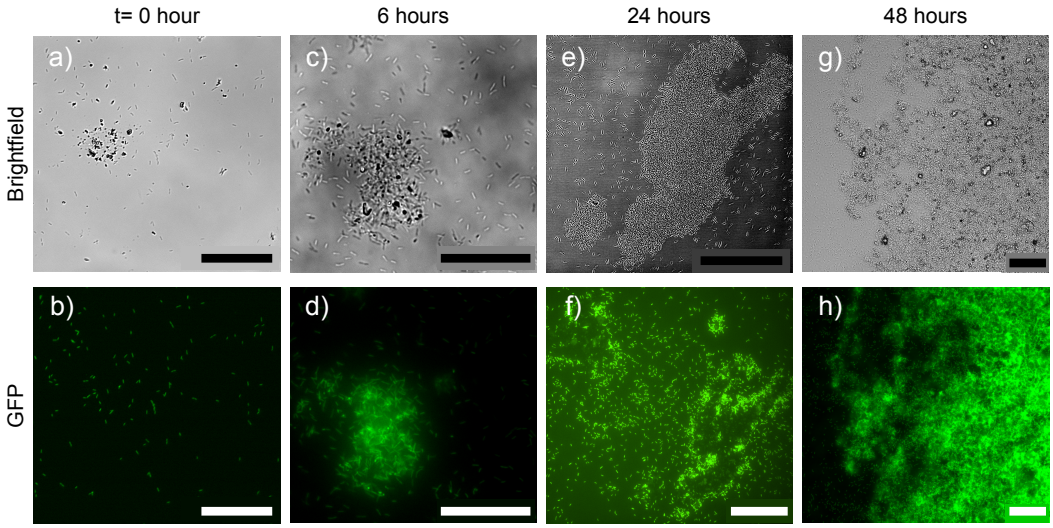

Figure 3.14: Microaggregate formation and development over the period of 48 hours time. The mixture of clay and bacteria was imaged from time zero to 48 hours after incubation on a slow shaker at room temperature, 21°C. Results demonstrate microaggregate formation from clay particles to an early stage of microaggregate to a mature microaggregate with size around 250 μm. The images are taken by fluorescent microscope with brightfield and GFP filters. Bars are 50 μm.

3.4 Discussion and conclusion

Soil carbon sequestration is a promising method to reduce atmospheric carbon dioxide concentrations, in which its ability to serve as a carbon sink is largely determined by the total amount of organic carbon remaining inaccessible to degradation in the soil. As such, microaggregates, which are the most stable fractions in soil and can keep organic materials for a very long time scale (100-300 years), are crucial elements in storing carbon. Many research studies have been focused on microaggregates structure and the interaction between bacteria and microaggregates. Despite this, there is relatively little knowledge as to how microaggregates are formed and how bacteria interact with each other in clay particles.

Building a model of microaggregates in the laboratory is an excellent way to gain a deeper understanding of (i) how microaggregates are formed, ii) how their structure will develop over time, and iii) the role of bacteria in formation and stability of microaggregates. Nonetheless, there are a number of technical challenges associated with this, one of which is the creation of a protocol, as there was previously no such protocol currently in existence. The design of a protocol is a complex process since there are many parameters that need to be optimised.

In particular, it is important to note that these parameters - such as temperature and aeration rate - are interrelated and that changing one parameter will have an effect on others.

In this chapter, a comprehensive protocol for creating a laboratory-scale model of microaggregates has been developed and optimized. Fig. 3.13(c-d) illustrates that the microaggregates developed in the laboratory can reach to the size of 250 μm which is on the larger end of the spectrum. Furthermore, the results revealed that the formation of microaggregates is largely driven by bacterial activity. Finally, the development of microaggregates over time in this chapter. Following the development of the laboratory model of microaggregates, the next chapter will examine the effect of clay particles on bacterial competition.

Chapter 4

Bacterial competition in soil microaggregates

4.1 Introduction

All ecosystems depend on bacteria to perform critical functions, including nutrient mineralisation, decomposition, and the removal of natural and anthropogenic toxins [207]. Many of these processes involve the conversion of insoluble substrates into smaller compounds, which the bacteria assimilate for growth and metabolism [161]. Aside from environments where readily metabolised nutrients are available, bacteria utilise secreted extracellular enzymes, such as digestive enzymes, to acquire nutrients [151].

Extracellular enzymes are chemical, secreted by a cell and functions outside that cell like signaling molecules, siderophores, and digestive enzymes [208]. These enzymes help bacteria to adopt and grow in different environments but their production is costly for the cell. Therefore, the cost to benefit ratio of producing these enzymes has to be sufficient for their producer cell to be able to continue producing it [209]. In this study, digestive enzyme is considered as the model system, in which the producer bacteria secret the enzyme to digest non-labile nutrients into soluble compounds to enable bacteria to acquire the carbon they need from their surrounding environment and grow [210].

Because these enzymes – also called "public goods" in the field of social evolution – function outside the cell, reaction products can diffuse away from the enzyme-secreting bacteria [211]. In environments with high diffusion rate, these nutrient-rich extracellular enzymes can be utilised by neighboring cells that may or may not be involved in their production [212]. Such bacteria that could intercept these products without secreting their own enzymes are generally called "cheaters"

or "free-loaders" in behavioural ecology, because they do not pay the cost of synthesising enzymes but benefit from the products they did not produce [126]. By avoiding this cost, cheaters can gain a competitive advantage and increase their individual fitness and reproduction rate compared to the enzyme producers [41]. Consequently, if the producer strain does not benefit from its secretions because they are diffused away from the producer cells or are uptaken by cheats, exploitation of the producer strain will become more likely [126].

With the absence of population spatial structure and high rates of mixing, a liquid culture is favourable for cheaters (non-producers), because all organisms compete directly in a relatively homogeneous resource pool, allowing cheaters to have equal access to enzymes supplied by producers. This gives cheaters a clear competitive advantage over producers to invade and take over the population as shown in Fig. 4.1 [213, 214].

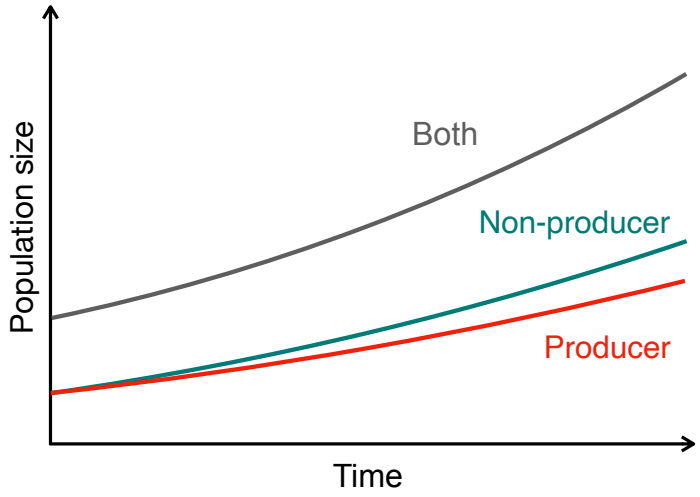

Figure 4.1: The costs and benefits of producing public goods. Shown are the growth rates of populations consisting of producers and non-producers (e.g., of a digestive enzyme) and producers in a population started with a 50:50 mixture of both. The graphs show that non-producers spread and out-compete producers in a well-mixed environment. Image reproduced from [215] with permission.

The stability of public good production in many systems is rather difficult to explain from an evolutionary perspective [216, 217]. In the bacterial population, selfish cheaters can put the public good producer cells at the risk of exploitation [218]. However, the question is how do the producer cells survive in this situation and how does the public good remain evolutionary stable?

Many natural systems contain a large degree of spatial heterogeneity [219, 220, 221, 222, 223] that is an important determinant of bacterial functions and popula-

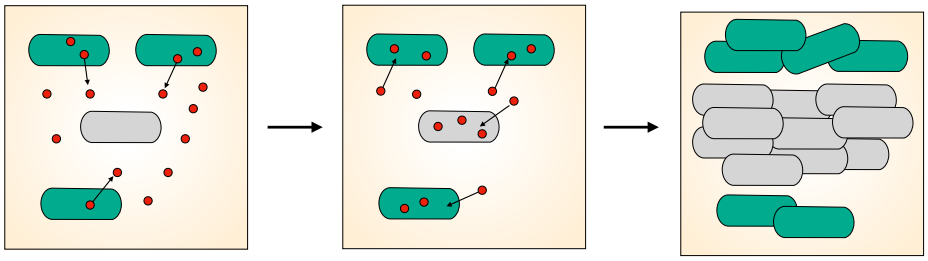

Figure 4.2: The tragedy of the commons with public goods. Cheats (gray cells) who do not pay the cost of producing public goods (red circles) can still exploit the benefits of public goods produced by other cells (green cells). This allows for cheats to increase their reproductive rate. Image reproduced from [215] with permission.

tion dynamics. It has been shown that populations often behave very differently in spatially heterogeneous structures as opposed to that which occurs in well-mixed environments [224]. For instance, previous research claimed that heterogeneity in the environment like in biofilm can increase the spatial segregation between two bacterial populations [138]. In fact, thicker biofilms provide an environment where the diffusion rate inside the structure is lower than the outside environment. As a result, the secreted enzymes can remain close to its producer cell and accumulate, meaning the producer cell can benefit from the digested nutrients in order to grow. This mechanism allows the producer cells and its secreted enzyme to remain evolutionary stable [133].

As discussed in Chapter 3, microaggregates are composed of diverse soil organic matter (SOM), soil minerals, such as clay particles, and biotic materials, such as soil bacteria, that bound together by wide range of physical, chemical and biological process [103, 225]. However, very little is known regarding the details of the microaggregate formation process.

Microaggregates host microbial populations whose stability partially relies on their activity. Living within a microaggregate structure can be beneficial for the bacteria. For instance, (i) lower diffusion rate within microaggregates can prevent the costly secretions from moving away from the cell that produce them, (ii) the physical property of microaggregate structure can protect bacteria against other predators, and (iii) the surface of the clay is able to adsorb chemical compounds, such as enzymes, SOM, nutrients, which makes them more accessible for bacteria to utilise. On the other hand, being within a microaggregate can pose a disadvantage to bacteria living within it because the physical structure of microaggregate may prevent bacteria from having access to the nutrients outside of this structure.

While there have been extensive experimental studies on the social evolution

of bacteria in homogeneous cultures, such as liquid, and heterogeneous environment, such as biofilm, [224, 226, 161], very little experimental studies were conducted in real soil microaggregates. Previous works have suggested that spatial structure and limited diffusion rate of an environment promote coexistence of cheater and producer strategies [138, 126, 133, 37, 227, 228]. It is important to note that the validity of this statement has not been challenged experimentally in soil microaggregate due to the complexity of such experimental processes. In fact, there have been no experimental quantification and visualisation of the way bacteria compete in microaggregates environments prior to this study.

One of the main features of microaggregates is their capability to provide a physical barrier in which bacteria can be protected against predators. This will be achieved by providing a physical structure that protects the enzymes produced by the bacteria and allows the bacteria to use the enzymes themselves in the context of an interaction with other bacteria. In this regard, there are multiple factors that can influence the interaction between producers and non-producers as listed below:

- **Reduced diffusion rate inside microaggregates:** Since microaggregates can potentially block the diffusion of secreted enzymes, the enzymes will remain inside the microaggregates, where they can be consumed preferentially by producers.

- **Chemical adsorption by clay particles:** The adsorption of clay particles in microaggregates demonstrates a remarkable capacity to adsorb different materials, such as organic substances and secreted enzymes, resulting in enhanced transport and bioavailability of chemical constituents and nutrients.

However, little is known on the structure of soil microaggregates and its impact on bacterial interactions and, consequently, on the outcome of bacterial competition. The purpose of this chapter is, therefore, to examine how bacteria behave and compete with one another in microaggregate structures using microscopic imaging and counting the number of cells at the end of the competition. Experiments of this type, however, are extremely challenging because:

1. The development of a laboratory model of soil microaggregates to accurately mimic the natural soil microaggregates is dependent on optimisation of several parameters, as described in detail in Chapter 3.

2. After the competition has taken place, it is necessary to quantify the number of both bacterial strains within microaggregates. To achieve this, the bacteria

need to be separated from the microaggregates, a process we call "breaking" process. Performing this procedure is very sensitive because it is extremely challenging to separate bacteria from microaggregates without killing the bacteria in the process.

3. Once the bacteria are separated from microaggregates, they need to be counted highly precisely and quickly to prevent potential sources of inaccuracy, such as bacterial aggregation and/or subsequent growth.

4.1.1 Aims of this chapter

This chapter aims to establish a laboratory-based system for examining bacterial competition within microaggregates and develop a protocol for assessing the results. In this regard, several technological advances have been made in order to overcome the challenges associated with breaking, counting, and microscopic imaging techniques so that accurate experimental results can be obtained in order to gain a deeper understanding of bacterial competition in soil microaggregates.

The rest of this chapter is as follows: In Section 4.2, the experiments for bacterial competition in clay environments will be designed in which several parameters, such as the type of bacterial strains and growth media, length of the experiment, and the laboratory conditions in which the bacteria compete, will be discussed in detail. Next in Section 4.3, several breaking techniques will be introduced, their effectiveness will be evaluated, and the best methods will be selected. Following this, a number of measurement and counting techniques will be discussed, their effectiveness will be evaluated experimentally, and the appropriate methods will be chosen in Section 4.4. In Section 4.5, microscopic studies will be utilised in an effort to get a better sense of how spatial structure affects bacterial competition. Lastly, Section 4.6 provides a detailed analysis of the results, which will be followed by a summary of this chapter.

4.2 Experimental design of bacterial competition in clay environments

In this section, two bacterial strains were selected to compete for a single resource, digested casein, in a clay environment. To have a better assessment on the role of microaggregates, bacterial growth was measured both in growth media containing clay and in media without clay. Furthermore, as a control, both bacterial strains competed in a media that does not require enzymes to metabolise. Throughout

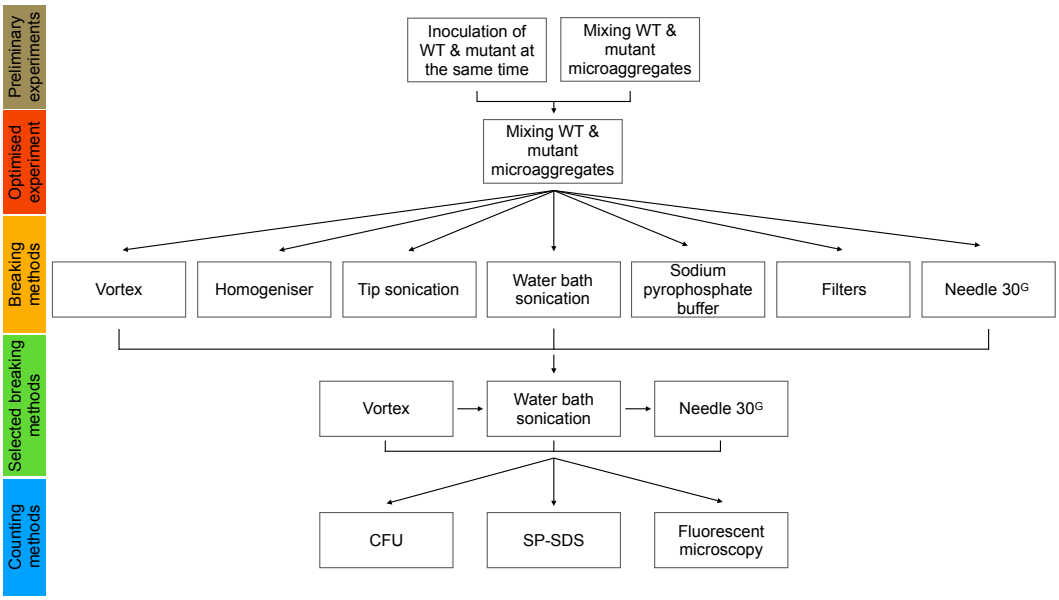

Figure 4.3: An illustration of the process of optimisation before and after the bacterial competition experiment in order to accurately analyse the results.

the following sections, the procedures involved in designing, optimizing, and conducting the experiment for the purpose of quantifying and assessing the bacterial competition will be described in detail.

4.2.1 Candidate bacterial strains and growth media

The model bacterium used in this project is *P. fluorescens*, which is a well-studied soil bacteria with versatile metabolism [229]. A detailed description of the characteristics of this psychrophilic soil bacterium, which is widely found in a soil environment, is given in Chapter 2. This section presents the reasons why this particular bacterium was selected for the bacterial competition.

Due to its versatile metabolism, *P. fluorescens* is able to survive in a wide variety of different environments, such as soil, decaying leaves, plants, milk and freshwater habitats [230]. The dairy industry has struggled with milk spoilage due to the proteolytic activity of *P. fluorescens* [231]. Studies have shown that *P. fluorescens* possesses an alkaline metalloprotease protease called AprX that digests casein, which is the main protein in milk [232]. The production of AprX protease is essential for *P. fluorescens* to digest casein and to thrive in an environment where it is the sole source of nutrition. In fact, an *aprX* mutant strain of *P. fluorescens* will not survive the same casein medium. Therefore, two strains in this project were used, ON2-WT which produces AprX and ON2-Δ*aprX* which does not produce AprX. Liquid casein was used as the medium in bacterial competition experiments. Also

as a control medium, casein was digested with filtered proteinase K, which bacteria did not need to produce AprX in order to grow in it [233].

4.2.2 Length of the experiment

Following the selection of the bacterial strains and the media, the next step involves determining the incubation time for the bacterial competition. The incubation time should be long enough for bacteria to utilise all the nutrients but before starvation and cell death occurred. Thus, an experiment was designed to grow ON2-WT and ON2-Δ*aprX* strains as mono-culture and co-culture in casein and digested casein media without clay on slow shaker with different incubation times. The time points of 24, 48, and 96 hours were considered, and the number of cells were counted from each time point as shown in Fig. 4.4. Comparing 24 and 48 hours time points, 4.4(a) and (b) respectively, it is indicated that the duration of 24 hours was not sufficient time for cells to grow. Also, between 48 and 96 hours time points shown in Figs. 4.4(b) and (c), the reduction in cell numbers after 96 hours suggests that the length of incubation was too prolonged for the cells. According to the results, during 48 hours of incubation, the bacterial cells will have sufficient time to grow and compete in the casein environment, but not so long that the number of bacteria starts to decrease.

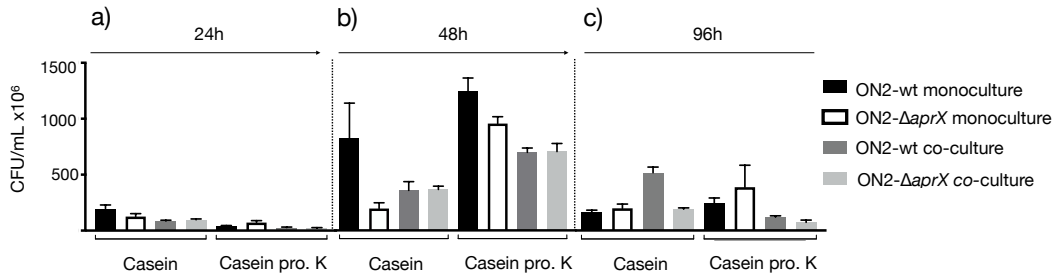

Figure 4.4: The optimal duration of the bacterial competition was determined to be 48 hours. The ON2-WT and ON2-Δ*aprX* were prepared as mono-culture and co-culture in casein and casein with proteinase K (digested casein) media without clay and incubated on a slow shaker† at the room temperature with three different incubation times, (a) 24 hours, and (b) 48 hours. Based on the CFU counting results, after 24 hours of incubation, there was still nutrient available in the cultures, suggesting that the incubation time needs to be extended in order to maximise the time for bacterial competition. Also, by comparing CFU counting results at 48 hours time point with (c) 96 hours, the reduction in number of cells after 96 hours incubation suggests that the length of incubation was too prolonged for the cells. Based on these results, 48 hours of incubation will give the cell enough time to grow and compete in casein.

ON2-WT and ON2-Δ*aprX* samples were prepared as a mono-culture and co-culture, respectively, and incubated at room temperature on a slow shaker (Laboratory shaker: IKA KS 260 basic S002) for the aforementioned three time periods. The details on sample preparation will be explained in Section 4.2.3.1. The results after 24 hours of incubation, shown in Fig. 4.4(a), indicates that the difference between WT and mutant mono-cultures in casein is beginning to reflect the disadvantage of the protease deficiency of ON2-Δ*aprX* in casein.

LB liquid medium was used to grow cells to the exponential phase before inoculating them into the casein-based media. As a result, residual LB medium is transferred into the casein and provides a small amount of nutrients that the protease deficient cells can be benefited from. Counting the number of cells after 48 hours and 96 hours of incubation shows that the difference between wild-type and mutant cells in mono-cultures is greatest after 48 hours as shown in Fig. 4.4(b), and the difference then decreases, as illustrated in Fig. 4.4(c). The reduction in results after 96 hours of incubation occurs due to cell lysis. This indicates that an incubation period of 48 hours is sufficient for ON2-WT to grow in casein before lysis occurs, which was observed after 96-hours of incubation.

4.2.2.1 Sample preparation for bacterial competition

P. fluorescens ON2-WT and ON2-Δ*aprX* strains were streaked from $-80°$C freezer stock onto LB agar plates without antibiotics and incubated at 30°C for 15 hours. A single colony was picked and resuspended in LB liquid for overnight growth at 30°C in a Stuart IS600 incubator shaker at 220 rpm. The growth of the overnight culture was measured using a Biochrom WPA Biowave DNA spectrophotometer at 600 nm (OD_{600nm}. Next, the overnight culture was inoculated into fresh LB liquid with a starting OD_{600nm} of 0.05.

To begin the experiments, cells were grown to the exponential phase (OD_{600nm} 0.2–0.4) in LB. In the case of mono-culture, the bacterial cells were inoculated into the considered fresh media (casein or digested casein) with an OD_{600nm} of 0.01.

In the co-culture sample, however, the start point OD_{600nm} of each bacterial strain was half that of the mono-culture. Thus, ON2-Δ*aprX* and ON2-WT were inoculated in a fresh media with an OD_{600nm} of 0.005. The total number of bacteria in co-culture equals the number of bacteria in mono-culture. The media with and without clay were prepared in this project where bacterial competition was examined. Details on how the clay media were prepared was thoroughly discussed in Chapter 3.

Samples with clay and without clay were placed on a slow shaker set to 110 rpm at room temperature for 48 hours. Once the incubation period is completed,

samples were collected, and the clay samples were prepared for microaggregate breaking treatment to determine the number of bacterial populations within the microaggregates. For the purpose of this project, which is to investigate the role of microaggregates in bacterial competition, the number of ON2-WT and ON2-Δ*aprX* cells were counted within microaggregates and in the liquid media separately to determine the fitness of each strain in each environment. To accomplish this, the fraction of the microaggregate samples needed to be separated from the liquid fraction with a minimal amount of mixing between the two functions.

4.2.3 Optimising the bacterial competition experiment

In Fig. 4.5, the CFU‡ counting and microscopic results of the co-culture of ON2-WT and ON2-Δ*aprX* in casein medium with clay was shown. In order to image single cells in media with or without clay, Nikon Ti-E inverted fluorescence microscope with CPI Plan Apochromat 60X Lambda oil objective was used. In this experiment, the number of ON2-WT and ON2-Δ*aprX* cells are very similar and there are no substantial differences between wildtype and mutant strains, as it is shown in Fig. 4.5(a).

Microscopic images of the co-culture sample in casein with clay, shown in Fig. 4.5(b), revealed that both producer and non-producer strains were well-mixed inside the microaggregates. In the event that both strains occupy the same space within the microaggregate (as it is illustrated in Fig. 4.6(a)), the digested casein produced by the AprX, secreted from the ON2-WT cell, will be accessible to the ON2-Δ*aprX* cell as well. Thus, the mixed genotypic population within microaggregates could explain the similarity between the number of ON2-WT and ON2-Δ*aprX* cells in the co-culture sample in casein with clay. The Fig. 4.5(b) is the image taken from co-culture of ON2-WT-CFP-Km^r and ON2-Δ*aprX*-YFP-Sm^r strains in casein medium with clay after 48 hours of incubation using fluorescent microscopy. In the natural habitat of the soil bacteria, due to the spatially heterogeneous structure of soil, the mixing rate of bacterial cells is reduced and cells in planktonic states are fewer than cells attached to soil surfaces [234]. Therefore, it is likely to expect soil bacterial cells to be more genotypically patchy.

4.2.3.1 Mixing monoclonal microaggregates in a co-culture

To increase the likelihood of ON2-Δ*aprX* and ON2-WT forming clonal patches within a microaggregate, the experiment was optimised to allow each bacterial

‡Refer to Section 4.4.1 for further information regarding the (Colony Forming Unit (CFU) counting technique.

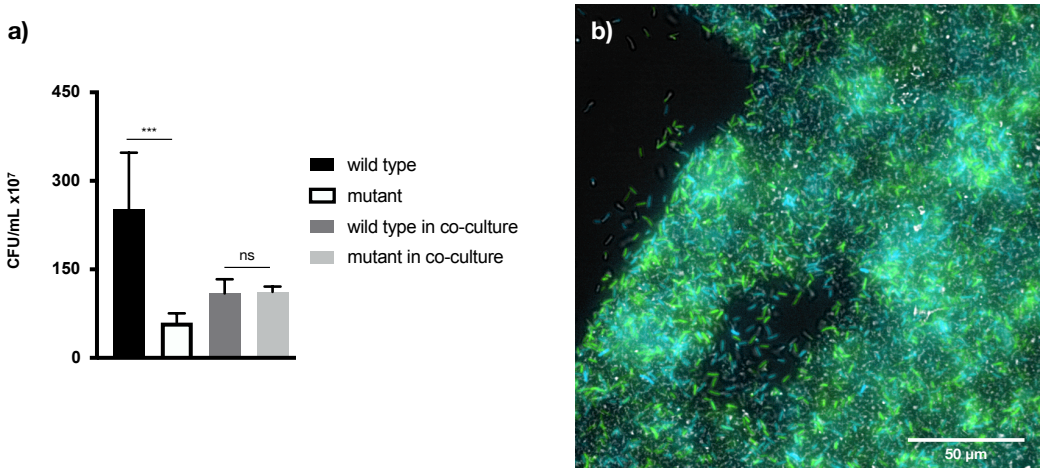

Figure 4.5: The ON2-Δ*aprX* cells in a genotypically mixed bacterial populations within a microaggregate can benefit from the ON2-WT secreted AprX; (a) result of the CFU counting of ON2-WT-CFP-Km^r and ON2-Δ*aprX*-YFP-Sm^r, mono-cultures and co-culture from microaggregates fraction in casein with clay medium after 48 hours of incubation; (b) fluorescence microscopic image of ON2-WT-CFP-Km^r and ON2-Δ*aprX*-YFP-Sm^r co-culture in casein clay medium after 48 hours of incubation. Error bars indicate mean and standard deviation *** p<0.005, ns (not statistically significant) p>0.05.

strain to get mixed with clay separately and form aggregates. In this respect, ON2-WT and ON2-Δ*aprX* strains were prepared as explained in Section 4.2.2.1 until the cells reach the exponential growth phase. Cells from the exponential phase were inoculated into separate tubes containing M63 clay medium and incubated at room temperature on a slow shaker with a speed of 110 rpm for 14 hours. It is noteworthy that both strains are predicted to grow equally well in M63 due to their access to labile nutrients. During this process, bacteria grow slowly and form microaggregates in clay M63 medium.

Upon completion of the incubation time, both tubes of ON2-WT and ON2-Δ*aprX* strains were gently transferred and mixed into one 50 ml Falcon tube, shown in Fig. 4.6(b). Mixing these two microaggregates together maximises clonal patchiness in the subsequent co-culture and for the experiments involving bacterial competition in clay media, this method was used to prepare samples. Figure 4.6 is an illustration of this process. The samples rested on a benchtop for 30 minutes so that the microaggregates sediment to the bottom of the tube. Next, the liquid supernatant containing the planktonic cells were removed without taking sedimented microaggregates. Then, 10 ml of a freshly prepared particular media, either casein or digested casein with proteinase K, was slowly added to the tubes

without disturbing microaggregates, and the tubes were placed on the slow shaker at room temperature to initiate the bacterial competition experiment. The rest of the experiments are conducted in the same manner.

It is important to emphasise that both bacterial strains started off at the same point, ensuring equal opportunity in the competition. Therefore, ON2-WT and ON2-Δ*aprX* mono-cultures in M63 with and without clay media were prepared and incubated for 14 hours along with the other samples. These tubes, which are called start-point tubes, were counted after 14 hours of incubation to represent the starting point for ON2-WT and ON2-Δ*aprX* cells in the competition experiment. In order to avoid frequency-dependent selection of bacterial competition, it was essential to start the experiment with an equal amount of ON2-WT and ON2-Δ*aprX* in the co-culture and to exclude any start point where the difference between ON2-WT and ON2-Δ*aprX* was by a factor of two or more. The CFU counting result shown in Fig. 4.7 presents the equal number of ON2-WT and ON2-Δ*aprX* cells in media without clay and with clay respectively.

4.2.3.2 Separation of solid and liquid fractions

Microaggregates formed during the incubation process and need to be separated from the liquid phase at the end of the competition. This step is necessary because the bacteria in the liquid fraction of the clay media are expected to behave similarly to bacteria in a liquid culture without clay. Since this study investigates the role of the spatial structure of microaggregate in bacterial competition, it is essential to avoid unnecessarily mixing these two fractions of clay media.

Following the incubation time, the tube sample was allowed to rest on the bench for 30 minutes to separate the microaggregates, as illustrated in Fig. 4.8(a). The resting process allowed the microaggregates to sediment to the bottom of the tube. The liquid fraction was then gently removed from the tube using a pipette as depicted in Fig. 4.8(b) until all liquid fractions have been removed from the sample as shown in Fig. 4.8(c). Afterwards, the microaggregates were prepared for the breaking treatment.

4.2.4 Post-competition treatments

Once the competition time for bacteria was completed and the supernatant fraction was separated from microaggregates, the samples were prepared for breaking and then enumerating cell density. By breaking aggregates, cells within microaggregates will separate from clay particles (as it is shown in Fig. 4.9), which is necessary in the process of accurate counting. The breaking and counting steps

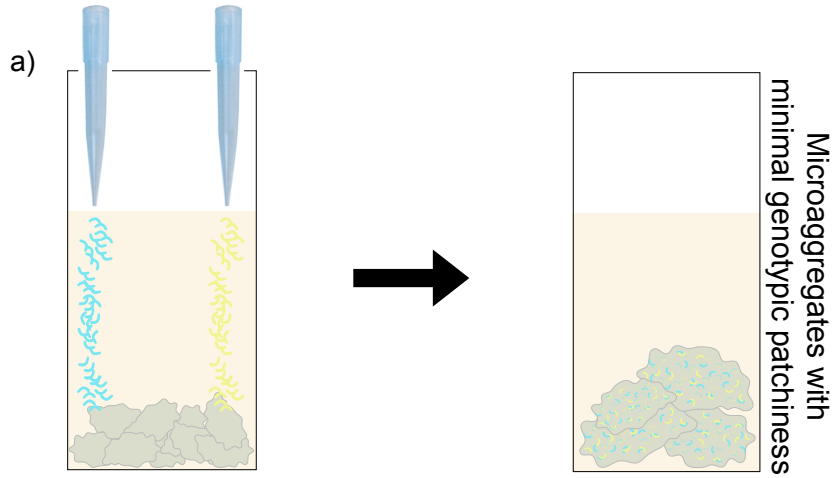

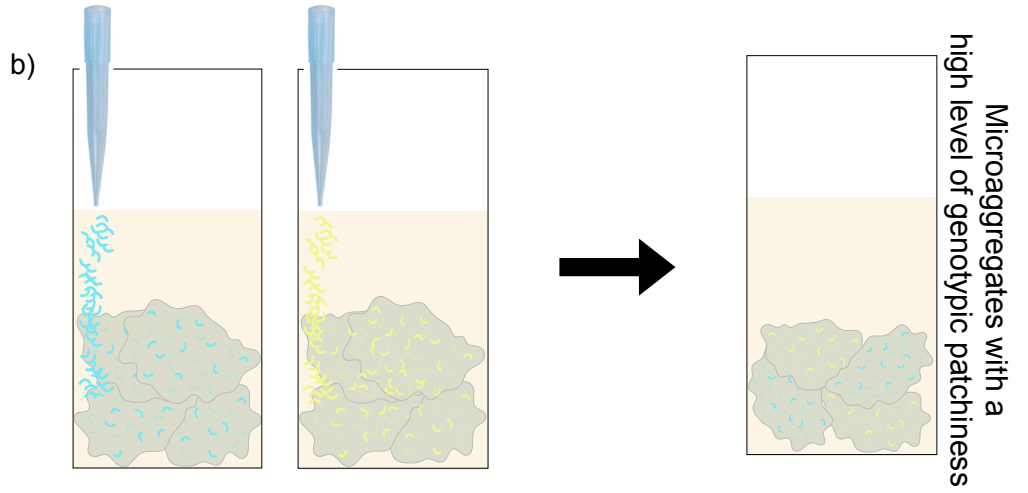

Figure 4.6: Experiment optimised to increase genotypic patchiness in microaggregates. In the previous experiment, both strains were added to the clay medium at the same time (a), which caused well-mixed bacterial strains in the microaggregates. However, by growing each bacterial strain in clay media separately (b), microaggregate will be formed with individual bacterial genotypes, and then two mono-cultures were mixed to prepare a co-culture sample. During this process, bacteria with the same genotype grow in microaggregates and form a high level of genotypic patchiness. Such genotypically patchy bacterial populations are expected in soil microaggregates due to the structure of the soil which limits mixing of bacterial populations and the fact that bacteria are more likely to be attached to soil surfaces rather than being in a planktonic state.

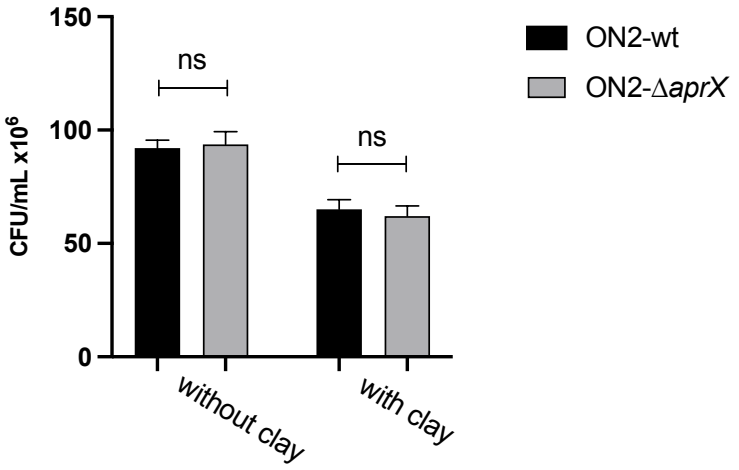

Figure 4.7: ON2-WT and ON2-Δ*aprX* strains had approximately the same cell density in the start point samples prior to the initiation of bacterial competition. The CFU counting was utilised to determine the number of bacterial cells. The ON2-WT and ON2-Δ*aprX* cells in M63 media with and without clay as the start point samples were placed on the slow shaker alongside other samples at room temperature for 24 hours. The start point samples were treated to be counted, while the rest of the samples were prepared for the bacterial competition. The difference between ON2-WT and ON2-Δ*aprX* in M63 medium without clay was statistically not significant as well as their difference in M63 with clay. Error bars indicate mean and standard deviation. ns: not statistically significant. p>0.05.

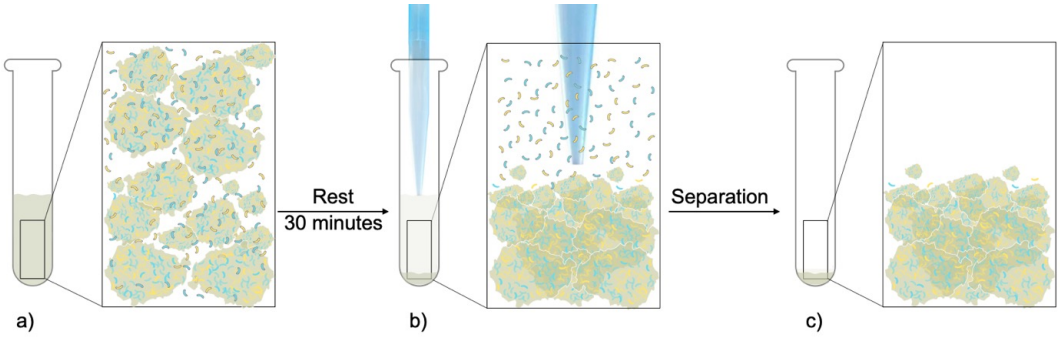

Figure 4.8: Separating the liquid fraction from the microaggregates is necessary to accurately measure the bacterial populations within microaggregates. (a) Upon completing the incubation time on the slow shaker, the microaggregates are suspended in the liquid culture. (b) Microaggregates are allowed sediment to the bottom of the tube after sitting on the bench for 30 minutes. Therefore, (c) the liquid and microaggregate fractions were separated. From one another bacterial populations in the liquid fraction are in the planktonic state and should not be mixed with bacterial populations within microaggregates during the breaking phase.

are essential for measuring and analysing bacterial populations inside microaggregates as they help us evaluate the relative fitness of each bacterial strain in a given environment and determine the outcome of the bacterial competition in different media.

The breaking step is when bacteria within a microaggregate can detach from the aggregates. Microaggregates are highly robust structures due to their bond between clay particles and bacteria. The strong binding between bacteria and clay particles may affect the accuracy of the measurement of density of different strains within microaggregates. Hence, the counting process needs to be accurate in order to assess the outcome of the bacterial competition in microaggregates precisely. It is of the utmost importance to determine and employ the most precise breaking and counting methods. Thus, in this study, different breaking and counting methods were utilised and a summary of all the optimisations can be found in Fig. 4.3. Although breaking and counting are two separate processes, a sample must be counted to assess the effectiveness of a breaking method by measuring the variability between technical replicates. As thoroughly discussed in the following section, the efficacy of each technique was evaluated by the CFU counting and microscopic imaging techniques.

4.3 Breaking treatment techniques

There are two factors which make the breaking process particularly challenging:

1. Microaggregates are robust and cannot be easily broken.
2. The breaking process must avoid damaging bacterial cells in order to accurately quantify the bacterial population within a microaggregate.

Many studies have been conducted on the bacterial population in soil fractions [235, 236, 237]. In the majority of these studies, it was essential to extract the cells from the soil without causing damage to the bacterial cells [238]. However, due to the strong bond between bacteria and clay particles, this process was not a straightforward process. Therefore, different mechanical and chemical methods were investigated in this study in order to determine the most effective method of disrupting microaggregates and other forms of aggregation without damaging the inside cells. [239].

To perform a breaking treatment, a mono-culture of ON2-WT-CFP and ON2-WT-YFP were grown on casein clay medium. First, samples were prepared using the same method explained in Section 4.2.3.1, and at the end of each bacterial

competition experiment, the solid phase was separated from the liquid phase as explained in the Section 4.2.3.2. The microaggregate fraction was then mixed with a buffer.

Phosphate-Buffered Saline (PBS) was the buffer used for mechanical breaking, while in the case of chemical treatment, a sodium pyrophosphate buffer was used instead in order to reduce aggregation of smectite clay particles.

The following section describes the implementation procedure for breaking techniques as well as their characteristics utilised in the study.

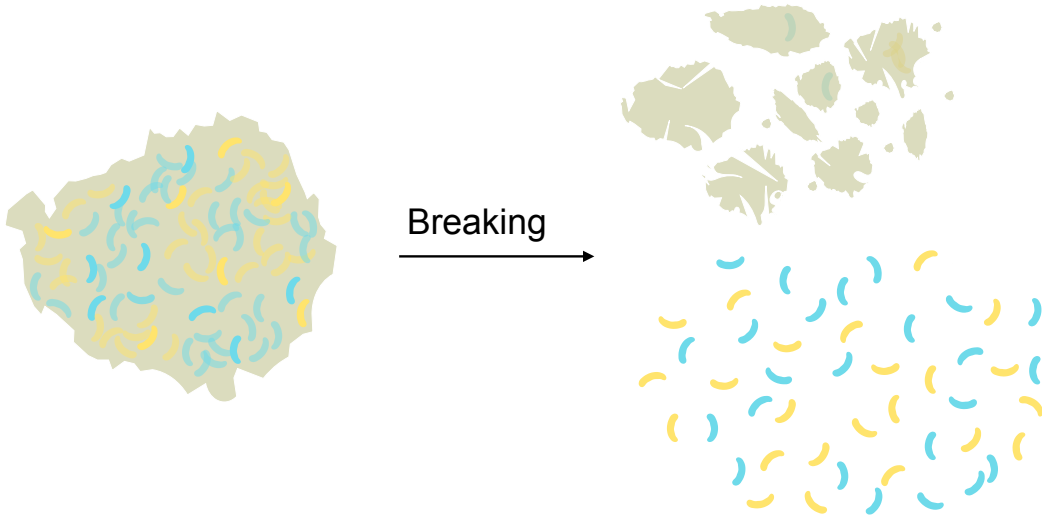

Figure 4.9: Breaking soil microaggregates in order to release bacterial cells attached to the clay particles.

4.3.1 Breaking microaggregates with vortex

Using vortexer to break up aggregates in culture is a common method of separating aggregations whilst limiting damage to the cells [233]. In this project, a Stuart Scientific SA8 Vortex Mixer was used, and samples were vortexed at a maximum speed of 2500 rpm for a duration of two minutes. The vortexing procedure was performed right after PBS was added to the separated solid part of the sample.

To evaluate the effectiveness of the vortex method in breaking the microaggregates, a drop of supernatant was placed on a microscopic slide. Microscopic images of the vortexed sample, shown in Fig. 4.10(a), however, indicated that there were still significant numbers of cells still attached to microaggregates. There is a tendency for *P. fluorescens* cells to aggregate and stick together. In fact, species of the genus *Pseudomonas* are known for exhibiting this behaviour in order to increase their survivability [240]. This occurs when the cells are in the stationary

phase, and bacteria are stressed as they have limited access to nutrients in their culture.

While the vortexing approach was able to loosen up the bonds of microaggregates, it was not able to completely break down their structures to extract bacteria, so using a stronger breaking method was necessary. It was concluded that this method can be used in conjunction with other methods to weaken bonds in aggregates before applying more aggressive methods.

4.3.2 Breaking microaggregates using a Homogeniser

A Homogeniser is a device that shakes the sample tubes vigorously to break up any aggregates and homogenise the sample. As well as vigorous shaking, using glass beads in the sample tubes could potentially enhance the homogenisation process. In this study, the homogenizing breaking approach was used to determine whether vigorous shaking with or without beads can break the microaggregates more effectively.

The device used here was a MP Biomedical FastPrep 24 Homogeniser with both glass and ceramic beads. The device has a range of speeds, and after evaluating their performance, speed levels of 4 m/s (equivalent to between 3700-4100 rpm) and 6 m/s (equivalent to between 3700-4500 rpm) [241] were chosen for a duration of 10, 20, and 30 seconds. The samples were treated with glass beads (Sigma-Aldrich), ceramic beads (Sigma-Aldrich) and without beads at each of these speeds.

First, six aliquots were prepared to test the homogeniser for no-bead cases at the speed levels 4 and 6, as well as at the time points of 10, 20, and 30 seconds. For each speed, an unhomogenised control sample was also prepared. Once the treatment was completed, the samples were allowed to rest for 30 minutes so that the clay aggregates could settle. Then a 100 μl from the supernatant fraction was spread on the LB-agar plate without antibiotics and the results of counting the number of cells was compared to the number of cells in the control sample.

As depicted in Fig. 4.11, a significant reduction in cells was observed in samples treated in this manner at both speeds when compared to the control sample. Furthermore, it can be deduced that increasing the shaking speed will result in even more damage to living cells. During the vigorous shaking, even small clay particles in the sample may cause the membrane of the bacteria to rupture and damage the cells. Therefore, the challenge of breaking the microaggregate was still unsolved as the vigorous shaking of the homogeniser could potentially break the microaggregates but this also damaged the bacteria.

The experiments were repeated with ceramic and glass beads, and the results

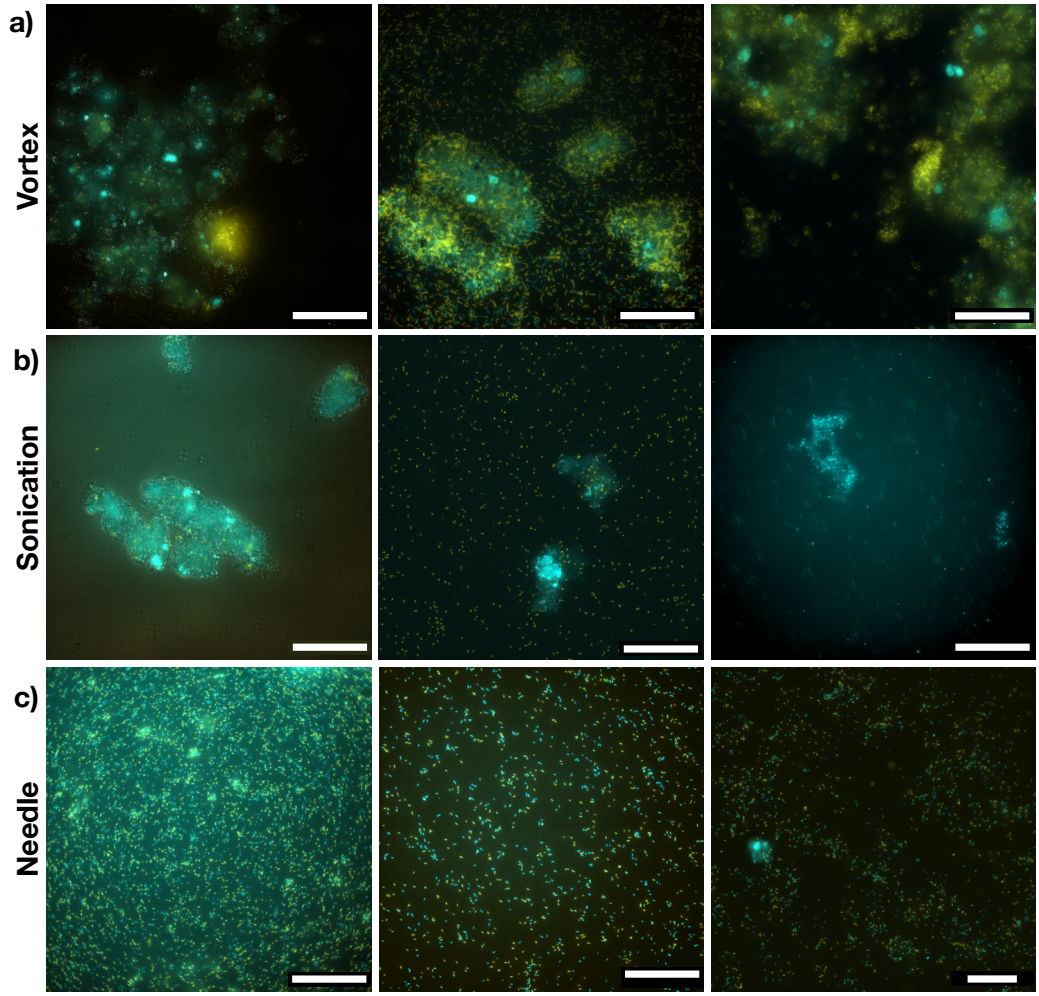

Figure 4.10: Microscopic images of different breaking techniques to break microaggregates. The samples are co-culture of ON2-WT and ON2-Δ*aprX* incubated in clay M63 for 48 hours at room temperature on the slow shaker. Then the supernatant fraction was removed and replaced with sterile PBS before breaking. After each breaking treatment, the samples were allowed to settle for 30 minutes on the bench at room temperature and the supernatant was collected for imaging using fluorescent microscopy with CFP and YFP filters. (a) samples treated by vortexer, (b) by vortexer and water bath sonication and (c) by vortexer, water-bath sonication and 30^G needle. For the purpose of microscopic imaging, ON2-WT was labelled with CFP and ON2-Δ*aprX* was labelled with YFP. Bars are 50 μm.

confirmed that the treatment with both types of beads resulted in a significant decline in the number of living cells (results are not shown). This breaking method was therefore not suitable to be used in this study.

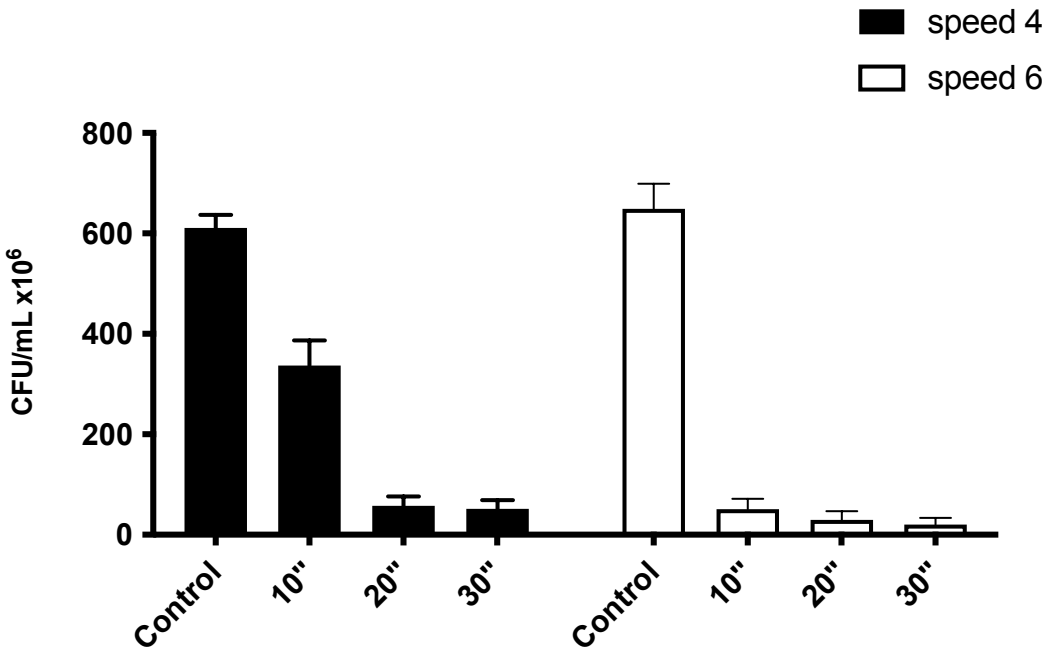

Figure 4.11: The effect of a homogeniser on cell viability. Homogeniser method was used to break aggregates and release cells inside microaggregates. The results shown in black are the ON2-WT in M63 clay that is agitated with speed 4 and results in white are agitated with speed 6. The control samples were only vortexed without being agitated by the homogeniser device.

4.3.3 Breaking using ultrasonic energy to destabilise microaggregates

Sonication is the act of applying sound energy to agitate particles in a sample in liquid. Ultrasonic frequencies (>20 kHz) are usually used, so the process is also known as ultrasonication. Ultrasonic tools are frequently used in wet labs for a wide variety of applications ranging from lysing cells for protein extraction to disrupting aggregate structure to cleaning microscopic glass slides.

Sonication can be conducted using either an ultrasonic water bath or an ultrasonic probe, also known as tip-sonicator. Both tip-sonication and water bath sonication were investigated in this study to evaluate their effectiveness in breaking microaggregates up without damaging the cells.

Tip-sonication is a direct method in which a probe - transmitting ultrasonic energy to the tube sample - is placed inside the tube and transmits the energy

directly to the sample, shown in Fig. 4.12(a). An ultrasonic tip in the laboratory produces a frequency between 20 kHz and 40 kHz, and by adjusting the amplitude of the tip-sonicator device, the intensity of the frequency can be adjusted.

In the case of the water bath sonication, the tube samples were placed in a water bath, and the ultrasonic energy is transmitted to the water first and then to the sample, as shown in Fig. 4.12(c). This method is considered to be less aggressive than the tip-sonication method, as the particles of the sample are agitated indirectly.

To test the efficiency of the tip and water bath sonication treatments, the cultures of ON2-WT bacterial strain were tested to grow in casein media with and without clay. The sample was prepared as a mono-culture, in which its details were explained in Section 4.2.3.2. The clay fraction was separated from the liquid phase following 48 hours of incubation at room temperature on a slow shaker. A 10 ml solution of sterile PBS was added to the microaggregates fraction and vortexed for one minute.

Three aliquots of 1 ml were separated from the same vortexed sample. One aliquot is used as a control sample that did not undergo any sonication treatment. The other tubes were treated with a tip sonicator with a minimum amplitude for three time periods of 5, 10, and 20 seconds. The tubes were placed on ice before breaking so that the heat generated by the tip-sonicator would not damage the cells. The samples were then diluted in PBS to the desired concentration and 100 ml were spread on LB agar plates without antibiotics. The plates were incubated at room temperature and the colonies were counted after 24 hours.

In the case of water bath sonication, sample preparation was carried out in the same manner as the tip sonication approach. In addition, the sample tubes - except the control sample that was not treated by any sonication treatment – were arranged on a floating foam rack so that they remained in the same position during the treatment, and all the tube samples received equal exposure to the ultrasonic energy. Ice was added to the water during sonication to keep the water cool as it tends to warms up during the sonication process.

The water-bath sonication process was conducted at three different time points, of 10, 20, and 30 minutes, in order to determine when the aggregates would be most effectively broken down. Following the sonication process, the samples as well as the control samples were allowed to rest for 30 minutes so aggregates could sediment. 100 μl of the supernatant was spread on LB agar plates without antibiotics. To evaluate the results, the CFU counting method was used. Figures 4.12(b) and (d) demonstrate the sonication results of tip and water bath sonication methods for a ON2-WT mono-culture grown in casein media with and without

clay, respectively. As shown in Fig. 4.12(b), increasing the duration of sonication increases the amount of damage to bacteria cells. In addition, the number of bacterial cells in the control sample is greater than in the two samples treated with tip-sonication, indicating even the lowest level of amplitude transmitted by the tip-sonicator damages bacterial cells.

On the other hand, because the ultrasonic energy is distributed in a more uniform and indirect manner when using the water bath sonication method, the CFU counting results show that this method increased the number of living bacterial cells, as shown in Fig. 4.12(d). This result indicates that cells were released from microaggregates to the liquid. Also, the number of cells increased when the sonication time was increased to 20 minutes, indicating that water bath sonication breaks the microaggregate structure without appreciably damaging bacterial cells. At the time point of 30 minutes, however, the number of cells dropped, suggesting that the sonication for 20 minutes was optimal.

In order to determine the level of homogeneity within the sample, the supernatants of samples that were subjected to 20 minutes of water bath sonication were examined using fluorescent microscopy. Although the CFU counting results indicated that the breaking process had improved, the microscopic images shown in Fig. 4.10(b), revealed that there are still large microaggregates in the supernatant fraction, which could adversely affect the outcome of the counting. The optimisation process was therefore continued to improve the breaking results obtained by vortexing and water bath sonication.

4.3.4 Breaking aggregates chemically, using sodium pyrophosphate

Counting bacterial cells in a soil-based environment requires detaching soil particles, including silt and clay particles, from cells [242]. This process has always been a limiting factor in studying soil-based microorganisms. Different chemical solutions have been used to affect the interaction between soil and the bacterial cell [243]. It is generally believed that, with the help of chemical substances, there is the possibility of weakening the bond between subunits of the soil aggregates [95].

The chemical agents used for separating bacteria from soil minerals could vary from diluted hydrofluoric acid (HF) to sodium pyrophosphate, polysorbate and polyphosphate [244]. Some of these agents are too harsh for living cells and will cause irreversible damage to the bacterial cells [245]. For example, harsh chemicals were used in some studies to lyse the cells and extract the DNA from the cells to measure the quantity of bacteria present in the soil using PCR techniques [246]. The objective of this project is, however, to count the number of living bacteria,

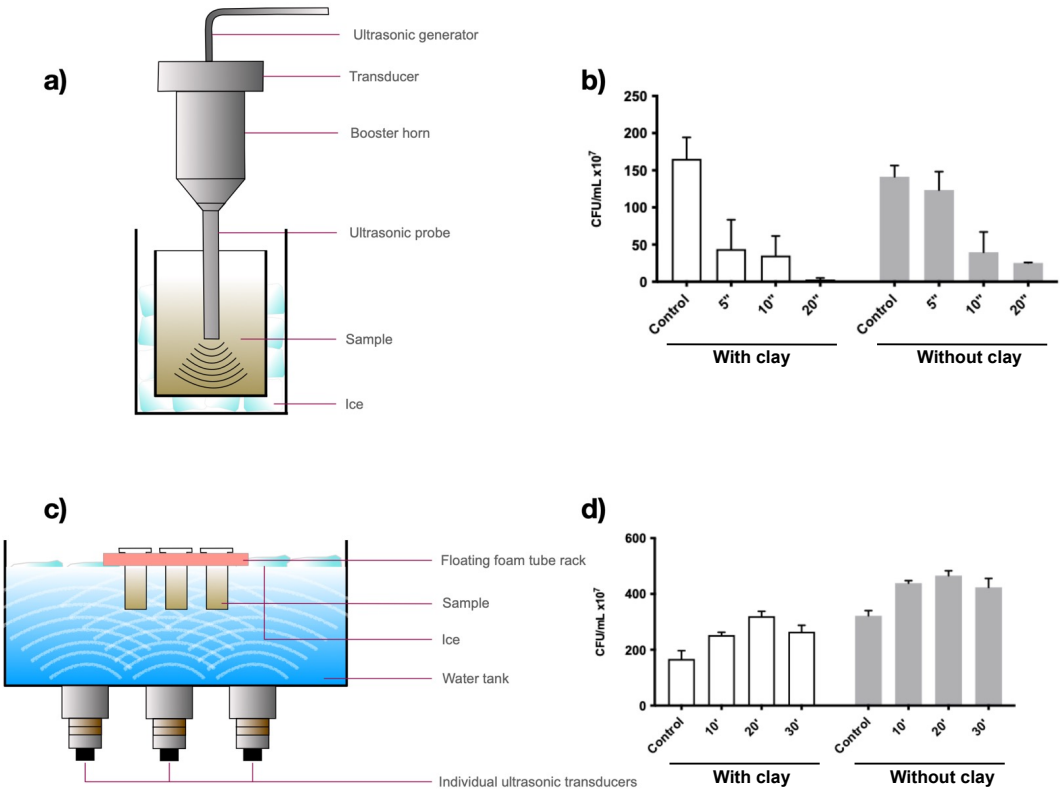

Figure 4.12: Water-bath sonication was a more effective way to break microaggregates without damaging cells compared to the tip-sonication. The incubation time was 48 hours at room temperature with a shaking speed of 110 rpm. The sample used in this step was ON2-WT with and without presence of clay in M63 medium. In each treatment, a control sample was vortexed for one minute following a 48-hour incubation period. (a) is representing a schematic image of a tip-sonicator that directly sonicate the sample, (b) is the result of CFU counting of samples treated by the tip-sonication, (c) a schematic image of the water-bath sonication that sonicate samples indirectly through water, and (d) represent the CFU counting result of samples after treating by water-bath sonication. After 48 hours of incubation, samples without clay (shown in white) and with clay (shown in grey) were treated by sonication devices.

therefore, the chemical agent must be harmless to bacteria.

Sodium pyrophosphate tetrabasic (SPT) is one of the buffers that is frequently used to detach bacteria from sediments [247, 248]. A sodium charged compound like SPT acts as a sodium chelator and facilitates weakening the strong chemical and electrostatic forces as well as hydrogen binding that causes cell attachment to the soil particles. In previous studies, sodium pyrophosphate is repeatedly used in the smectite dispersion process as it inhibits the attraction between clay particles and causes reduction in aggregation rate of clay particles [249, 250, 251].

The sodium pyrophosphate buffer does not have the nutrients needed for bacteria to grow but its pH was adjusted at 7 and it does not contain harsh chemicals to damage bacterial cells. Therefore, to facilitate detachment of bacteria from clay particles, 0.1 M SPT (Na4P2O7, $\geq$95%, Sigma-Aldrich) buffer was prepared by dissolving 0.1 g of sodium pyrophosphate in 100 ml sterile distilled water.

After the bacterial competition in the clay environment was completed, the samples were incubated on the bench for one hour and then the supernatant was removed very gently to prevent disturbance of the microaggregates. Then 9 ml of the 0.1 M sodium pyrophosphate was added in the microaggregate fraction and vortexed for 2 minutes. The mixture then was placed on the slow shaker for 18 hours at room temperature. The sample was then rested on a benchtop for one hour to allow the clay aggregates to settle in the bottom of the tube. The supernatant was collected and diluted in the PBS buffer for subsequent counting and microscopic study.

According to the microscopic images depicted in Fig.4.13, there are still many clumps present in the treated samples, which will impact the accuracy of the aggregate counting. This is because the clay aggregates have been broken up into smaller subunits and, therefore, suspended in the supernatant fraction rather than in the sediment fraction, further affecting the accuracy of this approach. This is confirmed by the CFU counting results, which did not demonstrate significant differences between samples treated with SPT buffer and untreated samples. In conclusion, the chemically-based approach was not appropriate for breaking, and was not chosen for further use in this study.

4.3.5 Breaking aggregates using filters

Previously, the SPT buffer was used as a chemical agent to aid in the detachment of cells from microaggregates, but aggregates remain in the solution with the unattached cells. This could potentially lead to inaccurate measurements since they could attach to the clay aggregates again. In this regard, another method of separating cells from aggregates is to pass them through filters [239]. Using

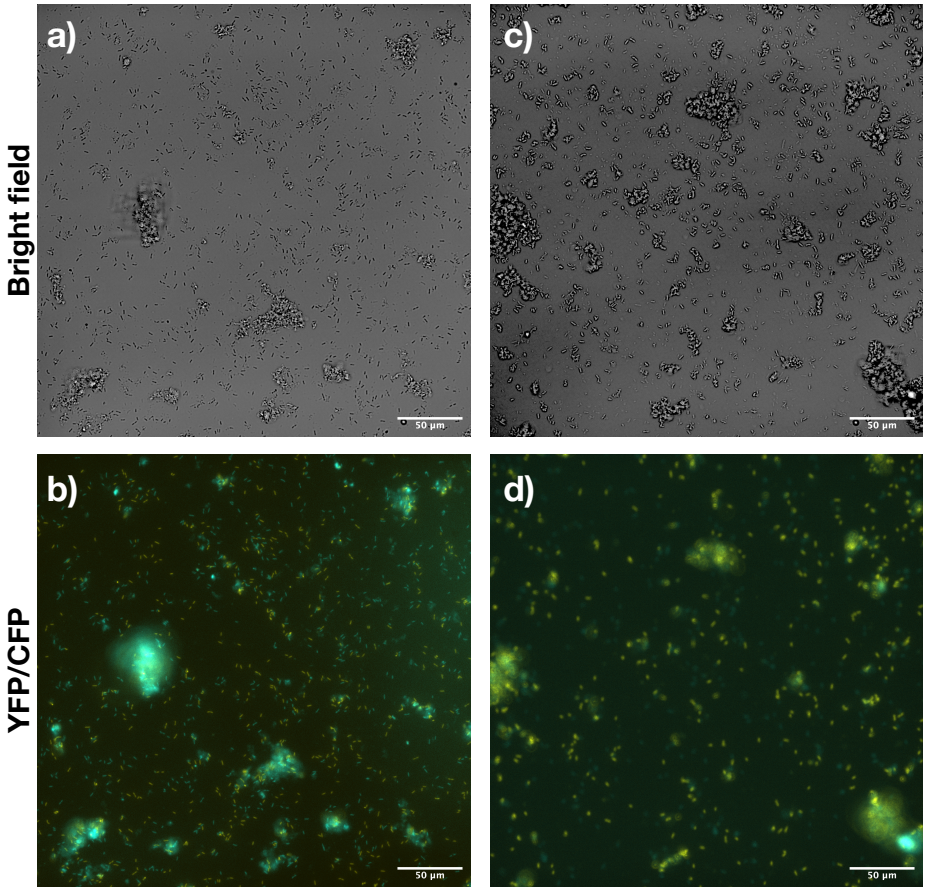

Figure 4.13: The SPT buffer did not sufficiently break microaggregates. The co-culture sample was incubated in clay casein medium for 48 hours, the supernatant was removed, and the clay fraction of the sample was mixed with 9 ml of the SPT buffer. The mixture was vortexed and transferred to water-bath sonication (a, b) and one sample (c, d) was treated only with SPT without vortex and sonication treatments and both samples were incubated on the slow shaker at room temperature for 24 hours. After 24 hours of incubation time, samples rested on the bench for 30 minutes until the solid and liquid phase were separated. The supernatants were collected to check the status of microaggregates after SPT treatment under microscope. Image (a) and (c) were taken with a bright-field filter and image (b, d) with YFP and CFP filters. No difference was observed between samples treated only with SPT and samples with vortex, water-bath sonication in SPT. Presence of small microaggregates with a significant number of cells attached to it shows SPT treatment was not an effective method to break and detach bacterial cells from microaggregates.

a syringe and passing the sample containing aggregates through the filter not only prevents the aggregates from remaining in the sample after breaking but also might facilitate the detachment of cells from aggregates.

In this study, filters with pore sizes of 5 μm, 11 μm, 30 μm, and 40 μm were used and their effectiveness were assessed. The selected filters came in two types: a loose paper filter, and a plastic disposable filter (Sigma-Aldrich Whatman Puradisc). Two sizes of 11 and 30 μm are loose paper filters that need to be cut in order to fit in the cylinder of a syringe.

In this approach, a mono-culture of ON2-WT bacteria in casein clay medium - the preparation is explained in Section 4.2.3.1 - was used. Once the sample was treated with 2 minutes of vortexing and 20 minutes of water bath sonication, 1 ml of the supernatant containing broken aggregates and cells was collected to filter with different pore sizes. The size of a *P. fluorescens* cell is about 1 μm in its smallest dimension, so the 5 μm pore size was selected as the smallest pore size and 40 μm as the filter with largest pore size in this experiment. Then, the supernatant was transferred into the syringe and passed through the filter. The results of using these different filters can be seen in Fig. 4.14.

Although filtering method has been previously used to detach bacteria from soil [252], it was not an effective method for separating bacteria from microaggregates; it was observed that the mesh of the filters with pore sizes of 5 μm, 11 μm, and 30 μm became fully blocked by the clay particles. In this project, the only filter that could pass the supernatant sample through was one with a pore size of 40 μm. The collected filtered sample, however, contained only a very small number of cells that were not representative of the bacterial populations present in the microaggregates (data not shown). This method did not improve breaking progress and, therefore, was not further considered as a breaking treatment in this study.

4.3.6 Applying pressure using fine syringes

In this study, fine needles were used as the last attempt to break down aggregates and release bacteria from microaggregates. Timing plays an extremely important role in the breaking process; if the bacterial culture and the buffer remain for too long, the number of cells will change, which would have a negative impact on the accuracy of the counting process. Therefore, the goal is to find a method to break down the microaggregates without affecting the competition results or the viability of the bacteria.

Breaking aggregates mechanically has the advantage of being relatively quick. One such mechanical technique that was tried in this project involved passing the clay-bacteria mixture through a syringe with a needle gauge size of 30 μm (Sigma

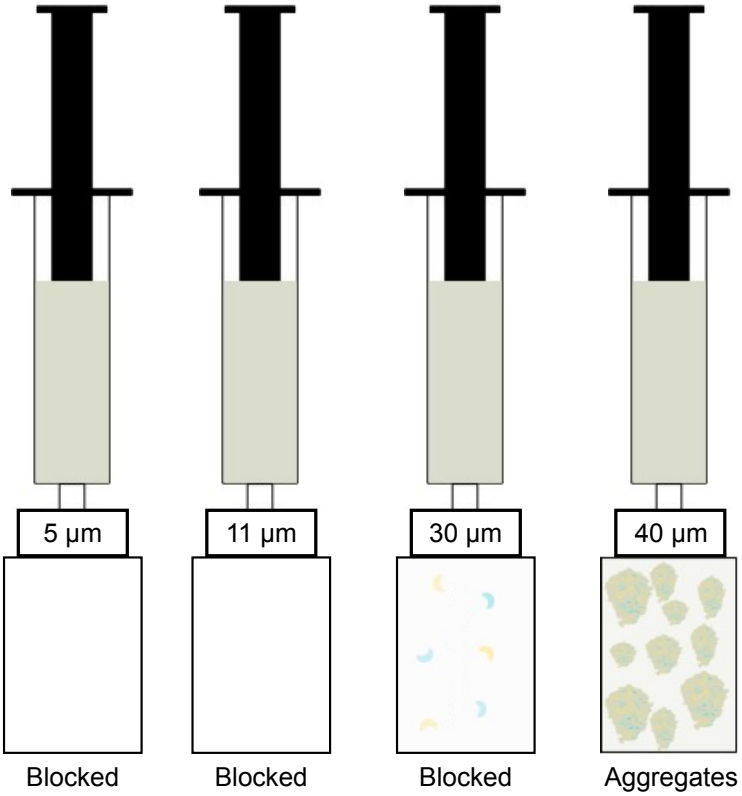

Figure 4.14: Using filters to separate cells from aggregates . Filters with smaller pores (5, 11, and 30 μm) were completely blocked by microaggregates. A few cells could find their way however the filtered sample was very transparent suggesting that the majority of the cells stayed with microaggregates. The 40 μm filter was the only filter that the supernatant could pass through but the microscopic images from filtered samples showed they also contained very few cells (data not shown).

Aldrich). Various needle gauge sizes were also tested, but finer needles generated larger shear stress to break aggregates, which was used in this study.

In this approach, the ON2-WT mono-culture, incubated at room temperature for 48 hours in casein medium with clay, was prepared for the breaking treatments as described previously. After undergoing two minutes of vortex treatment and 20 minutes of water bath sonication, the sample was then passed through a 30^G needle. The sample was collected from the needle using a 7 ml Bijou container. The passage through the needle was repeated five times in sequence. Using the 30^G needle, fewer clumps of clay-bacteria aggregates were observed under the microscope as shown in Fig. 4.10(c) which can improve the bacterial quantification process. The sequence of these breaking treatments (vortex, sonication and needle) was therefore the most effective way to break microaggregates and free up the bacteria that were attached to them found in this project.

4.4 Data analysis

To analyse and assess the results of the bacterial competition, bacterial growth must be measured [253]. However, quantifying the total abundance of the bacterial population and the interaction between bacterial populations in microaggregates has proven to be one of the most challenging aspects of this project.

During the breaking step, it was observed that the counting process was impacted by unbroken clay aggregates, resulting in considerable variation in counting. In this study, several counting techniques were also tested to achieve an optimum way to count the bacteria inside microaggregates.

The ON2-WT and ON2-Δ*aprX* strains were prepared in casein and digested casein media with and without clay as previously explained in Section 4.2.2.1 and microaggregates in mono-cultures were mixed as co-culture samples in both casein and digested casein media with clay. The optimum breaking method that was a combination of vortex, water bath sonication and needle was applied to break microaggregates after bacterial competition was finished. The extracted cells then were used to quantify bacterial cells using different counting techniques. The counting methods used are as follows:

4.4.1 Colony forming unit (CFU) counting

CFU is a classic counting method commonly used to estimate the number of viable bacterial cells in a sample. This method is one of the most reliable methods for determining the bacterial population in a bacterial culture. Following is a description of the sample preparation process to be used in CFU technique.

The samples for bacterial competition are prepared in casein and digested casein media with and without clay and incubated at room temperature with speed of 110 rpm for 48 hours. Upon completion of the incubation period, the tube samples were treated to break the microaggregates. Then, the cells were diluted in sterile distilled water or PBS to the desired dilution. On the LB agar plate with the appropriate antibiotic, diluted samples were spread to count the considered strain from the other strain in the co-culture samples. For each sample, the procedure was repeated five times in order to obtain the most accurate results. A variety of incubation times and temperatures were tested, and it was found that the optimal time and temperature for incubation were 48 hours and 21°C (room temperature), respectively.

Figure 4.15 shows the results of the CFU counting of ON2-WT and ON2-Δ*aprX* strains after 48 hours of competition in casein and digested casein media with and without clay. Results from Fig. 4.15(a) showed the wild-type and mutant strains grow similarly in a proteinase K digested casein media in mono-culture and co-culture without clay. This means that in the pre-digested casein medium, the AprX-deficiency is not a disadvantage for the ON2-Δ*aprX*, and the mutant strain was able to grow in the digested casein as well as the wildtype strain. Therefore, both strains have equal access to the digested casein to grow.

Similar results were observed in the case of mono-cultures and co-cultures of ON2-WT and ON2-Δ*aprX* in digested casein with clay as given in Fig. 4.15(b). The CFU counting result indicates that in presence of clay, both strains could grow equally as mono-cultures and co-culture in pre-digested casein medium. However, the CFU counts of the mono-culture samples in casein medium without clay demonstrated that the lack of AprX production in ON2-Δ*aprX* reflected its growth in mono-culture casein medium, shown in Fig. 4.15(c). On the other hand, in the co-culture samples in casein medium without clay, the number of the AprX-deficient cells are similar to the AprX-producer cells which is match with the hypothesis that AprX secreted by WT bacteria diffuses away as a public good and the digested casein can be consumed not only by AprX producers, but also by other non-producing cells within the vicinity.

Next medium was casein with clay which is the main goal of this study to determine whether clay could act as a protective element for the WT strain to keep the AprX and digested casein close to the producer cells or not. To begin with, it was necessary to ensure that the clay itself did not add any extra nutrients to the casein that would allow the ON2-Δ*aprX* cells to grow on it. For this purpose, the ON2-Δ*aprX* cells were inoculated in casein with and without clay and incubated at room temperature for 48 hours. Based on the results of this experiment, it can

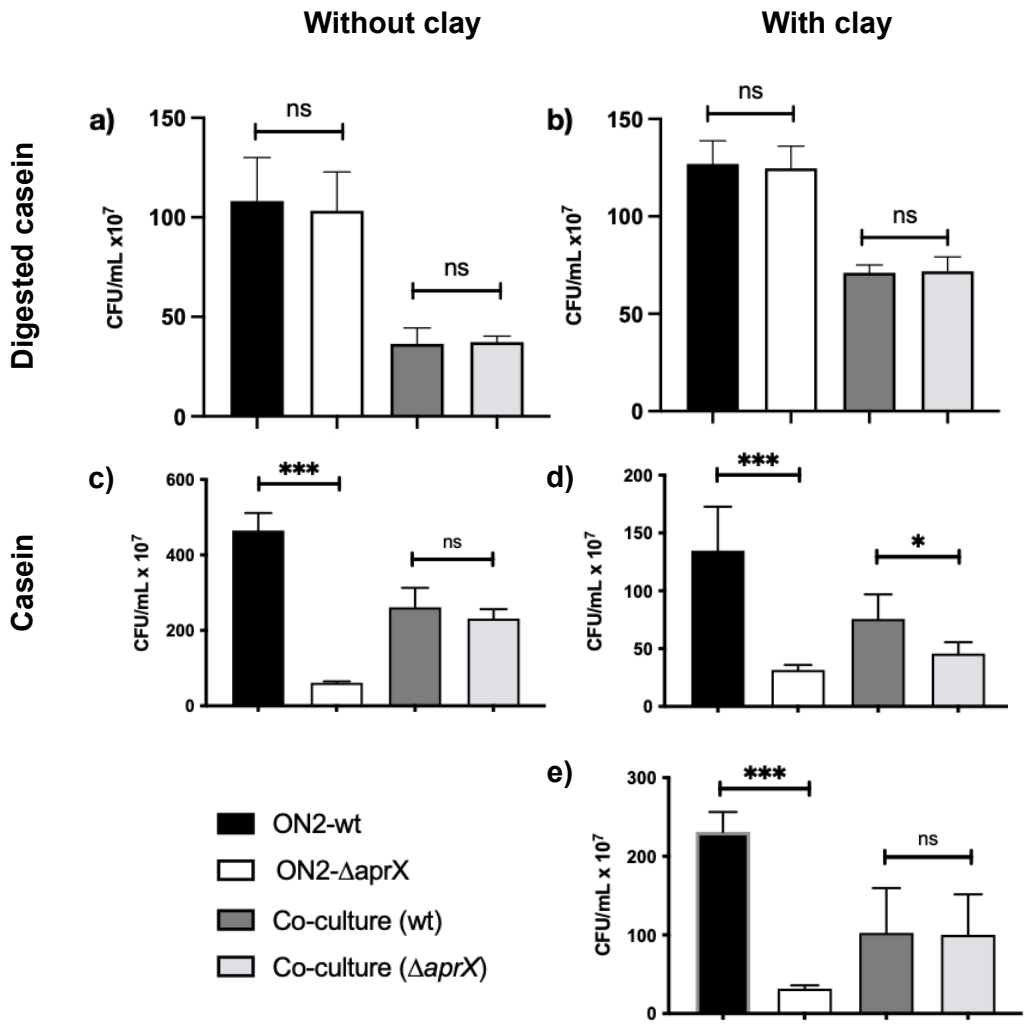

Figure 4.15: In the casein clay medium, different bacterial populations are found within microaggregates. The CFU counting results show the number of bacteria in mono-culture and co-culture in (a) digested casein medium without clay, (b) digested casein medium with clay, (c) casein medium without clay, and (d, e) casein medium with clay. Casein was digested with 5 mg/L of proteinase K and the digested casein was used as the control medium for the two bacterial strains, since both strains were able to grow on the digested casein without the need for AprX. The outcome of the bacterial competition in casein medium sometimes showed that (d) the ON2-WT could grow faster than ON2-Δ*aprX* in casein medium with clay and their difference is significant (p<0.05). However, in biological repeats, the CFU counting result showed that both AprX-producer and non-producer cells grew similarly (e), which suggested that the microaggregate could not be the barrier to protect AprX from diffusing away. Data presented as mean and standard deviation and data are compared using t test *** p<0.005, * p<0.05, ns (not statistically significant) p>0.05.

be concluded that clay does not contribute significantly to the addition of extra nutrients to the casein medium (data not shown). The co-culture sample in casein with clay is representative of bacterial competition and provides an opportunity to examine the presence of clay aggregates and its effect on the outcome of the bacterial competition.

The average of the CFU counting result of co-culture in casein clay, shown in Fig. 4.15(d), showed a significant difference (p<0.05) between AprX-producer and non-producer indicating that the ON2-WT within microaggregates could have access to its own secretions which resulted in faster growth rate for the ON2-WT strain. However, the bacterial competition experiment was repeated multiple times and surprisingly the CFU counting results in some of the biological repeats showed that the growth rate of the ON2-WT and ON2-Δ*aprX* strains in the co-culture with the presence of clay was not significantly different, as shown in Fig. 4.15(e). Unlike previous CFU counting results in Fig 4.15(d), the results shown in Fig. 4.15(e) indicate that the ON2-Δ*aprX* strain have similar access to the secreted AprX and the digested casein which leads to both AprX-producer and AprX non-producer strains to have similar growth. This experiment had several technical and biological repeats and a similar outcome as shown in Figs. 4.15(d) and (e), was observed every time. Due to the variability in the CFU counting results, further counting methods were used to investigate the outcome of bacterial competition in casein medium with clay. Therefore, another counting method was tested called SP-SDS which is a known method to estimate CFU numbers of bacteria by having more repeats from each sample.

4.4.2 Single Plate-Serial Dilution Spotting (SP-SDS) counting technique

SP-SDS is designed for CFU counting of microorganisms, such as bacteria and yeast, with no prior knowledge about their growth rate and viable counts [254].

In this method, usually up to six dilutions are chosen and for each dilution, and ten to twenty spots of bacterial culture with volume of 20 μl are placed on an agar plate. The sample preparation is similar to what was explained in Section 4.4.1, and three dilutions (10^3, 10^4, 10^5) were chosen to inoculate on agar plate containing appropriate antibiotics.

The plates were initially incubated at 30°C for 24 hours but the colonies grew to attach together very fast that caused inaccurate counting results. Therefore, different agar plate incubation time periods and temperatures were tested to find the optimum operating conditions. The temperature was reduced from 30°C to the room temperature and incubation time was extended to 48 hours. The reduced temperature and longer incubation time allowed cells to grow gradually to

colonies and to be counted before they attach together. The result of SP-SDS counting and the shape of colonies after incubation time were shown in Figs. 4.16(a) and (b), respectively.

The SP-SDS results demonstrated that ON2-WT and ON2-Δ*aprX* strains do not differ significantly when grown in mono-culture or co-culture in digested casein, and the presence of clay did not alter the results (see Fig. 4.16(a)). In the case of casein clay medium, the SP-SDS, shown in Fig. 4.16(b), confirmed a significant difference (p-value<0.005) between ON2-WT and ON2-Δ*aprX* mono-cultures, which is due to protease deficiency of the ON2-Δ*aprX* strain. However, in the case of co-culture samples in casein with clay, the difference between WT and mutant strains was still not significant (p-value>0.05).

As it was previously mentioned, colonies were counted after 48 hours of incubation at room temperature when they were fully grown. Each colony means that a single mother cell reproduces to make a group of genetically identical cells, and this group of cells form a mass. During the counting process, many colonies were found to be flattened transparent as shown in Fig. 4.16(c). However, in the next day, multiple colonies subsequently were observed within the flattened transparent colonies as it is shown in Fig. 4.16(d). These newly grown colonies were formed 24 hours after the counting, which caused variation in the number of counting results. By the time entire colonies formed, previous colonies had already joined together, making counting them impossible. This resulted in a significant variation in our ability to quantify bacterial competition. As a result, this technique was not considered for further use in this project.

Fluorescence microscope was another approach that was utilised to count cells after the breaking phase. It should be noted that presence of aggregates in the samples even after the breaking process is very common and it could affect the accuracy of counting results. In the following section, the fluorescence microscope provided images that helped detect presence of any aggregate and count both of the labelled bacterial strains in the sample.

4.4.3 Counting using fluorescence microscopy

Fluorescent microscopy was utilised to screen for the presence of aggregates, such as bacterial aggregates and microaggregates, to prevent variations in the outcome of competition. This would enable the detection and counting of any unbroken aggregates contained in the sample.

In this approach, a 96-well plate with optically clear flat bottom (THISTLE Scientific) was used. Following 48 hours of incubation on a slow shaker at room temperature, the sample was treated to break up the microaggregates. This step

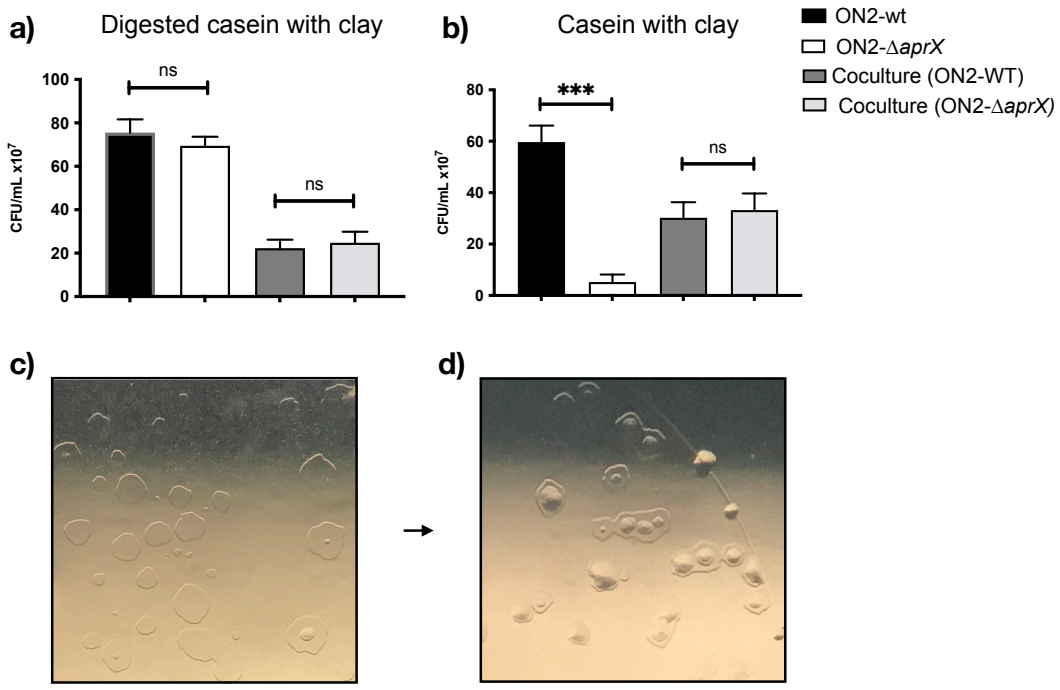

Figure 4.16: Additional colonies grew after the initial incubation period, resulting in incorrect SP-SDS counting. The samples were prepared for the breaking process (vortex (2 minutes), water-bath sonication (20 minutes) and needle breaking methods (five times)) after the competition was finished. Then bacterial cells were spotted on LB agar with respected antibiotics and incubated at room temperature for 48 hours before counting. (a) the SP-SDS CFU counting result of ON2-WT and ON2-Δ*aprX* in mono-cultures and co-culture in digested casein with clay and (b) in casein medium with clay. The start point samples for this experiment were counted and the result confirmed the similar number of ON2-WT and ON2-Δ*aprX* cells at the beginning of the bacterial competition experiment. If the number of cells in start point samples was unequal, the bacterial experiment was terminated and started with new sample preparation. Data presented as mean and standard deviation and data are compared using *t* test *** $p<0.005$, ns (not statistically significant) $p>0.05$.

was followed by 120 seconds of vortexing, 20 minutes of sonication, and 60 seconds of vortexing, and passing the supernatant through a 30^G needle five times. Afterward, 50 μl of the supernatant part of the samples was transferred to 96-well plates and for each condition, five biological replicates were considered. In order to spin down the cells on the surface, the 96-well plate was placed in a centrifuge with a speed of 3214*g at 18°C for 10 minutes.

The presence of aggregates in the samples was negligible and various methods used to count bacteria, such as manual visual counting, or counting using image processing applications, such as Fiji [255] or MATLAB Mathworks [256]. The cell counting results in casein clay medium are shown in Fig. 4.17(c), which is an average of five repetitions. Also, plots of each repetition in mono-culture as well as in co-culture are shown in Fig. 4.17(a) and Fig. 4.17(b), respectively.

On the basis of the number of ON2-WT and ON2-Δ*aprX* cells – as mono-culture and co-culture in casein with clay environment – an average of each sample was calculated to measure the ratio between ON2-WT and ON2-Δ*aprX* cells. According to the calculated ratio between WT and mutant mono-cultures, shown in Fig. 4.17(a), there is 5:1 ratio of ON2-WT to ON2-Δ*aprX* strains as mono-culture samples in casein clay, indicating the growth rate of ON2-WT cells in casein clay is substantially higher than ON2-Δ*aprX* cells. This ratio is consistent with the previous results from the CFU counting method shown in Fig. 4.15(d).

The results of counting the ON2-WT and ON2-Δ*aprX* strains as co-culture in casein clay medium are shown in Fig. 4.17(b). These counts are from the same samples with different technical repeats. In most replicates of the co-culture sample – three out of five cases – there was a ratio of approximately 2:1 between ON2-WT and ON2-Δ*aprX* cells. It can be derived that in these cases, being within microaggregates could protect the WT strain from losing its AprX enzyme, which was demonstrated by improving its growth rate compared to the ON2-Δ*aprX*. However, in some of the repeats - two out of five cases - the ratio between ON2-WT and ON2-Δ*aprX* cells was 1:1, indicating that the ON2-Δ*aprX* could grow as similar as the ON2-WT by having access to the digested casein, produced by AprX.

Overall, the average result of counting cells in co-culture samples in casein medium with clay, shown in Fig. 4.17(c), indicated that the ON2-WT cells grow more than ON2-Δ*aprX* cells (p-value<0.05), but the difference is not as significant as cells in mono-cultures with p-value<0.0001.

The variation in the results suggested that in the case of similar growth of of ON2-WT and ON2-Δ*aprX*, the mutant cells probably had access to the digested casein by leaking out from the microaggregates or the ON2-WT and ON2-Δ*aprX* population were mixed inside the microaggregates that the physical structure of

microaggregate could not be accounted for protecting AprX or digested casein from ON2-Δ*aprX* cells. With the SP-SDS technique, there is a high variation in the number of bacteria due to the growth of colonies after the incubation time. As a result, this method was not considered for quantifying cells after the competition. The CFU counting was the most reliable method to count the number of living cells after the competition. Additionally, a microscopic study was conducted in order to validate the counting results and also gain a more comprehensive understanding of microaggregates and bacterial competition within them.

4.5 Microscopic study on bacterial competition in microaggregates

This section focuses on the bacterial interaction within microaggregates by using fluorescence microscopy with high resolution oil-immersion objectives in order to gain a better understanding of the role of spatial structure of microaggregate in bacterial competition. Fluorescent proteins were used to label bacterial cells in order to analyse cells' position and their interactions within microaggregates.

Fluorescent microscopes have been used for studying bacteria since 1911 [257]. As a result of technological advancements in fluorescent microscopy, fluorescently labelled bacteria can be studied in more detail and with higher contrast [258]. A variety of fluorescently labelled proteins can be used to label bacterial cells, nevertheless, in bacterial co-cultures, in which two strains of bacteria are mixed in a culture, the two fluorescent labels need to be distinguished from one another. Therefore, it is necessary to use fluorescent proteins with different emission wavelengths to avoid overlap. Initially, red fluorescence protein (RFP) was used to label one of the strains, however, the labelled cells were not very bright under the fluorescence microscope. Thus, the two fluorescent proteins used in this research were yellow fluorescent protein (YFP) and cyan fluorescent protein (CFP) according to the process described in Section 2.3.1.3 in Chapter 2.

The microscopic studies will provide a visual representation of how bacteria compete within microaggregates. Such data will be critical for understanding the behaviour of bacteria within microaggregates, as well as their competition with each other. As previously stated, the CFP-labelled cells in bacterial competition within microaggregates could not be distinguished from clay due to the autofluorescence characteristic of hectorite clay.

Figure 4.18 illustrates an example of the autofluorescence property of hectorite clay, which profoundly impacts the signal of CFP-labelled cells. In Fig. 4.18(a), which is a merged image of yellow and cyan fluorescent channels, an area of a

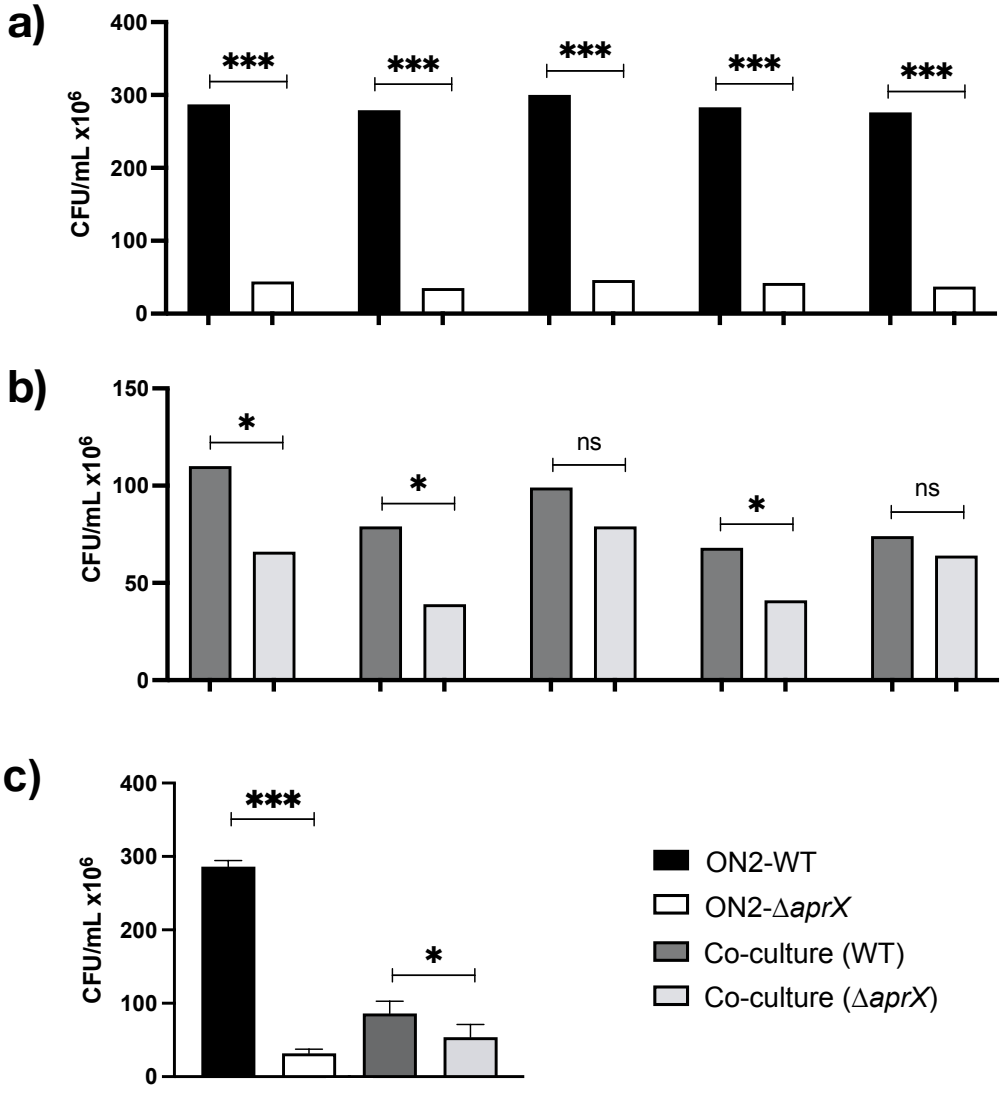

Figure 4.17: Quantification of the number of ON2-WT and ON2-Δ*aprX* cells in co-culture samples in casein medium with clay confirms that ON2-WT cells are doing better in microaggregates. (a) counting repeats of ON2-WT mono-culture sample and ON2-Δ*aprX* cells, (b) counting repeats of co-culture samples that ON2-WT from co-culture was shown in dark grey and ON2-Δ*aprX* cell number in light grey and (c) the average of the CFU counting of the mono-culture and co-culture samples. The CFU counting results belong to mono-cultures and co-culture samples from the same experiment. In the majority of the co-culture repeats, the ON2-WT cells are growing faster than ON2-Δ*aprX* in casein medium with clay which indicates the being inside microaggregate have helped producer cells to have access to the digested casein. Data presented as mean and standard deviation and data are compared using *t* test, ns (not statistically significant) $p>0.05$, **** $p<0.0001$, * $p<0.05$.

microaggregate has been selected and shown in orange square. As demonstrated in this image, the dominant bacterial population looks to be the YFP-labelled cells. However, the CFP-labelled cells were found to have a similar number as the YFP-labelled cells when the filters were separated, as shown in Figs. 4.18(b) and (c), respectively. The auto-fluorescent nature of the hectorite clay is a great challenge in this fluorescent microscopic study and in order to observe the population of each bacterial strain within microaggregates, multiple optimisations were required.

As a result of a variety of optimisation efforts, the most effective method for determining the dominant bacterial population within microaggregates was to switch fluorescent labels, CFP and YFP, between the bacterial strains, ON2-WT and ON2-Δ*aprX*. Thus, only the YFP-labelled cells, that are bright and distinguishable from background noise of clay, will be studied in the image.

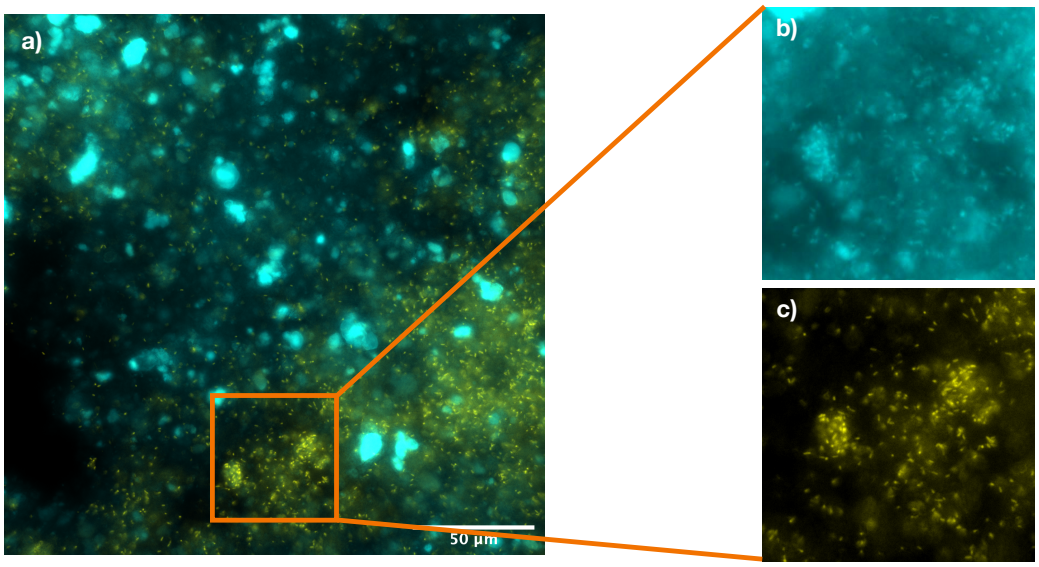

Figure 4.18: Hectorite clay's autofluorescence poses a great challenge to fluorescent microscopy imaging of CFP-labelled bacteria within microaggregates. The fluorescent microscopic image (a) represents a microaggregate with ON2-WT-CFP and ON2-Δ*aprX*-YFP cells after 48 hours of incubation in digested casein. An area containing both bacterial populations in microaggregate is magnified in the region shown by the orange square. The cyan and yellow filters of the merged image were separated in order to observe CFP and YFP-labelled populations separately. In image (a) both clay aggregates and CFP-labelled cells appeared in cyan fluorescent channel but in (b) cells labelled with YFP label are very bright and distinguishable from the background noise. It was later demonstrated that the total number of the CFP-labelled cells is very similar to that of the YFP-labelled cells using CFU counting method.

ON2-WT and ON2-Δ*aprX* bacterial strains were labelled with CFP and YFP, respectively, and two sets of co-cultures were prepared. In one co-culture, ON2-

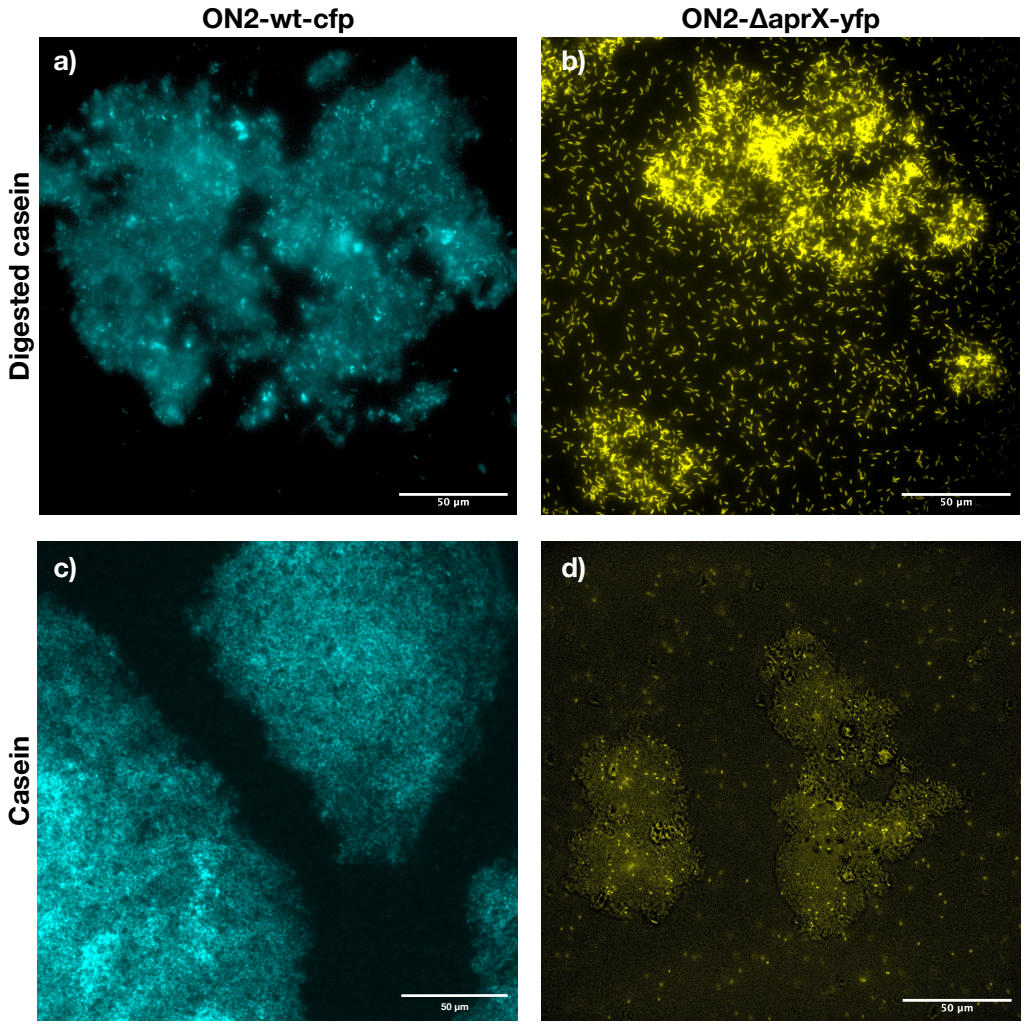

Figure 4.19: Significant growth reduction of ON2-Δ*aprX*-YFP in casein clay environment. Mono-cultures of ON2-WT-CFP and ON2-Δ*aprX*-YFP after incubation in clay with digested casein (a,b) and clay with casein (c,d) for 48 hours. The overnight cultures of ON2-WT-CFP and ON2-Δ*aprX*-YFP were inoculated into clay media with OD_{600nm} of 0.01. Digested casein clay is an environment that both ON2-WT-CFP and ON2-Δ*aprX*-YFP can grow in this medium and form microaggregates. However, in the casein clay environment, the ON2-Δ*aprX*-YFP strain unlike ON2-WT-CFP (c) is unable to digest the casein to consume it and grow (d). Size of microaggregates in (d) are smaller compared to (c) and its structure seems to be more fragile as well.

WT-CFP was mixed with ON2-Δ*aprX*-YFP, while in the other, ON2-WT-YFP was mixed with ON2-Δ*aprX*-CFP. Studying these two co-cultures provides a chance for both ON2-WT and ON2-Δ*aprX* strains to be visualised within microaggregate structure and provide a measure of the true density of each strain.

In this project, a variety of microscopy techniques were used to observe bacterial competition within microaggregates, in order to choose the most appropriate approach.

4.5.1 Epifluorescence microscopy

The epifluorescence microscopic imaging was used to observe the bacterial competition between ON2-WT and ON2-Δ*aprX* strains within microaggregates in casein and digested casein media with clay in order to assess the fitness of each strain in the presence of microaggregates. The objective The results of this experiment are presented as follows:

4.5.1.1 Comparison of bacterial mono-cultures in digested casein and casein with clay

The first step is growing ON2-WT and ON2-Δ*aprX* cells separately in microaggregates as mono-cultures and comparing their growth in casein and digested casein media. This is an essential step in determining the growth of each strain without any interference from other strains. Therefore, their behaviour in a given media can be compared to their behaviour in co-culture. In Section 4.2.3.1, protocols for preparing mono-cultures were thoroughly explained, but in short, cells from exponential phase were inoculated in clay M63 and incubated overnight on a slow shaker at room temperature. Following this, two tubes containing microaggregates of ON2-WT-CFP cells were mixed together as a mono-culture of ON2-WT-CFP cells, and the supernatant was replaced with a particular media (for instance, either casein or digested casein with proteinase K). The same procedure was repeated for the preparation of the ON2-Δ*aprX*-YFP mono-cultures to provide an equal condition of sample preparation for both mono-cultures and co-cultures.

Following the 48-hour incubation time at room temperature on a slow shaker, the samples were transferred on to a glass slide using a cut 1000 μl pipette tip as described in Chapter 3 for fluorescent microscopic imaging. As the CFU counting results shown in Figs. 4.15(a) and (b), the ON2-WT and ON2-Δ*aprX* mono-cultures have similar growth as mono-culture and co-culture in digested casein environment with and without clay. Figures 4.19(a) and (b) provide microscopic evidence that confirms the CFU results as both ON2-WT-CFP and ON2-Δ*aprX*-YFP

mono-cultures grow to similar levels in clay with digested casein.

However, Figs. 4.19(c) and (d), demonstrated a substantial difference between mono-cultures of ON2-WT-CFP and ON2-Δ*aprX*-YFP in casein with clay medium. Both strains were inoculated in casein clay medium and were incubated for 48 hours at room temperature on the slow shaker with speed of 110 rpm. Even though the auto-fluorescence feature of the hectorite clay saturates the signal coming from the ON2-WT-CFP cells, the presence of bacteria is still visible due to the considerable bacterial population within the microaggregates.

Additionally, the bacteria from both strains grew equally in digested casein medium as indicated by the CFU counting results in Fig. 4.15(c) and microscopic studies in Figs. 4.19(c) and (d). On the other hand, in casein, which is an AprX-dependent medium for bacteria to grow, the number of cells corresponding to WT strain was higher than the mutant cells in mono-culture samples. These results were previously observed by counting CFU of ON2-WT and ON2-Δ*aprX* mono-cultures in casein media with and without clay as shown in Fig. 4.15(b) and (d), as well as in microscopic images, shown in Figs. 4.19(c) and (d).

As a consequence of the inability to produce AprX enzyme, the ON2-Δ*aprX* strain was unable to digest casein and, therefore, did not grow as much as ON2-WT in the casein medium. The microscopy images in Figs. 4.19(c) and (d) confirmed that ON2-WT cells continue to grow and build up their population in the microaggregate, however the ON2-Δ*aprX* cells are unable to grow in casein and the microaggregate structure did not change this fact. In Fig. 4.19(d) the size of the microaggregates seems to be affected by low density of the bacterial cells compared to 4.19(c) which can potentially lead to a more fragile microaggregate structure.

4.5.1.2 Comparison of co-culture samples in digested casein medium with clay

In order to compare the population of ON2-WT with ON2-Δ*aprX* as co-culture in a clay environment, the samples were prepared in two sets of co-cultures. Since YFP has the highest contrast with clay, labelling both strains with YFP in separate co-cultures will allow both ON2-WT and ON2-Δ*aprX* have equal opportunity to be seen in the co-culture samples under fluorescence microscope. This step is imperative in comparing the outcome of the bacterial competition in microaggregates. Therefore, two sets of co-cultures were prepared with ON2-WT-CFP, ON2-WT-YFP as the first co-culture and ON2-Δ*aprX*-CFP and ON2-Δ*aprX*-YFP as the second one.

The co-culture is prepared in the same manner as outlined on optimisation of sample preparation in Section 4.2.3.1, but in short, the cells from the exponential

phase were inoculated in the clay M63 and incubated overnight on a slow shaker at room temperature. Next, the microaggregates containing ON2-WT cells were mixed with the microaggregates with ON2-Δ*aprX* cells in a tube, and the supernatant fraction was replaced with a fresh digested casein medium. The co-culture tubes were incubated on a slow shaker at room temperature for 48 hours. Once the competition was completed, the supernatant was replaced with sterile PBS, and microaggregates were collected using a cut-tip pipette and transferred to glass slides for microscopic imaging.

Figure 4.20 shows microscopic images of two sets of co-culture samples of ON2-WT and ON2-Δ*aprX* with switched fluorescent protein labels in digested casein with clay. Figures 4.20(a) and (b) on the top row demonstrate the co-culture contain ON2-WT-CFP and ON2-Δ*aprX*-YFP, respectively, while Figs. 4.20(c) to (d) on the bottom row depict the co-culture of ON2-WT-YFP and ON2-Δ*aprX*-CFP, respectively. In each case, two microscopic images are shown. In both samples with switched fluorescent protein labels, the ON2-WT and ON2-Δ*aprX* strains create a well-mixed bacterial population within microaggregates.

The results validate the ability of the ON2-Δ*aprX* cells to grow and expand their population within the microaggregates similar to the ON2-WT strain when the casein protein in the medium is digested. The similarity in growth between ON2-WT and ON2-Δ*aprX* strains within microaggregates in pre-digested casein was also observed in the result of the CFU counting, shown in Fig. 4.15(b).

4.5.1.3 Comparison of co-culture samples in casein medium with clay

The co-culture samples in casein medium with clay were prepared in the same way as the samples in digested casein with clay and after 48 hours of incubation the samples were prepared for imaging by fluorescence microscope. The microscopic results for co-cultures in the casein clay environment are shown in Fig. 4.21. The top row, Figs. 4.21(a) and (b), are two repeats of the co-culture with ON2-WT-CFP and ON2-Δ*aprX*-YFP, respectively, and in the bottom row, Figs. 4.21(c) and (d), the images are showing the co-culture of ON2-WT-YFP cells mixed with ON2-Δ*aprX*-CFP in casein medium with clay, respectively.

In Fig. 4.21(a), the signal representing YFP-labeled ON2-Δ*aprX* cells appeared to be weaker than that of ON2-WT-CFP cells. On the other hand, the information regarding the quantity of the ON2-WT-CFP cells is unclear due to the signal overlap with the hectorite clay. Hence, in the second co-culture, shown in Fig. 4.21(c), where WT is labeled with YFP, the population of wildtype strain is clearly recognisable. The YFP signal from these co-cultures, shown in Figs. 4.21(a) and (c), indicate that the ON2-WT cells grew faster than ON2-Δ*aprX* which led them

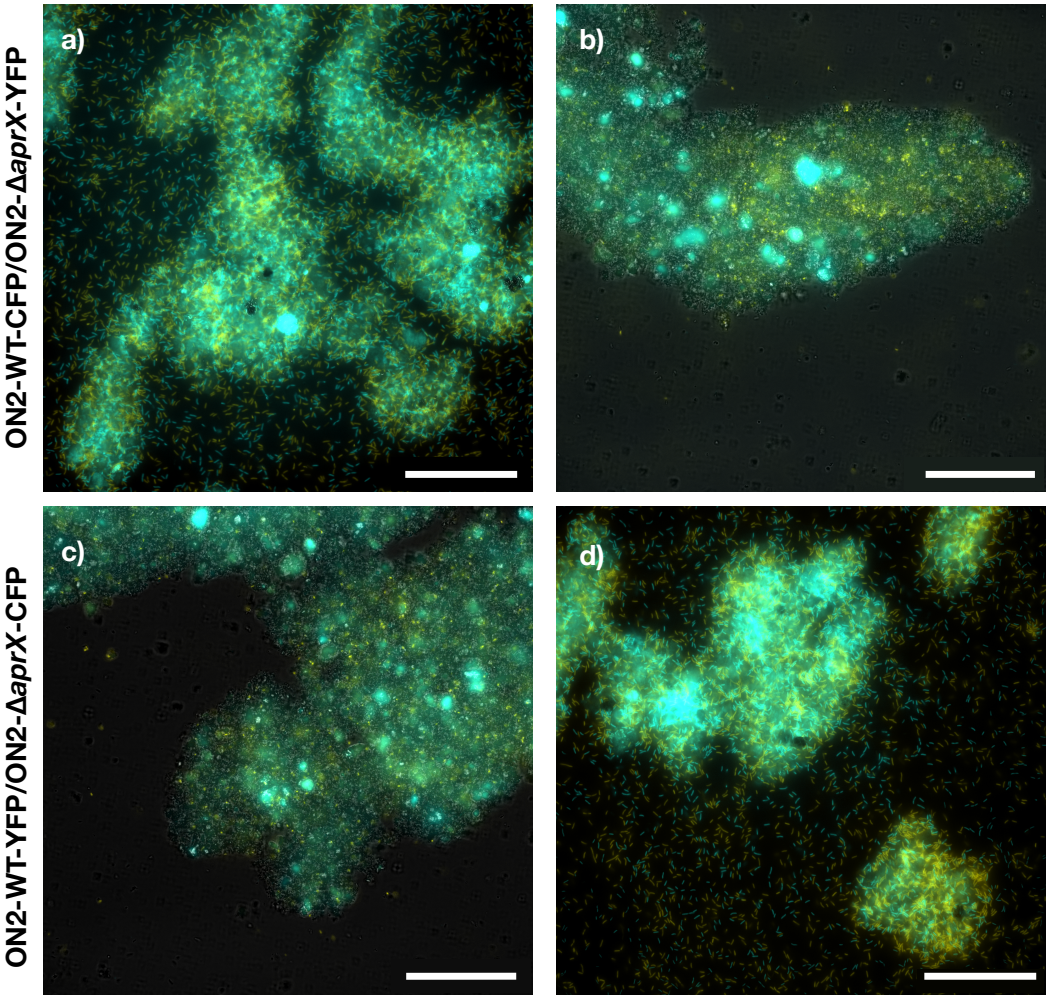

Figure 4.20: Well-mixed population of ON2-WT and ON2-Δ*aprX* when they grew in the pre-digested casein with clay medium. Two sets of co-culture were prepared, (a) and (b) ON2-WT-CFP mixed with ON2-Δ*aprX*-YFP and (c) and (d) ON2-WT-YFP was mixed with ON2-Δ*aprX*-CFP. The switching fluorescent labels were done to have a better observation of both bacterial populations in co-culture within microaggregates. Samples are prepared as it explained in Section 4.2.3.1. Bars are 50 μm.

to be the dominant population within microaggregates.

However, there were microaggregates in the same sample that exhibited a mixed population of wildtype and mutant strains within microaggregates, as it is shown in Figs. 4.21(b) and (d). The ON2-WT and ON2-Δ*aprX* cells grew similarly within these microaggregates, and switching fluorescent labels also repeated the same result. The variety in the bacterial population within microaggregates supports the variation in the CFU counting data observed in Figs. 4.15(d) and (e). The microscopic results of the bacterial competition, shown in Figs. 4.21(a) and (c), suggested that the ON2-WT strain is doing better than the ON2-Δ*aprX* strain and formed a high level of genotypic patchiness within microaggregates. It is important to note that these results provide valuable information on the role microaggregates play in bacterial competition by spatially separating cells, allowing the AprX producers to benefit from their own secretions and grow faster when they are within microaggregates in co-culture with non-producer cells.

While the process of sample preparation for microscopic study was the same for all the co-culture samples, the structure of each microaggregates was different and in individual microaggregates, there was a variation in the level of bacterial genotypic patchiness (as it is shown in Figs. 4.20 and 4.21). The clonal patchiness of ON2-WT in some microaggregates (Fig. 4.21(a) and (c)) indicates that the AprX is used by its producer cell which is why one can suggest that the structure of microaggregates could play a role in the bacterial competition within this structure. However, in some other cases, the ON2-WT and ON2-Δ*aprX* cells were mixed which suggest that the secreted AprX became a "public good".

These findings suggest that although in some cases the role of microaggregates in protecting secreted enzymes is negligible, however, higher growth rate of AprX-producer cells in the co-culture in casein was only observed in presence of clay in the culture. The findings of this study provide important evidence that the spatial structure of microaggregates influences the bacterial competition in soil where by providing an environment that allows the producer strain to benefit more from its secretions.

In order to gain a deeper understanding of the role of the microaggregates, further microscopic studies were conducted. As a next step, a microfluidic device was used to evaluate the bacterial competition as monolayer and also obtain a detailed fluorescent image of bacteria within microaggregates.

4.5.1.4 Studying bacterial interaction in microfluidic channel

Microfluidics revolutionised the study of microbial ecology by monitoring the behaviour of microorganisms in the nearest environment to their natural habitat

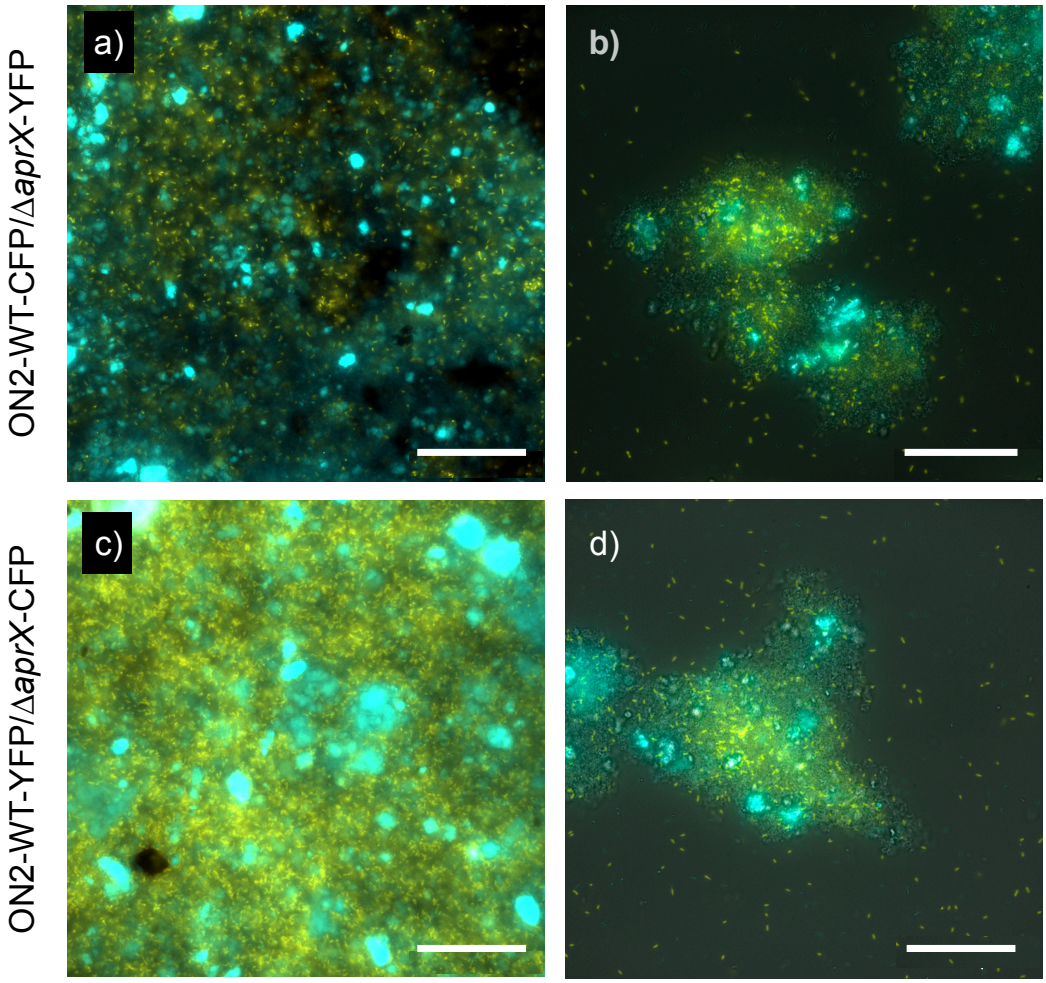

Figure 4.21: Co-culture of ON2-WT and ON2-Δ*aprX* strains in the casein clay environment after 48 hours of incubation. (a) and (b)are the co-culture samples in which ON2-WT was labeled with CFP and ON2-Δ*aprX* with YFP, and (c) and (d) are images of the co-culture sample that ON2-WT was labelled with YFP and ON2-Δ*aprX* labelled with CFP. In the co-culture sample that ON2-WT was labelled with CFP (a), the microscopic image showed that the CFP-labeled cells were dominant compared to YFP-labeled cells. However, due to the autofluorescence feature of hectorite clay, distinguishing the CFP-labeled bacterial population from clay aggregates is difficult. By switching the fluorescent labels of the bacterial strains in co-culture, the microscopic images (c) revealed that the ON2-WT-YFP is the dominant population compared to ON2-Δ*aprX*-CFP in the casein clay environment. However, from the same samples in which images (a) and (b) were taken, there are microaggregates with well-mixed bacterial strains, ON2-WT and ON2-Δ*aprX*, as shown in image (b) and (d). These results indicated that there are different degrees of bacterial genotypic patchiness within microaggregates. Scale bars show 50 μm.

[259]. Using this artificial micro-environment, the study environment can be customised in greater detail, such as chemical ingredients as well as the physical structure (the capability of applying a variety of geometric patterns to the microfluidic chamber) [260].

In this study, microfluidics approach was used to gain a better understanding on the interaction of ON2-WT and ON2-Δ*aprX* while the cells were still monolayer. Also, by adding clay in the chamber, the process of forming microaggregate could be investigated as well as studying the bacterial interaction within microaggregate. The microfluidic chambers were also used to replicate the natural environment in which soil bacteria live. This provides an opportunity to study the behaviour of soil bacterial cells in their natural environment, which could provide further insight into not only bacterial interactions overtime at high resolution but also their interaction with clay particles during the process of microaggregate formation.

The microfluidic chambers are made of 25 g of Polydimethylsiloxane (PDMS) mixed with 2.5 g of Silicone Elastomer curing agent. The bubble was removed under vacuum condition and the mixture was transferred in a microfluidic device mould and incubated at 42°C overnight to solidify. There are various types of chambers that can be used depending on the purpose of the experiment. Two types of chambers were employed in this project, namely linear and porous.

Bacterial samples were prepared in the same manner to be used in both chambers as follows:

A single colony of ON2-WT-CFP and ON2-Δ*aprX*-YFP was grown in fresh LB liquid without antibiotics at 25°C with and the shaking speed of 220 rpm overnight. The overnight culture was inoculated with OD_{600nm} 0.05 into fresh LB liquid without antibiotics and incubated at 25°C and the shaking speed of 220 rpm until they reached to the exponential phase, OD_{600nm} 0.2. The microfluidic device setup in the lab as shown in Fig. 4.22(a) was used in this study. The bacterial strains and media used in this study were ON2-WT-CFP and ON2-Δ*aprX*-YFP in co-culture as well as liquid casein and casein clay media, respectively.

4.5.1.5 Linear chamber

The linear chamber with 0.75 μm depth and 1 mm width as shown in Fig. 4.22(b) was used in this project. In this chamber, the co-culture with ratio 1:1 of ON2-WT-CFP and ON2-Δ*aprX*-YFP cells at exponential phase were planted on the surface of the chambers. Casein and digested casein flowed in two separate chambers. The flow rate in the microfluidic device also is adjustable to be close to the flow rate of the environment that bacteria live in. Also, keeping a constant flow of media allows for optimal oxygen and nutrient levels for the growth of bacteria. In

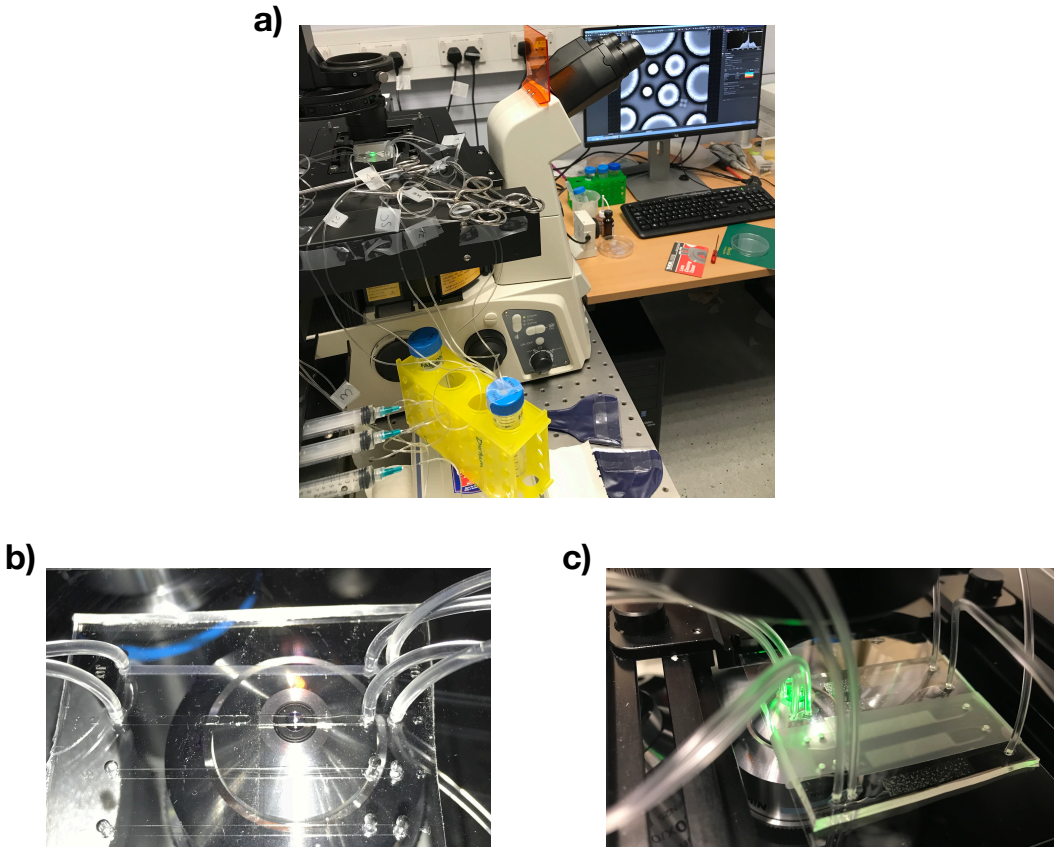

Figure 4.22: Microfluidic devices on fluorescent microscopy. Image (a) is showing the setup of an experiment using a microfluidic device, (b) a microfluidic device with linear channels and (c) a microfluidic device with porous channels.

this study, the flow rate was optimised at 0.01 ml per minute.

An image was taken from each casein and digested casein sample every hour for a period of 8 hours at room temperature using a fluorescent microscopy. Figure 4.23(a) represents the growth of ON2-WT-CFP and ON2-Δ*aprX*-YFP, while the casein flows in the chamber. It can be seen in Fig. 4.23(a) that the CFP-labelled ON2-WT cells are growing faster than the ON2-Δ*aprX*-YFP over period of 8 hours, indicating that the digested casein was likely washed away by the liquid flow. Therefore, due to limited access of ON2-Δ*aprX* to the digested casein, ON2-WT strain continued to grow faster than ON2-Δ*aprX*. On the other hand, it appears ON2-Δ*aprX*-YFP grows faster than ON2-WT-CFP in the predigested casein medium (shown in Fig. 4.23(b)), which is consistent with the fact that cheats can save their energy by not producing AprX, resulting in faster growth compared to the producers.

Although, the surface of the microfluidic chamber and the constant flow reduce the risk of up taking digested food by the ON2-Δ*aprX* cells, the flow rate is still higher than it would be inside the microaggregate. Also, the linear chamber is not wide enough to easily accommodate large clay aggregates that are dragged into the chambers. It was also observed that the size of the clay aggregates was not controllable and often large aggregates that were formed due to overgrowth, did stock at the beginning of the chamber and caused blockage of the flow and, consequently, damaged the device. To overcome this problem, a porous chamber was tested and the details of the experiment and results are discussed in the following section.

4.5.1.6 Porous chamber

Figure 4.22(c) shows a porous chamber with a width of 4 mm and a depth of 75 μm that is wider than a linear chamber. The middle part of this chamber is surrounded by a variety of cylinders ranging in size from 10 μm to 100 μm, as shown in Fig. 4.24(a). The presence of these cylinder-shaped objects in the chamber acts as an obstacle and causes disturbance in the flow.

Studying bacterial interaction in microfluidic device with a porous chamber can create a system such as one might see in soil [129]. In addition, the porous chamber has a wider entrance, which allows for larger clay aggregates to be accommodated in the chamber. This enables us to study the competition between bacteria in an environment that is more like that of soil microaggregates and also to observe how microaggregates develop over time by adding clay media to the chamber. Figure 4.24(b) presents microscopic image of the co-culture cells, ON2-WT-CFP and ON2-Δ*aprX*-YFP, in the porous chamber with casein flow as the

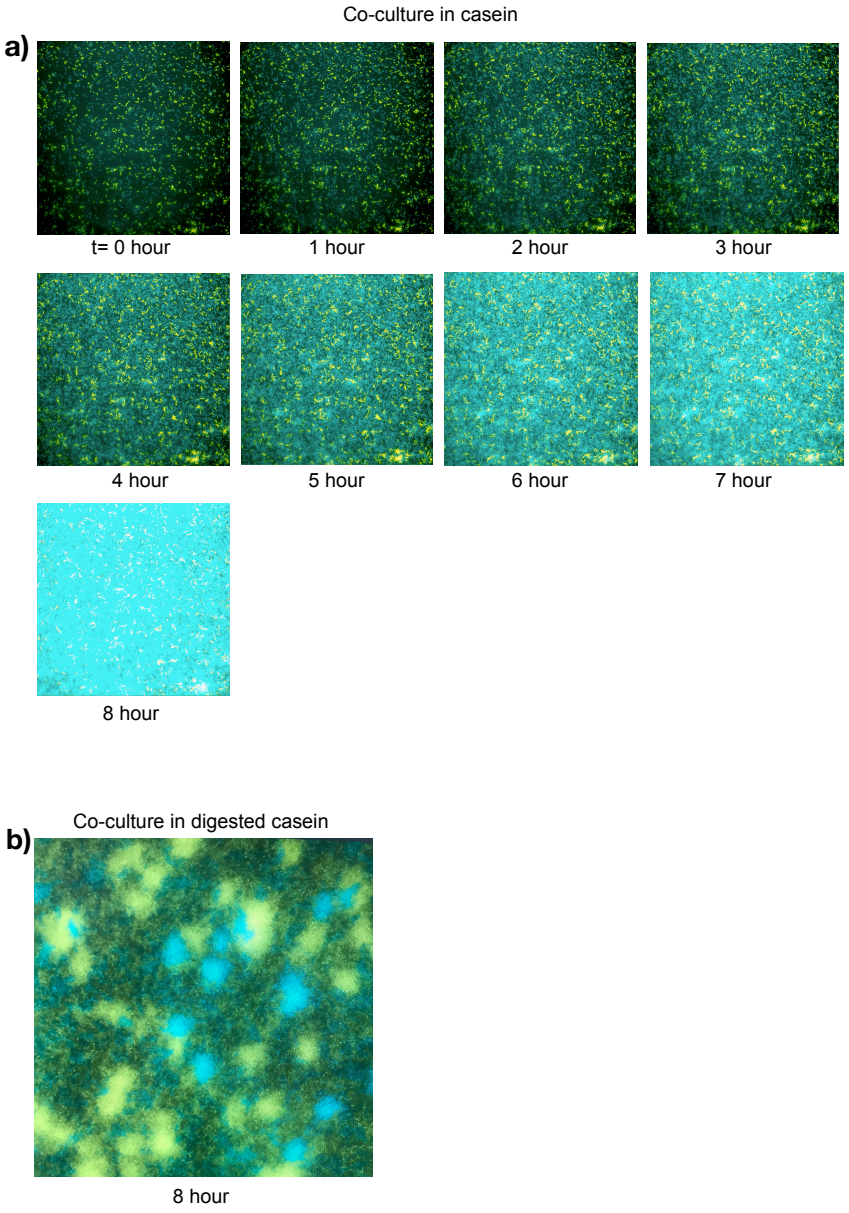

Figure 4.23: Growth comparison of ON2-WT-CFP and ON2-Δ*aprX*-YFP as co-culture in casein and predigested casein (using proteinase K) media on the surface of the linear chamber of the microfluidic device. (a) result of co-culture growth in casein in different time points (from time 0 hour to 8 hours). (b) co-culture sample in predigested casein after 8 hours of incubation. Results show that the ON2-WT-CFP could grow faster than ON2-Δ*aprX*-YFP in the casein medium flows as the only source of nutrient (a). However, in the predigested casein (b), the ON2-Δ*aprX*-YFP cells grew faster than and formed bigger patches than ON2-WT-CFP.

growth medium. Following seven hours of incubation, bacterial rings around the cylinders were formed, as shown in Fig. 4.24(c), but the thickness of the bacterial rings was not uniform around the cylinders. This is due to a different flow rate of the growth medium in the chamber, which is more favourable for the bacteria attached to one side of the cylinder than the other.

Moreover, as the bacteria grow, they generate patches with genotypic identical cells which can create a physical obstruction that can change both the pathway of the flow [129]. Further optimisation will, therefore, be required to understand the influence of flow rate on the growth of the bacteria in order to precisely analyse their competition.

Another attempt was to transfer ON2-WT-CFP and ON2-Δ*aprX*-YFP into the porous chamber and flow the clay media to the chamber. The aim of this experiment was to observe the process of microaggregate formation overtime alongside bacterial competition in the microaggregates. To do this, cells of both strains from the exponential growth phase were flowed into the channel and individual cells were planted on the surface of the chambers. Then, the flow of the cells was stopped, and casein clay medium started to flow into the chamber.

It was observed that the clay particles began to come through the porous chamber. At the beginning of the casein clay flow, it appeared that the clay particles and small clay aggregates are in the right size to enter the chamber and gradually build up a microaggregate structure. However, the bacteria and clay aggregates gradually got attached together over time and created large aggregates that blocked the entrance of the chamber as demonstrated in Fig. 4.24(d). The entry blockage of the chamber had a negative impact on the flow of medium and on the growth of bacteria in the chamber. Consequently, the microscopic images taken from the cells in the middle of the chamber proved not to be particularly insightful, nor did the large aggregates formed by the multi-layer combinations of cells and clay.

The results of the microfluidic device approach were not conclusive due to the reasons outlined above; nonetheless, it demonstrated considerable potential in exploring bacterial behaviour in great detail as future research. In order to gain a deeper understanding of the structure of microaggregates, confocal microscopy was performed to examine the structure of microaggregates at a greater level of detail.

4.5.2 Confocal microscopy

As discussed in the previous section, it is crucial to have a clear understanding of the structure of the microaggregates in order to explain the result of the bacterial competition in casein medium with clay. For this purpose, confocal microscopy

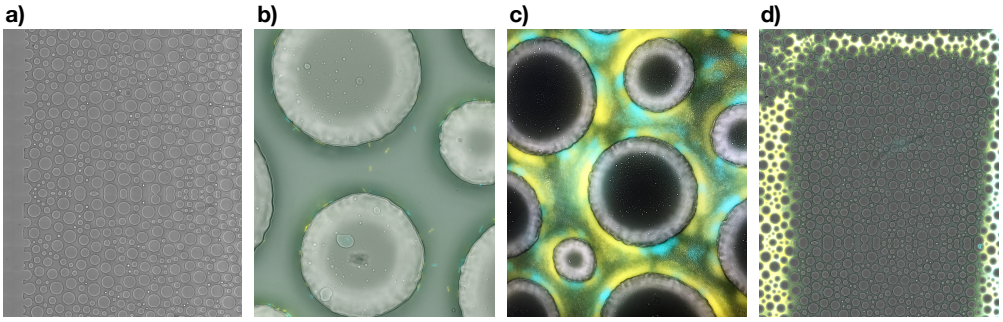

Figure 4.24: Microfluidic device with porous chamber used to create a similar environment to soil microaggregates. The growth of ON2-WT-CFP and ON2-Δ*aprX*-YFP in the casein co-culture on the surface of a porous chamber was investigated. Image (a) is the look of the porous chamber before transferring the cells. In image (b) the co-culture samples were transferred in the porous chamber, (c) after 5 hours of incubation in casein and d) is when the co-culture sample in microaggregates was transferred in the porous chamber. ON2-WT was labelled with CFP and ON2-Δ*aprX* labelled with YFP.

technique was also used to investigate the structure of the microaggregates in more depth. The purpose of confocal imaging in this study was to gain a better understanding of the spatial structure of microaggregates through optical sectioning, which allows the collection of multiple z-stacks in order to develop a three-dimensional image of the microaggregates. For this purpose, a mono-culture of ON2-WT labelled with YFP in casein medium with clay was selected. The sample preparation in confocal microscopy is similar to that of fluorescent microscopy, which was explained in Section 4.2.3.1. In short, ON2-WT-YFP cells from exponential phase were inoculated in casein clay medium and incubated on the slow shaker for 48 hours. Upon completion of incubation time, the microaggregate sample was transferred onto a microscope glass slide covered with a coverslip and confocal microscopy used for this experiment was Olympus FV1000 on a BX61 upright frame. Figure 4.25, represents different z-stacks of microaggregates, where the ON2-WT-YFP cells are shown in yellow and the clay due to its autofluorescence is shown in cyan.

Confocal images revealed that the structure of the microaggregates is very heterogeneous and complex. The microaggregates can be composed of small particles that form an intact and relatively closed structure with smaller pores, or they can be composed of larger clay particles and the arrangement of these particles creates larger pores within the microaggregates. It is well-known that the arrangement of clay particles, as building units, plays an important role in the establishment of interior pore spaces, which with the secreted substances from bacteria subse-

quently dictates the structure of microaggregates [103]. As a consequence, the permeability of this structure will vary depending on the arrangement of the clay particles.

Various z-stacks of the confocal images indicated that the structure of microaggregates can be in a way that allow bacteria to traverse the microaggregate structure in areas with larger pores (Figs. 4.25(a) to (i)). These images revealed that microaggregates contain clay particles of different shapes and sizes, which form pores of various sizes. In some microaggregates, pores are larger than in others, allowing cells outside of microaggregates to reach into the interior space. As a result, ON2-Δ*aprX* cells are likely to be neighbours of ON2-WT cells, allowing mutants to benefit from ON2-WT secretions that digest casein and grow fast. In this case, the role of microaggregates in isolating AprX-producing strain from mutant strain or preventing leakage of AprX enzyme from its producer cell is negligible, and ON2-WT and ON2-Δ*aprX* cells can grow a well-mixed population within the microaggregate. In contrast, the microaggregates containing smaller clay particles and pores may provide a more intact structure which producers can be isolated within the structure. The microaggregates with a relatively compact structure may also decrease the leakage of AprX and transform the AprX from a public good into a private good. Using these data is of great importance to understand how the spatial structure of soil microaggregates shapes the bacterial communities, since very little is known about the bacterial interactions within soil microaggregates.

4.6 Discussion and Conclusion

In this section, the counting and microscopic results are evaluated and their main features are discussed. Finally, a summary of this chapter is given in the conclusion section.

4.6.1 Discussion

After a series of optimisation procedures, a setup for the bacterial competition experiment in microaggregates was developed to grow microaggregates with bacterial mono-cultures and co-cultures in casein medium (where AprX enzyme was needed) and digested casein as the control medium. The co-culture samples are made from a combination of wildtype and mutant mono-cultures microaggregates in order to reduce the possibility of wildtype and mutant cells sharing the same space in the microaggregates. Following the competition, samples were treated with several different breaking techniques.

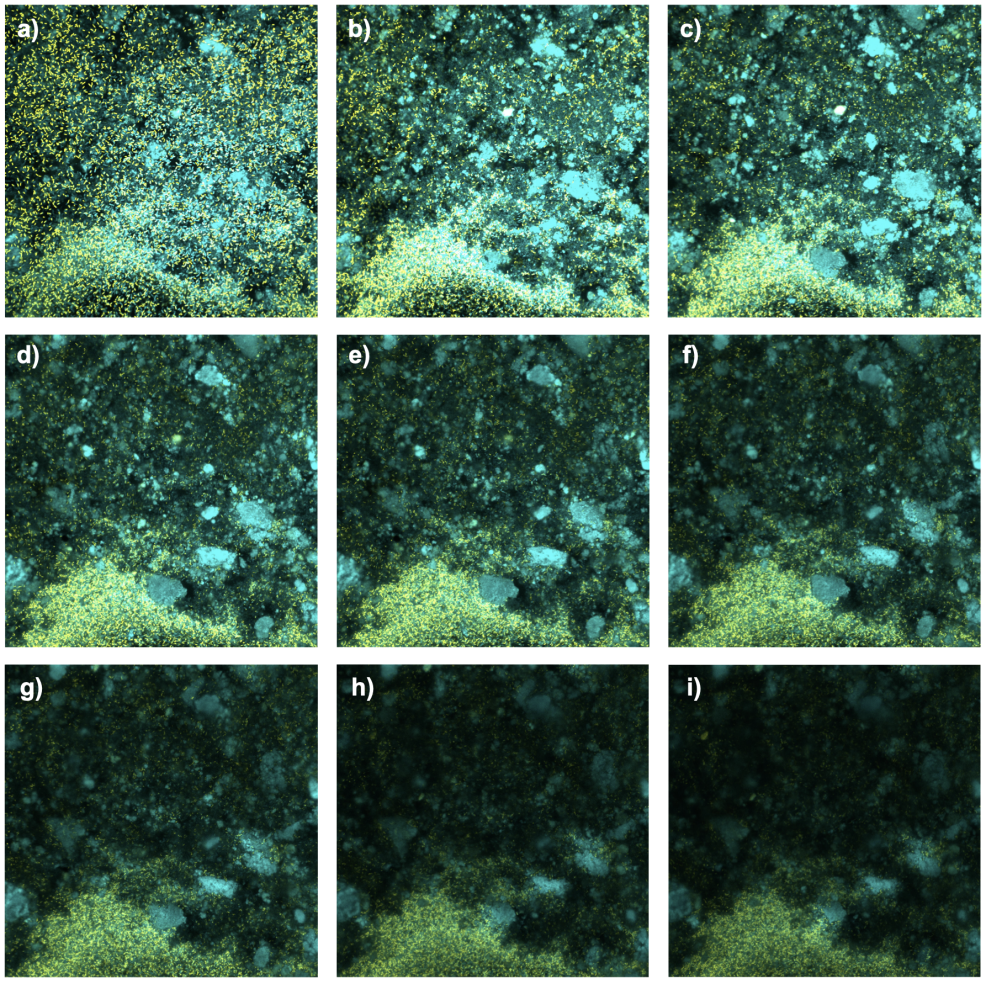

Figure 4.25: The structure of microaggregates depends on its base units, clay particles. Using confocal microscopy, the structure of the microaggregate was investigated. The sample was a mono-culture of ON2-WT-YFP in casein clay medium that was incubated for 48 hours at the slow shaker. Images from (a) to (i) show z-stacks of the microaggregate structure in cyan and the ON2-WT-YFP cells in yellow. The images taken with different z-stacks demonstrated bacterial movement in the microaggregate structure. The microaggregates built with larger clay particles contain larger pores. As a result of the presence of liquid in the clay media, bacterial cells are observed passing into the microaggregates through these pores. So, not all microaggregate structures are similar, and, depending on the pore size within the structure, the efficiency of the microaggregate as a physical barrier may differ. It is this phenomenon that explains the variation in the outcome of the bacterial competition.

A combination of four breaking treatments – consisting of a 120 second vortex, 20 minutes of water bath sonication, a short vortex, followed by passing the sample through a 30^G gauge size needle five times– enabled bacteria to be released from the sample with minimal damage. Multiple counting methods were also employed in order to have a clear understanding of the outcome of the bacterial competition in microaggregates.

CFU counting measurements were done on all the samples including ON2-WT and ON2-Δ*aprX* in mono-culture and co-culture in casein and digested casein with proteinase K media with and without clay. The outcome of CFU counting of mono-culture samples of ON2-WT and ON2-Δ*aprX* strains was always constant with minimum variation among technical and biological repeats. For instance, CFU counting of mono-culture samples in digested casein media with and without clay always showed that the difference between ON2-WT and ON2-Δ*aprX* was statistically not significant ($p< 0.05$) and in casein media with and without clay, their difference was always statistically significant ($p<0.005$).

Based on the CFU counting results, it is safe to consider that ON2-Δ*aprX* strain can grow as well as ON2-WT strain in digested casein but it is unable to grow in undigested casein due its AprX-deficiency caused by a clean deletion of *aprX* gene in its genome.

The CFU counting results showed that in casein and predigested casein media without clay, the standard deviations are relatively small as shown in Figs 4.15(a), 4.15(b) and 4.15(c), respectively. However, the CFU counting of the co-culture sample in the medium that the bacterial competition will be assessed, casein medium with clay, showed that the difference between ON2-WT and ON2-Δ*aprX* strains, can be vary from significant with $p<0.05$ to not significant with $p>0.05$, as shown in Fig. 4.15(d) and (e). This variation in data made analysing the outcome of bacterial competition very challenging.

The CFU counting results of the competition between ON2-WT and ON2-Δ*aprX* in the casein clay environment, shown in Fig. 4.15(d), indicates that the presence of microaggregate was beneficial for the ON2-WT strain and in co-culture sample with ON2-Δ*aprX* strain, AprX producer had access to the digested casein and could could grow faster than the AprX non-producer. However, in the CFU counting shown in Fig. 4.15(e), the result indicate that both AprX producer and non-producer cells can have similar access to the digested casein from AprX digestion. The variation in this result required more counting techniques to analyse the outcome of bacterial competition. The other counting methods including SP-SDS method and fluorescent microscopic imaging were tested. The results of the SP-SDS method were not informative due to continuous growth of bacterial colonies

after the incubation time.

With the aid of a fluorescence microscope, the number of bacteria in casein medium with clay was quantified and the outcome of bacterial competition after 48 hours was observed that the ON2-WT performed better than ON2-Δ*aprX* strain when clay was present (shown in Fig. 4.17), which can be the result of the microaggregate structure causing the AprX enzyme to remain close to the producer cells. The variability of counting results, however, encouraged epifluorescence and confocal microscopy to be used to study microaggregates in more detail.

Epifluorescence microscopic imaging on mono-cultures and co-cultures of ON2-WT and ON2-Δ*aprX* in casein media with clay was carried out. The results of microscopic imaging of mono-culture confirmed the counting results, as they indicated the similar growth of ON2-WT and ON2-Δ*aprX* strains in digested casein medium with clay but higher growth of ON2-WT compared to ON2-Δ*aprX* in case of casein medium with clay.

To have a better understanding of each bacterial population as co-culture within microaggregates, the ON2-WT and ON2-Δ*aprX* strains were labelled with CFP and YFP, as given Figs. 4.21(a) and 4.21(b), and with YFP and CFP as shown in Figs. 4.21(c) and 4.21(d). The outcome of bacterial competition in casein medium with clay after 48 hours of incubation revealed that the bacteria formed two types of distribution, mixed and patchy.

The mixed bacterial population within microaggregates, shown in Fig. 4.21(b) and (d), could suggest that the AprX-producer and non-producer cells are not isolated within microaggregate structure and ON2-Δ*aprX* still can get access to the digested casein which is very similar to the counting result where both strain grew similarly in co-culture sample in casein medium with clay, Fig. 4.15(e). Meanwhile, the higher growth of the AprX-producer cells and formation of genotypic patches of ON2-WT strain within microaggregates in the same sample, as shown in Figs. 4.21(a) and (c), visually is indicating that ON2-WT was growing faster than ON2-Δ*aprX* in casein medium in presence of clay, which is confirm the counting results shown in Fig. 4.15(d) and Fig. 4.17(c). These results indicated that microaggregates in one medium with equal condition have potential to be formed in different shapes and structures which can affect the outcome of bacterial competition.

These results also indicated that microaggregates in one medium with equal condition may form in various shapes and sizes, which can provide a unique environment for bacteria to attach to clay particles and grow with varying degrees of genotypic patchiness. As a result, each microaggregate can influence the outcome of bacterial competition in a different manner. However, by breaking the

aggregates, the counting results will represent an average over all the microaggregates in the sample, which may not reflect the bacterial populations within each microaggregates.

Additionally, fluorescence microscopy images of the linear microfluidic device revealed that AprX-producing cells attached to the surface of the microfluidic chamber grew faster than their neighbour cells, AprX non-producers, when the casein medium was flowing. However, when casein is predigested using proteinase K, AprX non-producers grew more rapidly than AprX producers.

Later, the confocal microscopy helped to gain a better understanding about the structure of microaggregate. The confocal images revealed that pores in the microaggregate structure can have different sizes and the large pores will facilitate the passage of bacterial cells within microaggregates (shown in Fig. 4.25). Also, the small pores which are smaller than a bacterial cell (approximately 1 μm) can make passage of bacteria difficult resulting in cells within microaggregates being isolated from the outside.

The microscopic findings are of great significance as they demonstrate that the structure of all microaggregates that formed during 48 hours of incubation are not identical. In some microaggregates, the AprX-producer could be isolated from AprX non-producers and benefit from its secretions, resulting in growth and formation of bacterial genotypic patches within microaggregates. In this regard, the size and arrangement of clay particles also play an important role in the formation of microaggregates [76]. This was not the case in other microaggregates, and it can be assumed that diffusion rates within microaggregates with relatively open structures are higher than those with relatively closed structures, which may increase the chance of enzyme leakage. This is an important factor determining whether an enzyme becomes "public good" or is kept as "private good".

In fact, as indicated above, the results of the experiment are highly dependent on the structural integrity of the microaggregates; if the arrangement of the clay particles leads to create a relatively compact microaggregate that will provide a relatively closed environment, there is a higher chance that the producer cells inside the microaggregates can get more access to the digested casein and grow faster than ON2-Δ*aprX* in casein clay after 48 hours, as the counting results shown in Figs. 4.15(d), and Fig. 4.17(c). To have a clear understanding of how microaggregates are formed at a micro-scale, further research is required, which is beyond the scope of this study.

A similar observation was also achieved from the fluorescence microscopic studies on the co-culture samples with the exact same condition. The microscopic images revealed that in some cases Fig. 4.21(a) and Fig. 4.21(c), a higher growth

and genotypic patchiness of the ON2-WT strain compared to the ON2-Δ*aprX* in the casein clay medium made the ON2-WT the dominant bacterial population. These results indicate that the microaggregate can protect AprX enzyme from exploitation by AprX non-producers and allow the ON2-WT strain to grow and create genotypic patchiness within microaggregates. However, there are some cases in the same sample that show mixed bacterial genotypes within microaggregates, as shown in Fig. 4.21(b) and 4.21(d).

4.6.2 Conclusion

Although bacterial competition in homogenised environments, such as liquid culture, has been the subject of significant literature studies, little is known about how bacteria interact with one another and compete in soil environments, as their natural habitat. The purpose of this chapter was, therefore, to develop a systematic framework for precisely investigating bacterial behaviour in soil, where soluble nutrients are scarce.

In order to determine the effects of spatial structure of microaggregate on bacterial competition, a microaggregate laboratory model - similar to that found in soil - was developed. A soil bacterium, P. fluorescens, with ON2 background carrying a gene responsible for producing a digestive enzyme called aprX, was used as a wildtype strain, ON2-WT. Also, this study used a two-step allelic replacement technique to replace the aprX gene in ON2-wt with a deleted version of *aprX*, which was called ON2-Δ*aprX*, to construct a proteinase deficient strain.

The media for bacterial competition were chosen to be casein with and without clay and as the control media, digested casein with and without clay was selected. Using a slow shaker, the samples were incubated at room temperature for the purpose of replicating the conditions in natural soil. After a series of optimisation procedures, a setup for the experiment was developed to grow microaggregates with each strain as mono-cultures and then combine two mono-culture microaggregates as co-cultures in order to reduce the possibility of WT and mutant cells sharing the same space in the microaggregates. The incubation period for the competition was determined by screening several time points.

Following the competition, the samples were treated with several microaggregate breaking techniques. A combination of four breaking treatments – consisting of a 120 second vortex, 20 minutes of water bath sonication, a short vortex, followed by passing the sample through a 30G gauge size needle – enabled bacteria to be released from the sample with minimal damage. To assess the bacterial population in the samples, different counting techniques were employed including CFU counting and counting bacterial cells using fluorescence microscopy. It

is important to note that the results obtained in this study are made under certain conditions as discussed previously and changing one or more experimental variables may result in a different outcome.

Results from bacterial competition in casein medium with clay indicated that there is a continuum of outcomes depending on the spatial structure of the microaggregate - ranging from a relatively closed structure that protects the extracellular enzymes, to a relatively open structure with large pores in which the extracellular enzymes leak outside of the microaggregate and become available to mutant bacteria. In fact, *most microbial communities studied in the laboratory are snapshots in time resulting from a history of interactions between individual cells and genotypes under certain conditions* [37]. These findings is of great significance as it not only demonstrates how the structure of the microaggregate, besides other environmental factors, impacts bacterial competition, but it also provides a platform for further studies on bacterial competition in soil that may have a great impact on carbon sequestration in soil.

Chapter 5

General Discussion

The desire to understand bacterial competition has driven generations of researchers to study bacterial competitive strategies of all kinds [28, 119, 37, 127, 133]. However, there are no comprehensive experimental investigations of bacterial competition in soil microaggregates. The goal of this research study was to investigate bacterial interaction and competition in a laboratory model of soil microaggregates.

In view of this, the majority of this thesis was devoted to optimising the experimental procedure, including sample preparation, aggregate breaking techniques, counting techniques, and microscopic studies. The solutions provided for the experimental challenges in this research provides a foundation for studying the bacterial population inside the microaggregates and will be valuable to anyone who wishes to study bacterial competition in soil environments.

This chapter is organised as follows: In Section 5.1, a summary of the tasks that were undertaken as part of this thesis will be presented, followed by the discussion. In Section 5.2 further research questions that were not addressed in this study are discussed which could offer additional insight into bacterial competition in microaggregates.

5.1 Discussion

Numerous studies explore mitigation strategies to help combat climate change due to the increasing concentration of carbon dioxide in the atmosphere [21]. The sequestration of carbon in soil would be a promising strategy to reverse this trend [261]. The capacity of soil to sequester carbon depends on numerous factors such as total soil organic carbon (SOC), properties of the soil, management of the soil, and climatic conditions [262, 225]. Different soil fractions, macroaggregates and

microaggregates, also have different capacities to sequestrate SOC [263]. The stability of SOC is reported to be weaker in macroaggregates compared to microaggregates due to the more transient structure of macroaggregates [89]. However, in microaggregates, the carbon turnover is much slower – approximately 300 years – compared to the other soil fractions [187, 68, 264]. Therefore, SOC can be stored in soil for a long time and be protected from decomposition or oxidation [192]. For decades, researchers have debated the mechanisms of soil carbon sequestration [265]. However, the latest studies support the soil continuum model, suggesting that the persistence of SOC is strongly influenced by the surrounding environment and the interplay between bacteria and soil minerals [266].

Bacteria play an integral role in all ecosystems, including the mineralisation of nutrients, decomposition, and the remediation of environmental pollution. A number of these processes involve the conversion of non-labile substrates into simpler compounds, which can be assimilated by bacteria to support growth and metabolism. Except in environments where simple nutrients are readily available, bacteria produce and secrete digestive enzymes in order to scavenge nutrients [267]. These enzymes, however, are costly for bacteria to produce [268, 269, 136], and in environments with high diffusion rates, such enzymes can be consumed by neighboring cells that were not involved in their production. The neighbouring cells, therefore, will gain a competitive advantage which will increase their fitness and therefore their frequency relative to population size in comparison with enzyme producers [175].

Our understanding of bacterial competition in homogeneous environments like liquid cultures is well-studied, however, our knowledge of bacterial interaction in spatially heterogeneous environments like soil is much more limited. Microaggregates are composed of a network of interconnected pores and voids of varying size, shape and geometry, which results in a complex biogeochemical network. The network allows the transport of liquids and gases, dissolved compounds and colloidal particles within some microaggregates [193]. In general, soil is an aggregate based environment where the soil microorganisms, such as bacteria, live in communities that are closely associated with soil aggregates [51]. However, the impact of the microaggregate on bacterial activities and their interaction is not well understood.

It has been suggested that limited diffusion and spatial structure promote coexistence of cheater and producer strategies [135], however, this statement has not been experimentally tested in soil microaggregates and no quantification or visualisation of how bacteria compete in this fraction of soil had been performed prior to this study. The objective of this thesis is, therefore, to develop a labora-

tory model of bacterial competition in soil microaggregates and to ascertain what factors are at play in different conditions.

To accomplish this, the first step was to create the competition environment, which includes the enzyme-producer strain and cheater strain that do not produce enzymes, labile and non-labile nutrients, and clay-based microaggregates, as follows:

- Producer bacterial strain (WT): This study utilised *Pseudomonas fluorescens* as an organism model. *P. fluorescens* is a gram-negative bacterium found throughout terrestrial habitats and plays a critical role in the breakdown of organic matter. *P. fluorescens* produces an alkaline metalloproteinase, commonly known as AprX, which is an exo-enzyme capable of breaking down complex proteins into a more labile form. Because *P. fluorescens* has a highly adaptable metabolic system, it is able to thrive in diverse environments and produces a broad range of exo-enzymes that allow it to digest non-labile nutrients to survive.

- Non-producer bacterial strain (ON2-Δ*aprX*): A strain lacking the AprX protein production, was constructed by deleting *aprX* gene from the the genome of *P. fluorescens* ON2, called ON2-Δ*aprX*. The ON2-Δ*aprX* is deficient in producing the extracellular AprX proteinase, preventing the organism from growing in casein medium. Thus this bacteria must rely on the AprX enzyme produced by ON2-WT cells to break down the casein into a labile form i.e. digested casein, to survive. Chapter 2 provides detailed information on how the construct protease deficient strain was generated in the ON2 *P. fluorescens* background.

- Media: Casein, a milk protein, and digested casein with and without clay were used as media in this study. Among the extracellular enzymes that *P. fluorescens* produces, AprX is a heat-stable metalloproteinase enzyme that is responsible for digesting casein and causing milk spoilage. A detailed description of how to prepare the media for bacterial competition was given Chapter 2.

- Microaggregate environment: In order to determine the effects of spatial structure of microaggregate on bacterial competition, a microaggregate laboratory model - similar to that found in soil - was developed. Because of the surface properties of clay particles, organic materials can accumulate on the surface of the clay and unite with the minerals to initiate forming microaggregate structures. In addition, microbial activity, such as polysaccharide secretion, are essential for the stability of microaggregates.

Bacteria play an important role in the formation and stabilisation of microaggregates, as they secrete their extracellular products to survive. These secreted substances act as cement and form the clay particles into clay aggregates and ultimately, form highly stable microaggregate structures over time.

Chapter 3 outlined a comprehensive protocol for creating a laboratory-based model of microaggregates, developed and optimised in this study. Following completion of a bacterial competition within microaggregates, bacteria were separated from microaggregates so that the growth of both bacterial strains - ON2-WT and ON2-Δ*aprX* - could be measured. The process proved difficult because it was extremely challenging to separate bacteria from their microaggregates without damaging or destroying them. Several breaking techniques – vortexing, using homogeniser, applying ultrasonic energy, using sodium pyrophosphate buffer, using filters, and using fine syringes– were introduced and their effectiveness were assessed thoroughly in Chapter 4.

The breaking treatment was optimised by combining four different types of breaking methods - including 120 seconds of vortexing, 20 minutes of water bath sonication, a short vortex, followed by passing the sample through a 30^G gauge needle. Experimental evidence demonstrated that this approach allowed bacteria to be released from the microaggregates with minimal damage. As soon as the bacteria have been separated from the microaggregates, it is important to count them quickly and accurately to prevent any bacterial re-aggregation. Chapter 4 discusses several counting methods, including CFU, SP-SDS, fluorescent microscopy, and the effectiveness of each was evaluated. To ensure the accuracy of the results, all samples were prepared under the same environmental condition.

The growth of both ON2-WT and ON2-Δ*aprX* strains as mono-cultures and co-culture in the predigested casein medium was very similar, Figs. 4.15(a) and (b), Figs. 4.19(a) and (b) and presence of clay in predigested casein did not seem to change the results. The microscopic images of the co-culture in predigested casein with clay showed a well-mixed population of both bacterial strains within microaggregates, Fig. 4.20, which can represent the CFU results of co-culture samples in digested casein with clay.

The counting results of the mono-culture samples showed that the ON2-Δ*aprX* strain, unlike ON2-WT, is unable to grow in casein-based media with or without clay (Figs. 4.15(c) and 4.15(d)), and this is due to a clean deletion of the *aprX* gene in the genome of the ON2-Δ*aprX* strain. The microscopic images of the mono-culture samples in casein with clay medium also confirmed the CFU counting results by showing a substantial difference between the microaggregates formed by ON2-WT cells and ON2-Δ*aprX* when they grew in casein (Figs. 4.19(c) and

4.19(d)).

The counting results of the bacterial competition in the casein medium without clay, showed that the difference between ON2-WT and ON2-Δ*aprX* was always insignificant (shown in Fig. 4.15(c)). However, in casein medium with clay, the counting results showed that sometimes ON2-WT strain is the winner of the competition, as shown in Figs. 4.15(d) and 4.17(c)) but most of the time the number of ON2-WT cells was not significantly different from the number of ON2-Δ*aprX* cells (Fig. 4.15(e)). It should be noted that the recent evidence of higher growth of ON2-WT strain in co-culture samples was observed only when clay was present in the casein medium.

The microscopic study provided additional insight into the impact of microaggregates on bacterial competition. The microscopic techniques were also utilised and optimised to gain a better visual understanding of how microaggregates affect bacterial interaction and competition. A detailed discussion of the implementation and optimisation of these techniques can be found in Chapter 4. Based on the microscopic findings of the co-culture sample in casein medium with clay, individual microaggregates showed different scenarios:

- In the first scenario, we observed a mixed population of the ON2-WT and ON2-Δ*aprX* cells within microaggregates and there was no statistically significant difference between two strains in casein medium containing clay. This result suggested that the AprX enzyme was not exclusive to its producer cell (i.e. public good), and the digested casein was accessible to the ON2-Δ*aprX* strain. In this scenario the microaggregates have a negligible protective role for the producer cells in casein clay environment.

- In the second scenario, we observed a high level of genotypic patchiness of the ON2-WT strain, and its higher growth compared to ON2-Δ*aprX*. This scenario is routinely observed in our microscopic images, from counting results, suggesting that the AprX-producers within microaggregates have potential access to their secreted AprX (i.e. private good) and digested casein. In this condition, it is hypothesised that the AprX producer was able to grow faster than non-producer strain within microaggregates in casein.

Figure 4.21 evidently show different bacterial populations within microaggregates in the same co-culture sample in casein medium with clay. These microscopic images demonstrated that the genotypic patchiness within microaggregates in the same sample can be highly variable and each microaggregates can exhibit a highly heterogeneous structure. There are times when the spatial structure of microaggregates creates an environment where the "public good" transforms into

a "private good" by successfully limiting the access of the AprX non-producer cells to the AprX and digested casein, Fig. 4.21(a) and 4.21(c), and there are times when it does not, Figs. 4.21(b) and 4.21(d). In the case of high genotypic patchiness of the ON2-WT strain within microaggregates, producer cells can benefit from their AprX enzyme production by consuming its product, digested casein, and growing faster in co-culture with ON2-Δ*aprX*.

The structure of soil microaggregates is described as a three-dimensional network of interconnected pores that provides an extremely heterogeneous biogeochemical interface on the internal and external surfaces [103]. Thus, there are many unknown geochemical factors that can directly or indirectly influence bacterial interaction within the microaggregates. Based on our intriguing microscopic results, it appears that spatial structure of microaggregates can influence the outcomes of bacterial competition. Our results suggest that the combination of clay particles and bacteria may form microaggregates with a compact form, resulting in a relatively closed environment in which AprX producer cells can be isolated from AprX non-producers. In this case, it is more likely that the ON2-WT strain could form a higher degree of genotypic patchiness which allows cells to have access to their secretions. On the other hand, if the arrangement of clay particles lead to form microaggregates with large pores, microaggregate with a closed spatial structure may not be developed, which results in a more open structure. There is a high probability that in the microaggregates with relatively open structures, cells can cross the microaggregate through the large pores, which makes them less isolated from outside of the microaggregates. This can result in a mixed bacterial population within microaggregate, making access to the AprX enzyme not exclusive to its producer cell.

5.2 Future Research Directions

The results of this project have opened up a number of new avenues for future research and the following are a few potential areas that could be explored:

Synthetic clay: It was observed in Chapter 4 that the porous structure of microaggregates are not uniform and it is possible that the secreted enzymes might leak from the microaggregate and become accessible to the non-producing bacteria. The various size and shape of hectorite clay particles may be a possible explanation for this event which is creating a nonuniform structure of microaggregates. To determine the role of clay particles in the structure of microaggregates, one potential future work is the use of laponite clay which is a manufactured smectite clay.

The physical and chemical properties of laponite is similar to hectorite clay [270], however, the particle size distribution of laponite is more uniform. Due to this property, a more homogeneous microaggregate with a compact structure may be achieved, preventing the leakage of nutrients from the outside of the microaggregates. Also, it would be interesting to know whether using laponite could facilitate the breaking process on a developed microaggregate. Moreover, this synthetic clay does not possess the autofluorescence properties of hectorite clay [271], thus offering great potential for fluorescent microscopic studies of bacterial interaction within microaggregates.

Microaggregate formation and structure by overproducing LapA in *P. fluorescens*: Further study is needed to explore the impact of microaggregate porous structure on the bacterial competition within the microaggregate. LapA is an extracellular protein found in *Pseudomonas fluorescens* that plays an essential role in the formation of biofilm when the cells are under stress. In unfavorable conditions, the LapA protein is secreted by an ABC transporter to facilitate attachment of cells to other surfaces. The LapA protein, which is responsible for the reversible binding of cells to surfaces, plays a key role in biofilm formation [272], (also as it is illustrated in Fig. 5.1(a)). In a condition when cells are in their favourable nutrient conditions, LapG degrades the LapA proteins and this, in turn, will let them return to planktonic state [273], as it is demonstrated in Fig. 5.1(b).

A preliminary experiment was made by growing *P. fluorescens* Pf0-1 strains, including Pf0-1 WT, Pf0-1-Δ*lapG* and Pf0-1-Δ*lapA*, in M63 with glucose medium with clay for 24 hours. Brightfield microscopic imaging was utilised on the microaggregates with these three strains and the results showed a larger microaggregate structure in bacterial sample Pf0-1-Δ*lapG* that overproduces LapA protein as shown in Fig. 5.1(c). These findings suggest that proteins that are involved in biofilm formation could influence the formation of microaggregates by increasing the chance of attachment of cells to clay particles (in the case of Pf0-1-Δ*lapG*) and gluing the clay particles together. Therefore, the next research questions include how the degree of biofilm compactness formed by Pf0-1-Δ*lapG* and Pf0-1-Δ*lapA* can affect the outcome of bacterial competition. Other interesting research questions, which were not covered in this thesis, are related to the fitness of bacteria under specific circumstances as follows:

The fitness of bacterial cells inside microaggregate: Another interesting research topic, which was not covered in this thesis, is related to the fitness of bacteria under specific circumstances as follows:

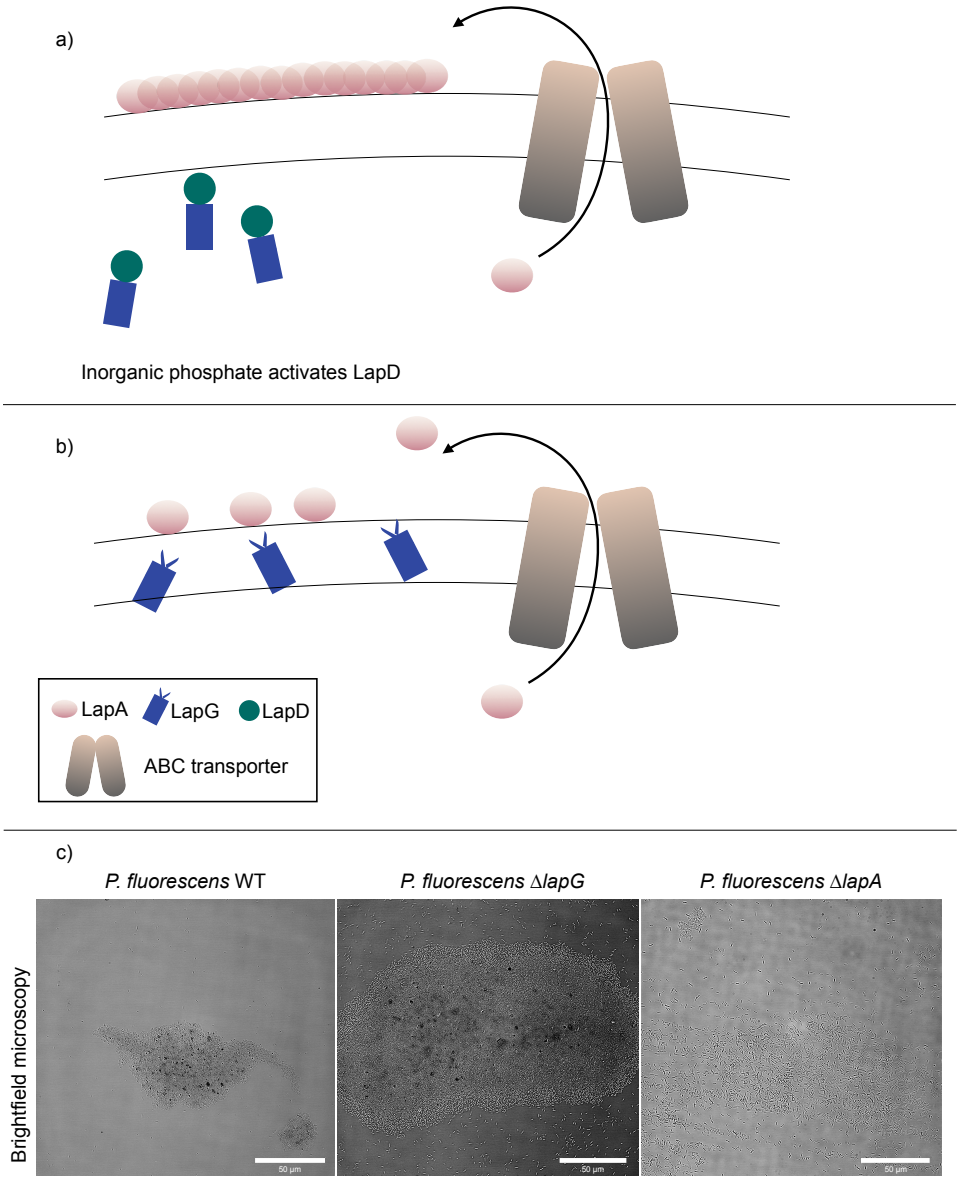

Figure 5.1: The role of an adhesive agent, LapA protein, on microaggregate formation. LapA acts as an adhesive agent on the cell surface of *P. fluorescens*. During periods of stress, (a) high level of inorganic phosphate acts as a signal to activate LapD which suppresses activity of LapG (LapG degrades LapA). Therefore, LapA accumulates on the cell surface and facilitates attachment of cells to other cells or surfaces. When the stress is eliminated, (b) LapD becomes inactive so LapG degrades the LapA protein that leads cells to return to their planktonic state. (c) Brightfield microscopic images of *P. fluorescens* Pf0-1 WT, Pf0-1-Δ*lapG* and Pf0-1-Δ*lapA* after 24 hours of incubation at room temperature with slow shaking speed.

- Certain strains of *Pseudomonas fluorescens* are resistant to certain concentrations of beta-lactam antibiotics and heavy metals [274, 275]. In order to grow in this environment, these bacteria secrete extracellular compounds that enable them to break down these toxic substances. This is similar to the condition where bacteria need to secrete AprX in order to digest casein and grow. As a consequence, the clay attachment might enable cells to locally reduce the concentration of toxic substances as clay particles act as physical barriers or due to their chemical properties that have the ability to adsorb chemical substrates on their surface. Thus, the possibility of higher survival rate of bacteria within microaggregates can be tested and compared with bacteria in planktonic state.

- Being enclosed in microaggregates might limit bacteria access to nutrients outside of the microaggregates, which could reduce bacterial growth rate compared with that in a non-enclosed space [276]. However, our knowledge of bacterial growth rate while they are in microaggregates is very limited. To tackle this question, a number of experiments can be performed, such as labeling the carbon source by a fluorescence label and measuring the fluorescent intensity overtime. By calculating the rate of carbon consumption of bacteria in a liquid culture, the result can be compared to the same culture with clay.

Microscopical study: The fluorescent microscopic imaging of bacterial competition in microaggregates, as described in Chapter 4, has been extremely challenging since the autofluorescence characteristics of the hectorite clay and thus poses a great technical challenge to observe the population of each bacterial strain inside microaggregates.

Another possibility to overcome the difficulty in imaging hectorite clay with fluorescence microscopy is using the spectral unmixing technique. A preliminary experiment was conducted using a Zeiss Airyscan Axiovert LSM 880 confocal microscope and the objective of this experiment was to determine whether this technique could allow us to distinguish the signal from clay from that of CFP-labelled cells. Spectral unmixing is a technique that facilitates the identification of different fluorescent compounds based upon their fluorescent emission patterns. In this approach, the emission is resolved as a function of wavelength using a variable wavelength beam splitter. As shown in Fig. 5.2, the Airyscan confocal microscope successfully distinguished clay signals from CFP-labeled cells using spectral demixing. Therefore, for further imaging of microaggregates, it is valuable to consider utilising this technique to distinguish between the signal from

clay and the signal from fluorescently labelled cells.

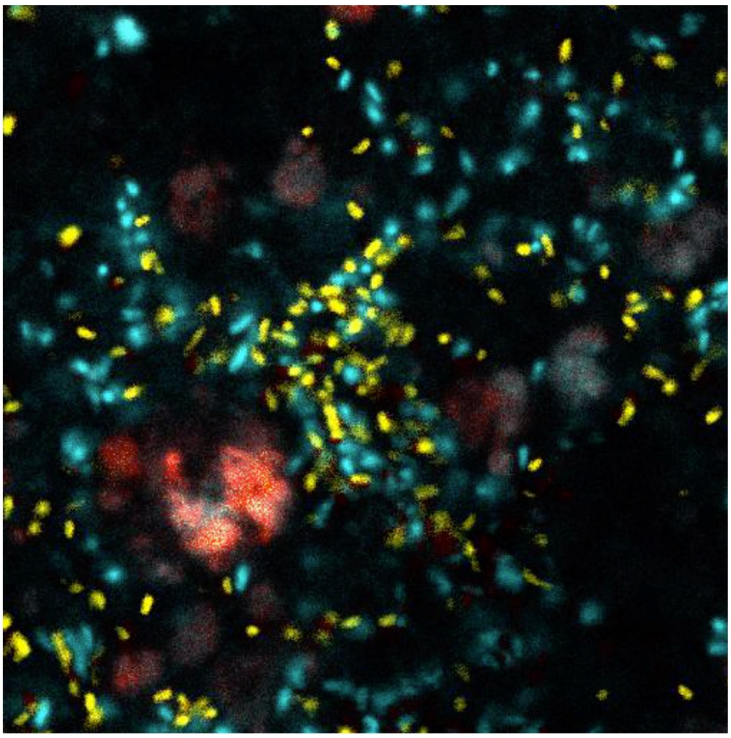

Figure 5.2: Confocal imaging of a co-culture sample, ON2-WT-CFP and ON2-Δ*aprX*-YFP in digested casein clay using Airy-scan microscopy. Using the spectral demixing feature of Airy-scan microscope, a unique signal from the wavelength of the hectorite clay was identified. This signal was marked with red colour which is easily distinguished from CFP and YFP labelled cells. Imaging the mixture of ON2-WT-CFP and ON2-Δ*aprX*-YFP in digested casein clay.

As shown in Fig. 5.2, the Airyscan confocal was successful to distinguish the clay signal from CFP-Labeled cells. Therefore, a comprehensive study using Airy-Scan microscopy to separate the signal from the hectorite clay and CFP-labelled cells is recommended for future research into microscopic imaging of bacterial competition in microaggregate.

In addition the following tasks are recommended for further exploration:

1. Optimising microfluidic-device chamber to accommodate microaggregates for further studies on bacterial competition and their interaction within microaggregates.

2. Structural study on microaggregates, using electron microscopy for instance, to compare the microaggregate structure made in the laboratory with those that occur naturally.

Theoretical studies: The experimental results presented in this thesis will facilitate future research in computational mathematics and modeling of bacterial competition in soil microaggregates. Several factors, including but not limited to diffusion rates and consumption rates of extracellular enzymes, bacteria dynamics, environmental parameters, and microaggregate structural parameters, can be incorporated into a mathematical model.

The computation model could be used not only to replicate the experimental results, but also, more importantly, to (i) uncover relationships between variables that are not obvious from experimental data, potentially allowing us to resolve how the competition between producer and cheater strains depends on a wider range of environmental parameters, (ii) to verify the predictions and scenarios on bacterial competition under certain conditions, and (iii) to identify the conditions that favour bacterial competition in soil microaggregate and the emergence of cooperative growth.

Bibliography

[1] Todd A Ontl and Lisa A Schulte. Soil carbon storage. *Nature Education Knowledge*, 3(10), 2012.

[2] Eric H Oelkers and David R Cole. Carbon dioxide sequestration a solution to a global problem. *Elements*, 4(5):305–310, 2008.

[3] RA Houghton. Balancing the global carbon budget. *Annual Review of Earth and Planetary Sciences*, 35(1):313–347, 2007.

[4] Paul G Falkowski, Tom Fenchel, and Edward F Delong. The microbial engines that drive earth's biogeochemical cycles. *science*, 320(5879):1034–1039, 2008.

[5] Wilfred M Post, Tsung-Hung Peng, William R Emanuel, Anthony W King, Virginia H Dale, Donald L DeAngelis, et al. The global carbon cycle. *American scientist*, 78(4):310–326, 1990.

[6] Yahai Lu and Ralf Conrad. In situ stable isotope probing of methanogenic archaea in the rice rhizosphere. *Science*, 309(5737):1088–1090, 2005.

[7] Susan Trumbore. Carbon respired by terrestrial ecosystems–recent progress and challenges. *Global Change Biology*, 12(2):141–153, 2006.

[8] James Ivor Prosser. Microorganisms cycling soil nutrients and their diversity. In *Modern soil microbiology*, pages 237–261. CRC Press, 2007.

[9] Myles R Allen, Opha Pauline Dube, William Solecki, Fernando Aragón-Durand, Wolfgang Cramer, Stephen Humphreys, Mikiko Kainuma, Jatin Kala, Natalie Mahowald, Yacob Mulugetta, et al. Framing and context. *Global warming of*, 1(5), 2018.

[10] Nadine Herold, Ingo Schöning, Beate Michalzik, Susan Trumbore, and Marion Schrumpf. Controls on soil carbon storage and turnover in german landscapes. *Biogeochemistry*, 119(1):435–451, 2014.

[11] MP Martin, Martin Wattenbach, P Smith, Jeroen Meersmans, Claudy Jolivet, Line Boulonne, and Dominique Arrouays. Spatial distribution of soil organic carbon stocks in france. *Biogeosciences*, 8(5):1053–1065, 2011.

[12] Janna Pietikäinen, Marie Pettersson, and Erland Bååth. Comparison of temperature effects on soil respiration and bacterial and fungal growth rates. *FEMS microbiology ecology*, 52(1):49–58, 2005.

[13] DH Mao, ZM Wang, L Li, ZH Miao, WH Ma, CC Song, CY Ren, and MM Jia. Soil organic carbon in the sanjiang plain of china: storage, distribution and controlling factors. *Biogeosciences*, 12(6):1635–1645, 2015.

[14] Christos Gougoulias, Joanna M Clark, and Liz J Shaw. The role of soil microbes in the global carbon cycle: tracking the below-ground microbial processing of plant-derived carbon for manipulating carbon dynamics in agricultural systems. *Journal of the Science of Food and Agriculture*, 94(12):2362–2371, 2014.

[15] Peter O'Neill. *Environmental chemistry*. Routledge, 2017.

[16] Jong-Su Seo, Young-Soo Keum, and Qing X Li. Bacterial degradation of aromatic compounds. *International journal of environmental research and public health*, 6(1):278–309, 2009.

[17] Nezha Tahri Joutey, Wifak Bahafid, Hanane Sayel, and Naïma El Ghachtouli. Biodegradation: involved microorganisms and genetically engineered microorganisms. *Biodegradation-life of science*, 1:289–320, 2013.

[18] S Pointing. Feasibility of bioremediation by white-rot fungi. *Applied microbiology and biotechnology*, 57(1):20–33, 2001.

[19] Richard D Bardgett, Chris Freeman, and Nicholas J Ostle. Microbial contributions to climate change through carbon cycle feedbacks. *The ISME journal*, 2(8):805–814, 2008.

[20] VL Jin and RD Evans. Elevated co2 increases microbial carbon substrate use and nitrogen cycling in mojave desert soils. *Global Change Biology*, 13(2):452–465, 2007.

[21] Brajesh K Singh, Richard D Bardgett, Pete Smith, and Dave S Reay. Microorganisms and climate change: terrestrial feedbacks and mitigation options. *Nature Reviews Microbiology*, 8(11):779–790, 2010.

[22] Carlos E Coviella, David JW Morgan, and John T Trumble. Interactions of elevated co2 and nitrogen fertilization: Effects on production of bacillus thuringiensis toxins in transgenic plants. *Environmental Entomology*, 29(4):781–787, 2000.

[23] Qiongfen Qiu, Ralf Conrad, and Yahai Lu. Cross-feeding of methane carbon among bacteria on rice roots revealed by dna-stable isotope probing. *Environmental Microbiology Reports*, 1(5):355–361, 2009.

[24] Michael J McInerney, Jessica R Sieber, and Robert P Gunsalus. Syntrophy in anaerobic global carbon cycles. *Current opinion in biotechnology*, 20(6):623–632, 2009.

[25] Elena Butaitė, Michael Baumgartner, Stefan Wyder, and Rolf Kümmerli. Siderophore cheating and cheating resistance shape competition for iron in soil and freshwater pseudomonas communities. *Nature communications*, 8(1):1–12, 2017.

[26] Ali R Zomorrodi and Daniel Segrè. Synthetic ecology of microbes: mathematical models and applications. *Journal of molecular biology*, 428(5):837–861, 2016.

[27] Maren L Friesen. Social evolution and cheating in plant pathogens. *Annual Review of Phytopathology*, 58:55–75, 2020.

[28] Michael E Hibbing, Clay Fuqua, Matthew R Parsek, and S Brook Peterson. Bacterial competition: surviving and thriving in the microbial jungle. *Nature reviews microbiology*, 8(1):15–25, 2010.

[29] Teri C Balser and Mary K Firestone. Linking microbial community composition and soil processes in a california annual grassland and mixed-conifer forest. *Biogeochemistry*, 73(2):395–415, 2005.

[30] Céline Mouginot, Rika Kawamura, Kristin L Matulich, Renaud Berlemont, Steven D Allison, Anthony S Amend, and Adam C Martiny. Elemental stoichiometry of fungi and bacteria strains from grassland leaf litter. *Soil Biology and Biochemistry*, 76:278–285, 2014.

[31] Yang Yang, Yanxing Dou, and Shaoshan An. Testing association between soil bacterial diversity and soil carbon storage on the loess plateau. *Science of the Total Environment*, 626:48–58, 2018.

[32] Joshua P Schimel and Sean M Schaeffer. Microbial control over carbon cycling in soil. *Frontiers in microbiology*, 3:348, 2012.

[33] Pankaj Trivedi, Manuel Delgado-Baquerizo, Chanda Trivedi, Hangwei Hu, Ian C Anderson, Thomas C Jeffries, Jizhong Zhou, and Brajesh K Singh. Microbial regulation of the soil carbon cycle: evidence from gene–enzyme relationships. *The ISME journal*, 10(11):2593–2604, 2016.

[34] M Dıaz-Zorita, E Perfect, and JH Grove. Disruptive methods for assessing soil structure. *Soil and Tillage research*, 64(1-2):3–22, 2002.

[35] Mette Burmølle, Dawei Ren, Thomas Bjarnsholt, and Søren J Sørensen. Interactions in multispecies biofilms: do they actually matter? *Trends in microbiology*, 22(2):84–91, 2014.

[36] Brent Cezairliyan and Frederick M Ausubel. Investment in secreted enzymes during nutrient-limited growth is utility dependent. *Proceedings of the National Academy of Sciences*, 114(37):E7796–E7802, 2017.

[37] Melanie Ghoul and Sara Mitri. The ecology and evolution of microbial competition. *Trends in microbiology*, 24(10):833–845, 2016.

[38] William D Hamilton. The genetical evolution of social behaviour. ii. *Journal of theoretical biology*, 7(1):17–52, 1964.

[39] Jeff Smith, J David Van Dyken, and Peter C Zee. A generalization of hamilton's rule for the evolution of microbial cooperation. *Science*, 328(5986):1700–1703, 2010.

[40] George R Price et al. Selection and covariance. *Nature*, 227:520–521, 1970.

[41] Jakob Worm, Linda E Jensen, Thomas S Hansen, Morten Søndergaard, and Ole Nybroe. Interactions between proteolytic and non-proteolytic pseudomonas fluorescens affect protein degradation in a model community. *FEMS microbiology ecology*, 32(2):103–109, 2000.

[42] C Clarholm. The microbial loop in the soil. 1994.

[43] Anje-Margriet Neutel, Johan AP Heesterbeek, and Peter C De Ruiter. Stability in real food webs: weak links in long loops. *Science*, 296(5570):1120–1123, 2002.

[44] Matthias C Rillig and Daniel L Mummey. Mycorrhizas and soil structure. *New Phytologist*, 171(1):41–53, 2006.

[45] G Jock Churchman. The philosophical status of soil science. *Geoderma*, 157(3-4):214–221, 2010.

[46] Patrick Lavelle, Thibaud Decaëns, Michaël Aubert, Sebastien Barot, Manuel Blouin, F Bureau, P Margerie, Philippe Mora, and J-P Rossi. Soil invertebrates and ecosystem services. *European journal of soil biology*, 42:S3–S15, 2006.

[47] Ohana YA Costa, Jos M Raaijmakers, and Eiko E Kuramae. Microbial extracellular polymeric substances: ecological function and impact on soil aggregation. *Frontiers in microbiology*, 9:1636, 2018.

[48] Simone Cristina Braga Bertini and Lucas Carvalho Basilio Azevedo. Soil microbe contributions in the regulation of the global carbon cycle. In *Microbiome Under Changing Climate*, pages 69–84. Elsevier, 2022.

[49] Judith M Tisdall and Jennifer Malcolm OADES. Organic matter and water-stable aggregates in soils. *Journal of soil science*, 33(2):141–163, 1982.

[50] BG Prove, RJ Loch, JL Foley, VJ Anderson, and DR Younger. Improvements in aggregation and infiltration characteristics of a krasnozem under maize with direct drill and stubble retention. *Soil Research*, 28(4):577–590, 1990.

[51] Regina L Wilpiszeski, Jayde A Aufrecht, Scott T Retterer, Matthew B Sullivan, David E Graham, Eric M Pierce, Olivier D Zablocki, Anthony V Palumbo, and Dwayne A Elias. Soil aggregate microbial communities: towards understanding microbiome interactions at biologically relevant scales. *Applied and Environmental Microbiology*, 85(14):e00324–19, 2019.

[52] Meichen Wang, Asuka A Orr, Joseph M Jakubowski, Kelsea E Bird, Colleen M Casey, Sara E Hearon, Phanourios Tamamis, and Timothy D Phillips. Enhanced adsorption of per-and polyfluoroalkyl substances (pfas) by edible, nutrient-amended montmorillonite clays. *Water research*, 188:116534, 2021.

[53] T. Hattori. Soil aggregates as microhabitats of microorganisms. 37:23–36, 1988.

[54] E Amézketa. Soil aggregate stability: a review. *Journal of sustainable agriculture*, 14(2-3):83–151, 1999.

[55] John R Nimmo. Porosity and pore size distribution. *Encyclopedia of Soils in the Environment*, 3(1):295–303, 2004.

[56] Martin J Shipitalo and Renee-Claire Le Bayon. 10 quantifying the effects of earthworms on soil aggregation and porosity. *Earthworm ecology*, page 183, 2004.

[57] Capowiez Yvan, Samartino Stéphane, Cadoux Stéphane, Bouchant Pierre, Richard Guy, and Boizard Hubert. Role of earthworms in regenerating soil structure after compaction in reduced tillage systems. *Soil Biology and Biochemistry*, 55:93–103, 2012.

[58] N Bottinelli, Pascal Jouquet, Yvan Capowiez, Pascal Podwojewski, Michel Grimaldi, and X Peng. Why is the influence of soil macrofauna on soil structure only considered by soil ecologists? *Soil and Tillage Research*, 146:118–124, 2015.

[59] V Pot, SOLAPLMF Peth, Olivier Monga, LE Vogel, A Genty, Patricia Garnier, L Vieublé-Gonod, Malte Ogurreck, Felix Beckmann, and PC Baveye. Three-dimensional distribution of water and air in soil pores: comparison of two-phase two-relaxation-times lattice-boltzmann and morphological model outputs with synchrotron x-ray computed tomography data. *Advances in water resources*, 84:87–102, 2015.

[60] Mitchell Pavao-Zuckerman. Soil ecology. In *Encyclopedia of Ecology, Five-Volume Set*, pages 3277–3283. Elsevier Inc., 2008.

[61] Eric Brevik. What do scientists see in soil pits? 2011.

[62] William B Whitman, David C Coleman, and William J Wiebe. Prokaryotes: the unseen majority. *Proceedings of the National Academy of Sciences*, 95(12):6578–6583, 1998.

[63] Luke R Thompson, Jon G Sanders, Daniel McDonald, Amnon Amir, Joshua Ladau, Kenneth J Locey, Robert J Prill, Anupriya Tripathi, Sean M Gibbons, Gail Ackermann, et al. A communal catalogue reveals earth's multiscale microbial diversity. *Nature*, 551(7681):457–463, 2017.

[64] Mohammad Bahram, Falk Hildebrand, Sofia K Forslund, Jennifer L Anderson, Nadejda A Soudzilovskaia, Peter M Bodegom, Johan Bengtsson-Palme, Sten Anslan, Luis Pedro Coelho, Helery Harend, et al. Structure and function of the global topsoil microbiome. *Nature*, 560(7717):233–237, 2018.

[65] Stilianos Louca, Florent Mazel, Michael Doebeli, and Laura Wegener Parfrey. A census-based estimate of earth's bacterial and archaeal diversity. *PLoS biology*, 17(2):e3000106, 2019.

[66] Manuel Delgado-Baquerizo, Angela M Oliverio, Tess E Brewer, Alberto Benavent-González, David J Eldridge, Richard D Bardgett, Fernando T

Maestre, Brajesh K Singh, and Noah Fierer. A global atlas of the dominant bacteria found in soil. *Science*, 359(6373):320–325, 2018.

[67] Hubert de Jonge and Marjo C Mittelmeijer-Hazeleger. Adsorption of co2 and n2 on soil organic matter: nature of porosity, surface area, and diffusion mechanisms. *Environmental Science & Technology*, 30(2):408–413, 1996.

[68] JAET Six, Edward T Elliott, and Keith Paustian. Soil macroaggregate turnover and microaggregate formation: a mechanism for c sequestration under no-tillage agriculture. *Soil biology and biochemistry*, 32(14):2099–2103, 2000.

[69] Felipe Bastida, David J Eldridge, Carlos García, G Kenny Png, Richard D Bardgett, and Manuel Delgado-Baquerizo. Soil microbial diversity–biomass relationships are driven by soil carbon content across global biomes. *The ISME journal*, 15(7):2081–2091, 2021.

[70] EU Onweremadu, VN Onyia, and MAN Anikwe. Carbon and nitrogen distribution in water-stable aggregates under two tillage techniques in fluvisols of owerri area, southeastern nigeria. *Soil and Tillage Research*, 97(2):195–206, 2007.

[71] Mariana Regina Durigan, Maurício Roberto Cherubin, Plínio Barbosa De Camargo, Joice Nunes Ferreira, Erika Berenguer, Toby Alan Gardner, Jos Barlow, Carlos Tadeu dos Santos Dias, Diana Signor, Raimundo Cosme de Oliveira Junior, et al. Soil organic matter responses to anthropogenic forest disturbance and land use change in the eastern brazilian amazon. *Sustainability*, 9(3):379, 2017.

[72] Abdelhakim Bouajila, Zohra Omar, and Ghalya Magherbi. Soil aggregation, aggregate-associated organic carbon, and total nitrogen under different land use in regosols of coastal arid lands in gabes, tunisia. *Arabian Journal of Geosciences*, 14(18):1–12, 2021.

[73] CA Cambardella and ET Elliott. Carbon and nitrogen distribution in aggregates from cultivated and native grassland soils. *Soil Science Society of America Journal*, 57(4):1071–1076, 1993.

[74] David C Coleman, MA Callaham Jr, and DA Crossley Jr. Secondary production: activities of heterotrophic organisms—microbes. *Fundamentals of Soil Ecology*, 3:47–76, 2018.

[75] JD Jastrow. Soil aggregate formation and the accrual of particulate and mineral-associated organic matter. *Soil Biology and Biochemistry*, 28(4-5):665–676, 1996.

[76] H Lünsdorf, RW Erb, WR Abraham, and KN Timmis. 'clay hutches': a novel interaction between bacteria and clay minerals. *Environmental Microbiology*, 2(2):161–168, 2000.

[77] AP Edwards and JM Bremner. Use of sonic vibration for separation of soil particles. *Canadian Journal of Soil Science*, 44(3):366–366, 1964.

[78] Julie A Howe and A Peyton Smith. The soil habitat. In *Principles and Applications of Soil Microbiology*, pages 23–55. Elsevier, 2021.

[79] R Paul Voroney. The soil habitat. In *Soil microbiology, ecology and biochemistry*, pages 25–49. Elsevier, 2007.

[80] Joshua Neuman. Soil organic matter maintenance in no-till and crop rotation management systems. 2017.

[81] Maja Ivanić, Neda Vdović, Sandra de Barreto, Vladimir Bermanec, and Ivan Sondi. Mineralogy, surface properties and electrokinetic behaviour of kaolin clays from the naturally occurring pegmatite deposits. *Geologia Croatica*, 68(2):139–145, 2015.

[82] Fred T Mackenzie. *Sediments, Diagenesis, and Sedimentary Rocks: Treatise on Geochemistry, Volume 7*, volume 7. Elsevier, 2005.

[83] SK Haldar and Josip Tišljar. Basic mineralogy. *Introduction to mineralogy and petrology*, pages 39–79, 2014.

[84] Muniram Budhu. *Soil mechanics fundamentals*. John Wiley & Sons, 2015.

[85] JM Huggett. Clay minerals, encyclopedia of geology, 2005.

[86] SK Haldar. Chapter 1-minerals and rocks. *Introduction to Mineralogy and Petrology (Second Edition). Ed. by SK Haldar. Second Edition. Oxford: Elsevier*, pages 1–51, 2020.

[87] Ming Zhang. The effect of clay minerals on copper and gold flotation. 2016.

[88] Sheikh M Fazle Rabbi, Heiko Daniel, Peter V Lockwood, C Macdonald, Lily Pereg, Matthew Tighe, Brian R Wilson, and Iain M Young. Physical soil architectural traits are functionally linked to carbon decomposition and bacterial diversity. *Scientific reports*, 6(1):1–9, 2016.

[89] Bent T Christensen. Physical fractionation of soil and structural and functional complexity in organic matter turnover. *European journal of soil science*, 52(3):345–353, 2001.

[90] Martin R Carter and Bobby A Stewart. *Structure and organic matter storage in agricultural soils*, volume 8. CRC press, 1995.

[91] D Vaughan and RE Malcolm. *Soil organic matter and biological activity*, volume 16. Springer Science & Business Media, 1985.

[92] JM Lynch and Elaine Bragg. Microorganisms and soil aggregate stability. In *Advances in soil science*, pages 133–171. Springer, 1985.

[93] RJ Haynes and RS Swift. Stability of soil aggregates in relation to organic constituents and soil water content. *Journal of soil science*, 41(1):73–83, 1990.

[94] Cliff T Johnston, Marika Santagata, and Mohammadhasan Sasar. Physical and chemical properties of layered clay mineral particle surfaces. In *Developments in Clay Science*, volume 10, pages 125–167. Elsevier, 2022.

[95] Dongxu Zhou, Amr I Abdel-Fattah, and Arturo A Keller. Clay particles destabilize engineered nanoparticles in aqueous environments[=. *Environmental science & technology*, 46(14):7520–7526, 2012.

[96] Holger Pagel, Katrin Ilg, Jan Siemens, and Martin Kaupenjohann. Total phosphorus determination in colloid-containing soil solutions by enhanced persulfate digestion. *Soil Science Society of America Journal*, 72(3):786–790, 2008.

[97] Claire Chenu and AF Plante. Clay-sized organo-mineral complexes in a cultivation chronosequence: Revisiting the concept of the 'primary organo-mineral complex'. *European journal of soil science*, 57(4):596–607, 2006.

[98] Johannes Lehmann, James Kinyangi, and Dawit Solomon. Organic matter stabilization in soil microaggregates: implications from spatial heterogeneity of organic carbon contents and carbon forms. *Biogeochemistry*, 85(1):45–57, 2007.

[99] Ingrid Kögel-Knabner, Georg Guggenberger, Markus Kleber, Ellen Kandeler, Karsten Kalbitz, Stefan Scheu, Karin Eusterhues, and Peter Leinweber. Organo-mineral associations in temperate soils: Integrating biology, mineralogy, and organic matter chemistry. *Journal of Plant Nutrition and Soil Science*, 171(1):61–82, 2008.

[100] Maki Asano and Rota Wagai. Evidence of aggregate hierarchy at micro-to submicron scales in an allophanic andisol. *Geoderma*, 216:62–74, 2014.

[101] Markus Kleber, Karin Eusterhues, Marco Keiluweit, Christian Mikutta, Robert Mikutta, and Peter S Nico. Mineral–organic associations: formation, properties, and relevance in soil environments. In *Advances in agronomy*, volume 130, pages 1–140. Elsevier, 2015.

[102] Alexandra N Kravchenko, Wakene C Negassa, Andrey K Guber, and Mark L Rivers. Protection of soil carbon within macro-aggregates depends on intra-aggregate pore characteristics. *Scientific Reports*, 5(1):1–10, 2015.

[103] Kai Uwe Totsche, Wulf Amelung, Martin H Gerzabek, Georg Guggenberger, Erwin Klumpp, Claudia Knief, Eva Lehndorff, Robert Mikutta, Stephan Peth, Alexander Prechtel, et al. Microaggregates in soils. *Journal of Plant Nutrition and Soil Science*, 181(1):104–136, 2018.

[104] Georg Guggenberger, Edward T Elliott, Serita D Frey, Johan Six, and Keith Paustian. Microbial contributions to the aggregation of a cultivated grassland soil amended with starch. *Soil Biology and Biochemistry*, 31(3):407–419, 1999.

[105] Steven K Lower, Christopher J Tadanier, and Michael F Hochella Jr. Measuring interfacial and adhesion forces between bacteria and mineral surfaces with biological force microscopy. *Geochimica et Cosmochimica Acta*, 64(18):3133–3139, 2000.

[106] Rodney M Donlan. Biofilms: microbial life on surfaces. *Emerging infectious diseases*, 8(9):881, 2002.

[107] Bent T Christensen. Physical fractionation of soil and structural and functional complexity in organic matter turnover. *European journal of soil science*, 52(3):345–353, 2001.

[108] Subburaj Suganya, Madhava Anil Kumar, and Soumya Haldar. Effect of bacterial attachment on permeable membranes aided by extracellular polymeric substances. In *Microbial and Natural Macromolecules*, pages 733–749. Elsevier, 2021.

[109] François Buscot, Ajit Varma, et al. Microorganisms in soils: roles in genesis and functions. 2005.

[110] Karl Ritz. *The architecture and biology of soils: Life in inner space*. Cabi, 2011.

[111] Peter K Robinson. Enzymes: principles and biotechnological applications. *Essays in biochemistry*, 59:1, 2015.

[112] Richard G Burns. Enzyme activity in soil: location and a possible role in microbial ecology. *Soil biology and biochemistry*, 14(5):423–427, 1982.

[113] RL Sinsabaugh and DL Moorhead. Resource allocation to extracellular enzyme production: a model for nitrogen and phosphorus control of litter decomposition. *Soil biology and biochemistry*, 26(10):1305–1311, 1994.

[114] J Frankena, HW Van Verseveld, and AH Stouthamer. Substrate and energy costs of the production of exocellular enzymes by bacillus licheniformis. *Biotechnology and bioengineering*, 32(6):803–812, 1988.

[115] ML Giuseppin, JW Almkerk, JC Heistek, and CT Verrips. Comparative study on the production of guar alpha-galactosidase by saccharomyces cerevisiae su50b and hansenula polymorpha 8/2 in continuous cultures. *Applied and environmental microbiology*, 59(1):52–59, 1993.

[116] Torben Christiansen and Jens Nielsen. Production of extracellular protease and glucose uptake in bacillus clausii in steady-state and transient continuous cultures. *Journal of biotechnology*, 97(3):265–273, 2002.

[117] Joel L Sachs, Ryan G Skophammer, and John U Regus. Evolutionary transitions in bacterial symbiosis. *Proceedings of the National Academy of Sciences*, 108(Supplement 2):10800–10807, 2011.

[118] Manasi S Gangan, Marcos M Vasconcelos, Urbashi Mitra, Odilon Câmara, and James Q Boedicker. Optimal strategy for public good production is set by balancing intertemporal trade-off between population growth rate and carrying capacity. *bioRxiv*, 2021.

[119] Carey D Nadell, Knut Drescher, and Kevin R Foster. Spatial structure, cooperation and competition in biofilms. *Nature Reviews Microbiology*, 14(9):589–600, 2016.

[120] Kelsi M Sandoz, Shelby M Mitzimberg, and Martin Schuster. Social cheating in pseudomonas aeruginosa quorum sensing. *Proceedings of the National Academy of Sciences*, 104(40):15876–15881, 2007.

[121] Susse Kirkelund Hansen, Paul B Rainey, Janus AJ Haagensen, and Søren Molin. Evolution of species interactions in a biofilm community. *Nature*, 445(7127):533–536, 2007.

[122] Thomas E Kehl-Fie and Eric P Skaar. Nutritional immunity beyond iron: a role for manganese and zinc. *Current opinion in chemical biology*, 14(2):218–224, 2010.

[123] Anat Bren, Yuval Hart, Erez Dekel, Daniel Koster, and Uri Alon. The last generation of bacterial growth in limiting nutrient. *BMC systems biology*, 7(1):1–9, 2013.

[124] Matthew F Barber and Nels C Elde. Buried treasure: evolutionary perspectives on microbial iron piracy. *Trends in Genetics*, 31(11):627–636, 2015.

[125] Louise Aldén, Fredrik Demoling, and E Baath. Rapid method of determining factors limiting bacterial growth in soil. *Applied and environmental microbiology*, 67(4):1830–1838, 2001.

[126] Steven D Allison, Lucy Lu, Alyssa G Kent, and Adam C Martiny. Extracellular enzyme production and cheating in pseudomonas fluorescens depend on diffusion rates. *Frontiers in microbiology*, 5:169, 2014.

[127] Sara Mitri, Ellen Clarke, and Kevin R Foster. Resource limitation drives spatial organization in microbial groups. *The ISME journal*, 10(6):1471–1482, 2016.

[128] James A Damore and Jeff Gore. Understanding microbial cooperation. *Journal of theoretical biology*, 299:31–41, 2012.

[129] Katharine Z Coyte, Hervé Tabuteau, Eamonn A Gaffney, Kevin R Foster, and William M Durham. Microbial competition in porous environments can select against rapid biofilm growth. *Proceedings of the National Academy of Sciences*, 114(2):E161–E170, 2017.

[130] Carey D Nadell, Kevin R Foster, and João B Xavier. Emergence of spatial structure in cell groups and the evolution of cooperation. *PLoS computational biology*, 6(3):e1000716, 2010.

[131] Oskar Hallatschek, Pascal Hersen, Sharad Ramanathan, and David R Nelson. Genetic drift at expanding frontiers promotes gene segregation. *Proceedings of the National Academy of Sciences*, 104(50):19926–19930, 2007.

[132] Sara Mitri, João B Xavier, and Kevin R Foster. Social evolution in multispecies biofilms. *Proceedings of the National Academy of Sciences*, 108(supplement_2):10839–10846, 2011.

[133] Knut Drescher, Carey D Nadell, Howard A Stone, Ned S Wingreen, and Bonnie L Bassler. Solutions to the public goods dilemma in bacterial biofilms. *Current Biology*, 24(1):50–55, 2014.

[134] Gregory J Velicer, Lee Kroos, and Richard E Lenski. Developmental cheating in the social bacterium myxococcus xanthus. *Nature*, 404(6778):598–601, 2000.

[135] Michiel Vos, Alexandra B Wolf, Sarah J Jennings, and George A Kowalchuk. Micro-scale determinants of bacterial diversity in soil. *FEMS microbiology reviews*, 37(6):936–954, 2013.

[136] Steven D Allison and Peter M Vitousek. Responses of extracellular enzymes to simple and complex nutrient inputs. *Soil Biology and Biochemistry*, 37(5):937–944, 2005.

[137] Farooq Azam and Francesca Malfatti. Microbial structuring of marine ecosystems. *Nature Reviews Microbiology*, 5(10):782–791, 2007.

[138] Ákos T Kovács. Impact of spatial distribution on the development of mutualism in microbes. *Frontiers in microbiology*, 5:649, 2014.

[139] Wei Zhang, Tadas Sileika, and Aaron I Packman. Effects of fluid flow conditions on interactions between species in biofilms. *FEMS microbiology ecology*, 84(2):344–354, 2013.

[140] Christoph Hauert and Michael Doebeli. Spatial structure often inhibits the evolution of cooperation in the snowdrift game. *Nature*, 428(6983):643–646, 2004.

[141] Philip S Stewart and Michael J Franklin. Physiological heterogeneity in biofilms. *Nature Reviews Microbiology*, 6(3):199–210, 2008.

[142] J David Van Dyken, Melanie JI Müller, Keenan ML Mack, and Michael M Desai. Spatial population expansion promotes the evolution of cooperation in an experimental prisoner's dilemma. *Current Biology*, 23(10):919–923, 2013.

[143] YA Vetter, JW Deming, Peter A Jumars, and BB Krieger-Brockett. A predictive model of bacterial foraging by means of freely released extracellular enzymes. *Microbial ecology*, 36(1):75–92, 1998.

[144] Emily E Curd, Jennifer BH Martiny, Huiying Li, and Thomas B Smith. Bacterial diversity is positively correlated with soil heterogeneity. *Ecosphere*, 9(1):e02079, 2018.

[145] Jizhong Zhou, Beicheng Xia, David S Treves, L-Y Wu, Terry L Marsh, Robert V O'Neill, Anthony V Palumbo, and James M Tiedje. Spatial and resource factors influencing high microbial diversity in soil. *Applied and Environmental Microbiology*, 68(1):326–334, 2002.

[146] Arnaud Dechesne, Dani Or, and Barth F Smets. Limited diffusive fluxes of substrate facilitate coexistence of two competing bacterial strains. *FEMS microbiology ecology*, 64(1):1–8, 2008.

[147] H Lünsdorf, RW Erb, WR Abraham, and KN Timmis. 'clay hutches': a novel interaction between bacteria and clay minerals. *Environmental Microbiology*, 2(2):161–168, 2000.

[148] Alexandra Alimova, M Roberts, A Katz, E Rudolph, JC Steiner, RR Alfano, and P Gottlieb. Effects of smectite clay on biofilm formation by microorganisms. *Biofilms*, 3(1):47, 2006.

[149] Mark W Silby, Ana M Cerdeño-Tárraga, Georgios S Vernikos, Stephen R Giddens, Robert W Jackson, Gail M Preston, Xue-Xian Zhang, Christina D Moon, Stefanie M Gehrig, Scott AC Godfrey, et al. Genomic and genetic analyses of diversity and plant interactions of pseudomonas fluorescens. *Genome biology*, 10(5):1–16, 2009.

[150] Muriel E Rhodes. The characterization of pseudomonas fluorescens. *Microbiology*, 21(1):221–263, 1959.

[151] Richard G Burns, Jared L DeForest, Jürgen Marxsen, Robert L Sinsabaugh, Mary E Stromberger, Matthew D Wallenstein, Michael N Weintraub, and Annamaria Zoppini. Soil enzymes in a changing environment: current knowledge and future directions. *Soil Biology and Biochemistry*, 58:216–234, 2013.

[152] JA Baldock and PN Nelson. Soil organic matter. CRC press, 2000.

[153] Guoqing Lu, Jamie Luhr, Andrew Stoecklein, Paige Warner, and William Tapprich. Complete genome sequences of pseudomonas fluorescens bacteriophages isolated from freshwater samples in omaha, nebraska. *Genome Announcements*, 5(12):e01501–16, 2017.

[154] Martin Wiedmann, Denise Weilmeier, Sean S Dineen, Robert Ralyea, and Kathryn J Boor. Molecular and phenotypic characterization of pseudomonas spp. isolated from milk. *Applied and Environmental Microbiology*, 66(5):2085–2095, 2000.

[155] JA Lucey, ME Johnson, and DS Horne. Invited review: perspectives on the basis of the rheology and texture properties of cheese. *Journal of Dairy Science*, 86(9):2725–2743, 2003.

[156] Pieter Walstra. *Dairy technology: principles of milk properties and processes*. CRC Press, 1999.

[157] C Holt. Structure and stability of bovine casein micelles. *Advances in protein chemistry*, 43:63–151, 1992.

[158] Ching-Hsing Liao and Daniel E McCallus. Biochemical and genetic characterization of an extracellular protease from pseudomonas fluorescens cy091. *Applied and Environmental Microbiology*, 64(3):914–921, 1998.

[159] Kirsten Christoffersen, Ole Nybroe, Klaus Jürgens, and Michael Hansen. Measurement of bacterivory by heterotrophic nanoflagellates using immunofluorescence labelling of ingested cells. *Aquatic microbial ecology*, 13(1):127–134, 1997.

[160] Mette H Nicolaisen, Jakob Worm, Niels OG Jørgensen, Mathias Middelboe, and Ole Nybroe. Proteinase production in pseudomonas fluorescens on2 is affected by carbon sources and allows surface-attached but not planktonic cells to utilize protein for growth in lake water. *FEMS microbiology ecology*, 80(1):168–178, 2012.

[161] Steven D Allison. Cheaters, diffusion and nutrients constrain decomposition by microbial enzymes in spatially structured environments. *Ecology Letters*, 8(6):626–635, 2005.

[162] Frank Duong, Chantal Soscia, Andrée Lazdunski, and Maryse Murgier. The pseudomonas fluorescens lipase has a c-terminal secretion signal and is secreted by a three-component bacterial abc-exporter system. *Molecular microbiology*, 11(6):1117–1126, 1994.

[163] Chunyue Zhang, Etske Bijl, Birgitta Svensson, and Kasper Hettinga. The extracellular protease aprx from pseudomonas and its spoilage potential for uht milk: A review. *Comprehensive reviews in food science and food safety*, 18(4):834–852, 2019.

[164] Robert MQ Shanks, Nicky C Caiazza, Shannon M Hinsa, Christine M Toutain, and George A O'Toole. Saccharomyces cerevisiae-based molecular tool kit for manipulation of genes from gram-negative bacteria. *Applied and environmental microbiology*, 72(7):5027–5036, 2006.

[165] Weng-Tat Chan, Chandra S Verma, David P Lane, and Samuel Ken-En Gan. A comparison and optimization of methods and factors affecting the transformation of escherichia coli. *Bioscience reports*, 33(6), 2013.

[166] Bacterial Transformation. The heat shock method [video file].(2017). *United States of America: JoVE. Retrieved December*, 10, 2017.

[167] MJ McBride and MJ Kempf. Development of techniques for the genetic manipulation of the gliding bacterium cytophaga johnsonae. *Journal of bacteriology*, 178(3):583–590, 1996.

[168] VI Brown and EJL Lowbury. Use of an improved cetrimide agar medium and other culture methods for pseudomonas aeruginosa. *Journal of clinical pathology*, 18(6):752–756, 1965.

[169] Nicholas Billinton and Andrew W Knight. Seeing the wood through the trees: a review of techniques for distinguishing green fluorescent protein from endogenous autofluorescence. *Analytical biochemistry*, 291(2):175–197, 2001.

[170] Christoffel Dinant, Martin E van Royen, Wim Vermeulen, and Adriaan B Houtsmuller. Fluorescence resonance energy transfer of gfp and yfp by spectral imaging and quantitative acceptor photobleaching. *Journal of microscopy*, 231(1):97–104, 2008.

[171] Kyoung-Hee Choi and Herbert P Schweizer. mini-tn7 insertion in bacteria with single atttn7 sites: example pseudomonas aeruginosa. *Nature protocols*, 1(1):153–161, 2006.

[172] Lotte Lambertsen, Claus Sternberg, and Søren Molin. Mini-tn7 transposons for site-specific tagging of bacteria with fluorescent proteins. *Environmental microbiology*, 6(7):726–732, 2004.

[173] JL Martinez and F Baquero. Mutation frequencies and antibiotic resistance. *Antimicrobial agents and chemotherapy*, 44(7):1771–1777, 2000.

[174] Wook Kim, Fernando Racimo, Jonas Schluter, Stuart B Levy, and Kevin R Foster. Importance of positioning for microbial evolution. *Proceedings of the National Academy of Sciences*, 111(16):E1639–E1647, 2014.

[175] Steven D Allison, Lucy Lu, Alyssa G Kent, and Adam C Martiny. Extracellular enzyme production and cheating in pseudomonas fluorescens depend on diffusion rates. *Frontiers in microbiology*, 5:169, 2014.

[176] Jacques Monod. The growth of bacterial cultures. *Annual review of microbiology*, 3(1):371–394, 1949.

[177] Oliver John Meacock. *Collective twitching motility in Pseudomonas aeruginosa and its evolutionary consequences*. PhD thesis, University of Oxford, 2019.

[178] Alberto Alvarez-Barrientos, Javier Arroyo, Rafael Cantón, César Nombela, and Miguel Sánchez-Pérez. Applications of flow cytometry to clinical microbiology. *Clinical microbiology reviews*, 13(2):167–195, 2000.

[179] Pierre Friedlingstein, Susan Solomon, GK Plattner, Reto Knutti, Philippe Ciais, and MR Raupach. Long-term climate implications of twenty-first century options for carbon dioxide emission mitigation. *Nature Climate Change*, 1(9):457–461, 2011.

[180] David S Powlson, Andrew P Whitmore, and Keith WT Goulding. Soil carbon sequestration to mitigate climate change: a critical re-examination to identify the true and the false. *European Journal of Soil Science*, 62(1):42–55, 2011.

[181] Esteban G Jobbágy and Robert B Jackson. The vertical distribution of soil organic carbon and its relation to climate and vegetation. *Ecological applications*, 10(2):423–436, 2000.

[182] Marie-France Dignac, Delphine Derrien, Pierre Barre, Sébastien Barot, Lauric Cécillon, Claire Chenu, Tiphaine Chevallier, Grégoire T Freschet, Patricia Garnier, Bertrand Guenet, et al. Increasing soil carbon storage: mechanisms, effects of agricultural practices and proxies. a review. *Agronomy for sustainable development*, 37(2):14, 2017.

[183] Henry Lin and H Lin. Understanding soil architecture and its functional manifestation across scales. *Hydropedology, ed. H. Lin (Amsterdam: Elsevier)*, pages 41–74, 2012.

[184] Vadakattu V.S.R. Gupta and James J. Germida. Soil aggregation: Influence on microbial biomass and implications for biological processes. *Soil Biology and Biochemistry*, 80:A3–A9, 2015.

[185] V.A. Snyder and M.A. Vázquez. Structure. pages 54–68, 2005.

[186] A Pl Edwards and JM Bremner. Microaggregates in soils 1. *Journal of Soil Science*, 18(1):64–73, 1967.

[187] Claire Chenu, Diego Cosentino, et al. Microbial regulation of soil structural dynamics. *The architecture and biology of soils: life in inner space*, pages 37–70, 2011.

[188] Svetlana Filimonova, Andrei Nossov, Alexander Dümig, Antoine Gédéon, Ingrid Kögel-Knabner, and Heike Knicker. Evaluating pore structures of soil components with a combination of "conventional" and hyperpolarised 129xe nmr studies. *Geoderma*, 162(1-2):96–106, 2011.

[189] Yu-Tuan Huang, David J Lowe, G Jock Churchman, Louis A Schipper, Ray Cursons, Heng Zhang, Tsan-Yao Chen, and Alan Cooper. Dna adsorption by nanocrystalline allophane spherules and nanoaggregates, and implications for carbon sequestration in andisols. *Applied Clay Science*, 120:40–50, 2016.

[190] Svetlana Filimonova, Stephan Kaufhold, Friedrich E Wagner, Werner Häusler, and Ingrid Kögel-Knabner. The role of allophane nano-structure and fe oxide speciation for hosting soil organic matter in an allophanic andosol. *Geochimica et Cosmochimica Acta*, 180:284–302, 2016.

[191] P Puget, DA Angers, and C Chenu. Nature of carbohydrates associated with water-stable aggregates of two cultivated soils. *Soil Biology and Biochemistry*, 31(1):55–63, 1998.

[192] Johan Six, Heleen Bossuyt, Stefan Degryze, and Karolien Denef. A history of research on the link between (micro) aggregates, soil biota, and soil organic matter dynamics. *Soil and Tillage Research*, 79(1):7–31, 2004.

[193] Kai U Totsche, Thilo Rennert, Martin H Gerzabek, Ingrid Kögel-Knabner, Kornelia Smalla, Michael Spiteller, and Hans-Jörg Vogel. Biogeochemical interfaces in soil: the interdisciplinary challenge for soil science. *Journal of Plant Nutrition and Soil Science*, 173(1):88–99, 2010.

[194] SM Fazle Rabbi, Brian R Wilson, Peter V Lockwood, Heiko Daniel, and Iain M Young. Aggregate hierarchy and carbon mineralization in two oxisols of new south wales, australia. *Soil and Tillage Research*, 146:193–203, 2015.

[195] M Van Gestel, Roel Merckx, and Karel Vlassak. Spatial distribution of microbial biomass in microaggregates of a silty-loam soil and the relation with the resistance of microorganisms to soil drying. *Soil Biology and Biochemistry*, 28(4-5):503–510, 1996.

[196] RJ Wodzinski and WC Frazier. Moisture requirements of bacteria: I. influence of temperature and ph on requirements of pseudomonas fluorescens. *Journal of bacteriology*, 79(4):572–578, 1960.

[197] Sabrina Juarez, Naoise Nunan, Anne-Claire Duday, Valérie Pouteau, Sonja Schmidt, Simona Hapca, Ruth Falconer, Wilfred Otten, and Claire Chenu. Effects of different soil structures on the decomposition of native and added organic carbon. *European journal of soil biology*, 58:81–90, 2013.

[198] Geneviève L Grundmann. Spatial scales of soil bacterial diversity–the size of a clone. *FEMS microbiology ecology*, 48(2):119–127, 2004.

[199] Naoise Nunan, Iain M Young, John W Crawford, and Karl Ritz. Bacterial interactions at the microscale–linking habitat to function in soil. *The spatial distribution of microbes in the environment*, pages 61–85, 2007.

[200] Iain M Young, John W Crawford, Naoise Nunan, Wilfred Otten, and Andrew Spiers. Microbial distribution in soils: physics and scaling. *Advances in agronomy*, 100:81–121, 2008.

[201] Celso Figueiredo Gomes, Jorge Hamilton Gomes, and Eduardo Ferreira da Silva. Bacteriostatic and bactericidal clays: an overview. *Environmental Geochemistry and Health*, pages 1–21, 2020.

[202] Jing Zhang, Chun Hui Zhou, Sabine Petit, and Hao Zhang. Hectorite: Synthesis, modification, assembly and applications. *Applied Clay Science*, 177:114–138, 2019.

[203] Lucjan Chmielarz, Andrzej Kowalczyk, Monika Skoczek, Małgorzata Rutkowska, Barbara Gil, Piotr Natkański, Marcelina Radko, Monika Motak, Radosław Dębek, and Janusz Ryczkowski. Porous clay heterostructures intercalated with multicomponent pillars as catalysts for dehydration of alcohols. *Applied Clay Science*, 160:116–125, 2018.

[204] Catherine N Mulligan, RN Yong, and BF Gibbs. Surfactant-enhanced remediation of contaminated soil: a review. *Engineering geology*, 60(1-4):371–380, 2001.

[205] Plinio Innocenzi, Luca Malfatti, Stefano Costacurta, Tongjit Kidchob, Massimo Piccinini, and Augusto Marcelli. Evaporation of ethanol and ethanol-water mixtures studied by time-resolved infrared spectroscopy. *The Journal of Physical Chemistry A*, 112(29):6512–6516, 2008.

[206] X Wang, K Xia, X Yang, and C Tang. Growth strategy of microbes on mixed carbon sources. nat commun 10 (1): 1279, 2019.

[207] Lynne Boddy. Fungi, ecosystems, and global change. In *The Fungi*, pages 361–400. Elsevier, 2016.

[208] Kelly I Ramin and Steven D Allison. Bacterial tradeoffs in growth rate and extracellular enzymes. *Frontiers in microbiology*, 10:2956, 2019.

[209] Michael A Brockhurst, Angus Buckling, Dan Racey, and Andy Gardner. Resource supply and the evolution of public-goods cooperation in bacteria. *BMC biology*, 6(1):1–6, 2008.

[210] AT Nasseri, S Rasoul-Amini, MH Morowvat, Y Ghasemi, et al. Single cell protein: production and process. *American Journal of food technology*, 6(2):103–116, 2011.

[211] Alexandre Persat, Carey D Nadell, Minyoung Kevin Kim, Francois Ingremeau, Albert Siryaporn, Knut Drescher, Ned S Wingreen, Bonnie L Bassler, Zemer Gitai, and Howard A Stone. The mechanical world of bacteria. *Cell*, 161(5):988–997, 2015.

[212] Paula Watnick and Roberto Kolter. Biofilm, city of microbes. *Journal of bacteriology*, 182(10):2675–2679, 2000.

[213] Douglas L Marshall and Ronald H Schmidt. Physiological evaluation of stimulated growth of listeria monocytogenes by pseudomonas species in milk. *Canadian journal of microbiology*, 37(8):594–599, 1991.

[214] Vincent Juillard, Sylviane Furlan, Catherine Foucaud, and Jean Richard. Mixed cultures of proteinase-positive and proteinase-negative strains of lactococcus lactis in milk. *Journal of dairy science*, 79(6):964–970, 1996.

[215] Stuart A West, Ashleigh S Griffin, Andy Gardner, and Stephen P Diggle. Social evolution theory for microorganisms. *Nature reviews microbiology*, 4(8):597–607, 2006.

[216] Laurent Keller. *Levels of selection in evolution*, volume 21. Princeton University Press, 1999.

[217] Joel L Sachs, Ulrich G Mueller, Thomas P Wilcox, and James J Bull. The evolution of cooperation. *The Quarterly review of biology*, 79(2):135–160, 2004.

[218] Joao B Xavier and Kevin R Foster. Cooperation and conflict in microbial biofilms. *Proceedings of the National Academy of Sciences*, 104(3):876–881, 2007.

[219] Peter Kareiva. Population dynamics in spatially complex environments: theory and data. *Philosophical Transactions of the Royal Society of London. Series B: Biological Sciences*, 330(1257):175–190, 1990.

[220] Stephen P Ellner, Edward McCauley, Bruce E Kendall, Cheryl J Briggs, Parveiz R Hosseini, Simon N Wood, Arne Janssen, Maurice W Sabelis, Peter Turchin, Roger M Nisbet, et al. Habitat structure and population persistence in an experimental community. *Nature*, 412(6846):538–543, 2001.

[221] Peter Chesson. General theory of competitive coexistence in spatially-varying environments. *Theoretical population biology*, 58(3):211–237, 2000.

[222] Jordl Bascompte and Ricard V Solé. Rethinking complexity: modelling spatiotemporal dynamics in ecology. *Trends in Ecology & Evolution*, 10(9):361–366, 1995.

[223] Misael B de Souza Júnior, Fernando F Ferreira, and Viviane M de Oliveira. Effects of the spatial heterogeneity on the diversity of ecosystems with resource competition. *Physica A: Statistical Mechanics and its Applications*, 393:312–319, 2014.

[224] Michelle GJL Habets, Daniel E Rozen, Rolf F Hoekstra, and J Arjan GM de Visser. The effect of population structure on the adaptive radiation of microbial populations evolving in spatially structured environments. *Ecology letters*, 9(9):1041–1048, 2006.

[225] Johannes Lehmann and Markus Kleber. The contentious nature of soil organic matter. *Nature*, 528(7580):60–68, 2015.

[226] Babak Momeni, Adam James Waite, and Wenying Shou. Spatial self-organization favors heterotypic cooperation over cheating. *Elife*, 2:e00960, 2013.

[227] S Bickel and D Or. Soil bacterial diversity mediated by microscale aqueous-phase processes across biomes. nat commun 11: 1–9, 2020.

[228] Monica I Abrudan, Fokko Smakman, Ard Jan Grimbergen, Sanne Westhoff, Eric L Miller, Gilles P Van Wezel, and Daniel E Rozen. Socially mediated induction and suppression of antibiosis during bacterial coexistence. *Proceedings of the National Academy of Sciences*, 112(35):11054–11059, 2015.

[229] Diana Di Gioia, Francesca Luziatelli, Andrea Negroni, Anna Grazia Ficca, Fabio Fava, and Maurizio Ruzzi. Metabolic engineering of pseudomonas fluorescens for the production of vanillin from ferulic acid. *Journal of biotechnology*, 156(4):309–316, 2011.

[230] Ian T Paulsen, Caroline M Press, Jacques Ravel, Donald Y Kobayashi, Garry SA Myers, Dmitri V Mavrodi, Robert T DeBoy, Rekha Seshadri, Qinghu Ren, Ramana Madupu, et al. Complete genome sequence of the plant commensal pseudomonas fluorescens pf-5. *Nature biotechnology*, 23(7):873–878, 2005.

[231] Eric Andriamahery Rasolofo, Daniel St-Gelais, Gisele LaPointe, and Denis Roy. Molecular analysis of bacterial population structure and dynamics during cold storage of untreated and treated milk. *International journal of food microbiology*, 138(1-2):108–118, 2010.

[232] Robert Jenness. Comparative aspects of milk proteins. *Journal of Dairy Research*, 46(2):197–210, 1979.

[233] Arthur H Totten, Li Xiao, Donna M Crabb, Amy E Ratliff, Kevin Dybvig, Ken B Waites, and T Prescott Atkinson. Shaken or stirred?: comparison of methods for dispersion of mycoplasma pneumoniae aggregates for persistence in vivo. *Journal of microbiological methods*, 132:56–62, 2017.

[234] Yichao Wu, Peng Cai, Xinxin Jing, Xueke Niu, Dandan Ji, Noha Mohamed Ashry, Chunhui Gao, and Qiaoyun Huang. Soil biofilm formation enhances microbial community diversity and metabolic activity. *Environment International*, 132:105116, 2019.

[235] D Harris and EA Paul. Measurement of bacterial growth rates in soil. *Applied Soil Ecology*, 1(4):277–290, 1994.

[236] Viggo Lindahl and Lars R Bakken. Evaluation of methods for extraction of bacteria from soil. *FEMS Microbiology Ecology*, 16(2):135–142, 1995.

[237] John E Hobbie, R Jasper Daley, and STTI977 Jasper. Use of nuclepore filters for counting bacteria by fluorescence microscopy. *Applied and environmental microbiology*, 33(5):1225–1228, 1977.

[238] Jens Boenigk. A disintegration method for direct counting of bacteria in clay-dominated sediments: dissolving silicates and subsequent fluorescent staining of bacteria. *Journal of microbiological Methods*, 56(2):151–159, 2004.

[239] Nanna Buesing and Mark O Gessner. Comparison of detachment procedures for direct counts of bacteria associated with sediment particles, plant litter and epiphytic biofilms. *Aquatic Microbial Ecology*, 27(1):29–36, 2002.

[240] Thomas Trunk, Hawzeen S Khalil, and Jack C Leo. Bacterial autoaggregation. *AIMS microbiology*, 4(1):140, 2018.

[241] Fastprep motion measurements.

[242] Jeonggil Lee, Han-Suk Kim, Ho Young Jo, and Man Jae Kwon. Revisiting soil bacterial counting methods: Optimal soil storage and pretreatment methods and comparison of culture-dependent and-independent methods. *PloS one*, 16(2):e0246142, 2021.

[243] JM Lynch. Interactions between biological processes, cultivation and soil structure. In *Biological Processes and Soil Fertility*, pages 307–318. Springer, 1984.

[244] Maria T Brandl and Steven Huynh. Effect of the surfactant tween 80 on the detachment and dispersal of salmonella enterica serovar thompson single cells and aggregates from cilantro leaves as revealed by image analysis. *Applied and environmental microbiology*, 80(16):5037–5042, 2014.

[245] Yuki Morono, Takeshi Terada, Noriaki Masui, and Fumio Inagaki. Discriminative detection and enumeration of microbial life in marine subsurface sediments. *The ISME journal*, 3(5):503–511, 2009.

[246] Noah Fierer, Jason A Jackson, Rytas Vilgalys, and Robert B Jackson. Assessment of soil microbial community structure by use of taxon-specific quantitative pcr assays. *Applied and environmental microbiology*, 71(7):4117–4120, 2005.

[247] Stefano Amalfitano and Stefano Fazi. Recovery and quantification of bacterial cells associated with streambed sediments. *Journal of microbiological methods*, 75(2):237–243, 2008.

[248] Juan Liu, Jingquan Li, Li Feng, Hui Cao, and Zhongli Cui. An improved method for extracting bacteria from soil for high molecular weight dna recovery and bac library construction. *The Journal of Microbiology*, 48(6):728–733, 2010.

[249] Céline Martin, Frédéric Pignon, Jean-Michel Piau, Albert Magnin, Peter Lindner, and Bernard Cabane. Dissociation of thixotropic clay gels. *Physical Review E*, 66(2):021401, 2002.

[250] Khushboo Suman and Yogesh M Joshi. Microstructure and soft glassy dynamics of an aqueous laponite dispersion. *Langmuir*, 34(44):13079–13103, 2018.

[251] Khushboo Suman, Mohit Mittal, and Yogesh M Joshi. Effect of sodium pyrophosphate and understanding microstructure of aqueous laponite® dispersion using dissolution study. *Journal of Physics: Condensed Matter*, 32(22):224002, 2020.

[252] V Krištfek, K Šimek, B Grunda, and P Punčochář. Use of nitrocellulose synpor filters for counting soil bacteria by epifluorescence microscopy. *Folia microbiologica*, 32(4):349–353, 1987.

[253] Hazel M Davey. Life, death, and in-between: meanings and methods in microbiology. *Applied and environmental microbiology*, 77(16):5571–5576, 2011.

[254] Pious Thomas, Aparna C Sekhar, Reshmi Upreti, Mohammad M Mujawar, and Sadiq S Pasha. Optimization of single plate-serial dilution spotting (sp-sds) with sample anchoring as an assured method for bacterial and yeast cfu enumeration and single colony isolation from diverse samples. *Biotechnology Reports*, 8:45–55, 2015.

[255] Ian Levenfus. *An efficient method for counting DAPI-stained cells using Fiji*. GRIN Verlag, 2011.

[256] B Venkatalakshmi and K Thilagavathi. Automatic red blood cell counting using hough transform. In *2013 IEEE Conference on Information & Communication Technologies*, pages 267–271. IEEE, 2013.

[257] Oskar Heimstädt. Das fluoreszenzmikroskop. *Z Wiss Mikrosk*, 28:330–337, 1911.

[258] Adam D Hoppe, Stephanie Seveau, and Joel A Swanson. Live cell fluorescence microscopy to study microbial pathogenesis. *Cellular microbiology*, 11(4):540–550, 2009.

[259] Roberto Rusconi, Melissa Garren, and Roman Stocker. Microfluidics expanding the frontiers of microbial ecology. *Annual review of biophysics*, 43:65–91, 2014.

[260] Todd A Duncombe, Augusto M Tentori, and Amy E Herr. Microfluidics: reframing biological enquiry. *Nature Reviews Molecular Cell Biology*, 16(9):554–567, 2015.

[261] Rattan Lal and JM Kimble. Conservation tillage for carbon sequestration. *Nutrient cycling in agroecosystems*, 49(1):243–253, 1997.

[262] Uta Stockmann, Mark A Adams, John W Crawford, Damien J Field, Nilusha Henakaarchchi, Meaghan Jenkins, Budiman Minasny, Alex B McBratney, Vivien de Remy De Courcelles, Kanika Singh, et al. The knowns, known unknowns and unknowns of sequestration of soil organic carbon. *Agriculture, Ecosystems & Environment*, 164:80–99, 2013.

[263] Sindhu Jagadamma and Rattan Lal. Distribution of organic carbon in physical fractions of soils as affected by agricultural management. *Biology and Fertility of Soils*, 46(6):543–554, 2010.

[264] Ingo Lobe, Alexandra Sandhage-Hofmann, Sonja Brodowski, Chris C Du Preez, and Wulf Amelung. Aggregate dynamics and associated soil organic matter contents as influenced by prolonged arable cropping in the south african highveld. *Geoderma*, 162(3-4):251–259, 2011.

[265] Rattan Lal. Soil carbon sequestration to mitigate climate change. *Geoderma*, 123(1-2):1–22, 2004.

[266] Michael WI Schmidt, Margaret S Torn, Samuel Abiven, Thorsten Dittmar, Georg Guggenberger, Ivan A Janssens, Markus Kleber, Ingrid Kögel-Knabner, Johannes Lehmann, David AC Manning, et al. Persistence of soil organic matter as an ecosystem property. *Nature*, 478(7367):49–56, 2011.

[267] An-Na Li, Sha Li, Yu-Jie Zhang, Xiang-Rong Xu, Yu-Ming Chen, and Hua-Bin Li. Resources and biological activities of natural polyphenols. *Nutrients*, 6(12):6020–6047, 2014.

[268] W Harder and L Dijkhuizen. Physiological responses to nutrient limitation. *Annual review of microbiology*, 37(1):1–23, 1983.

[269] Robert W Sterner and James J Elser. *Ecological stoichiometry*. Princeton university press, 2017.

[270] George E Christidis, Carlos Aldana, Georgios D Chryssikos, Vassilis Gionis, Hussein Kalo, Matthias Stöter, Josef Breu, and Jean-Louis Robert. The nature of laponite: pure hectorite or a mixture of different trioctahedral phases? *Minerals*, 8(8):314, 2018.

[271] Judy Q Yang, Xinning Zhang, Ian C Bourg, and Howard A Stone. 4d imaging reveals mechanisms of clay-carbon protection and release. *Nature communications*, 12(1):1–8, 2021.

[272] Russell D Monds, Peter D Newell, Robert H Gross, and George A O'Toole. Phosphate-dependent modulation of c-di-gmp levels regulates pseudomonas fluorescens pf0-1 biofilm formation by controlling secretion of the adhesin lapa. *Molecular microbiology*, 63(3):656–679, 2007.

[273] Shannon M Hinsa and George A O'Toole. Biofilm formation by pseudomonas fluorescens wcs365: a role for lapd. *Microbiology*, 152(5):1375–1383, 2006.

[274] Yan Zhou, Yan-Bin Xu, Jia-Xin Xu, Xiao-Hua Zhang, Shi-Hui Xu, and Qing-Ping Du. Combined toxic effects of heavy metals and antibiotics on a pseudomonas fluorescens strain zy2 isolated from swine wastewater. *International Journal of molecular sciences*, 16(2):2839–2850, 2015.

[275] Yimei Ying and Guoqiang Bai. Biosorption properties of some heavy metals by pseudomonas fluorescens in industrial wastewater. In *2011 5th International Conference on Bioinformatics and Biomedical Engineering*.

[276] Hang Du, Weili Xu, Zhizhou Zhang, and Xiaojun Han. Bacterial behavior in confined spaces. *Frontiers in Cell and Developmental Biology*, 9:524, 2021.